

EPSC2018  
**TP4 abstracts**

## LaRa (Lander Radioscience) on the ExoMars 2020 Surface Platform.

Véronique Dehant<sup>1,2</sup>, Sébastien Le Maistre<sup>1</sup>, Rose-Marie Baland<sup>1</sup>, Ögür Karatekin<sup>1</sup>, Michel Mitrovic<sup>1</sup>, Marie-Julie Péters<sup>1</sup>, Attilio Rivoldini<sup>1</sup>, Tim Van Hoolst<sup>1</sup>, Bart Van Hove<sup>1</sup>, and Marie Yseboodt<sup>1</sup>  
(1) Royal Observatory of Belgium, Brussels, Belgium, (2) Université catholique de Louvain, Louvain-la-Neuve, Belgium

### Abstract

The LaRa (Lander Radioscience) experiment will be described and the scientific objectives will be detailed.

### 1. Introduction

The LaRa experiment is designed to obtain coherent two-way Doppler measurements from the radio link between the 2020 ExoMars lander and the Earth over at least one Martian year. The Doppler measurements will be used to observe the orientation and rotation of Mars in space (precession, nutations, and length-of-day variations), as well as polar motion. The ultimate objective is to obtain information on the Martian interior and on the sublimation/condensation cycle of atmospheric CO<sub>2</sub>. Rotational variations will allow us to constrain the moment of inertia of the entire planet, including its mantle and core, the moment of inertia of the core, and seasonal mass transfer between the atmosphere and the ice caps.

### 2. The LaRa instrument

The Surface Platform of 2020 ExoMars will house a radio science experiment LaRa to support specific scientific objectives during the ExoMars mission. LaRa has been designed to transpond an X-band signal transmitted from an Earth ground station, back to the Earth. The relative radial velocity of the Earth and the Martian lander is inferred from Doppler effects measured at the Earth ground stations. The Doppler shifts are measured from the Doppler tracking observations called “Two-way” by comparing the frequency of the radio signal received from LaRa with the corresponding frequency of a ground-based reference signal.

As LaRa performs a coherent conversion of the uplink carrier to the downlink carrier, the Masers of

the Earth’s ground stations ensure the frequency stability of the LaRa radiosignal. The downlink carrier frequency is related to the uplink carrier by a multiplicative constant, the transponder ratio (880/749).

LaRa uses three X-band antennas to communicate with the Earth, one for receiving the signal and two (for redundancy) for retransmitting the signal. In order to minimize the radio blackout during the observation period of the Earth in the Martian sky, LaRa’s antennas are designed to obtain an optimal antenna gain centered on an elevation (angle of the line-of-sight from lander to Earth) of about 30-55°.



Figure 1: The LaRa transponder and its antennas (1 receiving antenna RX, 2 transmitting antennas TX).

The strong energy/mass restrictions (Power  $\leq$  39 Watt - Total Mass transponder + antennas  $\leq$  2.150 kg) and the payload interface compatibility (with thermal control system (TCS), data handling system (DHS) and electrical power system (EPS)) introduce significant constraints on the final design of LaRa. The transponder design maintains the coherency of the signal, and the global precision on the Doppler is expected to be better than 0.1 mm/s at a 60 second integration time (compared to the instrument precision requirement at the level of 0.02 mm/s at a 60 second integration time).

After landing, the transponder will be operated when an Earth ground station is available and when the Earth is in the sky of the lander. The position of the lander will be determined with the first passes as well as from the landing site characteristics and from the MOLA altimetric data [5]. LaRa will operate twice per week at least during the whole mission lifetime (twice per week during the minimum guaranteed mission and during the extended mission, with a possible relaxation to once per week during hibernation).

### 3. The LaRa science

Since Mars is oblate and rotating and since the equator is not parallel to the Mars-Sun line (Mars has an obliquity angle of about  $25^\circ$ ), Mars reacts as a spinning top to the gravitational torque exerted by the Sun. As a consequence, the rotation axis and the planet slowly move in space around the perpendicular to the orbital plane (see Figure 2). The time needed to perform one cycle around the orbit normal is about 171,000 years with a speed on the precession cone (so-called precession rate) of about 7.6 arcsecond/year at present. A first objective of LaRa is to very accurately determine the precession rate. Since precession is inversely proportional to the polar principal moment of inertia, LaRa will be able to accurately determine the moments of inertia of Mars, providing important constraints on the interior structure.

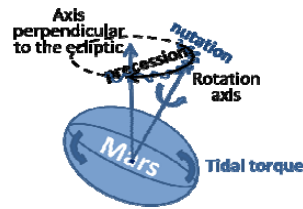


Figure 2: Representation of precession and nutation of Mars.

Because of the elliptical orbital motion of Mars and the orbital changes due for instance to interaction with other Solar System bodies, the gravitational torque on Mars changes with time. The variations in the torque induce periodic changes in the precession as well as variations in the obliquity, called nutations. The resulting motion of the pole due to precession and nutation is wiggly as illustrated in Figure 2. The periods of the nutations are related to the periods of the orbital motion and to the periods of the orbital

perturbations. The largest of these periodic nutations has a period of half the orbital period. Detailed explanations can be found in the Encyclopedia of the Solar System chapters of Dehant and Van Hoolst [1] and Van Hoolst and Rivoldini [6], in the book of Dehant and Mathews [2], and in the Treatise on Geophysics chapters on planetary rotation [3] [7].

The rotation changes are due to exchange of angular momentum with the atmosphere and to gravitational torques acting on Mars. The rotation rate of Mars is approximately uniform but variations in the Length-Of-Day (LOD) have already been observed and are mainly due to exchanges of mass and angular momentum between the atmosphere and surface. These exchanges occur mostly at seasonal periods through sublimation/condensation of the  $\text{CO}_2$  polar caps, mass redistributions in the atmosphere, and seasonally changing winds. LaRa will improve current estimates of the LOD variations (known at about 15% level, Konopliv et al., 2011) and thereby will place the best global constraints on the global mass redistribution in the atmosphere and ice caps and the atmospheric angular momentum.

### Acknowledgements

This work was financially supported by the Belgian PRODEX program managed by the European Space Agency in collaboration with the Belgian Federal Science Policy Office.

### References

- [1] Dehant, V., and Van Hoolst T. Encyclopedia of the Solar System, Chapter 8, 159-184, 2014.
- [2] Dehant V. and Mathews P.M., Precession, Nutation, and Wobble of the Earth. Book, Cambridge University Press, ISBN: 9781107092549, 536 pages, 2015.
- [3] Dehant V. and Mathews P.M., Treatise on Geophysics, Vol. 3 Geodesy, Section 3.10, ISBN: 9780444538024, 2015.
- [4] Konopliv A.S., Asmar S.W., Folkner W.M., Karatekin Ö., Nunes D.C., Smrekar S.E., Yoder C.F., Zuber M.T., Icarus, 211(1), 401-428, 2011.
- [5] Le Maistre S., InSight coordinates determination from direct-to-Earth radio-tracking and Mars topography model. Planetary and Space Science, 121, 1-9, 2016.
- [6] Van Hoolst T., and Rivoldini A., Encyclopedia of the Solar System, Chapter 18, 379-396, 2014.
- [7] Van Hoolst T., Treatise on Geophysics, Vol. 10 Planets and Moons, Section 10.04, ISBN: 9780444538024, 2015.

## CaSSIS – First images from science orbit

N. Thomas(1), G. Cremonese(2), M. Almeida(1), M. Banaszekiewicz(3), P. Becerra(1), J. Bridges(4), S. Byrne(5), V. Da Deppo(6), S. Debei(7), M.R. El-Maarry(19), E. Hauber(8), C.J. Hansen(9), A. Ivanov(10), L. Keszthelyi (11), R. Kirk(11), R. Kuzmin(12), N. Mangold(13), L. Marinangeli(14), W. Markiewicz(15†), M. Massironi(16), A.S. McEwen(5), C. Okubo(11), P. Orlean(3), M.R. Patel(17), A. Pommerol(1), V. Rolloff(1†), L. Tornabene(18), S. Tulyakov(10), P. Wajer(3), J. Wray(20), and R. Ziethe(1\*).

(1)Physikalisches Inst., University of Bern, Sidlerstrasse 5, CH-3012 Bern, Switzerland (nicolas.thomas@space.unibe.ch), (2)Osservatorio Astronomico di Padova, INAF, Padova, Italy, (3)Space Research Center, Polish Academy of Science, Warsaw, Poland, (4)University of Leicester, Leicester, UK, (5)Lunar and Planetary Laboratory, Tucson AZ, USA, (6)CNR-IFN UOS Padova, Italy, (7)Centro Interdipartimentale di Studi e Attività Spaziali, Padova, Italy, (8)Deutsches Zentrum für Luft- und Raumfahrt, Institut für Planetenforschung, Berlin, Germany, (9)Planetary Science Institute, St. George, Utah, USA, (10)École polytechnique fédérale de Lausanne, Lausanne, Switzerland, (11)USGS, Astrogeology Science Center, Flagstaff AZ, USA, (12)Vernadsky Inst. of Geochemistry and Analytical Chemistry of Russian Academy of Science, Moscow, Russia, (13)Université de Nantes, Nantes, France, (14)IRSPS - Università "G.D'Annunzio", Pescara, Italy, (15)Max-Planck-Institut für Sonnensystemforschung, Göttingen, Germany, (16)Dep.Geosciences, University of Padova, Padova, Italy, (17)Open University, Milton Keynes, UK, (18) Centre for Planetary Science & Exploration (CPSX), Western University, London, ON, Canada, (19) LASP, University of Colorado in Boulder, Boulder CO-80303, USA, (20) Georgia Inst. of Technology, School of Earth and Atmospheric Sciences, Atlanta GA, USA. \*Now at Micro-Cameras and Space Exploration, Neuchatel, Switzerland.

### Abstract

CaSSIS (Colour and Stereo Surface Imaging System) is the main imaging system for the ExoMars Trace Gas Orbiter (TGO) mission. The instrument was completed in October 2015 and launched in March 2016 [1]. This abstract describes the current status of CaSSIS and provides a first assessment of its observations from the start of the primary science mission.

### 1. Introduction

The objectives of CaSSIS are to (1) characterize sites which have been identified as potential sources of trace gases, (2) investigate dynamic surface processes (e.g. sublimation, erosional processes, volcanism) which may help to constrain the atmospheric gas inventory, and (3) certify potential future landing sites by characterizing local (down to ~10 m) slopes.

The technical aims foreseen were to (1) acquire imaging observations at a scale of <5 m/px, (2) produce images in 4 broad-band colours optimized for Mars photometry, (3) acquire a swath width >8 km, and (4) obtain quasi-simultaneous stereo pairs over the full swath width for high res. digital terrain models. These, combined with programmatic constraints, drove the design. The concept was discussed at EPSC in 2014 [1]. A full instrument description has been provided [2]. Details on the on-ground calibration of the instrument are provided in [3]. Spectral-image simulations to assess the colour and spatial capabilities of the instrument are shown in [4]. The full payload is described in [5].

CaSSIS was first switched-on on 7 April 2016 just over 3 weeks after launch and the first images of Mars in the Mars Capture Orbit (MCO) were acquired on 22 November 2016. CaSSIS was switched off during the aerobraking phase but rebooted on 20 March 2018. A flight software update was completed and transition to nominal imaging was made in April 2018. This paper will report on the latest imaging and show examples.

### 2. Observations

CaSSIS can acquire up to 3 compressed images per orbit. The number of images is controlled by the total data volume allocation and the time needed to compress. The time of passage of the spacecraft over the nightside is usually used to compress. The lossless compression gives a typical compression of 1.75:1. In the early phase of the mission, the data volume is such that high compression ratios (CR) are not normally needed and CR values of 3 are usual producing very high quality data. At times of very high data volume, raw uncompressed data can be obtained which may also be useful for calibration purposes.

In a typical one-week cycle at high data rate, CaSSIS will acquire around 100 targets. In our current observing plans, roughly half are acquired in stereo. The instrument has experienced some glitches such that imaging has not been continuous in the first weeks but the situation has been improving as more experience has been gained with commanding and control. At the time of writing, roughly 75% of the images are being acquired as planned. A further

flight software update is expected to resolve several of the outstanding issues.



Figure 1: Image of the rim of Korolev crater produced by combining the RED, PAN, and BLU channels of the CaSSIS image.

The image of the rim of Korolev crater (Figure 1) shows an example from the first medium term plan (MTP001). The image is a colour-composite using the RED, PAN, and BLU channels and was produced using ISIS3 and SPICE kernels that have now been optimized to account for instrument distortion and the telescope rotation mechanism. It is expected that production of these types of products will shortly become routine. Further improvement in the flat-field and bias subtraction are also to be expected.

Image acquisitions so far have been of a wide variety of target, although southern polar targets have been taken more frequently because of the current  $L_s$  (start of southern spring). Targets thus far have included layering in Terby crater (Figure 2), exposed layers in Hebes Chasma, dune fields in Herschel crater, and exposed bedrock in the southern highlands. Under clear conditions, the images acquired at 4.5 m/px are sharp and provide good contrast in PAN, RED and NIR. As expected the data in the BLU channel have the lowest signal to noise (SNR) but nonetheless provide good data. Binning of the BLU to 2x2 may become a standard mode for future observations to ensure good SNR.

The stereo pairs acquired so far have been reasonably well aligned despite the image timing not being finalized at this stage. Results from these first stereo acquisitions will be reported elsewhere.

### 3. Summary and Conclusions

The CaSSIS images under reasonable illumination conditions are of high quality. Both the colour and stereo capabilities of CaSSIS have been demonstrated in the initial phase. We expect CaSSIS to play an important role in investigations of surface properties over the coming years.

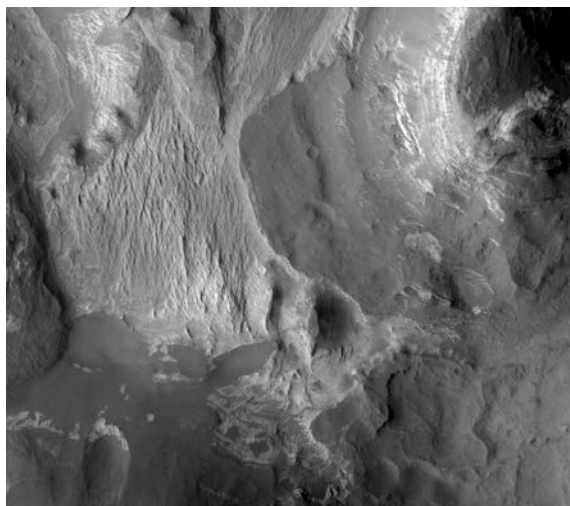


Figure 2: RED channel image of a part of Terby crater.

### Acknowledgements

The authors wish to thank the spacecraft and instrument engineering teams for the successful completion and operation of the instrument. CaSSIS is a project of the University of Bern and funded through the Swiss Space Office via ESA's PRODEX programme. The instrument hardware development was also supported by the Italian Space Agency (ASI) (ASI-INAF agreement no.I/018/12/0), INAF/Astronomical Observatory of Padova, and the Space Research Center (CBK) in Warsaw. Support from SGF (Budapest), the University of Arizona (Lunar and Planetary Lab.) and NASA are also gratefully acknowledged.

### References

- [1] Thomas, N. et al. (2014), The Colour and Stereo Surface Imaging System (CaSSIS) for ESA's Trace Gas Orbiter, EPSC abstract Vol. 9, id. EPSC2014-100.
- [2] Thomas, N. et al. (2017) Space Sci. Rev., 212, 1897
- [3] Roloff, V. et al. (2017) Space Sci. Rev., 212, 1871.
- [4] Tornabene, L.L. et al. (2018) Space Sci. Rev., 214, 18.
- [5] Vago, J., et al. (2015), ESA ExoMars program: The next step in exploring Mars, Solar System Research, 49, 518-528.

# CaSSIS – Targeting, Operations, and Data Reduction

N. Thomas(1), G. Cremonese(2), M. Almeida(1), J. Backer(3), P. Becerra(1), G. Borrini(1), S. Byrne(4), M. Gruber(1), P. Gubler(1), R. Heyd(4), A. Ivanov(5), L. Keszthelyi (3), C. Marriner(6), G. McArthur(4), A.S. McEwen(4), C. Okubo(3), M.R. Patel(6), A. Pommerol(1), C. Re(2), C. Schaller(4), S. Scheidt(4), E. Simioni(2), S. Sutton(4), S. Tulyakov(5), and C. Zimmermann(1).

(1)Physikalisches Inst., University of Bern, Sidlerstrasse 5, CH-3012 Bern, Switzerland (nicolas.thomas@space.unibe.ch), (2) Osservatorio Astronomico di Padova, INAF, Padova, Italy, (3)USGS, Astrogeology Science Center, Flagstaff AZ, US, (4)Lunar and Planetary Laboratory, Tucson AZ, USA, (5)École polytechnique fédérale de Lausanne, Lausanne, Switzerland, (6)Open University, Milton Keynes, UK.

## Abstract

CaSSIS (Colour and Stereo Surface Imaging System) is the main imaging system for the ExoMars Trace Gas Orbiter (TGO) mission. A scientifically compelling instrument was completed in October 2015 and launched in March 2016 [1]. This abstract describes the targeting, operations, and data reduction pipelines used to produce calibrated observations of selected targets.

## 1. Introduction

The scientific objectives of CaSSIS are to (1) characterize sites which have been identified as potential sources of trace gases, (2) investigate dynamic surface processes (e.g. sublimation, erosional processes, volcanism) which may help to constrain the atmospheric gas inventory, and (3) certify potential future landing sites by characterizing local (down to ~10 m) slopes.

The technical aims foreseen were to (1) acquire imaging observations at a scale of <5 m/px, (2) produce images in 4 broad-band colours optimized for Mars photometry, (3) acquire a swath width >8 km, and (4) obtain quasi-simultaneous stereo pairs over the full swath width for high res. digital terrain models. These technical aims combined with programmatic constraints drove the design.

The spacecraft has been in its primary science orbit since March 2016 and recently entered the primary science phase. CaSSIS uses planning tools based on the highly successful planning approach of HiRISE [2]. The elements specific to CaSSIS are covered by a set of IDL programs designed to generate the commands needed by the Science Operations Centre (SOC) in Madrid and the Mission Operations Centre (MOC) in Darmstadt. The data returned is then passed to an IDL pipeline for telemetry conversion and reduction. The output is in a pseudo PDS4

format (XML plus binary data files) that can be read into the ISIS software environment to produce mosaics and colour products. We describe here briefly the key elements of the operations.

## 2. Uplink Tools

The first step is time-independent target suggestions using the CaSSIS targeting tool (CaST), which is derived from HiWISH (<https://www.uahirise.org/hiwish/>). The detailed targeting tools are based around a GUI called PLAN-C – a derivative of the HiRISE tool, HiPLAN, in turn built on JMARS (<https://jmars.asu.edu/>). PLAN-C is seen as a layer within the JMARS environment and hence the user targeting CaSSIS has full access to the different layers available in JMARS for viewing maps and specific properties of the Martian surface. The user imports a state file that describes the orbit of TGO. The state file refers to planning SPICE kernels prepared in advance by the SOC. The user can then place targets along the orbit for CaSSIS to acquire. This is supported by a target database from CaST. The database can be imported as a separate layer into the JMARS environment and interacts with PLAN-C to support accurate targeting of interesting areas. PLAN-C also allows the setting of CaSSIS instrument parameters through a sub-element called the COGG. In this element, the filters may be chosen, the number of exposures in the sequence can be set, and the data compression selected. The result is a CaSSIS Target File (CTF) that has one line per image (a stereo pair produces two lines in the CTF).

Once the CTF has been produced, the file can be passed to an IDL code called C\_CTF2ITL. This produces the instrument timeline file (ITL) that the SOC needs to generate the spacecraft command files for all instruments on TGO. C\_CTF2ITL performs detailed error checking and ensures that data volume limits at bottlenecks within the instrument are not exceeded. The user can also program in instrument

reboots and other activities from the command line. The code automatically sets the timings of the commands within the timeline, opens and closes files in the spacecraft payload data handling unit (PDHU), and tracks the final data volume which is an input to the SOC.

### 3. Operations Monitoring and the Ground Reference Model

During execution and when the spacecraft is in ground contact, CaSSIS can be monitored through housekeeping telemetry (HK) transmitted on the 1553 bus. The HK is read semi-automatically from Darmstadt and is passed to an Influx database to which a Grafana interface has been written.

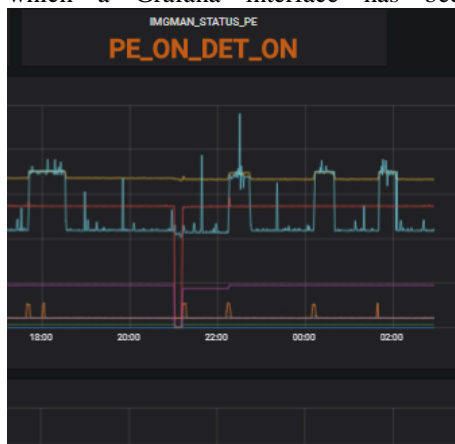


Figure 1: Part of the Grafana HK monitoring interface showing a system reboot (at 21:00) and image acquisitions increasing the current on the digital processor's 3.3 V line (in cyan).

The time available to build CaSSIS was extremely short and test time was reduced to a minimum to maintain the spacecraft schedule. The instrument has occasionally gone into safe mode during operations for reasons that might have been at first unclear. The Ground Reference Model (GRM) has been used to debug the system in these cases supported by the telemetry monitor.

### 4. Calibration Pipeline

Once the acquired data has been transferred from the MOC, it is passed to a calibration pipeline. This pipeline extracts the science telemetry packets and converts the data into a pseudo-PDS V4 format (binary data files with XML header information)

which is then passed to the radiometric calibration element of the pipeline. The conversion is performed on a framelet basis and is directly into reflectance (I/F). Preliminary studies (J. Fernando, pers. comm.) suggest good agreement with other instruments based on analysis of Phobos observations. The XML headers are also filled with geometry information. This information is based on SPICE kernels from the SOC. The orientation of the telescope is also required. C\_CTF2ITL generates the input for a C-kernel (produced using the SPICE toolkit) and this kernel can then be added to the SPICE kernel library to determine the pointing of CaSSIS. This allows the production of simple browse images (no instrument geometric distortion correction) of reasonable quality at a very early stage for validation purposes.

### 5. Geometry Processing – ISIS3 and DTM production

After completion of the radiometric calibration, the data can be assembled into mosaics. The SPICE I and F kernels have recently been improved. ISIS3 (<https://isis.astrogeology.usgs.gov/>) importers for CaSSIS data files have been written and tested. Export will be into a PDS4 compatible format. Tests with ISIS3 suggest that routine production of mosaiked products should be reasonably straightforward in this environment. Final product definition is being agreed at the time of writing.

The generation of digital terrain models (DTM) will be performed by individual institutes on a best effort basis. However, significant progress has been made (see elsewhere in this conference).

### Acknowledgements

The authors wish to thank the spacecraft and instrument engineering teams for the successful completion and operation of the instrument. CaSSIS is a project of the University of Bern and funded through the Swiss Space Office via ESA's PRODEX programme. The instrument hardware development was also supported by the Italian Space Agency (ASI) (ASI-INAF agreement no.I/018/12/0), INAF/Astronomical Observatory of Padova, and the Space Research Center (CBK) in Warsaw. Support from SGF (Budapest), the University of Arizona (Lunar and Planetary Lab.) and NASA are also gratefully acknowledged.

### References

- [1] Thomas, N. et al. (2017) Space Sci. Rev., 212, 1897
- [2] McEwen, A. et al. (2010), Icarus 205, 2.

# Mars INteractive Exploration based on Reconstruction and Visual Analysis: The MINERVA Concept

Gerhard Paar, Piluca Caballo (1), Christoph Traxler, Harald Piringer (2), Gerhard Triebnig, Fabian Schindler (3)

(1) JOANNEUM RESEARCH (JR), AT (gerhard.paar@joanneum.at); (2) VRVis Zentrum für Virtual Reality und Visualisierung Forschungs-GmbH, AT; (3) EOX IT Services GmbH, AT

## Abstract

MINERVA is a 3D GIS currently under development by JR, VRVis and EOX for a collaborative, holistic planetary science data infrastructure to allow members of different instrument teams to cooperate synergistically in virtual workspaces by sharing observation information, analysing and annotating the data. MINERVA is implementing a novel framework of interoperable and collaborative components based on an interactive 3D Viewer with GIS functionality, a database that maintains the knowledge about spatiotemporal data products, and a visual analytics platform that will help find new interconnections between the data coming from different instruments to discover new modes of scientific exploitation. MINERVA will be usable for the ExoMars Rover Mission (to be launched in 2020), which provides a heterogeneous set of scientific data captured by different instruments from the surface of the Red Planet. We will present the MINERVA concept, discuss various use cases and give selected details on representative ExoMars workflows and available & envisaged technical solutions.

## 1. MINERVA Scope

The ExoMars 2020 mission will provide a heterogeneous set of data from different instruments captured on the surface of Mars [1]. Imagery for science target selection, navigation, or close-up detailed visual analysis for geology, complemented by multi-spectral imagery from orbiters will be supplemented with georeferenced sensor data such as from the WISDOM ground penetrating radar instrument, looking into the Mars subsurface. The Analytic Laboratory Drawer inside the Rover body punctually observes samples acquired by a drill. A comprehensive and efficient analysis of this wealth of heterogeneous science data demands a sophisticated workflow that takes account for the heterogeneity of data and allows an overview of interconnections between different data entities.

Based on the instrument data and PDS4 archiving interfaces being established in the respective ROCC-to-Instrument ICDs<sup>1</sup>, concepts are required for the support of a holistic analysis of all the versatile scientific data from the entire rover mission. The MINERVA goal is to provide for the first time an integrative, holistic and analytic support for planetary scientists. This will not merely make the analysis more efficient but the tight integration of heterogeneous analysis methods in real time will allow insights, which would be hard or impossible to obtain using isolated methods. A major challenge is imposed by the huge & heterogeneous data volume. New interactive visualization methods based on, e.g., semantic annotations, meta-information and data modalities will be investigated. Beside the science claim in the mission itself, MINERVA will focus on the holistic workflow and on specific ExoMars requirements and the exploitation of the scheme for future missions and terrestrial applications.

## 2. MINERVA Components

The MINERVA prototype (Figure 1) will consist of three tightly integrated components:

- 1) A data base for scientific data products that also maintains analysis results [2]
- 2) A 3D Visualization Engine (PRo3D) [3] to navigate through 3D Mars surface reconstructions for extensive geological/morphologic interpretation [5] using a variety of interactive measurement tools. PRo3D offers important GIS functionalities such as orthographic view, superimposed rover tracks and data locations.
- 3) A non-spatial visualization component [4] for in-depth investigation of data, to discover relations, properties and coherencies otherwise hidden.

---

<sup>1</sup> ROCC...Rover Operations Control Centre;  
ICD...Interface Control Document

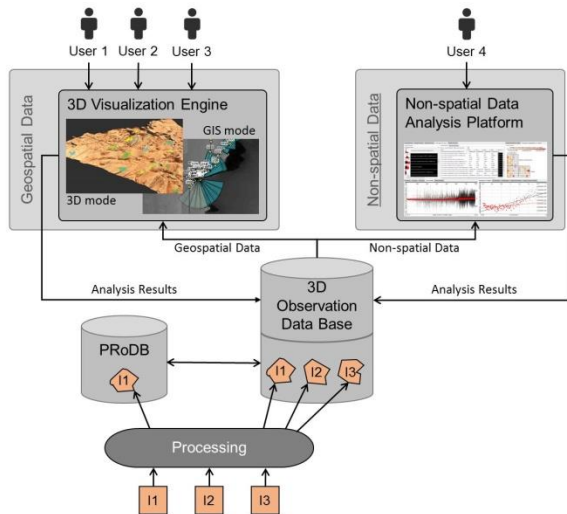


Figure 1: The Instrument Teams (I1...I3) use generic (PDS4) importer tools to ingest mission data into the 3D Observation Data Base. It is available to PRo3D with integrated GIS functionality, and the Non-spatial Data Analysis Platform. Users can share locations & observations and launch visual analysis of different instrument data at the same time.

### 3. MINERVA Use Cases

MINERVA will offer the users the opportunity to visualize, analyze, and annotate the mission data in a spatiotemporal context and in the context of other meta-information from the scientific measurements<sup>2</sup>:

- Support scientists in geo-referencing of scientific products (e.g. spectra) for the characterization of regions and the identification of their boundaries.
- To enable holistic overviews and correlations of product cues from multiple heterogeneous instruments. The scientists will be able to enrich the database by the output of interactive or semi-automatic tools for scientific assessment.
- Measure / annotate on 3D surfaces on PRo3D. Measurements/annotations are available in a data base and can be accessed by other users in PRo3D.
- Multi user handling to give different users different rights for loading and manipulating “session profiles” to support teams of scientists to exchange data e.g. on the same outcrops.

<sup>2</sup> The list is only a subset from many more. Further instrument collaboration use cases are being discussed with ExoMars instrument teams in workshops and direct communication.

- Search for spatial and temporal correlations in laboratory instruments data (spectrometers etc.).
- Get spatial overview of products’ locations having certain characteristics (e.g., a spectrum with a certain shape) and/or particular meta-information, e.g. rover orientations, focal length.
- Gain an overview of distribution of products by time / rover orientation / etc.
- Simultaneous inspection of ensembles of spectra / images. This may include a characterization of the overall dispersion, a pairwise comparison of particular products, and the clustering of products by their characteristics (e.g., the shape of their spectrum)
- Bidirectional relation of product locations to corresponding product characteristics, e.g., identify spectral bands with high values / strong variation / etc. within a region; identify potentially non-contiguous regions where objects have certain characteristics; inspect interpolated spectra between samples.

### References

- [1] Vago, J. L., Westall, F., Coates, A. J., Jaumann, R., Korabely, O., Ciarletti, V., ... & Rull, F. (2017). Habitability on early Mars and the search for biosignatures with the ExoMars Rover. *Astrobiology*, 17(6-7), 471-510.
- [2] Meissl, S., & Triebnig, G. (2010). Land Monitoring Network Services based on international geospatial standards: SOSI and geoland2/SDI Projects. *International Journal of Digital Earth*, 3(S1), 70-84.
- [3] Barnes, R., Gupta, S., Gunn, M., Paar, G., Huber, B., Bauer, A., ... & Ortner, T. (2017, March). Application of PRo3D to Quantitative Analysis of Stereo-Imagery Collected During the Mars Utah Rover Field Investigation (MURFI) Analogue Rover Trials. In *Lunar and Planetary Science Conference (Vol. 48)*.
- [4] Piringer, H., Tominski, C., Muigg, P., & Berger, W. (2009). A multi-threading architecture to support interactive visual exploration. *IEEE Transactions on Visualization and Computer Graphics*, 15(6), 1113-1120.
- [5] Balme, M., Robson, E., Barnes, R., Butcher, F., Fawdon, P., Huber, B., ... & Gupta, S. (2017). Surface-based 3D measurements of small aeolian bedforms on Mars and implications for estimating ExoMars rover traversability hazards. *Planetary and Space Science*.

### Acknowledgements

MINERVA is receiving funding from the Austrian Space Applications Programme (ASAP14) funded by BMVIT. JR, VRV is and EOX co-finance the activity.

## Spectral clustering applied on the ExoMars/CaSSIS simulated imagery dataset

**Maurizio Pajola** (1), Livio L. Tornabene (2), Frank P. Seelos (3), Giuseppe A. Marzo (4), Alice Lucchetti (1), Gabriele Cremonese (1), Antoine Pommerol (5), Patricio Becerra (5) and Nicholas Thomas (5)

(1) INAF, Osservatorio Astronomico di Padova, Vicolo dell'Osservatorio 5, 35122, Padova, Italy (maurizio.pajola@oapd.inaf.it), (2) Centre for Planetary Science and Exploration/Department of Earth Sciences, University of Western Ontario, London, Ontario N6A5B7, Canada, (3) Johns Hopkins University Applied Physics Laboratory, Laurel, MD, USA, (4) ENEA C. R. Casaccia, 00123, Roma, Italy, (5) Physikalisches Institut, University of Bern, Sidlerstr. 5, 3012 Bern, Switzerland

### Abstract

The Colour and Stereo Surface Imaging System (CaSSIS, [1]) is the scientific camera onboard the ExoMars Trace Gas Orbiter spacecraft. This instrument has three main aims: 1) to characterize possible surface/subsurface sources for methane and other trace gases, 2) to investigate dynamic surface processes that may contribute to atmospheric gases, and 3) to certify and characterize safety and hazards such as rocks and slopes, associated with candidate landing sites for ExoMars 2020 and other future surface missions [1]. To accomplish such goals, CaSSIS couples stereo topography and color observations with a spatial resolution of 4.6 m. The instrument has a suite of four filters (band 1 centered at 0.499  $\mu\text{m}$ , band 2 at 0.675  $\mu\text{m}$ , band 3 at 0.836  $\mu\text{m}$  and band 4 at 0.937  $\mu\text{m}$ ) that provides the means to discern the variations in the oxidation state of iron-bearing minerals and phases ( $\text{Fe}^{2+}$ ,  $\text{Fe}^{3+}$ ) [2].

Since its arrival at Mars on October 2016, the ExoMars spacecraft underwent an 18 months-long aerobraking phase that ended in April 2018. During this period, a CaSSIS-simulated imagery dataset was prepared and published [2] to fully assess both the colour capabilities and potential for spectral measurements of the instrument once the nominal mission begins (first weeks of May 2018). This dataset is characterized by two types of simulated products: the first is a partial simulated colour product (181 cubes) that provides the spectral bands of CaSSIS by convolving the VNIR spectral information obtained by the CRISM instrument [3] with the CaSSIS instrument response functions. These products maintain the spatial scale of the CRISM input cubes, i.e. 18-36 m/pixel (hence the "partial" designation). The second type are fully simulated products (33 cubes), produced by merging

the partial simulated colour cubes with a 32-bit radiometrically calibrated I/F panchromatic image from CTX [4] that is oversampled from 5-6 m/pixel to the nominal pixel-resolution of CaSSIS (4.6 m). As such, the fully simulated CaSSIS cube provides both the simulated colours and the spatial scales of an unbinned CaSSIS cube.

For this specific work, we decided to exploit some of the fully simulated colour products that cover the three final proposed landing sites for the NASA Mars 2020 rover (Jezero crater, N-E Syrtis and Columbia Hills) and the two finalists for the ExoMars 2020 rover (Oxia Planum and Mawrth Vallis). We focus on these targets to support the characterisation of landing sites (goal no. 3 in [1]). Moreover, these areas will be repeatedly observed by CaSSIS soon (targeting mode anticipated for late summer 2018) to see if any color and/or morphological changes may occur before the rover landings; hence, we provide high spatial scale analyses of simulations to expedite analysis of the actual CaSSIS data and provide pre-landing context.

We used the unsupervised K-means partitioning algorithm developed by [5] to investigate the spectral variability across the areas selected. This technique has been extensively validated using different spectral data sets on different areas of Mars [5-7], Mercury [8], Iapetus [9,10], Phobos [11] and Charon [12]. The statistical partitioning identifies different clusters on the study areas, based on the different exposed mineralogical signatures (see for example the Jezero crater case, Fig. 1). Each resulting cluster is characterized by its average and associated standard deviation. In addition, the geographical information of each spectrum is maintained in the process, hence the resulting clusters can be located on the studied surface and correlations with

geographical features can be investigated.

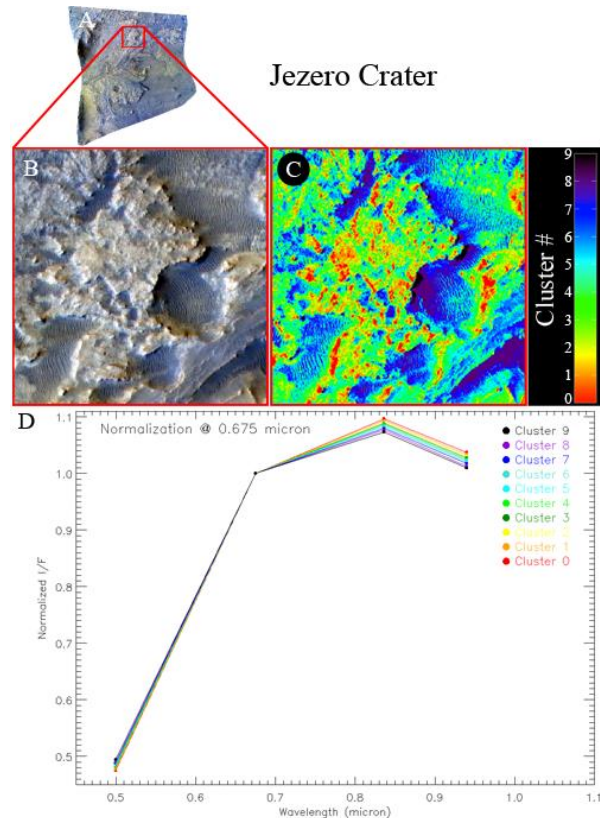


Fig. 1: A) Context image of the Jezero delta. This is one of the full simulated products called *cassis\_sim\_c\_05c5e\_x\_002387\_1987\_corr\_if\_nn\_4band\_composite*. B) The location on the Jezero delta where we applied the spectral clustering. C) The 10 clusters identified on the surface. D) The spectra of all clusters identified in C.

To highlight the different absorption strengths observable from the ferrous ( $\text{Fe}^{2+}$ ) or ferric ( $\text{Fe}^{3+}$ ) iron spectra, we normalized all spectra at 0.675  $\mu\text{m}$  (band 2). In this way, it is possible to highlight the inverse relationship between the behaviours of bands 3, 4 and band 1, i.e. in general, a deeper absorption at band 4 equates to a shallower absorption at band 1, and it appears to be sensitive to the presence of ferrous (or mafic) compositions, while the opposite is true for ferric altered compositions. This spectral trend is what we observe in our example on the Jezero delta (Fig. 1). A careful analysis shows that variations in the band 1 and 3,4 absorptions are not only related to the exposure of ferric and ferrous materials but also due to the physical mixing of these Fe-bearing components. Surface dust, which bears ferric Fe, also contributes to a band 1 absorption.

Mixing can be readily identified in our analyses as concentric gradients between spectral clusters. Deeper band 1 and shallower band 4 absorptions correlate with the inverted fan deposits (clusters 0 to 4); while clusters 5 to 8 are mainly related to basaltic mobilized material in the form of aeolian bedforms preferentially trapped in low-lying topographic areas. Cluster 9 is associated with the shadowed regions.

The simulated CaSSIS cubes provide spectral clusters at an unprecedented scale and coverage (e.g., aeolian bedforms are well resolved, so these products could be used for engineering constraints such as rover traverse ability). Similar spectral trends are observed on all five landing sites. Therefore, this analysis shows that when the spectral clustering technique is applied on the first CaSSIS color cubes, it will be an important tool to help distinguish different mineralogical deposits on Mars.

## Acknowledgements

The authors wish to thank the spacecraft and instrument engineering teams for the successful completion of the instrument. CaSSIS is a project of the University of Bern and funded through the Swiss Space Office via ESA's PRODEX programme. The instrument hardware development was also supported by the Italian Space Agency (ASI) (ASI-INAF agreement no.I/018/12/0), INAF/Astronomical Observatory of Padova, and the Space Research Center (CBK) in Warsaw. Support from SGF (Budapest), the University of Arizona (Lunar and Planetary Lab.) and NASA are also gratefully acknowledged.

## References

- [1] Thomas, N. et al., 2017. *Space Sci. Rev.* 212, 1897–1944.
- [2] Tornabene, L.L. et al., 2018. *Space Sci. Rev.* 214, 18.
- [3] Murchie, S. et al. 2007. *J. Geophys. Res., Planets* 112(E5), E05S03.
- [4] Malin, M.C., et al. 2007. *J. Geophys. Res.* 112, E05S04 (2007)
- [5] Marzo, G., et al., 2006. *J. Geophys. Res.* 111. E03002.
- [6] Marzo, G., et al., 2008. *J. Geophys. Res.* 113. E12009.
- [7] Fonti, S., Marzo, G.A., 2010. *Astron. Astrophys.* 512 (A51), 6 pp.
- [8] Lucchetti, et al., 2017. *48 Lunar and Planetary Science Conference*, 1964.
- [9] Pinilla-Alonso, N., et al., 2011. *Icarus* 215 (1), 75.
- [10] Dalle Ore, C., et al., 2012. *Icarus* 221 (2), 735.
- [11] Pajola, M. et al., 2018. *Planet. Space Sci.* 154, 63-71.
- [12] Dalle Ore, C., et al., 2018. *Icarus* 300, 21–32.

## The PanCam instrument for the ExoMars 2020 rover

**Andrew Coates** (1) for the ExoMars 2020 PanCam team(\*)  
(1) Mullard Space Science Laboratory, UCL, UK (a.coates@ucl.ac.uk)

### Abstract

The scientific objectives of the ExoMars rover are designed to answer several key questions in the search for life on Mars. In particular, the unique subsurface drill will address some of these questions for the first time, such as the possible existence and stability of sub-surface organics. PanCam will establish the surface geological and morphological context for the mission, working in collaboration with other context instruments. Here, we describe the PanCam scientific objectives in geology, atmospheric science and 3D vision. We discuss the design of PanCam, which includes a stereo pair of Wide Angle Cameras (WACs), each of which has an 11 position filter wheel, and a High Resolution Camera (HRC) for high resolution investigations of rock texture at a distance. The cameras and electronics are housed in an optical bench that provides the mechanical interface to the rover mast and a planetary protection barrier. The electronic interface is via the PanCam Interface Unit (PIU), and power conditioning is via a DC-DC converter. PanCam also includes a calibration target mounted on the rover deck for radiometric calibration, fiducial markers for geometric calibration and a rover inspection mirror.

\* A.J. Coates,<sup>1,2</sup> R. Jaumann,<sup>3</sup> A.D. Griffiths,<sup>1,2</sup> M. Carter,<sup>1,2</sup> C.E. Leff,<sup>1,2</sup> N. Schmitz,<sup>3</sup> J.-L. Josset,<sup>4</sup> G. Paar,<sup>5</sup> M. Gunn,<sup>6</sup> E. Hauber,<sup>3</sup> C.R. Cousins,<sup>7</sup> R.E. Cross,<sup>6</sup> P. Grindrod,<sup>2,8,15</sup> J.C. Bridges,<sup>9</sup> M. Balme,<sup>10</sup> S. Gupta,<sup>11</sup> I.A. Crawford,<sup>2,8</sup> P. Irwin,<sup>12</sup> R. Stabbins,<sup>1,2</sup> D. Tirsch,<sup>3</sup> J.L. Vago,<sup>13</sup> M. Caballo-Perucha,<sup>5</sup> G.R. Osinski,<sup>14</sup> and the PanCam Team

<sup>1</sup>Mullard Space Science Laboratory, University College London, Dorking, UK ([a.coates@ucl.ac.uk](mailto:a.coates@ucl.ac.uk))

<sup>2</sup>Centre for Planetary Science at UCL/Birkbeck, London, UK.

<sup>3</sup>Institute of Planetary Research, German Aerospace Centre (DLR), Berlin, Germany.

<sup>4</sup>Space Exploration Institute, Neuchâtel, Switzerland.

<sup>5</sup>Joanneum Research, Graz, Austria.

<sup>6</sup>Department of Physics, Aberystwyth University, Aberystwyth, UK.

<sup>7</sup>Department of Earth & Environmental Sciences, University of St Andrews, St Andrews, UK.

<sup>8</sup>Department of Earth and Planetary Sciences, Birkbeck, University of London, London, UK.

<sup>9</sup>Space Research Centre, University of Leicester, Leicester, UK.

<sup>10</sup>Department of Earth Sciences, Open University, Milton Keynes, UK.

<sup>11</sup>Department of Earth Science and Engineering, Imperial College London, UK.

<sup>12</sup>Department of Physics, University of Oxford, Oxford, UK.

<sup>13</sup>European Space Agency, Noordwijk, the Netherlands.

<sup>14</sup>Centre for Planetary Science & Exploration, U. Western Ontario, London, Canada

<sup>15</sup>Now at Natural History Museum, London, UK

# NOMAD on ExoMars Trace Gas Orbiter: status and preliminary results

**Ann C. Vandaele.** (1), Jose-Juan Lopez-Moreno (2), Giancarlo Bellucci (3), Manish R. Patel (4), Frank Daerden (1), Ian R. Thomas (1), Eddy Neefs (1), Bojan Ristic (1), Sophie Berkenbosch (1), Bram Beeckman (1), Roland Clairquin (1), Claudio Queirolo (1) and the NOMAD Team

(1) Royal Belgian Institute for Space Aeronomy (IASB-BIRA), av. Circulaire 3, 1180 Brussels, Belgium, (2) Instituto de Astrofísica de Andalucía (IAA/CSIC), Granada, Spain, (3) Istituto di Astrofisica e Planetologia Spaziali (IAPS/INAF), Via del Fosso del Cavaliere, 00133 Rome, Italy, (4) School of Physical Sciences, The Open University, Milton Keynes, UK - Space Science and Technology Department, STFC Rutherford Appleton Laboratory, UK (a-c.vandaele@aeronomie.be)

## Abstract

The NOMAD (“Nadir and Occultation for MARS Discovery”) spectrometer suite on board the ExoMars Trace Gas Orbiter (TGO) has been designed to investigate the composition of Mars’ atmosphere, with a particular focus on trace gases, clouds and dust. The detection sensitivity for trace gases is considerably improved compared to previous Mars missions, compliant with the science objectives of the TGO mission. This will allow for a major leap in our knowledge and understanding of the Martian atmospheric composition and the related physical and chemical processes. The instrument is a combination of three spectrometers, covering a spectral range from the UV to the mid-IR, and can perform solar occultation, nadir and limb observations. In this paper, we will report on the status of the instrument, and present the first results obtained during the commissioning phase and then the Science phase which started in April 2018.

## 1. Introduction

NOMAD will conduct a spectroscopic survey of Mars’ atmosphere in ultraviolet (UV), visible and infrared (IR) wavelengths covering large parts of the 0.2-4.3  $\mu\text{m}$  spectral range [1,2]. NOMAD is composed of 3 spectrometers: a solar occultation only spectrometer (SO – Solar Occultation) operating in the infrared (2.3-4.3  $\mu\text{m}$ ), a second infrared spectrometer (2.3-3.8  $\mu\text{m}$ ) capable of doing nadir, but also solar occultation and limb observations (LNO – Limb Nadir and solar Occultation) [3], and an ultraviolet/visible spectrometer (UVIS – UV visible, 200-650 nm) that can work in the three observation modes [4].

NOMAD will provide vertical profiling information for atmospheric constituents at unprecedented spatial and temporal resolution. Indeed, in solar occultation, the vertical resolution is less than 1 km for SO and UVIS, with a sampling rate of 1 s (one measurement every 1 km), and occultations will range from the surface to 200 km altitude (height-dependent sensitivities for species will be presented in this paper). NOMAD will also provide mapping of several constituents in nadir mode with an instantaneous footprint of 0.5 x 17  $\text{km}^2$  (LNO spectrometer) and 5  $\text{km}^2$  (UVIS spectrometer) respectively, with a repetition rate of 30 Martian days. The TGO orbit will allow NOMAD to sample a wide range of local times, hence strongly improving existing climatologies for water vapour and carbon monoxide, and developing new climatologies for e.g. HDO and methane. By providing the best-to-date measurements of  $\text{H}_2\text{O}$  and, co-located and simultaneously, HDO, hence D/H, NOMAD will contribute significantly to improve our knowledge of the Martian water cycle and the hydrogen escape process, and as such to the long-term fate of the Martian atmosphere. A highly sensitive monitoring of the well mixed, moderately long-lived gas CO will allow NOMAD to provide better insights in important mixing processes related to trace gases that are enriched upon condensation of the main atmospheric constituent,  $\text{CO}_2$ . NOMAD will also allow for a highly sensitive diurnal monitoring of  $\text{CH}_4$  throughout 1 Martian year, allowing for the first time to assess and understand the presence or absence of this unstable organic trace gas, and in the case of confirmed presence, to provide constraints to its origin and fate.

## 2. Status of the instrument

The Mars commissioning phase started in early March 2018 just after the end of the aerobraking operations which placed the spacecraft in its final circular orbit around Mars. A series of observations were planned to assess the state of the instrument, including calibration observations and observations dedicated to test the thermal dissipation within the instrument. Observations were performed to verify the pointing accuracy. We will present some results of this analysis showing that the instrument is performing as expected.

## 3. Preliminary results

Science phase started in April 2018. Since then NOMAD performed solar occultation and nadir observations using different options to test the instrument under various conditions. Several atmospheric species have been targeted, delivering profiles from solar occultation from 200km down to the surface and integrated abundances from nadir measurements. Observations optimized for the detection of dust and clouds have also been performed. The nominal strategy for solar occultations consist in measuring 5 different spectral intervals within 1 s, to derive densities for CO<sub>2</sub>, CO, H<sub>2</sub>O/HDO, CH<sub>4</sub>, and dust. Nadir observations were carried out using different numbers of spectral intervals recorded sequentially to investigate the signal to noise ratio. These measurements also focused on the same species as mentioned above. We will give an overview of the results so far obtained.

## Acknowledgements

The NOMAD experiment is led by the Royal Belgian Institute for Space Aeronomy (IASB-BIRA), assisted by Co-PI teams from Spain (IAA-CSIC), Italy (INAF-IAPS), and the United Kingdom (Open University). This project acknowledges funding by the Belgian Science Policy Office (BELSPO), with the financial and contractual coordination by the ESA Prodex Office (PEA 4000103401, 4000121493), by Spanish Ministry of Economy, Industry and Competitiveness and by FEDER funds under grant ESP2015-65064-C2-1-P (MINECO/ FEDER), as well as by UK Space Agency through grant ST/P000886/1 and Italian Space Agency through grant 2018-2-HH.0. The research was performed as part of the “Excellence of Science” project

“Evolution and Tracers of Habitability on Mars and the Earth” (FNRS 30442502).

## The NOMAD Team

*Scientific team:* Vandaele, Ann Carine; Lopez Moreno, Jose Juan; Bellucci, Giancarlo; Patel, Manish; Allen, Mark; Alonso-Rodrigo, Gustavo; Altieri, Francesca; Aoki, Shohei; Bauduin, Sophie; Bolsée, David; Clancy, Todd; Cloutis, Edward; Daerden, Frank; D'Aversa, Emiliano; Depiesse, Cédric; Erwin, Justin; Fedorova, Anna; Formisano, Vittorio; Funke, Bernd; Fussen, Didier; Garcia-Comas, Maia; Geminale, Anna; Gérard, Jean-Claude; Gillotay, Didier; Giuranna, Marco; Gonzalez-Galindo, Francisco; Hewson, Will; Homes, James; Ignatiev, Nicolai; Kaminski, Jacek; Karatekin, Ozgur; Kasaba, Yasumasa; Lanciano, Orietta; Lefèvre, Franck; Lewis, Stephen; López-Puertas, Manuel; López-Valverde, Miguel; Mahieux, Arnaud; Mason, Jon; Mc Connell, Jack; Mumma, Mike; Nakagawa, Hiromu, Neary, Lori; Neefs, Eddy; Novak, R.; Oliva, Fabrizio; Piccialli, Arianna; Renotte, Etienne; Robert, Severine; Sindoni, Giuseppe; Smith, Mike; Stiepen, Arnaud; Thomas, Ian; Trokhimovskiy, Alexander; Trompet, Loïc; Vander Auwera, Jean; Villanueva, Geronimo; Viscardy, Sébastien; Whiteway, Jim; Willame, Yannick; Wilquet, Valérie; Wolff, Michael; Wolkenberg, Paulina – *Tech team:* Alonso-Rodrigo, Gustavo; Aparicio del Moral, Beatriz; Barzin, Pascal; Beeckman, Bram; BenMoussa, Ali; Berkenbosch, Sophie; Biondi, David; Bonnewijn, Sabrina; Candini, Gian Paolo; Clairquin, Roland; Cubas, Javier; Giordanengo, Boris; Gissot, Samuel; Gomez, Alejandro; Hathi, Brijen; Jeronimo Zafra, Jose; Leese, Mark; Maes, Jeroen; Mazy, Emmanuel; Mazzoli, Alexandra; Meseguer, Jose; Morales, Rafael; Orban, Anne; Pastor-Morales, M; Perez-grande, Isabel; Queirolo, Claudio; Ristic, Bojan; Rodriguez Gomez, Julio; Saggin, Bortolino; Samain, Valérie; Sanz Andres, Angel; Sanz, Rosario; Simar, Juan-Felipe; Thibert, Tanguy

## References

- [1] Vandaele, A.C., et al., 2015. *Planet. Space Sci.* 119, 233-249.
- [2] Vandaele et al., 2018. *Space Sci. Rev.*
- [3] Neefs et al., 2015. *Applied Optics* 54, 8494-8520.
- [4] Patel et al., 2017. *Applied Optics* 56, 2771-2782.

# Thermal structure and aerosol content in the martian atmosphere from ACS-TIRVIM on board ExoMars/TGO

Sandrine Guerlet (1), N. Ignatiev (2), T. Fouchet (3), F. Forget (1), E. Millour (1), R.M.B. Young (1), L. Montabone (1,4), A. V. Grigoriev (2) A. Trokhimovskiy (2) F. Montmessin (5) and O. Korablev (2).

(1) Laboratoire de Météorologie Dynamique (LMD), Paris, France (2) Space Research Institute (IKI), Moscow, Russia (3) LESIA, Observatoire de Paris, Meudon, France (4) Space Science Institute, Boulder, CO, USA (5) LATMOS, Guyancourt, France. (sandrine.guerlet@lmd.jussieu.fr)

## Abstract

The ExoMars Trace Gas Orbiter (TGO), a mission by ESA and Roscosmos, was launched in March 2016. After a long aerobraking phase, it reached its final, near-circular 400 km orbit in February, 2018 then started its operational scientific phase in March, 2018. On board TGO, the ACS-TIRVIM instrument has the capability to map the thermal structure of the Martian atmosphere and its aerosol load at a great variety of local times. In this abstract, we describe our retrieval algorithm used to analyse TIRVIM data. We discuss synthetic retrievals performed for a great variety of scenes to fine-tune and evaluate the performance of our algorithm, then briefly present results obtained from the first orbits of TGO. In a second step (see EPSC abstract by [3]), the climatology dataset obtained from TIRVIM will be assimilated into the LMD Mars General Circulation Model to improve our understanding of the Martian atmospheric system.

## 1. The ACS-TIRVIM instrument

The Atmospheric Chemistry Suite (ACS) is a set of three spectrometers including a thermal-infrared channel, TIRVIM [2]. It is primarily dedicated to monitoring the thermal structure and aerosol content in the Martian atmosphere by acquiring spectra in nadir geometry. ACS-TIRVIM is a Fourier-transform spectrometer covering the range 600–6000  $\text{cm}^{-1}$  (1.7–17  $\mu\text{m}$ ) with a spectral resolution of 1.2  $\text{cm}^{-1}$ . We focus here on the range 600–1300  $\text{cm}^{-1}$ , which covers absorption by  $\text{CO}_2$  (centered at 667  $\text{cm}^{-1}$ ), water ice clouds (centered at 820  $\text{cm}^{-1}$ ) and dust (centered at 1100  $\text{cm}^{-1}$ ). TIRVIM is similar to the Thermal Emission Spectrometer (TES) on board Mars Global Surveyor or the Planetary Fourier Spectrometer (PFS) on board Mars Express, also operating in nadir geometry. The advantage of the TIRVIM data set over previous instruments comes from the TGO orbit,

which was designed to sample a complete daily cycle every two months. Hence, TIRVIM has the capacity to uniquely study both the diurnal and seasonal variability of the thermal structure, dust and ice cloud opacity, while previous instruments mainly sample(d) the atmosphere at  $\sim$ midday and  $\sim$ midnight.

## 2. Retrieval algorithm

We have developed a line-by-line radiative transfer model coupled to a bayesian retrieval algorithm to retrieve vertical profiles of the temperature from  $\sim$ 5 to  $\sim$ 45 km, surface temperature, and integrated optical depth of dust and water ice clouds. Following the method of [1], a priori temperature profiles are built from the TIRVIM spectra themselves. As nadir-viewing spectra cannot constrain the dust vertical profile, we assume that it is well mixed and retrieve a scaling factor to an a priori profile. Surface emissivity is taken from previously-derived TES emissivity maps. This algorithm will be described in more detail in a future publication.

## 3. Synthetic retrievals

In order to evaluate the performance of our algorithm and identify challenging cases, we performed synthetic retrievals for a great diversity of scenes. To start with, we extracted the surface and atmospheric state of the Martian atmosphere from the Mars Climate Database (MCD) for various locations (sampling different elevations), seasons, local times and aerosol scenarios. For each of these scenes, we computed a synthetic TIRVIM spectrum and added realistic noise. We then run our retrieval algorithm, starting from the aforementioned a priori profiles that are independent of the MCD.

Overall, the retrieved temperature profiles are close to the “true” profiles used to compute synthetic spectra, with a typical error of 2-3 K. The main

challenges lie in the retrieval of the temperature in the first scale height above the surface and close to the uppermost level probed by the core of the CO<sub>2</sub> band at 667 cm<sup>-1</sup> (near the 1-Pa level). In these altitude ranges, the contribution functions are quite broad, leading to significant degeneracy of the inverse problem. As a consequence, we are able to retrieve the mean temperature in these altitude ranges, but not the slope of the temperature profile.

Regarding dust and water ice clouds, our algorithm performs well in retrieving their integrated opacity during daytime (~9am - ~5pm), even if the assumed vertical distribution of aerosols is very different from the “true” profiles used to generate synthetic spectra. However, there are special cases for which the TIRVIM nadir spectra are insensitive to changes in the aerosol load, which implies that we cannot retrieve aerosol opacity. This occurs when the temperature contrast between the surface and the atmospheric layer with strong aerosol opacity is low (typically in the morning and evening). Examples of synthetic spectra at different local times and aerosol content are shown in Figure 1 to illustrate this issue.

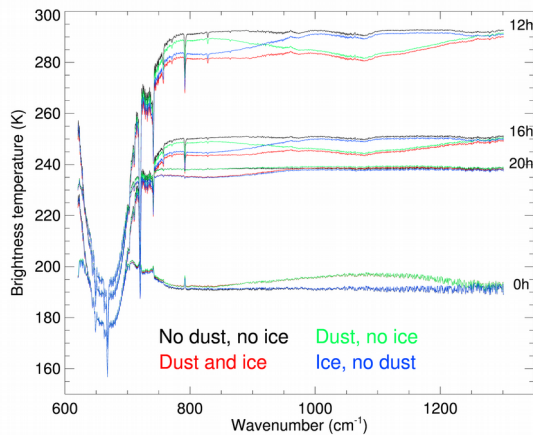


Figure 1: Examples of synthetic TIRVIM spectra computed at different local times, as labeled, with or without aerosol.

We highlight two special cases, for a given season and location: an example of a spectrum insensitive to cloud opacity (here at midnight) and an example of spectrum not sensitive to dust opacity (here at 20h).

#### 4. Application to ACS-TIRVIM

We have applied our algorithm to the TIRVIM data acquired during the two Mars Capture Orbits in November, 2016 and March, 2017. To validate the

retrieved temperature profiles, we searched for co-located measurements by the Mars Climate Sounder (MCS) on board Mars Reconnaissance Orbiter. This instrument operates in limb viewing geometry such that it measures the temperature with a much greater vertical resolution. It is however on a sun-synchronous orbit and acquires spectra only near 3am and 3pm. For these first TGO orbits, 6 ACS-TIRVIM data were colocated with MCS data, and the retrieved temperature profiles agreed well (typically within ~5K) except in one case (systematic difference of 10K). This work will be continued soon with the TIRVIM data acquired during the operational orbits, still being calibrated at IKI.

#### 5. Summary and Conclusions

We have developed a retrieval algorithm to analyse ACS-TIRVIM spectra acquired in nadir-viewing geometry. It is used to measure surface and atmospheric temperature (~5-45 km) as well as the integrated opacity of dust and water ice clouds. We have performed synthetic retrievals to evaluate its performance, identify challenging scenes and have applied it to TIRVIM data acquired during the Mars Capture Orbits. We validated the results using co-located MCS data. At the time of the EPSC meeting in September, we expect to have analyzed TIRVIM data acquired during the first few months of its operational phase and will discuss the results especially in term of the diurnal cycle of the temperature, aerosols, and comparisons with predictions from the LMD Mars GCM. Future efforts will focus on error characterization, a crucial aspect for upcoming data assimilation.

#### Acknowledgements

The ACS experiment is led by IKI in Moscow. We acknowledge support by CNES and Roscosmos.

#### References

- [1] Conrath, B. et al.: Mars Global Surveyor Thermal Emission Spectrometer (TES) observations: Atmospheric temperatures during aerobraking and science phasing, *Journal of Geophysical Research*, Vol. 105, Issue E4, p. 9509-9520, 2000.
- [2] Korablev, O. et al.: The Atmospheric Chemistry Suite (ACS) of Three Spectrometers for the ExoMars 2016 Trace Gas Orbiter, *Space Science Reviews*, Vol. 214, Issue 1, 2018.
- [3] Young, R. et al.: Preliminary assimilation of observations from ACS/TIRVIM on board ExoMars TGO into the LMD Mars GCM, EPSC 2018.

# Atmospheric model support for NOMAD on ExoMars/TGO

**Frank Daerden** (1), Lori Neary (1), Sébastien Viscardy (1), Justin Erwin (1), Séverine Robert (1), Shohei Aoki (1,13,14), Yannick Willame (1), Ann Carine Vandaele (1), Stephen Lewis (2), James Holmes (2), Paul Streeter (2), Manish Patel (2), Francisco González-Galindo (3), Miguel Angel Lopez-Valverde (3), José Juan Lopez-Moreno (3), Marco Giuranna (4), Giuseppe Sindoni (4), Francesca Altieri (4), Giancarlo Bellucci (4), Franck Lefèvre (5), Geronimo Villanueva (6), Michael J. Mumma (6), Michael D. Smith (6), Giuseppe Etiope (7, 4), James Whiteway (8), R. Todd Clancy (9), Michael J. Wolff (9), Robert E. Novak (10), Sophie Bauduin (11), Jacek W. Kaminski (12), Ian R. Thomas (1), Bojan Ristic (1), Cédric Depiesse (1), Jon Mason (2), and the NOMAD team.

(1) Royal Belgian Institute for Space Aeronomy BIRA-IASB, Brussels, Belgium, (2) Open University, Milton Keynes, UK, (3) Instituto de Astrofísica de Andalucía (IAA/CSIC), Granada, Spain, (4) Istituto di Astrofisica e Planetologia Spaziali (IAPS), Istituto Nazionale di Astrofisica (INAF), Rome, Italy, (5) LATMOS, Paris, France, (6) NASA Goddard Space Flight Center, Greenbelt, MD, USA, (7) Istituto Nazionale di Geofisica e Vulcanologia, Rome, Italy, (8) York University, Toronto, ON, Canada, (9) Space Science Institute, Boulder, CO, USA, (10) Iona College, New Rochelle NY, USA, (11) Université libre de Bruxelles, Belgium, (12) Institute of Geophysics, PAS, Atmospheric Physics, Warsaw, Poland, (13) Fonds National de la Recherche Scientifique, Belgium, (14) Tohoku University, Japan. ([Frank.Daerden@aeronomie.be](mailto:Frank.Daerden@aeronomie.be))

## Abstract

Mars atmospheric models have become increasingly important for the support of space missions to Mars and for the interpretation of the obtained observations. The NOMAD (“Nadir and Occultation for MArS Discovery”) spectrometer suite on board the ExoMars Trace Gas Orbiter (TGO) has been designed to investigate the composition of Mars’ atmosphere, with a particular focus on trace gases, clouds and dust, and started its science operations in April 2018. Within the NOMAD science team, a wealth of state-of-the-art models and related expertise has been incorporated to support and validate NOMAD in terms of (1) observation planning, (2) providing a priori for retrievals, (3) interpretation of observations and derivation of new science results, and (4) data assimilation. This abstract provides an overview of the modeling capability on the NOMAD science team and addresses how models can contribute to fulfill the main science objectives of the mission.

## 1. Introduction

The NOMAD team includes 3 of the most advanced Mars General Circulation Models (GCMs) to date: (1) the GEM-Mars model [1, 2], (2) the UK version of the LMD model [3, 4], and (3) the LMD model [3, 5]. Besides the parameterizations for atmospheric dynamics and physics, necessary to represent the atmospheric circulation and thermodynamic state, the applied GCMs uniquely contain modules for atmospheric chemistry, which is crucial to

understand and interpret the observations by NOMAD.

## 2. Planning of observations

The complexity of TGO’s operations, the observational constraints, and the specific capabilities of the various instruments and channels, impose a dedicated planning of observations for optimal science return. Atmospheric models can help in this planning by indicating which times, seasons and geolocations are of special interest, e.g. where current knowledge of atmospheric processes is known to be poor and requires specific observations. This may relate to the water cycle, photochemical cycles, dust storms etc. In the case of detection of special events, e.g. for methane, atmospheric models can provide new forecasts to support the mid-term observation planning.

## 3. A priori information for retrieval

At BIRA-IASB the GEM-Mars model has been applied to prepare atmospheric profiles to be used as a priori information in the retrieval algorithms. This work is presented in detail in an accompanying abstract at this conference by Erwin et al.

## 4. Interpretation of observations and new science results

TGO was designed to provide a refined search for atmospheric trace gases. Besides advancing the

detection limit for many species and creating inventories of them, the other main science objectives of TGO are (1) to understand the atmospheric processes that involve the detected trace gases, and (2) search for sources and sinks of the detected trace gases. This is where model support is vital, as it directly relates theoretical processes (reactions, sources, sinks, ...) to a 3D+time atmospheric state, that can be compared to the (sparse) set of observations. The differences between model and data provide direct insight in the plausibility of the imposed processes, and provide suggestions in how to modify them if necessary. In the case of detection of methane releases, the models can provide information on the source location by either doing an ensemble of forward simulations [Viscardy et al., this conference] or by calculating back trajectories [6].

## 5. Data assimilation

Data assimilation is a technique that allows to combine the dense 3D+time (theoretical) information from models with the sparse set of actual observations, in order to provide the most complete set of information of the atmospheric state and composition. The UK team has considerable expertise on data assimilation for Mars [7] and will extend this work with data assimilation of atmospheric state and chemical composition from the NOMAD observations. Data assimilation is also envisaged using the GEM-Mars model.

## Acknowledgements

The NOMAD experiment is led by the Royal Belgian Institute for Space Aeronomy (IASB-BIRA), assisted by Co-PI teams from Spain (IAA-CSIC), Italy (INAF-IAPS), and the United Kingdom (Open University). This project acknowledges funding by the Belgian Science Policy Office (BELSPO), with the financial and contractual coordination by the ESA Prodex Office (PEA 4000103401, 4000121493), by MICIIN through Plan Nacional (AYA2009-08190 and AYA2012-39691), by the Italian Space Agency through grant 2018-2-HH.0, as well as by UK Space Agency through grant ST/P000886/1. US investigators were supported by the National Aeronautics and Space Administration. The research was performed as part of the “Excellence of Science” project “Evolution and Tracers of Habitability on Mars and the Earth” (FNRS 30442502).

## The NOMAD Team

*Scientific team:* Vandaele, Ann Carine; Lopez Moreno, Jose Juan; Bellucci, Giancarlo; Patel, Manish; Allen, Mark; Alonso-Rodrigo, Gustavo; Altieri, Francesca; Aoki, Shohei; Bauduin, Sophie; Bolsée, David; Clancy, Todd; Cloutis, Edward; Daerden, Frank; D’Aversa, Emiliano; Depiesse, Cédric; Erwin, Justin; Fedorova, Anna; Formisano, Vittorio; Funke, Bernd; Fussen, Didier; Garcia-Comas, Maia; Geminale, Anna; Gérard, Jean-Claude; Gillotay, Didier; Giuranna, Marco; Gonzalez-Galindo, Francisco; Hewson, Will; Homes, James; Ignatiev, Nicolai; Kaminski, Jacek; Karatekin, Ozgur; Kasaba, Yasumasa; Lanciano, Orietta; Lefèvre, Franck; Lewis, Stephen; López-Puertas, Manuel; López-Valverde, Miguel; Mahieux, Arnaud; Mason, Jon; Mc Connell, Jack; Mumma, Mike; Nakagawa, Hiromu, Neary, Lori; Neefs, Eddy; Novak, R.; Oliva, Fabrizio; Piccialli, Arianna; Renotte, Etienne; Robert, Severine; Sindoni, Giuseppe; Smith, Mike; Stiepen, Arnaud; Thomas, Ian; Trokhimovskiy, Alexander; Vander Auwera, Jean; Villanueva, Geronimo; Viscardy, Sébastien; Whiteway, Jim; Willame, Yannick; Wilquet, Valérie; Wolff, Michael; Wolkenberg, Paulina – *Tech team:* Alonso-Rodrigo, Gustavo; Aparicio del Moral, Beatriz; Barzin, Pascal; Beeckman, Bram; BenMoussa, Ali; Berkenbosch, Sophie; Biondi, David; Bonnewijn, Sabrina; Candini, Gian Paolo; Clairquin, Roland; Cubas, Javier; Giordanengo, Boris; Gissot, Samuel; Gomez, Alejandro; Hathi, Brijen; Jeronimo Zafra, Jose; Leese, Mark; Maes, Jeroen; Mazy, Emmanuel; Mazzoli, Alexandra; Meseguer, Jose; Morales, Rafael; Orban, Anne; Pastor-Morales, M; Perez-grande, Isabel; Queirolo, Claudio; Ristic, Bojan; Rodriguez Gomez, Julio; Saggin, Bortolino; Samain, Valérie; Sanz Andres, Angel; Sanz, Rosario; Simar, Juan-Felipe; Thibert, Tanguy

## References

- [1] Neary, L., and F. Daerden (2018), *Icarus*, 300, 458–476
- [2] Daerden, F., et al., in prep.
- [3] Forget, F., et al. (1999), *J. Geophys. Res.* 104 (E10) 24,155–24,175.
- [4] Holmes, J. A., et al. (2017), *Icarus*, 282, 104–117
- [5] González-Galindo, F., et al. (2015), *J. Geophys. Res. Planets*, 120, 2020–2035
- [6] Daerden, F., et al. (2015), *Geophys. Res. Lett.*, 42, 7319–7326
- [7] Steele, L. J., et al. (2014), *Icarus*, 237, 97–115

# Recent results for the space radiation environment aboard ExoMars TGO provided by FRENDS's Liulin-MO dosimeter

Jordanka Semkova (1) and the Team Liulin-MO-FREND

(1) Space Research and Technology Institute, Bulgarian Academy of Sciences, Sofia, Bulgaria, ([jsemkova@stil.bas.bg](mailto:jsemkova@stil.bas.bg))

## Abstract

We present recent results from measurements of the charged particle fluxes, dose rates, linear energy transfer spectra and estimation of dose equivalent rates in the interplanetary space, in high elliptic Mars's orbit and first data in TGO science orbit, provided by Liulin-MO dosimeter of FRENDS instrument aboard TGO.

The obtained data show that during the cruise to Mars and back (6 months in each direction), taken during the declining of solar activity, the crewmembers of future manned flights to Mars will accumulate at least 60% of the total dose limit of 1 Sv for the cosmonauts/ astronauts career in case their shielding conditions are close to the average shielding of Liulin-MO detectors - about  $10 \text{ g cm}^{-2}$ .

The comparison of flux and dose rate measurements carried out by Liulin-MO dosimeter during the cruise of TGO to Mars with calculation based on galactic cosmic rays (GCR) models show surplus of measured flux and dose rate on calculated.

The dosimetric measurements in high elliptic Mars' orbit were used to estimate the flux shadow by Mars effect. Results of 23 TGO pericenter crossing were investigated. The "shadow effect" amounted to 30%, but as a rule was less than calculated one.

The results are important for future manned mission to Mars radiation risk estimations.

## 1. Introduction

The estimation of the radiation effects for a long-duration manned space mission requires: i) Knowledge and modeling of the particle radiation environment; ii) Calculation of primary and

secondary particle transport through shielding materials; and iii) Assessment of the biological effect of the dose.

The FRENDS's dosimetry module Liulin-MO provided information about the radiation environment during the cruise stage and now - on Mars' orbit.

The main goal of the Liulin-MO dosimetric experiment is investigation of the radiation conditions in the heliosphere at distances from 1 to 1.5 AU from the Sun. The main scientific objectives of the Liulin-MO investigation are: a) To measure the dose and determine the dose equivalent rates for human explorers during the interplanetary cruise and in Mars orbit; b) Measurement of the fluxes of GCR, solar energetic particles and secondary charged particles during the cruise and in Mars orbit; c) Together with other detectors of the FRENDS instrument to provide data for verification and benchmarking of the radiation environment models and assessment of the radiation risk to the crewmembers of future exploratory flights.

## 2. Methodology and measured parameters of Liulin-MO

Liulin-MO contains two dosimetric telescopes - A&B, and C&D arranged at two perpendicular directions [1]. Each pair of the dosimetric telescopes consists of two  $300 \mu\text{m}$  thick,  $20 \times 10 \text{ mm}$  area rectangular Si PIN photodiodes. The parameters, provided by Liulin-MO simultaneously for two perpendicular directions have the following ranges: absorbed dose rate from  $10^{-7} \text{ Gy h}^{-1}$  to  $0.1 \text{ Gy h}^{-1}$ ; particle flux in the range  $0 - 10^4 \text{ cm}^{-2} \text{ s}^{-1}$ ; energy deposition spectrum and coincidence energy deposition spectrum in the range  $0.08 - 190 \text{ MeV}$ .

### 3. Liulin-MO data during the TGO cruise, in high elliptic Mars' orbit and first data in Mars' science orbit

The average flux from GCR during the transit to Mars for the period April 22 - September 15, 2016 is  $3.12 \text{ cm}^{-2} \text{ s}^{-1}$  and  $3.29 \text{ cm}^{-2} \text{ s}^{-1}$  in two perpendicular directions. For November 01, 2016 - January 17, 2017 in MCO1 it is 3.26 and  $3.42 \text{ cm}^{-2} \text{ s}^{-1}$  in two perpendicular directions. In the pericenter the average decrease of the particle flux is  $0.77 \text{ cm}^{-2} \text{ s}^{-1}$ . The flux for February 24, 2017 - March 07, 2017 in MCO2 is slightly higher.

The dosimetric measurements in high elliptic Mars' orbit demonstrate strong dependence of the GCR fluxes near the TGO pericenter on satellite's field of view shadowed by Mars.

The average flux from GCR for April 16-May 13, 2018 in Mars science orbit is 2.96 and  $3.06 \text{ cm}^{-2} \text{ s}^{-1}$  in two perpendicular directions.

The measured flux and dose rate during the TGO transit to Mars were compared with calculations based on galactic cosmic ray models. The results show surplus of measured on calculated values.

Table 1 summarizes the dose rate in silicon, the quality factors and dose equivalent rates obtained during the different phases of TGO flight.

Table 1. Dose rate in Si D (Si), quality factors Q and dose equivalent rates H during different TGO phases

Time frame/TGO phase	D (Si) (AB)/ D (Si) (DC) $\mu\text{Gy d}^{-1}$	Q (AB)/ Q (DC)	H (AB)/ H (DC) $\text{mSv d}^{-1}$
April 22 - September 15, 2016/ Cruise	372 ± 37/ 390 ± 39	4.08 ± 0.3/ 4.02 ± 0.3	1.97± 0.4/ 2.04± 0.4
November 01, 2016 - January 17, 2017/ MCO1	405.6 ± 41/ 422 ± 42	4.23 ± 0.33/ 4.12 ± 0.3	2.23± 0.5/ 2.26± 0.5

February 24 - March 07, 2017/ MCO2	410 ± 41/ 425 ± 42.5	4.31 ± 0.33/ 4.17 ± 0.3	2.3± 0.55
April 16 – May 13, 2018/ Mars Science Orbit	337± 34/ 354± 35	3.5±0.26	1.53±0.3/ 1.61±0.32

### 4. Summary and Conclusions

The increase of the charged particles dose rate and flux measured from April 22, 2016 to March 07, 2017 corresponds to the increase of GCR intensity during the declining phase of the solar activity.

The obtained data show that during the cruise to Mars and back (6 months in each direction), taken during the declining of solar activity, the crewmembers of future manned flights to Mars will accumulate at least 60% of the total dose limit of 1 Sv for the cosmonauts/ astronauts career in case their shielding conditions are close to the average shielding of Liulin-MO detectors - about  $10 \text{ g cm}^{-2}$ .

Very first Liulin-MO data in Mars' Science Orbit show that close to the Solar activity minimum the dose equivalent rate is about  $1.2\div 1.6 \text{ mSv d}^{-1}$ .

A similar module, called Liulin-ML for investigation of the radiation environment on Mars' surface as a part of the active detector of neutrons and gamma rays ADRON-EM on the Surface Platform is under preparation for ExoMars 2020 mission.

### Acknowledgements

Thanks: Contracts N 503/2-13 and 63/4-14 between IKI-RAS and SRTI-BAS; Agreement between RAS and BAS on fundamental space research; Contract No. 4000117692/16/NL/NDe Funded by the Government of Bulgaria through an ESA Contract under the PECS.

### References

[1] Semkova, J., *et al*: Charged particles radiation measurements with Liulin-MO dosimeter of FREND instrument aboard ExoMars Trace Gas Orbiter during the transit and in high elliptic Mars orbit, Icarus 303, pp. 53–66, 2018, <https://doi.org/10.1016/j.icarus.2017.12.034>.

## **Ices, frosts and clouds on Mars observed by CaSSIS during the first months of TGO's primary science mission**

A. Pommerol (1), N. Thomas (1), Z. Yoldi (1), V. Rolloff (1), M. Almeida (1), P. Becerra (1), S. Tulyakov (2), L. Tornabene (3), F. Seelos (4), J. Bapst (5), C. J. Hansen (6), G. Portyankina (7), A. Lucchetti (8), M. Pajola (8), S. Douté (9), M. Patel (10) and G. Cremonese (8).

(1) Physikalisches Inst., University of Bern, Sidlerstrasse 5, CH-3012 Bern, Switzerland (antoine.pommerol@space.unibe.ch), (2) Ecole Polytechnique Federale de Lausanne, Switzerland, (3) Centre for Planetary Science & Exploration (CPSX), Western University, London, ON, Canada, (4) Johns Hopkins University Applied Physics Laboratory, Laurel, Maryland, USA, (5) LPL, University of Arizona, Tucson AZ, USA, (6) Planetary Science Institute, Tucson AZ, USA, (7) Laboratory for Atmospheric and Space Physics, University of Colorado, USA, (8) INAF-OAPD, Astronomical Observatory of Padova, Italy, (9) Institut de Planétologie et d'Astrophysique de Grenoble, Université Grenoble Alpes/CNRS, France, (10) School of Physical Sciences, The Open University, Milton Keynes MK7 6AA, UK.

### **Abstract**

The CaSSIS (Colour and Stereo Surface Imaging System) [1] of the ExoMars Trace Gas Orbiter (TGO) has already acquired numerous images of Mars that show seasonal and diurnal ices and frosts at the surface as well as clouds and fog in the atmosphere. Simulations of the CaSSIS signal in all four colour filters from laboratory measurements with analogues and data from other missions will be helpful to interpret these new observations.

### **1. Introduction**

The original 74°-inclination non-Sun-synchronous orbit of the TGO spacecraft coupled with the abilities of CaSSIS to image the surface:

- in up to four colour band
- with sufficient signal-to-noise to provide good quality images in low-light conditions
- with the possibility of quasi-simultaneous stereo acquisitions

provide new opportunities to study the seasonal and diurnal cycles of volatiles (H<sub>2</sub>O and CO<sub>2</sub>) at the surface of Mars. In particular, the regions around 70° latitude in both hemispheres are strongly affected by seasonal changes and can be studied in great details, with short revisit times and possibilities of observations at variable local time during all seasons.

In order to interpret the colour images in terms of ice properties relevant for our understanding of volatiles cycles, we have followed two types of approaches in preparation for scientific exploitation of CaSSIS data:

- Simulation of the CaSSIS spectral signal from laboratory experiments conducted with well-characterized analogues of Martian icy surfaces. This approach is detailed in a companion abstract [2].

- Simulation of CaSSIS spectral-images from data acquired by the HiRISE, CRISM and CTX imagers of MRO. The simulated data provide a thorough assessment of how the colour capabilities of CaSSIS address the relevant science and will be key for cross-calibration, comparison and change-detection with the actual CaSSIS images [3].

### **2. Observations**

Since the beginning of the primary science phase in April 2018, CaSSIS has already acquired a large number of images, regularly increasing, showing the presence of H<sub>2</sub>O and CO<sub>2</sub> ice and frosts at the surface and occasionally clouds and fogs in the atmosphere.

The first observations performed under low-light conditions have confirmed the ability of CaSSIS to provide high-quality images even under challenging illumination conditions. As expected, data from the BLU filter generally show a lower signal-to-noise than the other filters because of the low reflectance of the Martian surface at short visible wavelengths but excel at revealing the presence of even small amounts of ice at the surface or in the atmosphere because of their high reflectance. We are currently focusing our efforts on updating the laboratory calibration of data from the BLU and NIR filters [4] using in-flight data.

Colour composite images assembled from data acquired in the BLU filter combined with PAN and either RED or NIR filter can provide a wealth of information on the occurrence and properties of ices and the processes involved in their deposition and evolution. For instance, the RED-PAN-BLU image of the Northern rim of crater Korolev (73° North) shown by [5] and publically released on the 26<sup>th</sup> of April 2018 (<http://exploration.esa.int/mars/60235->

[exomars-images-korolev-crater/](#) was acquired at early local solar time (07:14 AM) with an incidence angle of 77°.



Figure 1: CaSSIS colour (RED-PAN-BLU) image of the Southern rim of crater Ross (252°E, 57°S). The image is 6 km wide, at a resolution of 4.5m/px. The north-facing slopes appear already defrosted at  $L_s=170^\circ$ , with the exception of the channels of numerous gullies, whereas the floor of the crater and the southern facing slopes are still covered by bright seasonal  $\text{CO}_2$  ice. CaSSIS image: CAS-M01-2018-05-05T19.25.42.020-RED-PAN-BLU.

This colour image shows icy terrains with a rich variety of albedo, colours and textures. Because the image was acquired shortly before the fall equinox in the northern hemisphere, it is likely that the ice seen at the surface consists of both perennial water ice deposits that have survived the entire summer and freshly deposited water frost. On-going comparisons with laboratory data [2] should help with the

interpretation of observed colours and albedo in terms of ice properties.

In the other hemisphere, the external edges of the southern seasonal cap start sublimating as we approach spring equinox. Figure 1 shows an example of the sublimation of the seasonal ice on the North-facing slopes of the southern rim of crater Ross. TES temperature measurements at this location and season in previous Martian years [6] are compatible with the partial defrosting seen by CaSSIS. Of particular interest is also the observation of  $\text{CO}_2$  ice inside the channels of gullies, as it has recently been hypothesized that the  $\text{CO}_2$  cycle is associated to the gullies formation process [7].

### 3. Summary and future work

Many of the first images acquired by CaSSIS at the beginning of TGO's primary science missions show ices, frosts and clouds. In addition, the quality of the images, considering those acquired under challenging low-light conditions, prove the ability of the instrument to make a significant contribution to the understanding of volatiles cycles on Mars.

Simulations of CaSSIS spectral signal from both laboratory analogues and instruments on other missions are key for the interpretation of CaSSIS colour observations. Results obtained during the first months of the primary science phase will guide future laboratory experiments.

### Acknowledgements

The authors wish to thank the spacecraft and instrument engineering teams for the successful completion and operation of the instrument. CaSSIS is a project of the University of Bern and funded through the Swiss Space Office via ESA's PRODEX programme. The instrument hardware development was also supported by the Italian Space Agency (ASI) (ASI-INAF agreement no.I/018/12/0), INAF/Astronomical Observatory of Padova, and the Space Research Center (CBK) in Warsaw. Support from SGF (Budapest), the University of Arizona (Lunar and Planetary Lab.) and NASA are also gratefully acknowledged. The laboratory work has been carried out within the framework of the NCCR PlanetS supported by the Swiss National Science Foundation.

### References

- [1] Thomas, N. et al. (2017) Space Sci. Rev., 212, 1897
- [2] Yoldi et al., this conference.
- [3] Tornabene, L. L. et al. (2018) Space Sci. Rev., 214, 18.
- [4] Roloff, V. et al. (2018) Space Sci. Rev., 214, xx.
- [5] Thomas, N. et al., this conference.
- [6] Bapst, J. et al. (2015) Icarus 260.
- [7] Vincendon, M. et al. (2015) JGR, 120.

## Meteorites as Environmental Witness Plates for Mars Sample Return Consideration

A. W. Tait<sup>1</sup>, C. Schröder<sup>1</sup>, J. W. Ashley<sup>2</sup>, M. A. Velbel<sup>3</sup>, P. J. Boston<sup>4</sup>, B. L. Carrier<sup>2</sup>, B. A. Cohen<sup>5</sup> and P. A. Bland<sup>6</sup>,  
(1) Biological and Environmental Sciences, University of Stirling, Stirling FK9 4LA, UK, (alastair.tait@stir.ac.uk), (2) Jet  
Propulsion Laboratory, Pasadena, CA, United States, (3) Michigan State University, East Lansing, MI, United States, (4)  
NASA Ames Research Center, Moffett Field, CA, United States, (5) NASA Marshall Space Flight Center, Huntsville, AL,  
United States, (6) Curtin University, Perth, WA, Australia.

### 1. Introduction

Returning samples from Mars is a mutual science goal for NASA and ESA administrations. The discussion of what samples to target and bring back is well underway [1]. ‘Samples of Opportunity’ (SOO) are serendipitously discovered targets that contain scientific-value, that otherwise would not be searched for due to their aleatory distribution. Meteorites found on Mars, in particular ordinary chondrites (OCs), are one such SOO. Over 24 iron and stony-iron meteorites have been identified on the Martian surface by the Mars Exploration Rovers (MERs) [2-5] and the Mars Science Laboratory (MSL) rover Curiosity [6-9] (Figure 1). These Martian finds are different from the SNC meteorites that are fragments of Martian crust found on Earth, and often referred to as Martian meteorites. If available to laboratory study, the Martian finds can significantly enhance understanding of geologic, geochemical, atmospheric, and potentially biological processes on the Red Planet because meteorite baseline compositions are known with much higher precision from curated terrestrial falls than that of Martian rocks. Therefore any deviations in meteorite geochemical, mineralogical, and isotopic composition, while resident on Mars, would be the sole result of alteration by the Martian environment. Therefore, an OC might act like a ‘Rosetta stone’, helping to decipher Martian surface history. The ability to record environmental weathering and potential biosignatures against a known baseline should make stony-meteorites primary SOO in the upcoming Mars2020 stage of the sample return endeavour.

### 2. Insights Gained from Meteorites

#### 2.1 Atmospheric Evolution

Meteorite accumulation rates and the average size of meteorite fragments is to first order a function of the density of the atmosphere [10, 11]. For example, the martian iron-meteorite Block Island has been used to argue that the atmosphere was at least an order of magnitude denser when it fell [12], although, others argue this could be a recent fall under current conditions with a shallow entry angle [13].



Figure 1: (Sol 1713) “Santorini” is a stony-iron meteorite discovered at Meridiani Planum by MER Opportunity.

#### 2.2 Weathering Environment

Metallic phases in meteorites make them extremely sensitive tracers to the presence of water [14]. None of the iron meteorites discovered on Mars so far show widespread signs of rust. They do, however, display patches of coating that is associated with iron oxidation [2,5,15]. This coating may have formed during periods of burial or ice exposure during high obliquity cycling [5]. Iron oxidation rates of stony-meteorites discovered by MER Opportunity are determined to be 1-4 orders of magnitude slower than

the Antarctic weathering rate of similar materials [16]. Meteorites on Earth are found to contain Fe-(oxy)hydroxides, sulfates, carbonates, salts, and smectites. These alterations reflect both different stages of weathering [17], and environmental conditions [18]. By investigating the mineralogy of these alteration products of weathered meteorites on Mars, it would be possible to reconstruct paleo-environments. Such alteration could also provide a regional alteration baseline, providing value for other returned samples.

### 2.3 Putative Biosignatures

The search for life on Mars requires unambiguous biosignatures. The compositions of Ordinary Chondrites (OC) are well known, making the detection of modifications by putative organisms easier to recognise [18]. In fact, ordinary chondrites make attractive habitats for terrestrial microorganisms in arid environments because they become hygroscopic and contain abundant metal, sulfur and even organics as energy sources [18]. Meteorites recovered from the Nullarbor Plain, Australia, were found to contain various cryptoendolithic and chasmoendolithic communities of bacteria and archaea [18]. 16S rRNA gene analysis of meteorites from the Nullarbor Plain showed microbial colonisation by a variety of microorganisms including some iron- and sulfur-metabolising genera such as *Geobacter sp* and *Desulfovibrio sp* [19], potentially leaving  $\delta^{34}\text{S}$  signatures in the secondary weathering products [18]. Many microbial communities exacerbate weathering and form biofilms on mineral surfaces, where they can also become entombed by secondary minerals and preserved [19].

### 3. Open Questions and Conclusions

Ordinary chondrites would be the most suitable targets to be considered among the list of exogenic samples of opportunity for MSR. They are the most common meteorite type found on Earth, and the same is expected for Mars [10]. So far, however, the observed Martian finds are dominated by iron and stony-iron meteorites [2-4] (Figure 1), with only one candidate OC. Is this an observational sampling bias, or is there another environmental reason [8]? Indeed, how can OCs be identified by imagery and other remote sensing observations [e.g., 14]?

When considering a weathered ordinary chondrite for sample return, is there sufficient scientific value independent of exposure age? Given the potential upper limit of Noachian resident ages [12,16], can OCs not only survive but also preserve geochemical and isotopic signatures for billions of years?

These are some of the questions that need to be addressed to assess the viability of OCs as samples of opportunity for MSR. A focused study of an ordinary chondrite candidate by either Opportunity or Curiosity, if encountered, would assist greatly with the assessment. Additional studies of samples from warm and cold deserts could enhance our understanding in advance of such encounters on Mars.

### Acknowledgements

A. Tait's Rutherford Fellowship is funded through the Commonwealth Scholarship Commission, UK. C. S. acknowledges funding by the UK Space Agency (ST/R001278/1).

### References

- [1] iMOST (2018), *2nd IMSR Conference (Berlin)*, #6120
- [2] Schröder C. et al. (2008) *JGR*, *113*, E06S22, 10.1029/2007JE002990.
- [3] Ashley J. W. (2009) *LPS XL*, #2468.
- [4] Schröder C. et al. (2010) *JGR*, *115*, E00F09, 10.1029/2010JE003616.
- [5] Ashley J. W. (2011) *JGR*, *116*, E00F20, 10.1029/2010JE003672.
- [6] Wellington D. F. et al. (2018) *LPSC XLIX*, #1832
- [7] Johnson J. R. et al. (2014) AGU Fall Meeting, P51E-3989.
- [8] Ashley J. W. and Herkenhoff K. E. (2017) *LPS XLVII*, #2656.
- [9] Wiens R. C. et al. (2017) *Metsoc*, # 6168.
- [10] Bland P. A. and Smith T. B. (2000) *Icarus*, *144*, 21–26.
- [11] Chappelow J. E. and Sharpton V. L. (2006) *Icarus*, *184*, 424–435.
- [12] Beech M. and Coulson I. M. (2010) *Mon. Not. R. Astron. Soc.*, *404*, 1457–1463.
- [13] Chappelow J. E. and Golombek M. P. (2010) *JGR*, *115*, E00F07, 10.1029/2010JE003666.
- [14] Ashley J. W. and Wright S. P. (2004) *LPS XXXV*, #1750.
- [15] Fleischer I. et al. (2011) *Meteoritics & Planet. Sci.*, *46*, 21–34.
- [16] Schröder C. et al. (2016) *Nat. Commun.*, *7*, 13459, 10.1038/ncomms13459.
- [17] Wlotzka F., (1993) *Meteoritics*, *28*, 460.
- [18] Tait A. W. et al. (2017) *GCA*, *215*, 1–16.
- [19] Tait A. W. et al. (2017) *Front. Microbiol.*, *8*, 10.3389/fmicb.2017.01227

## 3DPD application to the first CaSSIS DTMs

Emanuele Simioni (1), Cristina Re(1), Teo Mudric( 1), Maurizio Pajola (1), Alice Lucchetti (1), Riccardo Pozzobon (2), Pamela Cambianica (2), Gabriele Cremonese(1), Antoine Pommerol (3), and Nicolas Thomas (3)  
(1) INAF, Osservatorio Astronomico di Padova, Vicolo dell'Osservatorio 5, 35122, Padova, Italy  
([emanuele.simioni@oapd.inaf.it](mailto:emanuele.simioni@oapd.inaf.it)), (2) Dept. of Geoscience, University of Padova, Italy, (3) Physikalisches Institut, University of Bern, Sidlerstr. 5, 3012 Bern, Switzerland

### Abstract

The main objective of the ExoMars Trace Gas Orbiter (TGO) is the search for traces of atmospheric gases that could be the signature of biological activity on Mars. Among different onboard instruments, the spacecraft includes an imaging and photogrammetric camera called Colour and Stereo Surface Imaging System (CaSSIS, [1]) that is a narrow angle telescope dedicated to i) imaging with four filters (centered at 0.499  $\mu\text{m}$ , 0.675  $\mu\text{m}$ , 0.836  $\mu\text{m}$  and 0.937  $\mu\text{m}$ ) and a spatial scale < 5m and ii) to 3D reconstruct specific targets of interest through stereo capabilities. INAF-OAPD institute (The Astronomical Observatory of Padova), as part of the CaSSIS team, leads the Digital Terrain Models (DTMs) generation in association with other team members. In addition, INAF-OAPD is responsible for DTMs archiving [2]. Here, a preliminary DTM is shown, as example.

### 1. Introduction

The stereo satellite photogrammetry is generally based on push-broom acquisition systems. Different push-broom instruments have provided DTMs from Mars planetary images even without an actual stereo configuration, like NASA's CTX [3] and HiRISE [4] cameras.

Nowadays, the push frame approach is replacing the push broom in missions oriented to photogrammetry. The use of 2D images, buffered while the spacecraft moves, increase the geometry information avoiding registration problems. This is the case of CaSSIS: a common telescope configuration (oriented  $10^\circ$  with respect to the nadir pointing) taking advantage of a rotational unit to perform imaging in different directions.

To obtain a stereo couple, CaSSIS firstly acquires a set of "framelets" while looking forward along the orbit. Consequently the telescope rotates  $180^\circ$

degrees and, looking backward along the orbit, it acquires a second set of "framelets" covering the same area imaged by the first set. This approach guarantees a sufficient baseline to reach a vertical precision equal to the pixel on-ground.

Since its arrival around Mars in October 2016, CaSSIS already demonstrated its stereo performance despite a non-nominal orbit. Indeed, the first CaSSIS DTM of a Deep Seated Gravitational Slope Deformation (DSGSD) was reconstructed [5] and analysed [6]. At the end of April 2018, TGO started its commissioning phase and it is now ready for its nominal science mission phase.

### 2. 3DPD

INAF-OAPD developed a stereo pipeline for the 3D reconstruction of planetary surfaces, rooting its know-how from the design of the stereo camera STC [7] on board the BepiColombo mission. Despite STC and CaSSIS instruments are different in terms of optical design and stereo strategy, they both share the push-frame approach. Therefore, these contexts brought to the development of a ad-hoc DTM generation software, called 3DPD (three-Dimensional reconstruction of Planetary Data), which can be used for both the instruments.

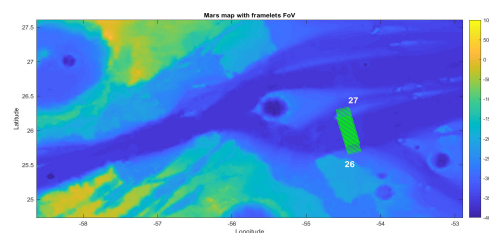


Figure 1: Screenshot of the 3DPD user interface showing the two CaSSIS frames' FoVs projected on the Mars surface that are used for the DTM generation.

The software includes a user interface for CaSSIS acquisition visualisation, as shown in Figure 1.

The full pipeline of the software [8] includes i) the geometrical distortion calibration [9], ii) the mosaicking of the images on the MOLA quote, iii) the definition of SURF tie-points and iv) a sequential use of both pyramidal NCC(Normalize Cross Correlation) and ALSM(Adaptive Least Square Matching) algorithms for the definition of disparity maps. The final steps leading to the resulting DTM production include v) the outliers detection and filling holes based on dephormable models [10] and vi) the triangulation phase. Tests will be also conducted to improve the level of details in the DEMs by photoclinometry [10].

### 3. CaSSIS first Stereo Images

During the first commissioning orbits (STP003 phase) CaSSIS acquired more than 800 panchromatic framelets, returning a total of 30 frames. Among them, eight frames are stereo couples.

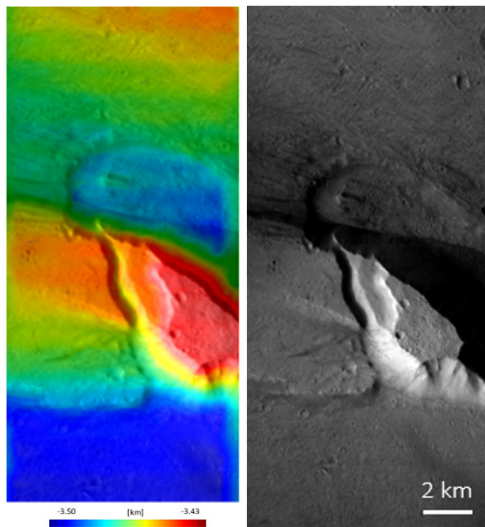


Figure 2: Preliminary height map reconstruction (texturized) of the structure (left hand side) and one of the two stereo images obtained after mosaicking process

(right-hand side). The quotes are referred to mean MOLA radius.

On May, 7, 2018, at 14:09:08 UT, the CaSSIS camera acquired the frames no. 26-27 covering a section of the Kasei Vallis canyon (the southernmost channel of the Kasei Valles) located at 26° N, -54.3°. Fig. 1 shows the FoV positions of the two CaSSIS frames, while the colorbar represents the MOLA elevation in metres. The stereo couple covers part of the outflow channels' outlet towards the Chryse Planitia, south-east of one of the largest teardrop shaped islands located in the area. Such location lies right at the boundary between the Noachian highland unit (Nhu) and the Amazonian and Hesperian impact unit (AHi) of the Mars global geology of [10]. The preliminary DTM result is presented in Fig. 2 and covers an incised dome/structure that is 4.4 km long, 1.9 km wide and 60 meters taller than the local plane. The CaSSIS DTMs will be integrated with multi-band orthorectified images provided by the color filters adding valuable compositional information to the reconstructed topography.

### Acknowledgements

The authors would like to express their gratitude to the CaSSIS team for the calibration during the commissioning phase and the Italian Space Agency (ASI) for providing us the opportunity to give our contribution to the project (ASI-INAF agreement no.I/018/12/0).

### References

- [1] Thomas, N., et al. 2014, 8th International Conference on Mars. 2014.
- [2] Cremonese G. et al 2018, EPSC
- [3] Bell III, J. F., et al., 2013, International Journal of Mars Science and Exploration 8: 1-14
- [4] McEwen, Alfred S., et al. 2007, Journal of Geophysical Research: Planets 112.E5.
- [5] Cremonese, G., et al.2017. LPSC. Vol. 48.
- [6] Massironi, M., et al., 2017, EPSC2017-618-1
- [7] G. Cremonese, et al, 2006, Mem. S.A.It. Suppl. 9, pp. 173-175 . ISSN: 1824-0178.
- [8] Simioni, E., et al.,2017, ISPRS 42: 133-139.
- [9] Tulyakov, Stepan, et al.2018, Advances in space research 61.1: 487-496.
- [10] Simioni, E, et al. 2011, PE&RS 77.5: 495-507.
- [11] Douté, S., et al. 2018 EPSC 2018.
- [12] Tanaka et al., 2014.. Planet. Space Sci. 95, 11-24.

# **Fine Resolution Epithermal Neutron Detector (FRIEND) onboard TGO. First results from cruise, elliptical capture orbit and science mapping phase**

**Igor Mitrofanov**(1), Maxim Litvak(1), Anton Sanin(1), Dmitry Golovin(1), Alexey Malakhov(1), Alexander Kozyrev(1), Maxim Mokrousov(1), Andrey Vostrukhin(1), Sergey Nikiforov(1), Jordanka Semkova(2), Rositza Koleva(2), Krasimir Krastev(2), Victor Benghin(3), Tsvetan Dachev(2), Yuri Matviichuk(2), Borislav Tomov(2), Stephan Maltchev(2), Plamen Dimitrov(2)

(1) Space Research Institute, Moscow, Russia, (2) Space Research and Technology Institute, Sofia, Bulgaria, (3) Institute of Biomedical Problems, Moscow, Russia

## **Abstract**

ExoMars is a two-launch mission undertaken by Roscosmos and European Space Agency. Trace Gas Orbiter, a satellite part of the 2016 launch carries the Fine Resolution Epithermal Neutron Detector instrument as part of its payload. The instrument aims at mapping hydrogen content in the upper meter of Martian soil with high spatial resolution of up to 60 km diameter spot. The instrument's neutron collimator, the first of its kind to map Martian neutrons flux, explains this capability.

Since launch in March 2016, FRIEND operated in three major mission phases: cruise to Mars, between April and September 2016, Mars Capture Orbit, between November 2016 and March 2017, and Science Orbit, from April 2018 up until now.

We will present our measurements' results from all three phases mentioned above. Cruise data provides for measurements of galactic cosmic rays in Earth-Mars transfer, an important input for future Martian missions planning. Data from the elliptical Mars Capture Orbit are an important step in instrument calibration needed for interpretation of routine measurements. Science orbit measurements are the first glance on Martian neutrons, and hence, hydrogen content at a high resolution.

## Occultation results by ACS TIRVIM at ExoMars TGO: aerosols and gases

Alexey Grigoriev (1), **Alexey Shakun** (1), Nikolay Ignatiev (1), Boris Moshkin (1), Dmitry Patsaev (1), Alexander Zharkov (1), Igor Maslov (1), Dmitry Gorinov (1), Andrey Kungurov (1), Aleksandr Santos-Skripko (1), Viktor Shashkin (1), Fedor Martynovich (1), Oleg Sazonov (1), Igor Stupin (1), Dmitry Merzlyakov (1), Yury Nikolskiy (1), Mikhail Luginin (1), Alexander Trokhimovskiy (1), Franck Montmessin (2), and Oleg Korablev (1)  
(1) Space Research Institute (IKI), Moscow, Russia, (2) LATMOS-CNRS, Guyancourt, France ([avshakun@iki.rssi.ru](mailto:avshakun@iki.rssi.ru))

### Abstract

ACS is a set of three spectrometers (NIR, MIR, and TIRVIM) observing the Mars atmosphere in solar occultations, nadir and limb geometry. It was built by Space Research Institute (IKI) in Moscow (Russia) [1]. ACS TIRVIM is a Fourier-spectrometer built around a 2-inch double-pendulum interferometer with cryogenically-cooled HgCdTe detector, allowing operation in nadir and in solar occultation. The primary goal of TIRVIM is the long-term monitoring of atmospheric temperature profiles and aerosol state in nadir (see Ignatiev et al. EPSC 2018).

TIRVIM is the first Fourier-spectrometer able to observe Sun occultations at Mars giving an access to a broad spectral range from near-IR through thermal IR: 1.7-17  $\mu\text{m}$ . A dedicated solar port with limited aperture, or the full 2" nadir aperture could be used to observe occultations. In either case the FOV diameter is 2.5°, while the spectral resolution changes from 0.8  $\text{cm}^{-1}$  when observing through the solar port (the "climatology" observation mode) to 0.13  $\text{cm}^{-1}$  when observing with full nadir aperture. This latter "sensitive" mode requires dedicated spacecraft pointing, but allows for sensitive measurements of trace atmospheric gases.

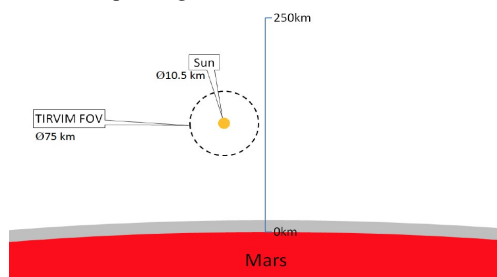


Figure 1: A sketch of TIRVIM observation geometry in occultation.

At the limb the FOV encompasses a circle of 75 km while the Sun disk diameter is 10.5 km. In the short-wavelength (SW) part of the spectrum the Sun radiation dominates and the Sun diameter mostly determines the effective FOV. In the long-wavelength (LW) part the infrared emission from Mars and the atmosphere is significant or dominates and the full FOV works. The vertical sampling in the "climatology" mode is as low as 0.4 km.

The first Sun occultations showed that the following gaseous bands are well visible in the TIRVIM spectra: multiple  $\text{CO}_2$  bands, CO at 4.7  $\mu\text{m}$ ,  $\text{H}_2\text{O}$  at 6.3  $\mu\text{m}$ . All these gases are routinely observed in "climatology" mode allowing for vertical profiling. The  $\text{CO}_2$  in the 15- $\mu\text{m}$  band is detectable up to the altitude of ~200 km, with a signature of non-LTE effects.

The "climatology" spectra reveal vertical structure of aerosols, sometimes layered. The spectra show  $\text{H}_2\text{O}$  ice features at around 3  $\mu\text{m}$  and 12  $\mu\text{m}$ . An interesting optical phenomenon is observed around the 12- $\mu\text{m}$  ice and 9- $\mu\text{m}$  silicate dust bands. When the Sun approaches the horizon, a sort of emission with a particularly strong and sharp peak around 9-10  $\mu\text{m}$  appears. The intensity increases by an order of magnitude in 10 s and remains at this level even when the Sun falls ~16 km below the horizon. Our preliminary interpretation is that the large TIRVIM FOV acquires the Sun IR light forward-scattered by the silicate dust particles. Just the same but time-reversed picture is visible at the sunrise. We call this effect "Silicate Dawn-Dusk" (SDD). SDD is observed in both hemispheres, at different places. A detailed interpretation of SDD effect would involve comprehensive modeling (Luginin et al., EPSC 2018) but should deliver a lot of information about aerosols.

TIRVIM occultations observed with the "sensitive" pointing allow to profile trace components. So far

CO<sub>2</sub> isotopic bands including 628 were observed. Less pronounced but detectable is O<sub>3</sub> at 9.6 μm; for NH<sub>3</sub> an existing upper limit of 8 ppb [2] could be improved.

The TIRVIM occultation results available will be reviewed, and the progress of their interpretation summarized.

## **Acknowledgements**

ExoMars is the space mission of ESA and Roscosmos. The ACS experiment is led by IKI Space Research Institute in Moscow. The project acknowledges funding by Roscosmos and CNES. Science operations of ACS are funded by Roscosmos and ESA.

## **References**

[1] Korablev, O., Montmessin, F., and ACS Team: The Atmospheric Chemistry Suite (ACS) of three spectrometers for the ExoMars 2016 Trace Gas Orbiter, *Space Sci. Rev.*, 214:7, 2018.

[2] Maguire, W.C.: Martian isotopic ratios and upper limits for possible minor constituents as derived from Mariner 9 infrared spectrometer data, *Icarus*, 32:85-97, 1977.

# Short-Term Equatorial Albedo Changes on Mars: Deliquescence or Dust?

Alfred McEwen (1), Nicolas Thomas (2), Antoine Pommerol (2), Cecilia Leung (1), Sarah Sutton (1), Jason Perry (1), Stephen Scheidt (1), Matthew Chojnacki (1).

(1) LPL, University of Arizona, USA, (2) Physikalisches Inst., University of Bern, Sidlerstrasse 5, CH-3012 Bern, Switzerland.

## Abstract

Puzzling short-term albedo changes have been seen on colluvial fans associated with Recurring Slope Lineae (RSL), especially within Valles Marineris, often associated with episodes of high dust opacity [1, 2]. Two leading hypotheses are (1) deliquescence associated with the lower daytime temperatures under dusty air, and (2) removal and redeposition of thin layers of surface dust. If (1) is correct, we should see dark areas in morning imaging by TGO/CaSSIS that disappear in the afternoon when observed by MRO's HiRISE and CTX. If (2) is correct, colour variations consistent with dust removal and deposition should be observed.

## 1. Introduction

CaSSIS (Colour and Stereo Surface Imaging System) on the ExoMars Trace Gas Orbiter (TGO) began systematic observing of Mars in May of 2018 [3,4], and provides the unique ability to observe equatorial Mars at all local times of day within each season. However, to distinguish seasonal albedo changes from shorter-term changes, we also need to rely on the High Resolution Imaging Science Experiment (HiRISE) [5] and the Context Imager (CTX) [6] on Mars Reconnaissance Orbiter (MRO), which observe the dayside at mid-afternoon local times.

## 2. Puzzling RSL

RSL are transient low-albedo features that initiate at bedrock outcrops and extend down steep slopes [1]. Individual slopes may have hundreds of lineae, with widths up to 5 m and lengths up to 1.5 km, so the largest lineae will be detectable by CaSSIS at  $\sim 4.5$  m/pixel. RSL are active during the warmest seasons and are associated with the transient presence of hydrated salts [7], which suggests some role for salty water. But if the RSL were caused by fluid flow, they

should not be precisely confined to angle-of-repose or steeper slopes ( $>28$  deg.) [8], so these seem to be dry granular flows whose activity is somehow associated with small amounts of water.

One key unknown about RSL is the time of day when they are most active; MRO can only observe in the middle afternoon, the driest time of day. The  $74^\circ$  inclined orbit of TGO rotates through  $\sim 24$  hours local time 1-2 times per Mars season, affording unique opportunities to image Mars in the morning when deliquescent liquids are most stable on the surface [9]. If the RSL or their fans are transiently dark due to deliquescence, then this process probably isn't restricted to steep slopes, rather it triggers granular flows (RSL) only on steep slopes. A goal of CaSSIS is to detect anomalous and transient dark patches in the morning. Although CaSSIS can re-image these locations in the mid-afternoon several Earth months before or after the morning images, seasonal changes complicate identification of diurnal changes. Fortunately, MRO can often image these sites within a couple of weeks of the morning image.

## 3. Puzzling Albedo Changes

One mystery is the transient relative darkening of large ( $>100$  m) fans upon which RSL terminate, such as in Valles Marineris [1,2]. Although the monitoring is far from uniform in space and time, there seems to be an association with periods of dusty air in Valles Marineris. Regional dust storms (area  $> 1.6 \times 10^6$  km<sup>2</sup>, and persisting for  $\geq 3$  sols) occur 18 to 50 times per Mars year, with the more opaque dust storms occurring between  $L_s = 134^\circ - 49^\circ$  [10]. About half of these regional storms follow the Acidalia storm track from north to south and tend to spread into eastern and central Valles Marineris. Some of the widespread RSL fans and nearby dune fields become relatively darker (compared to surroundings) during or shortly after these dusty periods, returning

to their previous appearance within weeks when the air is back to normal. How can we explain this observation? We explore two hypotheses:

(1) Daytime surface temperatures are lower and nighttime temperatures are higher, each by  $\sim 10^{\circ}\text{C}$ , when the air is very dusty [11]. Given the anticorrelation between temperature and relative humidity, this means that conditions needed for deliquescence may exist for extended periods of the day when the air is dusty, and the conditions needed for efflorescence should be reduced mid-day [9]. However, we are ignorant about actual relative humidity levels at these times and places except via modeling, and about local salt compositions and concentrations.

(2) Increased winds associated with the Acidalia storms could lead to increased saltation of sand, which kicks up and removes dust from sandy surfaces. This includes active sand ripples frequently observed on RSL fans [2]. As the winds die down, the dust is redeposited, increasing the albedo most markedly over the darkest surfaces. This seems like a straightforward explanation, but in detail some fans and dunes darken while others do not, and in some cases the darkening appears to be due to a greater density of RSL.

## 4. Joint CaSSIS-HiRISE Planning and Data Analysis

TGO plans observations at least 8 weeks prior to execution, and controls the orbit to match the plan. In contrast, MRO lets the orbits drift to minimize fuel use, but has a later planning cycle. This works well for joint observations, because the CaSSIS imaging plans will be known well in advance, so HiRISE and CTX can target the same locations within  $\sim 2$  weeks, given MRO's ability to point up to 30 degrees off-nadir.

These morning-afternoon image pairs will not be easy to compare because the lighting angles will be completely different over sloping terrain. Digital terrain models (from CaSSIS, CTX or HiRISE) will be used to model and remove topographic shading from the images. The detection of morning dark patches and their patterns in space and time will test the deliquescence hypothesis for the origin of water affecting RSL. If there is sufficient deliquescence on the surface to detect darkening, that should be

happening over many places, not just over steep slopes. Analysis of surface colour variations is complicated by dusty air which makes dark dust-free surfaces resemble dusty surfaces [12].

## 5. Summary and Conclusions

We are entering both the peak season for regional dust storms and the highest data rate period this summer (on Earth), so there should be many useful MRO-TGO image comparisons to present and discuss at the conference.

## References

- [1] McEwen, A. S., et al.: Recurring slope lineae in equatorial regions of Mars, *Nat. Geosci.*, 7(1), 53–58, doi:10.1038/ngeo2014, 2013.
- [2] Chojnacki M. et al.: Geologic context of recurring slope lineae in Melas and Coprates Chasmata, Mars. *J. Geophys. Res. Planets* 121, 1204-1231, doi: 10.1002/ 2015JE004991, 2016.
- [3] Thomas, N. et al.: The Colour and Stereo Surface Imaging System (CaSSIS) for the ExoMars Trace Gas Orbiter. *Space Sci. Rev.*, 212, 1897, 2017.
- [4] Thomas, N. et al.: CaSSIS – First images from science orbit, this conference, 2018.
- [5] McEwen, A.S., et al.: Mars Reconnaissance Orbiter's High Resolution Imaging Science Experiment (HiRISE). *J. Geophys. Res.* 112, E05S02, 2007.
- [6] Malin, M.C., et al.: Context camera investigation on board the Mars Reconnaissance Orbiter. *J. Geophys. Res.* 112 (E5). doi:10.1029/2006JE002808, 2007.
- [7] Ojha, L., et al.: Spectral evidence for hydrated salts in recurring slope lineae on Mars, *Nature Geoscience* 8, 829-832, doi:10.1038/NGEO2546, 2015.
- [8] Dundas, C. M., et al.: Granular flows at recurring slope lineae on Mars indicate a limited role for liquid water , *Nature Geoscience*, doi: 10.1038/s41561-017-0012-5, 2017.
- [9] Gough, R. V., V. F. Chevrier, and M. A. Tolbert: Formation of aqueous solutions on Mars via deliquescence of chloride-perchlorate binary mixtures, *Earth Planet. Sci. Lett.* 393, 73–82, doi:10.1016/j.epsl.2014.02.002, 2014.
- [10] Cantor, B.A., Malin, M.C., Edgett, K.E.: Martian Dust Storms—Observations by MGS-MOC and MRO-MARCI. Eighth International Conference on Mars, LPI Contribution No. 1791, p.1316, 2014.
- [11] Ryan, J.A., Henry, R.M.: Mars atmospheric phenomena during major dust storms, as measured at surface. *J. Geophys. Res.* 84, 2821-2829, 1979.
- [12] Fernando, J. et al.: Mars Atmospheric Dust Contamination of Surface Albedo and Color Measurements. 48th Lunar and Planetary Science Conference, LPI Contribution No. 1964, id.1635, 2017.

## Exploring HDO and H<sub>2</sub>O on Mars with the ACS instrument onboard TGO

Franck Montmessin (1), Anna Fedorova (2), Oleg Korablev (2), Alexander Trokhimovskiy (2), Kevin Olsen (1), L. Rossi (1), T. Fouchet (3), T. Encrenaz (3), E. Lellouch (3), Jean-Loup Bertaux (1,2) and the ACS team.

(1) LATMOS-UVSQ, Guyancourt, France; (2) Space Research Institute (IKI), Moscow, Russia, (3) LESIA, Observatoire de Paris, Meudon, France. (franck.montmessin@latmos.ipsl.fr)

### Abstract

#### 1. Introduction

The Trace Gas Orbiter (TGO) of the ESA-Roscosmos ExoMars mission has ended its trip to Mars, reaching the planet in October 2016. After more than a year-long aerobraking phase, its scientific mission has begun on April 22<sup>nd</sup> 2018 with the execution of the first solar occultation. The primary objective of TGO is to detect, map and locate trace gas sources, possibly revealing a residual geophysical (or even biological) activity on Mars. The instrument of interest here is the infrared spectrometer Atmospheric Chemistry Suite (ACS). ACS covers a wavelength range from 0.7 to 17  $\mu\text{m}$  at very high spectral resolution ( $\lambda / \Delta\lambda$  from 5,000 to 50,000). ACS operates in nadir and in solar occultation. Its performance and scientific objectives make it complementary to NOMAD, the other spectrometer dedicated to trace gas characterization.

The objectives of ACS [1] lie at the core of TGO mission goals (TGO will eventually serve as a telemetry relay for the ExoMars 2020 rover). However, the versatility of ACS makes it possible to contribute, beyond the sole topic of trace gases, to the more general knowledge of the Martian atmosphere, by characterizing in particular the Martian water cycle and that of its isotope HDO.

#### 2. The water and heavy water cycles

Several members of our team have long been involved in the study of Martian HDO, having described their theoretical approach with several original works [2,3,4].

The D / H ratio, determined via the isotope ratio of the water vapor, is more than five times higher than the reference ratio of the terrestrial oceans. This relative enrichment of D appears as the result of a differentiated escape suggesting that a quantity of water at least five times higher was once present on Mars (the Earth managed how to preserve all of its water). What we know today about Martian D / H has been developed essentially from observations made from Earth. The latter have substantially increased in number thanks to several groups [5,6,7,8].

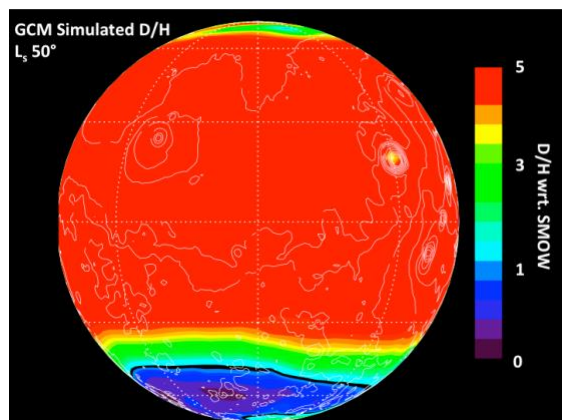


Figure: Map of the D/H ratio on Mars at Ls 50° as predicted by the GCM presented in [4].

During condensation, a fractionation process takes place between H<sub>2</sub>O and HDO, the latter tends to concentrate in the ice phase, distilling an air depleted in deuterium. In fact, an isotopic gradient must theoretically settle between the cold regions subject to condensation and the warmer regions (see Figure). The comparison of predictions of the 3D model published in [4] and ground observations agree well on the existence of a meridional gradient of D/H between the hot and humid summer hemisphere and the cold, dry winter hemisphere.

However, the observations also revealed a D/H contrast in longitude that contradicts model predictions [9]. No viable hypothesis can yet explain the presence of such a gradient. A fractionation action by adsorption / desorption of water in the regolith is theoretically possible, but such a phenomenon requires an exchange flux with the atmosphere that is too high. Many puzzles remain, and the field of HDO needs to be explored by observation.

### 3. Heavy water vapor: a major goal for ACS

The ACS measurements will produce the first vertical profiles obtained simultaneously for HDO and H<sub>2</sub>O in an altitude range limited in its lower part by the thick layer of aerosols (around 10 km typically) and in its upper part (above 80 km) by the gradual decrease in the concentration of these two species and that of the air mass factor. Nevertheless, these profiles will make it possible to identify the altitudes where it a sudden collapse of the two species is expected as a consequence of their condensation (hygropause), the associated formation of clouds (observed by ACS instrument too) and consequently the resulting fractionation. In fact, ACS shall be able to characterize in detail the space-time variability of H<sub>2</sub>O and HDO.

### Acknowledgements

ExoMars is a space mission of ESA and Roscosmos. The ACS experiment is led by IKI Space Research Institute in Moscow. The project acknowledges funding by Roscosmos and CNES. Science operations of ACS are funded by Roscosmos and ESA. FM, KO, TF and EL activity within ACS is supported by CNRS and CNES.

### References

[1] Korabiev, O., Montmessin, F., and ACS Team: The Atmospheric Chemistry Suite (ACS) of three spectrometers for the ExoMars 2016 Trace Gas Orbiter, *Space Sci. Rev.*, 214:7, 2018.

[2] Fouchet, T., and E. Lellouch. 2000. *Icarus* 144 (March): 114–23.

[3] Bertaux, J.-L., and F. Montmessin. 2001. *Journal of Geophysical Research (Planets)* 106 (December): 32879–

84. <https://doi.org/10.1029/2000JE001358>. Bertaux and Montmessin 2001,

[4] Montmessin, F., T. Fouchet, and F. Forget. 2005. *Journal of Geophysical Research (Planets)* 110 (March): 3006. <https://doi.org/10.1029/2004JE002357>. Montmessin et al., 2005.

[5] Encrenaz, T., C. DeWitt, M. J. Richter, T. K. Greathouse, T. Fouchet, F. Montmessin, F. Lefèvre, et al. 2016. “*Astronomy & Astrophysics* 586 (February): A62. <https://doi.org/10.1051/0004-6361/201527018>.

[6] Encrenaz, T., C. DeWitt, M. J. Richter, T. K. Greathouse, T. Fouchet, F. Montmessin, F. Lefèvre, et al. 2018. *Astronomy & Astrophysics* 612 (April): A112. <https://doi.org/10.1051/0004-6361/201732367>. Aoki et al., 2015.

[7] Aoki, S., Nakagawa, H., Sagawa, H., et al. 2015, *Icarus*, 260.

[8] Krasnopolsky, V. A. 2015, *Icarus*, 257, 377.

[9] Villanueva, G. L., Mumma, M. J., Novak, R. E., et al. 2015, *Science*, 348, 218.

## Performance of the ACS NIR channel and O<sub>2</sub> profiles

Anna Fedorova (1), Alexander Trokhimovskiy (1), Oleg Korablev (1), Franck Montmessin (2), Karim Gizatullin (1,3), Daria Betsis (1), Alexander Lomakin (1, 3), Andrey Patrakeev (1), Nikita Kokonkov (1), Alexey Shakun (1), Jean-Loup Bertaux (1,2) and the ACS team  
(1) Space Research Institute(IKI), Moscow, Russia, (2) LATMOS-UVSQ, Guyancourt, France; (3) MIPT, Dolgoprudnyi, Russia ([fedorova@iki.rssi.ru](mailto:fedorova@iki.rssi.ru))

### Abstract

The Atmospheric Chemistry Suite (ACS) is a set of three spectrometers (-NIR, -MIR, and -TIRVIM) intended to observe Mars atmosphere onboard the ESA-Roscosmos ExoMars 2016 Trace Gas Orbiter (TGO) mission. [1]. The near infrared channel (NIR) is a compact spectrometer operating in the range of 0.7–1.7  $\mu\text{m}$  with a resolving power of  $\lambda/\Delta\lambda \sim 25,000$ . It is designed to operate in nadir and in solar occultation modes. The spectrometer employs an acousto-optic tunable filter (AOTF) to select diffraction orders in an echelle spectrometer. During one measurement cycle it is possible to register up to ten different diffraction orders, each corresponding to an instantaneous spectral range of 10–20 nm.

The main task of NIR channel in nadir will be measurements of the water vapor in 1.38  $\mu\text{m}$  and the O<sub>2</sub> ( $a^1\Delta_g$ ) emission as a tracer of ozone at 1.27  $\mu\text{m}$ . The solar occultation is mostly aimed to study vertical distribution of water vapor and CO<sub>2</sub> density. Figure 1 illustrates the NIR sequence during a solar occultation, which includes measuring of 10 diffraction orders. Three orders are dedicated to different CO<sub>2</sub> bands, allowing one to profile the atmospheric density over a wide range of altitudes, three orders for H<sub>2</sub>O, one mixed order, two orders without significant gaseous absorption for measuring aerosols, and one order aimed for the O<sub>2</sub> at 0.76  $\mu\text{m}$  band.

A vertical profiling of the O<sub>2</sub> density is a unique feature of the ACS NIR science in occultation. No other instrument on a Mars orbiting platform being sensitive to O<sub>2</sub> from 10 to 60 km altitude range.

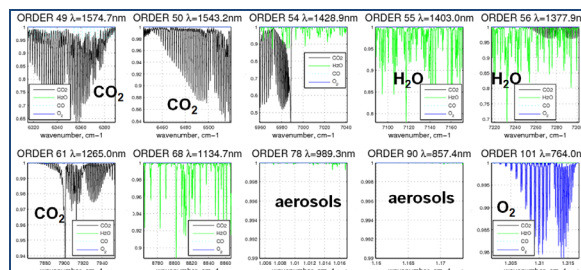


Figure 1: Standard measurement sequence of NIR in solar occultation includes 10 diffraction orders in the range of 0.76–1.58  $\mu\text{m}$

Here we present the calibration status, performances and first results of the O<sub>2</sub> density retrievals and H<sub>2</sub>O vertical profiles from the ACS/NIR solar occultations.

The status, constraints on the signal-to-noise ratio of NIR nadir measurements will be as well presented along with preliminary retrievals of H<sub>2</sub>O column abundance and the O<sub>2</sub> airglow intensity.

### Acknowledgements

ExoMars is the space mission of ESA and Roscosmos. The ACS experiment is led by IKI Space Research Institute in Moscow. The project acknowledges funding by Roscosmos and CNES. Science operations of ACS are funded by Roscosmos and ESA.

### References

- [1] Korablev, O., Montmessin, F., and ACS Team: The Atmospheric Chemistry Suite (ACS) of three spectrometers for the ExoMars 2016 Trace Gas Orbiter, Space Sci. Rev., 214:7, 2018.

# Improved near-infrared high-resolution solar spectrum from ACS NIR onboard TGO

**Karim Gizatullin** (1,2), Alexander Trokhimovskiy (1), Anna Fedorova (1) Oleg Korablev (1), Franck Montmessin (3), Daria Betsis(1), Jean-Loup Bertaux (1,3), Monique Spite (4) , and the ACS Team

(1) Space Research Institute (IKI), Moscow, Russia, (2) Moscow Institute of Physics and Technology (MIPT), Dolgoprudny, Russia, (3) LATMOS/IPSL, UVSQ Université Paris-Saclay, UPMC Univ. Paris 06, CNRS, Guyancourt, France, (4) GEPI Observatoire de Paris, CNRS, Guyancourt, France

## 1 Introduction

The Atmospheric Chemistry Suite (ACS) is Russian contribution to ESA-Roscosmos ExoMars 2016 Trace Gas Orbiter (TGO) mission [1], [2]. It arrived to Mars in October 2016. ACS is a package of three high sensitive infrared spectrometers with high resolve power ( $>10,000$ ) and cover from  $0.7$  to  $17\mu m$  — the visible to thermal infrared range [1].

In this work we present first results for high resolution solar spectra observed by ACS NIR [3] instrument in near infrared range.

## 2. Observations

The ACS NIR is a near infrared spectrometer, extension of SPICAM-IR instrument family [4], the main concept of which relies on the combination of an acousto-optic tunable filter (AOTF) and an echelle diffraction grating [1]. This combination gives resolving power  $\frac{\lambda}{\Delta\lambda} \approx 25,000$  in spectral range of  $0.73 - 1.65\mu m$  that corresponds to the echelle diffraction orders from 48 through 105. This is the first instrument that can measure with such high resolution in near-IR range outside the atmosphere. Here we present results that were obtained in June 2016 during Mid Cruise Checkout TGO Payload (MCC) observations of Sun. The NIR solar spectrum shows some undiscovered lines and differences from the known solar spectra in the range of  $1.3 - 1.5\mu m$  where the strong water absorption in the Earth atmosphere prevents from getting pure solar spectrum. The comparison with the Continuum Absorption at Visible and Infrared Wavelengths and its Atmospheric Relevance (CAVIAR) [5] solar spectrum and theoretical solar spectrum will be presented here.

## References

- [1] O. Korablev, F. Montmessin, A. Trokhimovskiy, A. A. Fedorova, A. V. Shakun, A. V. Grigoriev, B. E. Moshkin, N. I. Ignatiev, F. Forget, F. Lefèvre, K. Anufreychik, I. Dzuban, Y. S. Ivanov, Y. K. Kalinnikov, T. O. Kozlova, A. Kungurov, V. Makarov, F. Martynovich, I. Maslov, D. Merzlyakov, P. P. Moiseev, Y. Nikolskiy, A. Patrakeeve, D. Patsaev, A. Santos-Skripko, O. Sazonov, N. Semena, A. Semenov, V. Shashkin, A. Sidorov, A. V. Stepanov, I. Stupin, D. Timonin, A. Y. Titov, A. Viktorov, A. Zharkov, F. Altieri, G. Arnold, D. A. Belyaev, J. L. Bertaux, D. S. Betsis, N. Duxbury, T. Encrenaz, T. Fouchet, J.-C. Gérard, D. Grassi, S. Guerlet, P. Harrogh, Y. Kasaba, I. Khatuntsev, V. A. Krasnopolsky, R. O. Kuzmin, E. Lellouch, M. A. Lopez-Valverde, M. Luginin, A. Määttänen, E. Marcq, J. Martin Torres, A. S. Medvedev, E. Millour, K. S. Olsen, M. R. Patel, C. Quantin-Nataf, A. V. Rodin, V. I. Shematovich, I. Thomas, N. Thomas, L. Vazquez, M. Vincendon, V. Wilquet, C. F. Wilson, L. V. Zasova, L. M. Zelenyi, and M. P. Zorzano, “The atmospheric chemistry suite (acs) of three spectrometers for the exomars 2016 trace gas orbiter,” *Space Science Reviews*, vol. 214, p. 7, Nov 2017.
- [2] O. Korablev, A. Trokhimovsky, A. V. Grigoriev, A. Shakun, Y. S. Ivanov, B. Moshkin, K. Anufreychik, D. N. Timonin, I. Dziuban, Y. K. Kalinnikov, *et al.*, “Three infrared spectrometers, an atmospheric chemistry suite for the exomars 2016 trace gas orbiter,” *Journal of Applied Remote Sensing*, vol. 8, no. 1, p. 084983, 2014.
- [3] A. Trokhimovskiy, O. Korablev, Y. K. Kalinnikov, A. Fedorova, A. V. Stepanov, A. Y. Titov, I. Dziuban, A. Patrakeeve, and F. Montmessin, “Near-infrared echelle-aotf spectrometer acs-nir for the exomars trace gas orbiter,” in *Infrared Remote Sensing and Instrumentation XXIII*, vol. 9608, p. 960809, International Society for Optics and Photonics, 2015.
- [4] O. Korablev, J.-L. Bertaux, A. Fedorova, D. Fonteyn, A. Stepanov, Y. Kalinnikov, A. Kiselev, A. Grigoriev,

V. Jegoulev, S. Perrier, *et al.*, “Spicam ir acousto-optic spectrometer experiment on mars express,” *Journal of Geophysical Research: Planets*, vol. 111, no. E9, 2006.

- [5] K. P. Menang, M. D. Coleman, T. D. Gardiner, I. V. Ptashnik, and K. P. Shine, “A high-resolution near-infrared extraterrestrial solar spectrum derived from ground-based fourier transform spectrometer measurements,” *Journal of Geophysical Research: Atmospheres*, vol. 118, no. 11, pp. 5319–5331, 2013.

## Solar wind modulation of galactic cosmic rays observed on board of ExoMars TGO

**Rositza Koleva** (1), Jordanka Semkova (1), Victor Benghin (2), Tsvetan Dachev (1), Yuri Matviichuk (1), Borislav Tomov (1), Krasimir Krastev (1), Stephan Maltchev (1), Plamen Dimitrov (1), Igor Mitrofanov (3), Alexey Malahov (3), Dmitry Golovin (3), Maxim Mokrousov (3), Yuriy Yermolaev (3), Sergey Drobyshev (2)  
(1) Space Research and Technology Institute, Bulgarian Academy of Sciences, Sofia, Bulgaria, (2) Institute of Biomedical Problems of the Russian Academy of Sciences, Moscow, Russia, (3) Space Research Institute, Russian Academy of Sciences, Moscow, Russia  
rkoleva@stil.bas.bg

### Abstract

The FRIEND dosimeter Liulin-MO on board ExoMars TGO [6] in 2016 – 2017 measured GCR fluxes during TGO transit to Mars and on Mars high ecliptic orbit. During the interplanetary transit of TGO a good agreement between the fluxes provided by Liulin-MO and those measured by SIS instrument aboard ACE is observed. On high elliptic Mars orbit (31.10.2016 – 07.03.2017) Liulin-MO data match SIS data “delayed” by 5 days in average. During these periods no CME hit the Earth but multiple HSS were observed. We investigate the relation of GCR short-term variations to the observed solar wind parameters as measured aboard ACE to find how the flux depletions are related to the particular HSS.

### 1. Introduction

The 27 day variations in GCR intensities have been observed for many decades since the first announcement by Forbush [1]. On a short-term scale the GCR flux is modulated by interaction with non-homogeneous structures – high speed streams (HSS) and the interplanetary manifestations of coronal mass ejections that could be magnetic clouds (MC) and interplanetary coronal mass ejections (ICME) (e.g. [2], [3], [4]). These effects have been studied extensively using data from ground-based neutron monitors. Thus recorded GCR fluxes bear the effects of their interaction with the magnetosphere and the interaction of the primary and secondary particles with the atmosphere.

We focus on GCR variations caused by HSS and the leading them corotating interaction regions (CIRs). Different mechanisms were proposed to cause the

onset of GCR depression, including solar wind speed increases at stream edges, magnetic sector boundaries, magnetic field enhancements, and stream interfaces. Richardson [5] studied the effects of CIRs on GCR fluxes using data from several space probes. He concluded that interfaces between fast and slow solar wind streams and the leading edges of CIRs are responsible for the depression onset.

### 2. Data and results

Liulin-MO GCR fluxes in two perpendicular directions and the proton flux > 30 MeV by SIS instrument on ACE satellite [7] (located at L1 libration point at about 1 500 000 km from Earth) obtained from 22.04.2016 to 07.03.2017 are compared in Fig. 1. Note that Liulin-MO is not able to measure protons with energies below 30 MeV due to the shielding of its detectors. During the interplanetary transit of TGO a good agreement between the fluxes provided by the two instruments is observed. In high elliptic Mars orbit (31.10.2016 – 07.03.2017) Liulin-MO data match SIS data “delayed” by 5 days in average

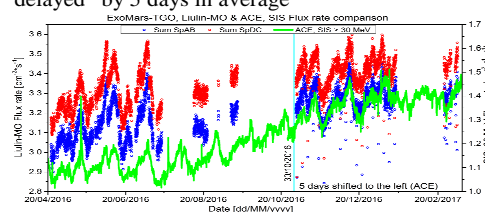


Figure 1. Liulin-MO GCR fluxes in two perpendicular directions and proton flux > 30 MeV by SIS instrument on ACE satellite obtained from 22.04.2016 to 07.03.2017

During the plotted period no CME hit the Earth but multiple HSS were observed according to NOAA Preliminary Reports and Forecasts of Solar Geophysical Data. Therefore it were HSS, which modulated SIS and Liulin-MO fluxes. As a first step we used the WSA-Enlil model (<http://iswa.ccmc.gsfc.nasa.gov/>) to look at the propagation of a possible HSS. During April – first half of July the Earth and Mars are located on near-by magnetic field lines and the HSS fronts reach both planets (and TGO still nearer to Earth than to Mars) roughly simultaneously. During November 2016 a possible HSS reaches Mars first and only after approximately 4 days reaches the Earth. At the end of the period – the beginning of March 2017 this delay is already about 6 days. In the scale of Fig. 1. an average delay of 5 days of ACE SIS data gives an admissible agreement with Liulin-MO GCR fluxes. The overall increase of the fluxes in both instruments observed from 22.04.2016 to 07.03.2017 can be attributed to the increase of GCR intensity during the declining phase of the solar activity.

We investigate the relation between GCR small-scale variations recorded by Liulin-MO on TGO transit to Mars and ACE SIS and solar wind (SW) disturbances - CIR and HSS - recorded on board ACE. To identify the SW disturbed regions we used velocity, density, proton temperature, module and components of IMF, proton thermal pressure, proton plasma  $\beta$  parameters (ratio of thermal and magnetic field pressures) and the method described in [8]. We identified about 15 regions with HSS. Usually CIRs/corotating high-speed streams depress the cosmic ray intensity, but there were two regions of HSS where no GCR flux depression was observed. The average depression in our cases is ~4%. In individual streams, the cosmic ray intensity and solar wind speed tend to be highly anti-correlated but exceptions occur. The recovery phase is more gradual than the onset phase. The depression onset is observed in different regions of the HSS – sometimes it is associated with the leading edge of the stream and the stream interface; with the leading or trailing edge of the CIR; or even inside the HSS. The depression maximum occurs around the maximum of SW speed, but it is rarely located in the vicinity of CIR trailing edge.

### 3. Summary and Conclusion

We presented a comparison between GCR fluxes measured aboard TGO by the FRENDO dosimeter

Liulin-MO and those measured by SIS instrument on ACE. Modelling of interplanetary medium during the investigated period showed that GCR small-scale variations observed by both instruments at different locations in the heliosphere are caused by one and the same HSS. Analyses of SW parameters measured on ACE showed that the onset of GCR flux depletions occur in different regions of the HSS. This does not give ground to make any conclusions about the mechanism of GCR-HSS interaction.

### Acknowledgements

This work was supported by: Contracts N 503/2-13 and 63/4-14 between IKI-RAS and SRTI-BAS; Agreement between RAS and BAS on fundamental space research; Contract No. 4000117692/16/NL/NDe Funded by the Government of Bulgaria through an ESA Contract under the PECS..

### References

- [1] Forbush, S. E.: On cosmic-ray effects associated with magnetic storms, *Terr. Magn. Atmos. Electr.*, Vol. 43, pp. 203–218, 1938
- [2] Badruddin ; Cosmic ray modulation: effects of high-speed solar wind streams, *Astrophys. and Space Sci.*, Vol. 246, pp. 171-191,1997.
- [3] Barouch E., Burlaga L.F.; Causes of Forbush decreases and other cosmic ray variations, *J. Geophys. Res.*, Vol. 80, pp. 449-456, 1975.
- [4] Cane H. V.; Coronal mass ejections and Forbush decreases, *Space Sci. Rev.*, Vol. 93, pp. 55-77, 2000
- [5] Richardson, I. G.; Energetic particles and corotating interaction regions in the solar wind, *Space Sci. Rev.*, Vol. 111, pp. 267–376, 2004
- [6] Semkova, J., et al.; Charged particles radiation measurements with Liulin-MO dosimeter of FRENDO instrument aboard ExoMars Trace Gas Orbiter during the transit and in high elliptic Mars orbit, *Icarus* Vol. 303, pp. 53–66, 2018.
- [7] Stone, E.C., et al.; "The Solar Isotope Spectrometer for the Advanced Composition Explorer". *Space Science Reviews*. Vol. 86, pp. 357–408, 1998
- [8] Yermolaev, Y. I., et al.; Catalog of large-scale solar wind phenomena during 1976–2000, *Kosm. Issled.*, Vol. 47(2), pp. 99–113. [Cosmic Research, pp. 81–94.]

# MA\_MISS: a miniaturized spectrometer on the ExoMars Drill System

M.C. De Sanctis (1), F. Altieri (1), E. Ammannito (2), S. De Angelis (1), M. Ferrari (1), D. Biondi (1) P. Tinivelli (1), R. Mugnuolo (2), S. Pirrotta (2) and the MA\_MISS team.

(1) Istituto di Astrofisica e Planetologia Spaziali (INAF-IAPS), Rome, Italy, mariacristina.desanctis@iaps.inaf.it, (2) Agenzia Spaziale Italiana, ASI, Italy

## Abstract

Ma\_MISS (Mars Multispectral Imager for Subsurface Studies) is the Visible and Near Infrared (VNIR) miniaturized spectrometer hosted by the drill system of the ExoMars 2020 rover. It will perform spectral reflectance investigations in the 0.4–2.2  $\mu\text{m}$  range to characterize the mineralogy of the excavated borehole wall at different depths ( $\leq 2$  m). Ma\_MISS has been completed and calibrated in early 2018 and is now on the way to be integrated on the rover.

## Introduction

Search for life on Mars is primarily focused on the analysis on the subsurface layers. Due to the very tenuous Martian atmosphere, potential chemical biosignatures at or in the vicinity of the Martian surface could have been degraded or destroyed by i) ultraviolet (UV) radiation ii) UV-induced photochemistry producing reactive oxidant species, and iii) ionizing radiation. The effects of the radiation decrease with depth: organic molecules and potential biomarkers could be better preserved in the subsurface. Thus, ExoMars rover is devoted to subsurface investigations for possible indicators of past life. Ma\_MISS instrument [1] is a miniaturized imaging spectrometer designed to provide spectra in the VNIR (0.4–2.2  $\mu\text{m}$ ) wavelength region. The spectral sampling is 20 nm while the spatial resolution is 120  $\mu\text{m}$ . By operating during pauses in drilling activity, it will produce spectra of the drill's borehole. Ma\_MISS is the only instrument in the rover's Pasteur payload able to analyze subsurface material in its natural condition (in situ), prior to extracting samples for further analysis. Ma\_MISS findings will help to refine criteria for deciding from where to collect samples.

## 1. MA\_MISS scientific objectives

Ma\_MISS will accomplish the following scientific objectives:

- 1) *determine the composition of subsurface materials:* MA\_MISS spectral range and high spatial resolution will allow identifying differences in lithologies. Analysis of absorption bands can be used to identify different mineralogical phases, such as iron-bearing minerals, silicates, oxides, hydrated materials, etc. [2, 3].
- 2) *map the distribution of subsurface ices:* Currently ice deposits in the Martian shallow subsurface have been inferred from remote-sensing detection of hydrogen [4], from permafrost evidences[5] and the detections of low latitude H<sub>2</sub>O frost on pole facing slopes [6]. Both H<sub>2</sub>O and CO<sub>2</sub> ices show diagnostic features in the Ma\_MISS spectral range.
- 3) *characterize important optical and physical properties of materials:* The study of spectral parameters, such as continuum reflectance level and slope can help to determine important physical parameters like the different grain sizes in materials that can help us to assess the type and state of sediments in the subsurface.
- 4) *produce a local stratigraphy of the subsurface:* Mars surface is rich in sedimentary outcrops that exhibit stratigraphic features at a range of spatial scales. Having access to the Martian subsurface will be fundamental to constrain the nature of processes at the ExoMars rover locations.

## 2. Instrument Description

The spectrometer is placed in a box on the side wall of the drill box (fig.1). The light from a 5W lamp is collected and carried, through an optical fiber bundle, to the miniaturized Optical Head (OH), hosted within the drill tip. A Sapphire Window (SW) with high hardness and transparency on the drill tip protects the Ma\_MISS OH allowing to observe the borehole wall. Different depths can be reached by the use of 3 extension rods, 50 cm long, each containing optical



## Modeling of aerosols from TIRVIM solar occultations onboard ExoMars/TGO

**Mikhail Luginin** (1), N. Ignatiev (1), A. Fedorova (1), A. Grigoriev (1), A. Shakun (1), A. Trokhimovsky (1), F. Montmessin (2), and O. Korablev (1)  
(1) Space Research Institute (IKI), Moscow, Russia (2) LATMOS, Guyancourt, France  
(mikhail.luginin@phystech.edu)

The ExoMars Trace Gas Orbiter (TGO) is a joint ESA-Roscosmos mission to Mars that has been launched in March 2016. The aerobreaking phase has ended in February 2018 followed by the start of nominal scientific work on the near-circular 400 km orbit in April 2018. The Atmospheric Chemistry Suite (ACS) is a set of three spectrometers (NIR, MIR, and TIRVIM), capable to observe Mars atmosphere in solar occultations, nadir and limb geometry [1]. TIRVIM instrument is a Fourier-spectrometer operating in the 1.7 to 17  $\mu\text{m}$  spectral range in solar occultation and nadir operation modes.

The main fraction of aerosols on Mars consists of mineral dust, while  $\text{H}_2\text{O}$  ice and  $\text{CO}_2$  ice crystals are also encountered depending on the season and location. TIRVIM with its wide spectral range permits a spectral separation between dust and  $\text{H}_2\text{O}$  ice clouds particles. This work is dedicated to aerosols modeling in the solar occultation mode. Preliminary analysis of the transmission spectra retrieved from the TIRVIM solar occultation data shows presence of both dust and  $\text{H}_2\text{O}$  ice aerosol particles on some altitudes.

### Acknowledgements

ExoMars is the space mission of ESA and Roscosmos. The ACS experiment is led by IKI Space Research Institute in Moscow. The project acknowledges funding by Roscosmos and CNES. Science operations of ACS are funded by Roscosmos and ESA. M. Luginin acknowledges the support from the Ministry of Education and Science of the Russian Federation, grant №14.W03.31.0017.

### References

- [1] Korablev, O. et al. The Atmospheric Chemistry Suite (ACS) of Three Spectrometers for the ExoMars 2016 Trace Gas Orbiter. *Space Science Reviews*, 214(1), 7, 2018. <http://doi.org/10.1007/s11214-017-0437-6>

# The NOMAD Spectrometer Suite on ExoMars Trace Gas Orbiter: Data Products, Format and Availability in the ESA Planetary Science Archive

Ian R. Thomas (1), Ann Carine Vandaele (1), Frank Daerden (1), Cédric Depiesse (1), Yannick Willame (1), Loïc Trompet (1), Sophie Berkenbosch (1), Roland Clairquin (1), Bram Beeckman (1), Bojan Ristic (1), Claudio Queirolo (1), Eddy Neefs (1), Jon Mason (2), Graham Sellers (2), Mark Leese (2), Brijen Hathi (2) Manish R. Patel (2), Giancarlo Bellucci (3), José Juan Lopez Moreno (4) and the NOMAD Team.

(1) BIRA-IASB, Brussels, Belgium; (2) Open University, Milton Keynes, U.K.; (3) IAPS/INAF, Rome, Italy; (4) IAA/CSIC, Granada, Spain (ian.thomas@aeronomie.be)

## Introduction

NOMAD, one of four scientific instruments on the ExoMars Trace Gas Orbiter (TGO), is a suite of three spectrometers operating in the UV-visible and infrared spectral ranges [3]. It was launched 2 years ago and, at the time of writing (May 2018), has begun making measurements as part of the TGO nominal science phase.

Data taken by NOMAD will be made available to the public and Mars community in NASA PDS4 format ([pds.jpl.nasa.gov/](http://pds.jpl.nasa.gov/)), the current standard for space science missions, via the ESA Planetary Science Archive ([archives.esac.esa.int/psa/](http://archives.esac.esa.int/psa/)). At the time of writing this abstract, the data is still under embargo - though this will be lifted soon, and therefore now is an opportune time to present the dataset to the scientific community.

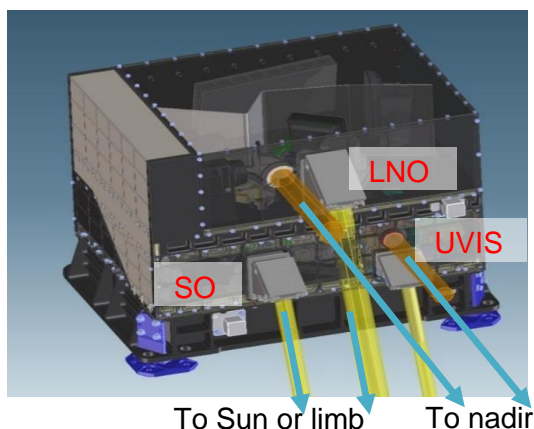


Figure 1: The NOMAD spectrometer suite.

There are three spectrometers within NOMAD, performing two main types of observations:

**Solar occultations**, where the sun is continually observed as the field of view passes through the atmosphere, have extremely high signal to noise ratios, but can only be performed when the orbital

position of the spacecraft allows it. On some occultations, the field of view never reaches the surface – these are known as grazing occultations.

**Nadir observations**, where the field of view is pointed to the ground directly below the spacecraft, and reflected sunlight is observed by the spectrometer. These can be measured regularly, but the trade-off is a lower signal to noise ratio.

The three channels are as follows:

**SO** (2.2-4.3 $\mu$ m, resolving power  $\sim$ 20000 and SNR $>$ 1000) which operates in solar occultation mode.

**LNO** (2.2-3.8 $\mu$ m, resolving power  $\sim$ 15000), which operates in nadir mode but can also measure in occultation and/or limb mode also.

**UVIS** (200-650nm), which operates in both solar occultation and nadir mode, and potentially in limb mode in future.

Both SO and LNO do not typically measure their entire spectral range every observation (though it is possible to do so). Instead, the range is split into  $\sim$ 100 diffraction orders, a selection of which are measured in an observation [1]. An acousto-optic crystal (AOTF) acts as a pass-band order-sorting filter, allowing radiation for the desired diffraction order to enter the spectrometer for a measurement, before the crystal driver frequency is changed to shift the pass-band onto another diffraction order [1]. Typically, up to 12 diffraction orders are measured during a solar occultation, and 2, 3 or 4 are measured during a nadir pass, however these values can be adapted depending on the observation conditions e.g. surface solar illumination angle. The choice of diffraction orders, the speed through which the diffraction orders are cycled, the detector readout rows (which affects the FOV direction), integration time, and many other parameters can also be varied – meaning that SO and LNO data can be complex to understand.

UVIS typically returns a full spectrum for each observation [2] (though a limited spectral range is also possible), and therefore no AOTF or diffraction order options exist. Multiple observation modes are possible, such as un-binned mode, where each pixel is read out individually (increasing SNR) rather than onboard binning if sufficient data volumes are available, and the nadir integration time depends on the surface illumination for a given observation.

## Data Products

The data products in the PSA are grouped as follows:

**Raw products:** these contain only uncalibrated housekeeping and science data.

**Partially processed products:** these contain a mixture of calibrated and uncalibrated datasets. The housekeeping (e.g. temperatures, voltages, etc.) are converted into SI units while the detector and observation parameters (e.g. AOTF driver frequency) remains in a raw format.

**Calibrated products:** these contain calibrated housekeeping, science and ancillary data. The process for calibrating the data is described in the next section.

**Derived products:** these are higher-level products created from single or multiple observations e.g. atmospheric densities or gas species maps.

## Data Pipeline

The three channels and multiple observation modes makes it very difficult to describe all possible variations. In general terms though, the nominal science data is calibrated as follows:

1. Housekeeping and observation parameters converted to SI units.
2. Geometry parameters added e.g. latitude, longitude, occultation tangent height,  $L_s$ , sub-solar and sub-TGO parameters, etc.
3. Spectral calibration (including temperature dependency and AOTF for SO/LNO).
4. Detector data corrections e.g. dark subtraction and/or vertical binning of detector rows (if applicable), correction/detection of bad pixels and other anomalies.
5. Straylight correction (UVIS only).
6. Radiometric calibration. For solar occultations by both UVIS and SO, the data is converted to

transmittance (where 1=top of atmosphere and 0=no signal). For nadir and limb observations, UVIS data is converted to radiance and LNO data is converted to either radiance factor or radiance. The resulting datasets will form the basis of the PSA calibrated products.

## Data Format

The NOMAD PSA collection is comprised of .xml label files which reference tabulated data stored in ASCII in .tab files. Metadata, such as observation parameters (e.g. time, diffraction order, start/end geometry) will be included here, allowing the searching and filtering of specific datasets using the PSA interface.

The tabulated data products contain one spectrum per line, including housekeeping, geometry, spectral calibration (e.g. wavelengths (UVIS) or wavenumbers (SO/LNO), AOTF function (SO/LNO), etc.), radiometric calibration (e.g. radiance), and radiometric calibration error (e.g. uncertainty in radiance).

## Acknowledgements

**The authors would like to thank everyone who has contributed to the design, construction, testing, operations and management of NOMAD and TGO.** The NOMAD experiment is led by the Royal Belgian Institute for Space Aeronomy (IASB-BIRA), assisted by Co-PI teams from Spain (IAA-CSIC), Italy (INAF-IAPS), and the United Kingdom (Open University). This project acknowledges funding by the Belgian Science Policy Office (BELSPO), with the financial and contractual coordination by the ESA Prodex Office (PEA 4000103401, 4000121493), by the Spanish Ministry of Economy, Industry and Competitiveness, by FEDER funds under grant ESP2015-65064-C2-1-P (MINECO/FEDER), and by the UK Space Agency through grant ST/P000886/1 and Italian Space Agency through grant 2018-2-HH.0.

## References

- [1] Neefs et al.: NOMAD spectrometer on the ExoMars trace gas orbiter mission: part 1 - design, manufacturing and testing of the infrared channels. Appl. Opt. 54:28. 2015.
- [2] Patel et al.: NOMAD spectrometer on the ExoMars trace gas orbiter mission: part 2 - design, manufacturing and testing of the UVIS channel. Appl. Opt. 56:10. 2017.
- [3] Vandaele A.C. et al.: Science objectives and performances of NOMAD, a spectrometer suite for the ExoMars TGO mission. PSS, 119:15. 2015.

# The NOMAD Spectrometer Suite on ExoMars Trace Gas Orbiter: First Results from the Commissioning and Nominal Science Phases

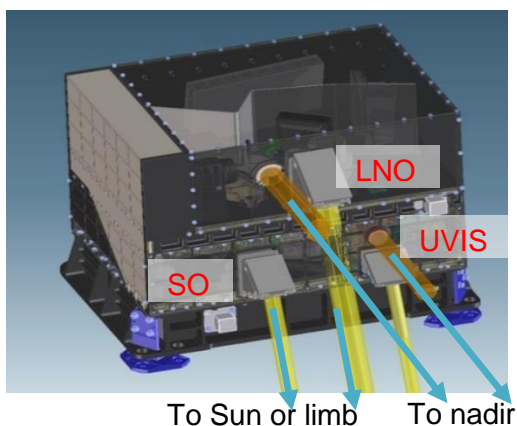
Ian R. Thomas (1), Ann Carine Vandaele (1), Séverine Robert (1), Loïc Trompet (1), Shohei Aoki (1,2, 3), Cédric Depiesse (1), Yannick Willame (1), Valérie Wilquet (1), Arianna Piccialli (1), Bojan Ristic (1), Claudio Queirolo (1), Frank Daerden (1), Justin T. Erwin (1), Lori Neary (1), Sébastien Viscardy (1), Sophie Berkenbosch (1), Roland Clairquin (1), Bram Beekman (1), Eddy Neefs (1), Jon Mason (4), Manish R. Patel (4), Giancarlo Bellucci (5), José Juan Lopez Moreno (6) and the NOMAD Team.

(1) BIRA-IASB, Brussels, Belgium; (2) Fonds National de la Recherche Scientifique, Belgium, (3) Tohoku University, Japan, (4) Open University, U.K; (5) IAPS/INAF, Rome, Italy; (6) IAA/CSIC, Granada, Spain (ian.thomas@aeronomie.be)

## Abstract

NOMAD, one of four scientific instruments on the ExoMars Trace Gas Orbiter, is a suite of spectrometers operating in the ultraviolet, visible and infrared spectrum. It was launched in 2016 and, at the time of writing, has just started the nominal science phase after one month of in-orbit commissioning. This presentation will describe some of the first results from all three spectrometers within NOMAD, in addition to detailing our plans for making future observations and analysing the incoming data to increase our understanding of Mars.

## 1. Scientific Objectives



Detection and mapping of new and existing gas species are the highest priority science objectives for NOMAD [4]. Many atmospheric constituents that can be measured are important markers of geophysical and/or biogenic activity, and therefore detecting the presence of such molecules and mapping their sources and sinks will greatly improve our knowledge of the red planet. Optical properties, such as particle size distributions of dust and ice aerosols, and measurements of the UV surface radiation

environment will also be repeatedly monitored by NOMAD over the course of the TGO mission, in addition to the continued mapping of water, carbon, ozone and other climatologic cycles occurring in the atmosphere of Mars [4].

## 2. The NOMAD Channels

There are two main types of observations performed by NOMAD:

**Solar occultations**, where the sun is continually observed as the instrument field of view passes through the atmosphere, have extremely high signal to noise ratios, but can only be performed when the orbital position of the spacecraft allows such observations to be made.

**Nadir observations**, where the instrument field of view is pointed towards the surface directly below the spacecraft, and reflected sunlight is observed. These observations can be measured on all orbits, but the trade-off is a lower signal to noise ratio than for solar occultations.

When atmospheric vertical profiles from solar occultations - taken by the SO and UVIS channels - and spectra from nadir observations - taken by the LNO and UVIS channels - are combined, they will provide an immense dataset for probing the composition of the atmosphere in great detail. Both infrared channels have a similar spectral range (2.2-4.3 $\mu\text{m}$  for SO; 2.2-3.8 $\mu\text{m}$  for LNO) and very high spectral resolution ( $\sim 0.1\text{-}0.2\text{cm}^{-1}$  for SO and  $\sim 0.15\text{-}0.25\text{cm}^{-1}$  for LNO, depending on wavenumber) allowing gas absorption lines to be measured in unprecedented detail [1]. The infrared spectral range covers many major and minor constituents, such as  $\text{CO}_2$ ,  $\text{CO}$ ,  $\text{H}_2\text{O}$ ,  $\text{HDO}$ ,  $\text{NO}_2$ ,  $\text{N}_2\text{O}$ ,  $\text{O}_3$ ,  $\text{CH}_4$ ,  $\text{C}_2\text{H}_2$ ,  $\text{C}_2\text{H}_4$ ,  $\text{C}_2\text{H}_6$ ,  $\text{H}_2\text{CO}$ ,  $\text{HCN}$ ,  $\text{OCS}$ ,  $\text{SO}_2$ ,  $\text{HCl}$ ,  $\text{HO}_2$ , and  $\text{H}_2\text{S}$  [3,4]. UVIS operates in the 200-650nm region, with a spectral resolution of  $\sim 1.2\text{-}1.6\text{nm}$ , providing crucial

data on the ultraviolet and visible regions of the spectrum - observing simultaneously with the SO and LNO channels - to detect O<sub>3</sub>, SO<sub>2</sub>, dust/ice opacities and clouds, among others [2].

### 3. Observations

All channels of NOMAD are highly configurable, and therefore planning observations effectively is a high priority for the team. The SO and LNO channels do not typically measure the entire spectral range in each observation. Instead, specific spectral ranges are chosen based on the absorption lines visible, and are measured repeatedly throughout a single nadir or solar occultation. The optimum number of spectral regions chosen is a trade-off between SNR and molecular detection: the greater the number of spectral ranges measured in an observation, the more molecules can be measured simultaneously, but at the expense of SNR. For solar occultations, SNR is not an issue, therefore up to 12 spectral regions are measured every occultation; however in nadir signals are much lower therefore normally only 2, 3 or 4 spectral regions are used. Also, the noise is reduced when the instrument temperature is lower; therefore LNO is not run on every orbit, allowing NOMAD to remain in its optimum thermal range. Similar options exist for UVIS, namely variations in integration time, and whether to run in binned or unbinned detector mode (the latter gives higher SNRs but requires more data volume).

Observations are chosen based on solar illumination angle, interesting surface sites, available data rates, etc. At present the allocated data volume is very high, however this will decrease as we move towards solar conjunction, forcing all the instruments on board to prioritise certain observations over others. All these trade-offs must be studied and the results fed back into the planning of future observations to optimise the science return from NOMAD.

### 4. Results

The nominal science phase has just begun, and so results at present are limited. NOMAD has performed one month of nadir-only measurements in the spacecraft commissioning period, and has now started the nominal science period where normal solar occultations measurements can be performed. Special measurements, such as limb measurements, grazing solar occultations (where the tangent altitude never reaches the surface), and *fullscans* (where the whole spectral range is measured) are all to be tested in this nominal science phase, plus a wide range of

calibration measurements are to be performed also. Results from all types of observations will be analysed and presented.

## 5. Summary and Conclusions

At the time of writing this abstract, the nominal science period has just begun and the incoming data is just starting to be calibrated and analysed. By the time of the conference, around 5 months of data will have been taken, and once analysed there will be many results to report. The aim of this presentation is to give the audience a general overview of the observations, data acquired, initial results, and future plans for the three channels onboard NOMAD.

## Acknowledgements

**The authors would like to thank everyone who has contributed to the design, construction, testing, operations and management of NOMAD and the TGO.** The NOMAD experiment is led by the Royal Belgian Institute for Space Aeronomy (IASB-BIRA), assisted by Co-PI teams from Spain (IAA-CSIC), Italy (INAF-IAPS), and the United Kingdom (Open University). This project acknowledges funding by the Belgian Science Policy Office (BELSPO), with the financial and contractual coordination by the ESA Prodex Office (PEA 4000103401, 4000121493), by the Spanish Ministry of Economy, Industry and Competitiveness, by FEDER funds under grant ESP2015-65064-C2-1-P (MINECO/FEDER), and by the UK Space Agency through grant ST/P000886/1 and Italian Space Agency through grant 2018-2-HH.0. This research was also performed as part of the "Excellence of Science" project "Evolution and Tracers of Habitability on Mars and the Earth" (FNRS 30442502) and supported by the BrainBe SCOOP and CRAMIC (FNRS) projects.

## References

- [1] Neefs et al.: NOMAD spectrometer on the ExoMars trace gas orbiter mission: design, manufacturing and testing of the infrared channels. *Appl. Opt.* 54:28. 2015.
- [2] Patel et al.: NOMAD spectrometer on the ExoMars trace gas orbiter mission: part 2 - design, manufacturing and testing of the UVIS channel. *Appl. Opt.* 56:10. 2017.
- [3] Robert, S., et al., "Expected performances of the NOMAD/ExoMars instrument", *Planetary and Space Science*, 124 94-104. 2016
- [4] Vandaele A.C. et al.: Science objectives and performances of NOMAD, a spectrometer suite for the ExoMars TGO mission. *PSS*, 119:15. 2015.

## First measurements of Martian CO by NOMAD/EMTGO

**Séverine Robert** (1), Justin T. Erwin (1), Shohei Aoki (1, 2, 3), Loïc Trompet (1), Ann Carine Vandaele (1), Ian R. Thomas (1), Michael D. Smith (4), Geronimo L. Villanueva (4), Marco Giuranna (5), Brittany Hill (6), Bernd Funke (6), Manuel Lopez Pueras (6), Miguel A. Lopez Valverde (6), Frank Daerden (1), Lori Neary (1), Bojan Ristic (1), Sébastien Viscardy (1), Arianna Piccialli (1), Valérie Wilquet (1), Giuseppe Sindoni (5), Giancarlo Bellucci (5), José Juan Lopez-Moreno (6), Manish R. Patel (7) and the NOMAD team

(1) Royal Belgian Institute for Space Aeronomy, BIRA-IASB, Belgium, (2) Fonds National de la Recherche Scientifique,FRS-FNRS, Belgium, (3) Tohoku University, Japan, (4) NASA Goddard Space Flight Center, Greenbelt, MD, USA, (5) Istituto di Astrofisica e Planetologia Spaziali (IAPS), Istituto Nazionale di Astrofisica (INAF), Rome, Italy, (6) Instituto de Astrofisica de Andalucia (IAA/CSIC), Granada, Spain, (7) Open University, Milton Keynes, UK, (severine.robert@aeronomie.be)

### Abstract

As of 21st April 2018, ExoMars Trace Gas Orbiter entered the Science Phase. The first measurements of NOMAD onboard EMTGO were planned, driven both by validation and by science. Spectra of Martian CO were recorded using the two infrared channels of NOMAD, in nadir with NOMAD-LNO and in solar occultation with NOMAD-SO. A preliminary analysis has been performed leading to the first vertical profiles of CO and a sparse map of CO. These results will be presented and compared to the latest results of CRISM/MRO and PFS/MEX.

### 1. The NOMAD instrument

NOMAD, the "Nadir and Occultation for MARS Discovery" spectrometer suite [1] is part of the payload of the ExoMars Trace Gas Orbiter mission 2016. The instrument will conduct a spectroscopic survey of Mars' atmosphere in UV, visible and IR wavelengths covering the 0.2 - 0.65 and 2.3 - 4.3  $\mu\text{m}$  spectral ranges. NOMAD is composed of 3 channels: a solar occultation channel (SO) operating in the infrared wavelength domain, a second infrared channel observing nadir, but also able to perform solar occultation and limb observations (LNO), and an ultraviolet/visible channel (UVIS) that can work in all observational modes. The spectral resolution of SO and LNO surpasses previous surveys in the infrared by more than one order of magnitude ( $\lambda/d\lambda \sim 15000$ ).

Both SO and LNO consist of an echelle grating in combination with an acousto-optic tunable filter (AOTF): the dispersive element provides the spectral

discrimination, while the filter selects the diffraction order [1]. An infrared detector array is actively cooled in order to maximise the signal-to-noise ratio. The design of the three channels has been fully described in [3] and in [4] for the UVIS and the IR channels respectively.

Calibration and validation have been performed and will be discussed in [5]. Level 1.0 data were made available to the NOMAD team in order to fully exploit the analysis.

### 2. Martian carbon monoxide

Carbon monoxide is a non-condensable species playing a major role in the photochemical cycle of CO<sub>2</sub>. Local and seasonal variations are expected and will give valuable constraints to model the dynamical processes in the Martian atmosphere. A climatology has been established recently using the CRISM data[6]. Continuous monitoring of the Martian water, carbon, ozone and dust cycles is part of the NOMAD science objectives. This would enable to extend existing datasets made by successive space missions in the past decades. In this presentation, we will focus on carbon monoxide (CO). The 2-0 band of CO centered at 2.35  $\mu\text{m}$  is measured by NOMAD-LNO and NOMAD-SO channels, mainly in its diffraction orders 189-191. The corresponding wavenumbers are given in Table 1.

#### 2.1. In nadir, with NOMAD-LNO

The footprint of a 15 sec measurement will cover a spatial region from 0.5x68 km<sup>2</sup> up to 17x51 km<sup>2</sup> for NOMAD-LNO. Considering the circular orbit

Table 1: Wavenumber limits in  $\text{cm}^{-1}$  of the diffraction orders for the two infrared channels of NOMAD.

	SO	LNO
189	4247.48-4281.33	4248.36-4282.30
190	4269.95-4303.99	4270.84-4304.96
191	4292.42-4326.64	4293.32-4327.61

of EMTGO, a global revisit time of 7 sols with varying local times is expected. These characteristics enable us to derive a first map of CO column-integrated abundances using the NOMAD-LNO measurements. The a priori information and the results of the retrievals will be presented. If any overlap with previous measurements of CRISM[6] and PFS[7] is obtained, the comparison will be shown.

## 2.2. In solar occultation, with NOMAD-SO

The sampling rate for the solar occultation measurement is 1 km, which provides unprecedented vertical resolution spanning altitudes from the surface to 200 km. This allows us to investigate vertical profiles of the atmospheric constituents. Solar occultation spectra have not been analysed yet but the transmittances were calculated using the method developed for the SOIR/VEX instrument[8]. The first profiles of CO abundances will be retrieved using these transmittances.

## Acknowledgements

The NOMAD experiment is led by the Royal Belgian Institute for Space Aeronomy (IASB-BIRA), assisted by Co-PI teams from Spain (IAA-CSIC), Italy (INAF-IAPS), and the United Kingdom (Open University). This project acknowledges funding by the Belgian Science Policy Office (BELSPO), with the financial and contractual coordination by the ESA Prodex Office (PEA 4000103401, 4000121493), by Spanish Ministry of Economy, Industry and Competitiveness, by FEDER funds under grant ESP2015-65064-C2-1-P (MINECO/FEDER), as well as by UK Space Agency through grant ST/P000886/1 and by Italian Space Agency through grant 2018-2-HH.0. The research was performed as part of the ‘‘Excellence of

Science’’ project ‘‘Evolution and Tracers of Habitability on Mars and the Earth’’ (FNRS 30442502). This research was supported by the FNRS CRAMIC project under grant number T.0171.16 and by the BrainBe SCOOP project. US investigators were supported by the National Aeronautics and Space Administration.

## References

- [1] Neefs, E., Vandaele, A.C., Drummond, R., Thomas, I.R. et al.: NOMAD spectrometer on the ExoMars trace gas orbiter mission: part I – design, manufacturing and testing of the infrared channels, *Applied Optics*, Vol. 54(28), pp. 8494-8520, 2015.
- [2] Vandaele, A.C., Neefs, E., Drummond, R., Thomas, I.R., Daerden, F. et al.: Science objectives and performances of NOMAD, a spectrometer suite for the ExoMars TGO mission, *Planetary and Space Science*, Vol. 119, pp. 233-249, 2015.
- [3] Vandaele, A.C., Willame, Y., Depiesse, C., Thomas, I.R., et al.: Optical and radiometric models of the NOMAD instrument part I: the UVIS channel, *Optics Express*, Vol. 23(23), pp. 30028-30042, 2015.
- [4] Thomas, I.R., Vandaele, A.C., Robert, S., Neefs, E. et al.: Optical and radiometric models of the NOMAD instrument part II: the infrared channels - SO and LNO, *Optics Express*, Vol. 24(4), pp. 3790-3805, 2016.
- [5] Thomas, I.R. et al., EPSC 2018
- [6] Smith, M.D., Daerden, F., Neary, L. and Khayat, A.: The climatology of carbon monoxide and water vapor on Mars as observed by CRISM and modeled by the GEM-Mars general circulation model, *Icarus*, Vol. 301, pp. 117-131, 2018.
- [7] Giuranna, M., Carraro, F., Wolkenberg, P., Grassi, D., Aronica, A., Aoki, S., Scaccabarozzi, D., Saggini, B., Formisano, V., and the PFS team: New dataset of atmospheric parameters retrieved by PFS-MEx, Scientific Workshop: ‘‘From Mars Express to ExoMars’’, 27-28 February 2018, ESAC Madrid, Spain.
- [8] Trompet, L., Mahieux, A., Ristic, B., Robert, S., Wilquet, V., Thomas, I.R., Vandaele, A.C. and Bertaux, J.-L.: Improved algorithm for the transmittance estimation of spectra obtained with SOIR/Venus Express, *Applied Optics*, Vol. 55(32), pp. 9275-9281, 2016.

# “Lucky Strike”: A terrestrial analog for hydrothermal fields on ancient Mars with implications for the ExoMars rover

Ottaviano Ruesch (1), Jorge L. Vago (1), Thibaut Barreyre (2)

(1) European Space Agency, ESTEC, Keplerlaan 1, 2201 AZ Noordwijk, The Netherlands, (ottaviano.ruesch@esa.int). (2) Norwegian Marine Robotics Facility, KG Jebsen Centre for Deep Sea Research, University of Berger, Bergen, Norway.

## Abstract

If hydrothermal systems developed on ancient Mars they are likely to have hosted favorable conditions for life and its emergence. Thus, the identification and study of hydrothermal contexts on Mars by robotic exploration (e.g., ExoMars) is currently a high priority. Here we use terrestrial submarine hydrothermal fields as analog to investigate the morphological and mineralogical characteristics of putative hydrothermal deposits developed during the Early- to Middle-Noachian periods of Mars and their potential preservation up to recent times.

## 1. Introduction

The environment of Mars during the Early- to Middle-Noachian periods was characterized by a higher internal heat flux and denser atmosphere relative to today's Amazonian Mars, likely producing temperatures around 273 K at the surface [1]. The internal radiogenic heat was probably dissipated through the young crust along tectonic systems and, at the surface, in spatially limited areas such as volcanic centers. Water from magmatic outgassing and exogenous delivery by impacts was probably globally abundant and interacted with the volcanic centers. The subsurface and surface interaction led to the development of geologic features that, as proposed below, were not dissimilar to current submarine hydrothermal fields on Earth. During the Hesperian, the diminishing availability of surface water and intensity of volcanism has possibly limited hydrothermalism to impact craters [2].

This inferred context has been determined to be one of the most likely ancient habitable environment of Mars [1, 3], based on the fact that hydrothermal systems of the Archean Earth are recognized as a very favorable environment for the concentration of

organics and subsequent emergence of life [4]. For example, the analysis of a 3.3 Ga old Archean Earth chert sample belonging to a hydrothermal, shallow-marine depositional setting revealed that hydrothermal fluids can sustain a high biomass [5]. For this reason, the candidate landing sites of the ExoMars rover are on Noachian-aged terrains [1]. Current submarine hydrothermal fields in volcanic areas on Earth are reasonable analogs for some type of environment on ancient Mars. The exact geological properties of hydrothermal sites that might have existed on Noachian Mars are unknown and might have been diverse, including settings such as subaerial, shallow submarine and deep submarine, and with morphologies such as diffuse or focused outflow. Here we focus on a particular site with the following characteristics [6, 7]: (i) a submarine context different from subaerial systems [8]; (ii) strongly influenced by tectonics in a low-spreading context, (iii) a relatively well studied area for which remote sensing observations have been recently acquired. (iv) is currently active with pristine features. We first review the geomorphology and mineralogy of this site and then consider the modification of a similar putative hydrothermal field on Mars during the Hesperian and Amazonian periods on the base of additional terrestrial analogs.

## 2. The Mid-Atlantic Ridge hydrothermal field “Lucky Strike”

The Lucky Strike segment on the low-spreading Mid-Atlantic Ridge is located at  $\sim 37^{\circ}2'$  N/ $\sim 32^{\circ}2'$  W, about 400 km southwest from the Azores Islands. The hydrothermal site was discovered in 1992 on the 13-km wide Lucky Strike volcano, itself found within an axial rift valley of the ridge [9, 10]. The hydrothermal vent field extends over 1 km<sup>2</sup> (Figure 1) with both low and high temperature venting, diverse

outflow morphologies, various substrata and faults [7]. Outflow morphologies include active sulfide mounds 1-20 m wide and several meters high with associated highly-porous chimneys and flanges; extinct mounds composed of sulfide blocks and rubble; patches of diffuse venting with no topographic relief, and networks of cracks. The substrate is primarily basalt covered by sulfide deposits, hydrothermally cemented breccia or talus material. Active venting is observed to be generally within 10 m from fault scarps, indicating that the extensive fault system is controlling the hydrothermal discharge [6, 7]. In addition to faults, the outflows are associated with volcanic morphologies such as a lava lake and volcanic cones. Several of the geologic properties of this field are identifiable in the local topography at a 1-m spatial resolution (Figure 1). Morphological detection of diffuse venting and surface cracking, instead, requires optical imagery at a sub-meter spatial resolution.

### 3. Post-formation modification of a putative hydrothermal field

In order to understand the post-formation modifications occurred during the Hesperian and Amazonian periods of a putative, Noachian-aged hydrothermal field, we consider massive sulfide deposits on Earth [12]. The deposits are remnants of hydrothermal fields after burial by sediments, diagenesis and exhumation. They are the only large-scale remnant feature that might be identified with remote sensing data without relying on in situ chemical analysis. Massive sulfide deposits correspond to Archean or younger sulfide mounds and consist of a massive lens of variable shape (mound, sheet), configuration (single, stacked, disseminated), and size (10-100s m) in a host rock of a different lithologic property [12]. The massive lens is associated with concordant exhalites and a discordant zone of veins in a host rock altered into clays and chlorites [12].

During burial, the mineralogy of massive sulfide deposit will not exceed the greenschist facies on Mars, corresponding to <10 km burial material. Chemical weathering, however, will probably replace sulfides with oxides, sulfates and quartz (gossan) [12, 13]. On Mars, the original context of formation of massive sulfide deposits could be modified by impact excavation and ejecta emplacement, rather than subduction and orogenesis.

We will discuss the differences between the Noachian context and today's spreading ridges on Earth, in particular the effect of the absence of plate tectonics (e.g., rift systems, subduction, orogenesis) on the factors controlling the small-scale geology of a hydrothermal field (heat source and permeability). We will further discuss the preservation of Noachian-aged hydrothermal deposits, and whether future in situ measurements by the ExoMars rover might be able to identify and assess ancient hydrothermal conditions.

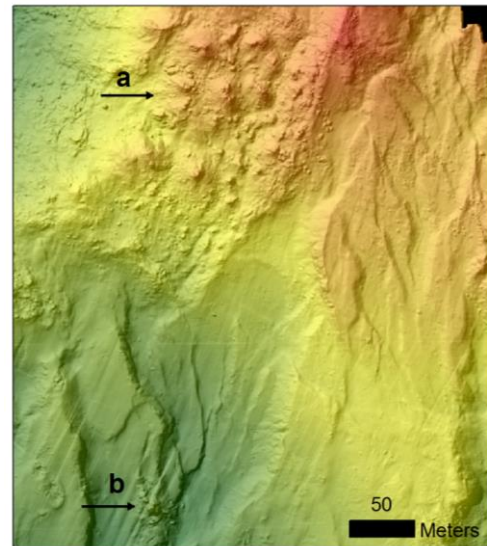


**Figure 1:** Hill-shaded map with color-coded topography (red: -1600 m, blue -1700 m) of an area within the Lucky Strike hydrothermal field. Mounds clusters (labelled a and b) are identified as isolated topographic peaks. Figure modified from [6].

### 4. References

- [1] Vago, J., et al., *Astrobiology*, vol. 17, 6-7, 471-510, (2017).
- [2] Marzo, G. A., *Icarus*, v. 208, 667-683, (2010).
- [3] Westall, F., in *Frontiers of astrobiology*, (2012).
- [4] Russell, M. J., et al., *Astrobiology*, vol. 14, 308-343, (2014).
- [5] Westall, F., et al., *Geology*, vol. 43, 615-618, (2015).
- [6] Ondreas, H., et al., *Geochem. Geophys. Geosyst.*, Vol. 10, 2, (2009).
- [7] Barreyre, T., et al., *Geochem. Geophys. Geosyst.*, vol. 13, 4, (2012).
- [8] Rossi P. A., et al., *J. Geophys. Res.*, vol. 113, E08016, (2008).
- [9] Langmuir, C. H., et al., *EOS Trans. AGU* 74: 99 (1993).
- [10] Langmuir, C. H. et al. *Earth Plan Sci Lett* 148: 69-91, (1997).
- [11] Schardt, C., and Large, R.R., *Ore Geology Review*, vol. 35, 335-351, (2009).
- [12] Shanks, W. C. P., and Thurston R. Eds. *Volcanogenic Massive sulfide occurrence model*, USGS report 2010-5070-C.
- [13] Burns, R. G., and Fisher, D. S., *J. Geophys. Res.* Vol. 95, B9, 14169-14173, (1990).

## Calibration of the NOMAD-UVIS channel

**Cédric Depiesse** (1), Yannick Willame (1), Ann Carine Vandaele (1), Ian R. Thomas (1), David Bolsée (1), Eddy Neefs (1), Sophie Berkenbosch (1), Roland Clairquin (1), Manish R. Patel (2), Jon Mason (2), Mark Leese (2), Brijen Hathi (2), Mike J. Wolff (3), R. Todd Clancy (3), Francesca Altieri (4), Giancarlo Bellucci (4), Jose-Juan Lopez-Moreno (5), Tanguy Thibert (6) and the NOMAD team

(1) Royal Belgian Institute for Space Aeronomy, Belgium, (2) Open University, UK, (3) SSI - Space Science Institute, Boulder, USA (4) Italian National Institute for Astrophysics, Italy, (5) IAA-CSIC, Spain, (6) Centre Spatial de Liège, Belgium (cedric.depiesse@aeronomie.be)

### Abstract

NOMAD (Nadir and Occultation for Mars Discovery) [1,2] is one of the four instruments on-board the ExoMars 2016 Trace Gas Orbiter (TGO). It consists of three high-resolution spectrometers (SO, LNO and UVIS). We present here the calibration of the NOMAD-UVIS channel.

### 1. The NOMAD-UVIS channel

The NOMAD-UVIS channel consists of a grating spectrometer in the Czerny-Turner configuration ranging from 200 nm to 650 nm with a resolution of 1.5 nm and a second order filter. Observations are obtained both in nadir and Solar Occultation (SO) through two dedicated telescopes. A mechanical selector drives the optical fibers to the entrance of the spectrometer. The detector is a CCD with [256 x 1024] pixels that can operate in full frame or vertically binned mode, where the latter is used to increase the signal-to-noise ratio and to reduce the data rate.

### 2. Ground calibration campaign

The calibration campaign took place at the Centre Spatial de Liège during thermal tests performed just before the integration of NOMAD onto TGO. The calibration measurements were performed at 5 different temperatures from -15° to +20°C. The Optical Ground Support Equipment (OGSE) consisted of a structure containing a set of 3 radiometrically calibrated lamps covering the bandwidth of the NOMAD-UVIS channel: 4 Pen-Ray lamps and an absorption cell containing SO<sub>2</sub> gas facing the nadir telescope, where the assembly was aligned using lasers. The SO will operate in transmittance and as it is considered to be a self-calibrating observation, no specific ground

calibration was performed. Assessment of the performance will rely on in-flight relative measurements and direct solar observations.

### 3. Results of the calibration

The analysis of the data obtained during the calibration campaign have allowed us to characterize the response of the spectrometer and to convert the raw data into real physical quantities (i.e., radiometric calibration):

- We have determined a mask for the “bad pixels” (essentially a list of the identified problematic pixels);
- The dark current is subtracted using measurements recorded before and after each set of observations. This approach allows on to take into account the variation of the temperature during an observation. The same process is used for in-flight data;
- The linearity of the detector’s response as function of both the integration time and the temperature;
- The pixel-wavelength relation (i.e., wavelength calibration) based on the lines of the Pen-Ray lamps and confirmed by in-flight measurements of solar lines. No temperature-dependence of the wavelength was observed;
- The radiometric calibration was determined using the 3 standard lamps to cover the wavelength range of UVIS;

- characterization of a straylight component, which is much larger in the UV than would be ideal (see next section).

#### 4. The straylight issue

A significant straylight signal has been identified, but unfortunately well after the calibration of the flight model calibration campaign. To better characterize it, we have used the NOMAD “flight spare” model. Tests and measurements with this model show that there are two components of the straylight. One “internal” (or in-band), coming from light within the bandwidth of the spectrometer (200 nm – 650 nm) called UV-visible straylight. A second component originates from outside the observed range (650 nm – 1100 nm), which we call IR straylight. The calibration must treat these two components explicitly, but separately. The UV-visible straylight will be corrected using the Zhong method [3] which consist in characterizing the instrument’s response to a set of monochromatic laser sources that cover the instrument’s spectral range. One obtains a spectral stray light signal distribution matrix that quantifies the magnitude of the spectral stray light signal within the instrument. By use of these data, a spectral stray light correction matrix is derived and the instrument’s response can be corrected with a simple matrix multiplication. For the IR straylight component, we studied it using a set of 50 nm bandpass filters. This allowed us to derive the quantity of straylight for each wavelength interval. The current method to IR straylight characterization requires a robust estimation of the actual radiance in the 650 to 1100nm spectral range. This is currently achieved using a typical IR radiance spectrum of Mars rescaled to the value measured at 600nm with the NOMAD-UVIS channel (wavelength where the straylight quantity is minimum in the spectrometer). The result for the straylight removal method obtained on the spare model is then extrapolated to the flight model.

#### Acknowledgements

The NOMAD experiment is led by the Royal Belgian Institute for Space Aeronomy (BIRA-IASB), assisted by Co-PI teams from Spain (IAA-CSIC), Italy (INAF-IAPS), and the United Kingdom (Open University). This project acknowledges funding by the Belgian Science Policy Office (BELSPO), with the financial and contractual coordination by the ESA Prodex Office (PEA 4000103401, 4000121493), by

MICIIN through Plan Nacional (AYA2009-08190 and AYA2012-39691), by UK Space Agency through grant ST/P000886/1, as well as and Italian Space Agency through grant 2018-2-HH.0.

#### References

- [1] Vandaele, A.C., et al.: Science objectives and performances of NOMAD, a spectrometer suite for the ExoMars TGO mission, *Planet. Space Sci.*, Vol. 119, pp 233-249, 2015.
- [2] Neefs, E., et al.: NOMAD spectrometer on the ExoMars trace gas orbiter mission: part1 – design, manufacturing and testing of the infrared channels, *Appl. Opt.*, Vol. 54(28), pp 8494-8520, 2015.
- [3] Y. Zong, S. Brown, B. Johnson, K. Lykke, and Y. Ohno, "Simple spectral stray light correction method for array spectroradiometers," *Appl. Opt.* 45, 1111-1119 (2006).

## Definition of a surface index based on previous datasets, to be used on NOMAD/EMTGO spectra

Séverine Robert (1), Ozgur Karatekin (2), Elodie Gloesener (2,3), Louis Ruel (1,2), Filippo Giacomo Carrozzo (4), Francesca Altieri (4), Ann Carine Vandaele (1), Frank Daerden (1), Ian R. Thomas (1), Bojan Ristic (1), Giancarlo Bellucci (4), Manish R. Patel (5), José Juan Lopez-Moreno (6) and the NOMAD team

(1) Royal Belgian Institute for Space Aeronomy, BIRA-IASB, Belgium, (2) Royal Observatory of Belgium, KSB-ORB, Belgium, (3) Université Catholique de Louvain, Belgium, (4) Istituto di Astrofisica e Planetologia Spaziali (IAPS), Istituto Nazionale di Astrofisica (INAF), Rome, Italy, (5) Open University, Milton Keynes, UK, (6) Instituto de Astrofisica de Andalucia (IAA/CSIC), Granada, Spain (severine.robert@aeronomie.be)

### Abstract

The NOMAD instrument onboard ExoMars Trace Gas Orbiter is composed of three channels. One of those is called LNO, for "Limb, Nadir and Occultation". It is an echelle grating coupled to an Acousto-Optic Tunable Filter that enables us to measure the radiation in the nadir viewing geometry with a spectral resolution of  $0.20\text{-}0.30\text{ cm}^{-1}$ . The  $2.2\text{ - }3.8\text{ }\mu\text{m}$  spectral range can be spanned through different diffraction orders of  $20\text{-}25\text{ cm}^{-1}$  width. This complicates any investigation related to broad spectral features such as those produced by aerosols or surface characteristics. Nevertheless, we establish a strategy based on a surface index, i.e. the ratio between the radiation at two wavelengths. This was determined through an investigation done on already existing datasets, from CRISM/MRO and OMEGA/MEX. It enabled us to assess which diffraction orders of NOMAD should be measured. This focus was borne in mind when planning the first scientific observations of NOMAD, done in April 2018. The spectra have been analysed and a preliminary conclusion will be presented.

### 1. The NOMAD instrument

NOMAD, the "Nadir and Occultation for Mars Discovery" spectrometer suite [1] was selected as part of the payload of the ExoMars Trace Gas Orbiter mission 2016. The instrument will conduct a spectroscopic survey of Mars' atmosphere in UV, visible and IR wavelengths covering the  $0.2\text{ - }0.65$  and  $2.3\text{ - }4.3\text{ }\mu\text{m}$  spectral ranges. NOMAD is composed of 3 channels: a solar occultation channel (SO) operating in the infrared wavelength domain, a second infrared channel observing nadir, but also able to perform solar occultation and limb observations (LNO), and

an ultraviolet/visible channel (UVIS) that can work in all observation modes. The design of the three channels has been fully described in [2] and in [3] for the UVIS channel and the IR channels respectively.

In the scientific preparation of the mission, we wondered how NOMAD-LNO may contribute to the surface characterization. This topic will be addressed in this abstract and in the associated presentation.

### 2. Characterization of the Martian surface using an index

The Martian surface has been studied by several instruments before the ExoMars mission. Among them, the imaging spectrometers OMEGA (Observatoire pour la Minéralogie, l'Eau, les Glaces et l'Activité) and CRISM (Compact Reconnaissance Imaging Spectrometer for Mars) have been observing the surface of Mars since 2004 and 2006 respectively. The measurements of these instruments, both operating in the visible to near infrared range, have dramatically sharpened our view of mineralogical and icy surface components in terms of composition. Especially, the data recorded by OMEGA and CRISM have provided useful information for the investigation of the surface and subsurface ice evolution as well as the presence of stable liquid water in the past of Mars. As an example, recent observations of erosional scarps performed by CRISM revealed the vertical structure of geologically young, ice-rich mantling deposits, near  $\pm 55^\circ$  latitude, likely formed during Mars' high-obliquity periods [4].

In order to evaluate the contribution of NOMAD to that topic, we analysed a set of data of CRISM and

OMEGA at similar location and  $L_S$ . On Fig. 1 and 2, we present the CRISM spectra at 5 different points of the surface at  $85^\circ\text{N}$  and  $-21^\circ\text{E}$  at  $L_S=133.8^\circ$ .

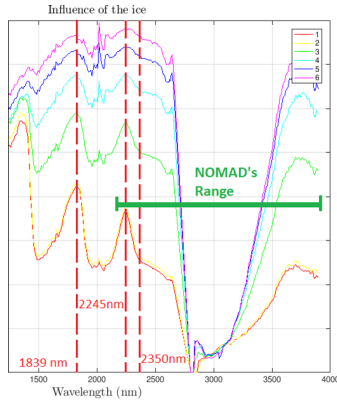


Figure 1: Corrected CRISM spectra (ref. Frt00002f7f)

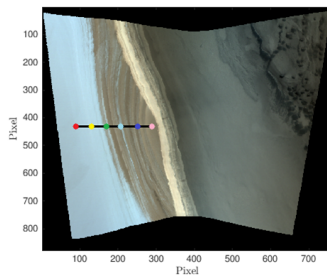


Figure 2: Projected map corresponding to the CRISM spectra

Fig. 3 shows a global map of OMEGA observations during MY 27,  $L_S=90-180^\circ$ . The colorbar gives an indication of the surface ice index. We concluded that the slope between 2245 and 2350 nm can be used as an indicator of the presence of ices. With OMEGA data we verified on a global scale that negative slopes about  $< -0.1$  can map the presence of water ice (surface or thick clouds) while positive values about  $> 0.1$  are diagnostic of the presence of surface  $\text{CO}_2$  ice. These wavelengths correspond to the NOMAD diffraction orders 189 and 197. These two orders have then been integrated in the nominal observation and measured during the Commissioning Phase. The analysis of these spectra are ongoing and should lead to interesting perspectives that will be presented.

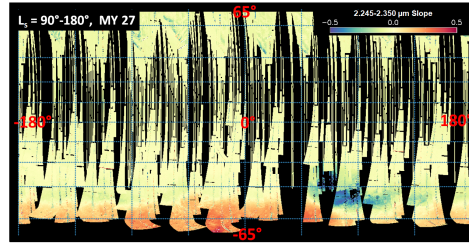


Figure 3: Surface ice index map using OMEGA data

## Acknowledgements

The NOMAD experiment is led by the Royal Belgian Institute for Space Aeronomy (IASB-BIRA), assisted by Co-PI teams from Spain (IAA-CSIC), Italy (INAF-IAPS), and the United Kingdom (Open University). This project acknowledges funding by the Belgian Science Policy Office (BELSPO), with the financial and contractual coordination by the ESA Prodex Office (PEA 4000103401, 4000121493), by MICHN through Plan Nacional (AYA2009-08190 and AYA2012-39691), as well as by UK Space Agency through grant ST/P000886/1 and Italian Space Agency through grant 2018-2-HH.0. The research was performed as part of the "Excellence of Science" project "Evolution and Tracers of Habitability on Mars and the Earth" (FNRS 30442502).

## References

- [1] Neefs, E., Vandaele, A.C., Drummond, R., Thomas, I.R. et al.: NOMAD spectrometer on the ExoMars trace gas orbiter mission: part 1 – design, manufacturing and testing of the infrared channels, *Applied Optics*, Vol. 54(28), pp. 8494-8520, 2015.
- [2] Vandaele, A.C., Willame, Y., Depiesse, C., Thomas, I.R., et al.: Optical and radiometric models of the NOMAD instrument part I: the UVIS channel, *Optics Express*, Vol. 23(23), pp. 30028-30042, 2015.
- [3] Thomas, I.R., Vandaele, A.C., Robert, S., Neefs, E. et al.: Optical and radiometric models of the NOMAD instrument part II: the infrared channels - SO and LNO, *Optics Express*, Vol. 24(4), pp. 3790-3805, 2016.
- [4] Dundas, C. M., Bramson, A. M., Ojha, L., Wray, J. J. et al.: Exposed subsurface ice sheets in the Martian mid-latitudes, *Science*, Vol. 359(6372), pp. 199-201, 2018.

## Status of METEO-P pressure and METEO-H humidity device development for the ExoMars 2020 mission

Timo Nikkanen (1,2,3), **Maria Genzer** (1), Maria Hieta (1,2), Matias Meskanen (1), Ari-Matti Harri (1) and Jouni Polkko (1)  
(1) Planetary Research and Space Technology research group, Finnish Meteorological Institute, Helsinki, Finland, (2) Aalto University, Finland, (3) Reaktor Space Lab, Helsinki, Finland (timo.nikkanen@fmi.fi)

### Abstract

Finnish Meteorological Institute (FMI) has developed a compact instrument pair for the ExoMars 2020 mission, consisting of the METEO-P pressure and METEO-H humidity measurement devices. The instruments have novel features, but the core technologies have extensive heritage from FMI's previous Mars missions. The devices are part of the METEO meteorological instrument package on board the Russian led Surface Platform (SP) element of the mission. METEO package includes also a thermometer and an anemometer from IKI, Russia, as well as the RDM Radiation and dust sensors, and the AMR magnetic field sensors from INTA, Spain. The Surface Platform is a stationary lander hosting a set of science investigations and delivering the European Space Agency rover element to the surface of Mars.[1]

### 1. Introduction

The miniature low-power instrument pair operations are managed by the instrument controller integrated on the METEO-P board. Mass of the pressure device is ca. 75 g and mass of the humidity device is ca. 45 g. During a pressure or humidity measurement sequence the instrument pair uses ca. 100-120 mW of power.

METEO-P is located in the same internal warm compartment with the METEO Central Electronics Unit (CEU), and interfaces with the CEU using an RS-422 data interface. The instrument controller handles power distribution and measurement collection of the two pressure transducer on board METEO-P and the one humidity transducer on METEO-H located on top of the meteorological mast. An automotive microcontroller (MCU), the Freescale MC9S12XEP100 is used for the METEO-P/H instrument control. The MCU was custom qualified for Mars missions by FMI in frame of the DREAMS-P and DREAMS-H pressure and humidity instrument pair for the ExoMars 2016 Schiaparelli mission[2].

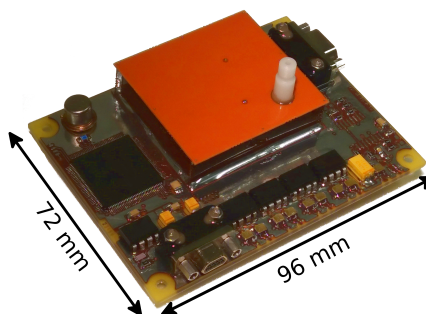


Figure 1: METEO-P pressure device STM

The measurement devices are based on capacitive Vaisala Barocap<sup>®</sup> pressure and Humicap<sup>®</sup> humidity sensors. Similar sensors have been flown on FMI's 6 previous Mars instrument projects and the Cassini-Huygens Titan lander. NASA's Curiosity rover is currently operating FMI's REMS-P and REMS-H devices in Mars.

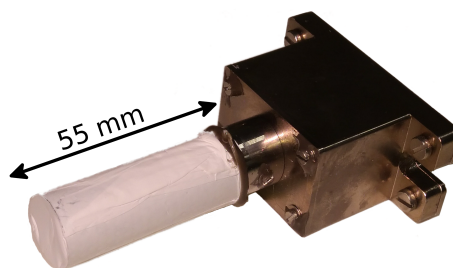


Figure 2: METEO-H humidity device STM

Compared to previous FMI designs, METEO-H uses a new type of Humicap<sup>®</sup> humidity sensors. The

new sensors offer a higher dynamic range and better knowledge of the sensor chip temperature through temperature sensors integrated on the chip. Measurement circuit for these PT1000 sensors has been implemented on the instrument controller on METEO-P board. Also, humidity sensor regeneration is now implemented through a PWM modulated voltage line and will heat up the humidity sensor heads to the required 160-165 °C regeneration temperature inside a wide range of environmental atmospheric temperatures.

## 2. Development status

Because of significant heritage of pressure and humidity devices developed by FMI, a lightweight model philosophy was selected for METEO-P and METEO-H development, including the following models:

- Structural and Thermal Model (STM)
- Electrical Interface Model (EIM)
- Protoflight Model (PFM)
- Flight Spare (FS)
- Humidity sensor Ground reference model

Both METEO-P and METEO-H STMs were manufactured in 2017 and delivered from FMI to IKI in Fall 2017.

The METEO-H Electrical Interface Model is fully representative and almost identical to the PFM. The METEO-P pressure device EIM is almost fully representative compared to PFM, but the type of the connectors was changed, the PCB corners rounded and few lay-out mistakes fixed to the PFM design. The EIMs have also been delivered from FMI to IKI.

PFM, FS and the ground reference model for METEO-H have been manufactured. As of May 2018, these models of the humidity device are now waiting for the beginning of humidity calibration process. The PFM and FS models of the METEO-P pressure device are under manufacturing and are expected to be completed in the beginning of June 2018. METEO-P PFM and FS will be then functionally tested and the pressure calibration process will be started.

## 3. Calibration

Both METEO-P and METEO-H are calibrated by FMI in FMI facilities.

For METEO-H the calibration of relative humidity requires in minimum two humidity points - dry

(0%RH) and (near)saturation (95-100%RH) - over the expected operational temperature and pressure range of the device. We have developed a custom-made, small, relatively low-cost calibration chamber able to produce both dry points and saturation points in Martian range pressure CO<sub>2</sub>, in temperatures down to -70 °C. The system utilizes a commercially available temperature chamber for temperature control, vacuum vessels and pumps. In this system dry point, low-pressure CO<sub>2</sub> environment is achieved by filling the main pressure vessel with dry CO<sub>2</sub> gas until the desired pressure is achieved. The saturation point is then achieved by adding some water vapor from the saturation chamber to the main pressure vessel.[3]

METEO-P is calibrated in different constant temperature and pressure points in vacuum and in Martian pressure, in changing temperature and in rapidly changing pressure. Calibrations are performed inside a small vacuum chamber placed inside a temperature test station. Pressure is controlled with a commercial pressure controller and calibrations are calculated against Mars-range pressure references traceable to national standards.

## References

- [1] ESA website ExoMars mission (2020)
- [2] T. Nikkanen (1,2), W. Schmidt (1), A.-M. Harri (1), M. Genzer (1), M. Hieta (1,2), H. Haukka (1) and O. Kempinen: Space qualification of an automotive microcontroller for the DREAMS-P/H pressure and humidity instrument on board the ExoMars 2016 Schiaparelli lander. European Planetary Science Congress 2015. EPSC Abstracts, Vol. 10, EPSC2015-465.
- [3] M. Genzer (1), J. Polkko (1), T. Nikkanen (1,2,3), M. Hieta (1,2) and A.-M. Harri (1): Calibration of Relative Humidity Devices in Low-pressure, Low-temperature CO<sub>2</sub> Environment. EGU General Assembly 2017. Geophysical Research Abstracts, Vol. 19, EGU2017-19164

# Preliminary results of dust and ice clouds retrieval using NOMAD/UVIS nadir measurements

**Yannick Willame** (1), Ann Carine Vandaele (1), Cédric Depiesse (1), Ian R. Thomas (1), Shohei Aoki (1), Arianna Piccialli (1), Frank Daerden (1), Bojan Ristic (1), Will Hewson (2), Manish R. Patel (2), Jon Mason (2), Michael J. Wolff (3), Fabrizio Oliva (4), Emiliano D'Aversa (4), Francesca Altieri (4), Giancarlo Bellucci (4), José Juan Lopez-Moreno (5) and the NOMAD team

(1) IASB-BIRA, Royal Belgian Institute for Space Aeronomy, Belgium, (2) OU, Open University, UK, (3) SSI, Space Science Institute, Boulder, CO, USA, (4) INAF/IAPS, Istituto di Astrofisica e Planetologia Spaziali, Italy, (5) IAA, Instituto de Astrofísica de Andalucía, Spain. (email: [yannick.willame@aeronomie.be](mailto:yannick.willame@aeronomie.be))

## Abstract

The NOMAD instrument, onboard the ExoMars Trace Gas Orbiter (TGO) mission, began scientific measurements in mid-April 2018. The UV-visible channel UVIS will be used to monitor dust and ice clouds present in the Martian atmosphere. In this presentation, the analysis of these data will be discussed and preliminary results will be presented.

## 1. The NOMAD instrument

NOMAD is an instrument suite [1] onboard the ExoMars TGO. It is composed of 3 channels. Two of these are spectrometers designed for measurement in the infrared (IR) between 2.3 and 4.3  $\mu\text{m}$  [2]: LNO for limb and nadir measurement and SO for solar occultation. The third channel is that of the UVIS [3], a spectrometer for measurements in the ultraviolet (UV) and visible range, between 200 and 650 nm with a spectral resolution of about 1.5 nm. UVIS can operate in limb, nadir and occultation modes.

The UVIS channel is dedicated to the study of the ozone abundances as well as dust and ice clouds.

## 2. Dust and ice clouds in the UV

UVIS nadir measurements will be used to monitor the dust optical depth (OD) and the ice cloud OD, as well as the ozone column (see abstract [4]). The goal of these measurements is to derive new climatologies, which will extend and provide comparisons to previous ones. Naturally included in such a dataset is the important spatial and temporal behaviours of these species. Previous studies have shown that ice clouds have repeatable seasonal patterns (i.e., from one year to the next), while dust is known to show

relatively important interannual variations that are mainly related to dust storm events (e.g. [5]).

Preliminary results of dust and ice cloud retrievals will be presented and compared to previous works.

## 3. Retrieval method

The analysis of UVIS data at IASB-BIRA will be performed using a retrieval algorithm specifically developed for nadir UV-visible. The code is based on the iterative use of the optimal estimation [6] and the radiative transfer model LIDORT [7] which includes accurate treatment of multiple scattering. Our retrieval method has already been used for SPICAM/UV measurements and allowed us to analyze more than 4 Martian years of data [8].

Within the NOMAD team, other institutes have also developed their retrieval method: The NEMESIS radiative [4] transfer model developed at the Open University; the MITRA code developed at IAPS-INAF [9, 10]; the ARS RT model from [11]; and the DISORT-based retrieval [12] developed at SSI. Comparisons between the results obtained by the different codes will also be presented.

## Acknowledgements

The NOMAD experiment is led by the Royal Belgian Institute for Space Aeronomy (BIRA-IASB), assisted by Co-PI teams from Spain (IAA-CSIC), Italy (INAF-IAPS), and the United Kingdom (Open University). This project acknowledges funding by the Belgian Science Policy Office (BELSPO), with the financial and contractual coordination by the ESA Prodex Office (PEA 4000103401, 4000121493), by MICIIN through Plan Nacional (AYA2009-08190 and AYA2012-39691), as well as by UK Space Agency through grant ST/P000886/1 and Italian

Space Agency through grant 2018-2-HH.0. The research was performed as part of the “Excellence of Science” project “Evolution and Tracers of Habitability on Mars and the Earth” (FNRS 30442502). This research was supported by the FNRS CRAMIC project under grant number T.0171.16 and by the BrainBe SCOOP project.

## References

- [1] Neefs, E., Vandaele, A.C., Drummond, R., Thomas, I.R. et al.: NOMAD spectrometer on the ExoMars trace gas orbiter mission: part 1 – design, manufacturing and testing of the infrared channels, *Applied Optics*, Vol. 54(28), pp. 8494-8520, 2015.
- [2] Thomas, I.R., Vandaele, A.C., Robert, S., Neefs, E. et al.: Optical and radiometric models of the NOMAD instrument part II: the infrared channels - SO and LNO, *Optics Express*, Vol. 24(4), pp. 3790-3805, 2016.
- [3] Vandaele, A.C., Willame, Y., Depiesse, C., Thomas, I.R., et al.: Optical and radiometric models of the NOMAD instrument part I: the UVIS channel, *Optics Express*, Vol. 23(23), pp. 30028-30042, 2015.
- [4] Hewson et al. ExoMars TGO O3 and dust mapping with the NOMAD-UVIS spectrometer. EPSC, 2018
- [5] Smith, 2008. Spacecraft Observations of the Martian Atmosphere. *Annual Review of Earth and Planetary Sciences*, 36(May), 191-219.
- [6] Rodgers, 2000. *Inverse Methods for Atmospheric Sounding - Theory and Practice*. Series on Atmospheric Oceanic and Planetary Physics, vol. 2. World Scientific Publishing Co.
- [7] Spurr et al., 2001. A linearized discrete ordinate radiative transfer model for atmospheric remote-sensing retrieval. *Journal of Quantitative Spectroscopy and Radiative Transfer*, 68(Mar.), 689-735.
- [8] Y. Willame, A.C. Vandaele, C. Depiesse, et al.: Retrieving cloud, dust and ozone abundances in the Martian atmosphere using SPICAM/UV nadir spectra, *Planetary and Space Science*, Volume 142, 2017.
- [9] Oliva, F., Adriani, A., Moriconi, M.L., Liberti, G.L., D’Aversa, E., Filacchione, G., 2016. Clouds and hazes vertical structure of a Saturn’s giant vortex from Cassini/VIMS-V data analysis. *Icarus* 278, 215–237. doi: 10.1016/j.icarus.2016.06.021.
- [10] Sindoni, G., Adriani, A., Mayorov, B., Aoki, S., Grassi, D., Moriconi, M., Oliva, F., 2013. Development of a Monte-Carlo radiative transfer code for the Juno/JIRAM limb measurements. European Planetary Science Congress 2013, held 8-13 September in London, UK.
- [11] Ignatiev, N.I., Grassi, D., Zasova, L.V., 2005. Planetary Fourier spectrometer data analysis: fast radiative transfer models. *Planet. Space Sci.* 53 (10), 1035–1042.
- [12] Wolff, M. J., M. D. Smith, R. T. Clancy, R. et al. (2009). "Wavelength dependence of dust aerosol single scattering albedo as observed by the Compact Reconnaissance Imaging Spectrometer." *Journal of Geophysical Research (Planets)* 114: E00D04.

## ExoMars-2020 Surface Platform scientific investigation

**Daniel Rodionov** (1), Lev Zelenyi (1), Oleg Korablev (1), Ilya Chuldov (1) and Jorge Vago (2)  
(1) Space Research Institute (IKI), Moscow, Russia, (2) European Space Research and Technology Centre (ESTEC), Noordwijk, Netherlands (rodionov@iki.rssi.ru)

### Abstract

ESA and Roscosmos have signed a cooperation agreement to work in partnership to develop and launch two ExoMars missions—in 2016 and 2020. The first mission is currently in progress, aiming to study Mars' atmospheric composition in unprecedented detail.

ExoMars-2020 mission will deliver the ExoMars Rover and a Landing Platform to the surface of Mars. The ExoMars Rover will carry a comprehensive suite of instruments dedicated to exobiology and geology research named after Louis Pasteur. The Rover will search for signs of life, past and present. It will have the capability to drill to depths of 2 m to collect and analyze samples that have been shielded from the harsh conditions prevailing on the surface, where radiation and oxidants can destroy organic materials [1].

The Landing Platform (LP) will be equipped with instruments to study the Martian environment. After the Rover egress the Landing Platform will serve as long-lived stationary platform (expected lifetime is two Earth years) to study surface environment with suite of scientific instruments [2]. The scientific objectives of the Landing Platform are:

- Context imaging.
- Long-term climate monitoring and atmospheric investigations.
- Studies of subsurface water distribution at the landing site.
- Atmosphere/surface volatile exchange.
- Monitoring of the radiation environment.
- Geophysical investigations of Mars' internal structure.

To address these objectives scientific payload has been selected and is currently in development.

Payload currently consists of 13 instruments with total mass of 45 kg. (including harness):

Instrument	Short description
BIP	Block of interfaces and memory. Commands the science payload of LP
TSPP	Set of 4 cameras to create surface panoramas and assist Rover egress
ADRON-EM	Neutron gamma-spectrometer and dosimeter
MGAK	Gas Analytical package
PK (Dust Suite)	Dust dynamics near the surfaces
MTK (Meteo Suite)	Set of meteo sensors (temperature, humidity, wind velocity, pressure, solar irradiance, dust). Magnetic sensor. EDL measurements.
SEM	Small seismometer.
MAIGRET	Magnetometer.
RAT-M	Passive radiometer.
FAST	Fourier IR spectrometer.
M-DLS	Martian Multichannel Diode Laser Spectrometer.
LARA	Lander Radio science.
HABIT	Habitability, Brine Irradiation and Temperature.

Landing Platform scientific payload is being developed by Space Research Institute (Moscow) with contribution from ESA (LARA, HABIT, sensors in MTK and MAIGRET).

## **Acknowledgements**

Space Research Institute acknowledges support from Roscosmos in development and operation of Russian scientific instruments for all elements of ExoMars mission.

## **References**

[1] Vago, J., Westall, F. et al.: Habitability on Early Mars and the Search for Biosignatures with the ExoMars Rover, *Astrobiology* Vol. 17, No. 6-7, 2017.

[2] Zelenyi L., Korablev O., Rodionov D. et al: Scientific objectives of the scientific equipment of the landing platform of the ExoMars-2018 mission, *Sol Syst Res* (2015)

## Model expectations for the D/H distribution on Mars as observed by NOMAD

**Frank Daerden** (1), Lori Neary (1), Sébastien Viscardy (1), Shohei Aoki (1,8,9), Arianna Picciali (1), Séverine Robert (1), Valérie Wilquet (1), Ian B. Thomas (1), Bojan Ristic (1), Ann Carine Vandaele (1), Geronimo Villanueva (2), Michael J. Mumma (2), Robert E. Novak (3), Thérèse Encrenaz (4), Stephen Lewis (5), James Holmes (5), José Juan Lopez-Moreno (6), Giancarlo Bellucci (7), Manish Patel (6), and the NOMAD team.

(1) Royal Belgian Institute for Space Aeronomy BIRA-IASB, Brussels, Belgium, (2) NASA Goddard Space Flight Center, Greenbelt, MD, USA, (3) Iona College, New Rochelle NY, USA, (4) LESIA, Observatoire de Paris, CNRS, UPMC, UPD, Meudon, France, (5) Open University, Milton Keynes, UK, (6) Instituto de Astrofísica de Andalucía (IAA-CSIC), Granada, Spain, (7) Instituto di Astrofisica e Planetologia Spaziali (IAPS), Istituto Nazionale di Astrofisica (INAF), Rome, Italy, (8) Fonds National de la Recherche Scientifique, Belgium, (9) Tohoku University, Japan ([Frank.Daerden@aeronomie.be](mailto:Frank.Daerden@aeronomie.be))

### Abstract

The NOMAD (“Nadir and Occultation for Mars Discovery”) spectrometer suite on board the ExoMars Trace Gas Orbiter (TGO) has been designed to investigate the composition of Mars’ atmosphere, with a particular focus on trace gases, clouds and dust, and started its science operations in April 2018. One of the primary science objectives of NOMAD is the detailed investigation of semiheavy water (HDO), both in nadir (total columns) and in solar occultation (vertical profiles). Interestingly, NOMAD has the capability to simultaneously retrieve H<sub>2</sub>O and HDO, hence the very important D/H ratio. This ratio provides information on cloud formation and atmospheric escape. The GEM-Mars model was recently extended with HDO fractionation. We present some first results that will be useful to guide the interpretation of D/H data from NOMAD.

### Introduction

The isotopic composition of fresh water on Earth has been defined by the Vienna Standard Mean Ocean Water (VSMOW), in which the HDO isotopologue of water has a relative abundance (D/H or  $\frac{1}{2} \times \text{HDO}/\text{H}_2\text{O}$ ) of  $155.76 \pm 0.1$  ppm (parts per million). In the atmosphere of Mars, D/H has been found to be enhanced by 5-7 times compared to Earth [1, 2 and references therein], indicating a stronger atmospheric depletion of H<sub>2</sub>O on Mars compared to Earth. Until now, HDO and D/H have been observed from Earth, and NOMAD will be the first instrument in orbit to provide detailed measurements. D/H fractionation is expected to occur in the Martian atmosphere following two processes: upon condensation/

evaporation of water, where the heavier isotopologue will condense/vaporize at slightly higher temperature, and by photolysis, where HDO has a lower absorption cross-section in the UV [3]. Also, the heavier isotope will escape less readily above the exobase during Jeans escape. Also the D/H ratio in ancient water ice reservoirs, such as the permanent water ice cap, is expected to impact on the atmospheric value [2].

### Modeling the D/H ratio on Mars

The GEM-Mars General Circulation Model [4] includes both the formation of water ice clouds and photochemistry. As such, it is well equipped to do simulations of the D/H fractionation. First results will be presented and interesting features will be highlighted. Model expectations will be discussed in view of the observational geometries of NOMAD and if possible compared to first results (which will be presented in Aoki et al., this session). For example, the model can help to understand how representative observed D/H ratios are in the solar occultation mode, where measurements are confined to the terminator and could be affected by morning/evening cloud and fog formation.

### Acknowledgements

The NOMAD experiment is led by the Royal Belgian Institute for Space Aeronomy (IASB-BIRA), assisted by Co-PI teams from Spain (IAA-CSIC), Italy (INAF-IAPS), and the United Kingdom (Open University). This project acknowledges funding by the Belgian Science Policy Office (BELSPO), with the financial and contractual coordination by the ESA

Prodex Office (PEA 4000103401, 4000121493), by the Spanish Ministry of Economy, Industry and Competitiveness and by FEDER funds under grant ESP2015-65064-C2-1-P (MINECO/FEDER), by the Italian Space Agency through grant 2018-2-HH.0, as well as by UK Space Agency through grant ST/P000886/1. US investigators were supported by the National Aeronautics and Space Administration. The research was performed as part of the “Excellence of Science” project “Evolution and Tracers of Habitability on Mars and the Earth” (FNRS 30442502).

## The NOMAD Team

*Scientific team:* Vandaele, Ann Carine; Lopez Moreno, Jose Juan; Bellucci, Giancarlo; Patel, Manish; Allen, Mark; Alonso-Rodrigo, Gustavo; Altieri, Francesca; Aoki, Shohei; Bauduin, Sophie; Bolsée, David; Clancy, Todd; Cloutis, Edward; Daerden, Frank; D'Aversa, Emiliano; Depiesse, Cédric; Erwin, Justin; Fedorova, Anna; Formisano, Vittorio; Funke, Bernd; Fussen, Didier; Garcia-Comas, Maia; Geminale, Anna; Gérard, Jean-Claude; Gillotay, Didier; Giuranna, Marco; Gonzalez-Galindo, Francisco; Hewson, Will; Homes, James; Ignatiev, Nicolai; Kaminski, Jacek; Karatekin, Ozgur; Kasaba, Yasumasa; Lanciano, Orietta; Lefèvre, Franck; Lewis, Stephen; López-Puertas, Manuel; López-Valverde, Miguel; Mahieux, Arnaud; Mason, Jon; Mc Connell, Jack; Mumma, Mike; Nakagawa, Hiromu; Neary, Lori; Neefs, Eddy; Novak, R.; Oliva, Fabrizio; Piccialli, Arianna; Renotte, Etienne; Robert, Severine; Sindoni, Giuseppe; Smith, Mike; Stiepen, Arnaud; Thomas, Ian; Trokhimovskiy, Alexander; Vander Auwera, Jean; Villanueva, Geronimo; Viscardy, Sébastien; Whiteway, Jim; Willame, Yannick; Wilquet, Valérie; Wolff, Michael; Wolkenberg, Paulina – *Tech team:* Alonso-Rodrigo, Gustavo; Aparicio del Moral, Beatriz; Barzin, Pascal; Beeckman, Bram; BenMoussa, Ali; Berkenbosch, Sophie; Biondi, David; Bonnewijn, Sabrina; Candini, Gian Paolo; Clairquin, Roland; Cubas, Javier; Giordanengo, Boris; Gissot, Samuel; Gomez, Alejandro; Hathi, Brijen; Jeronimo Zafra, Jose; Leese, Mark; Maes, Jeroen; Mazy, Emmanuel; Mazzoli, Alexandra; Meseguer, Jose; Morales, Rafael; Orban, Anne; Pastor-Morales, M; Perez-grande, Isabel; Queirolo, Claudio; Ristic, Bojan; Rodriguez Gomez, Julio; Saggin, Bortolino; Samain, Valérie; Sanz Andres, Angel; Sanz, Rosario; Simar, Juan-Felipe; Thibert, Tanguy

## References

- [1] Owen, T., et al. (1988), *Science*, 240, 1767.
- [2] Villanueva, G.L. et al. (2015), *Science* 348, 218.
- [3] Bertaux, J., and F. Montmessin (2001), *J. Geophys. Res.*, 106(E12), 32,879– 32,884.
- [4] Neary, L., and F. Daerden (2018), *Icarus*, 300, 458–476.

# Electromagnetic wave analyzer module for the ExoMars 2020 surface platform

**O. Santolik** (1,2), I. Kolmasova (1,2), and A. Skalsky (3)

(1) Department of Space Physics, IAP CAS, Prague, Czechia, (2) Charles University, Prague, Czechia,

(3) Institute of Space Research, Moscow, Russia

## Abstract

The ExoMars 2020 Surface Platform will conduct environmental and geophysical measurements with the aim to study the Martian surface and subsurface environment at the landing location. The Surface Platform instrumentation will include the Wave analyzer module, consisting of an assembly of magnetic and electric antennae and dedicated electronics, as a part of the Martian ground electromagnetic tool instrument. Science questions which we plan to address have never been answered by direct observations on the surface of the planet.

## 1. Introduction

Recent observations of the Mars Atmosphere and Volatile Evolution (MAVEN) mission on the Mars orbit have shown plasma waves [1] similar to those observed in the Earth's magnetosphere [2].

Although no experimental proof exists up to now, analogy with penetration of whistler mode waves through the Earth's ionosphere [3] and theoretical considerations [4] indicate that these waves might penetrate to the surface of Mars during night time.

By analogy with the terrestrial dust storms and volcanic eruptions [5] it can be theoretically expected that dust grains in the Martian dust storms or dust devils may be electrically charged by triboelectric effects [6]. Laboratory experiments also show that under specific conditions electrostatic discharges might occur in the dusty Martian atmosphere [7].

These discharges would emit broadband electromagnetic emissions [8] which have also been found in the laboratory experiments [9]. Moreover, remote measurements from the Earth using a 34-m Deep Space Network antenna have shown a non-

thermal component of electromagnetic radiation from Mars which has been attributed to the effects of electrostatic discharges in the dust storms [10]. Measurements of effect of terrestrial dust devils have also shown a detectable electromagnetic radiation [11].

The subject, however, remains controversial. No optical counterparts of the electrical discharges inside the images of Martian dust devils and dust storms have been identified up to now, and sprite-like discharges above the dust devils or dust storms will most likely be absent on Mars [12].

Additionally, observations of the radar receiver onboard the Mars Express spacecraft [13] lead the instrument team to a conclusion that no credible radio signals between 4 and 5.5 MHz coming from Martian lightning could be detected, although the receiver would be able to easily detect terrestrial lightning. These results, however, did not rule out the possibility of discharges that radiate at much lower or at much higher frequencies.

## 2. Science questions

The following science questions stem from previous research and will be addressed by the Wave analyzer module on the ExoMars 2020 surface platform:

A. Can we observe electromagnetic radiation propagating from the interplanetary space down to the surface of the planet? If yes, then

A1. Which frequencies and plasma wave modes can penetrate down to the surface of Mars?

A2. What are the conditions under which we observe the penetration of electromagnetic radiation from interplanetary space down to the surface of Mars?

A3. What state of the Martian ionosphere is the most favorable for the penetration to happen?

B. Can we observe electromagnetic radiation from electric discharges in the Martian dust storms? If yes, then:

B1. Are the waveforms of the electromagnetic radiation from Martian discharges similar to the waveforms radiated from the terrestrial lightning?

B2. Which processes lead to initial break-down of Martian discharges and how are these processes reflected in the detectable electromagnetic radiation?

B3. Which special meteorological conditions lead to initiation of Martian discharges?

To address all these questions a statistical analysis of a sufficiently long time series of electromagnetic measurements on the surface of Mars would be needed.

### 3. The wave analyzer module

Electromagnetic waves will be measured by the sensor assembly of the module which will be integrated with one of the solar panels of the Surface platform: a magnetic search coil antenna for frequencies up to 20 kHz and additional electric antenna for frequencies up to 8 MHz.

The electronics of the module will then use sophisticated onboard analysis methods in order to maximize the scientific return with the limited telemetry resources by science-based compression.

The data products will include time and frequency averaged survey mode spectra of electric and magnetic field, high-resolution burst mode spectra, and selected high-resolution waveform burst mode snapshots.

Onboard storage mechanisms and selective download, as well as triggering and selection algorithms will be adjustable by telecommands.

Autonomous night-time operations are proposed to increase the detection probability of waves propagating through the ionosphere. A positive side effect is absence of interferences from solar panels.

## References

- [1] Harada, Y., et al. (2016), MAVEN observations of electron-induced whistler mode waves in the Martian magnetosphere, *J. Geophys. Res. Space Physics*, 121, doi:10.1002/2016JA023194.
- [2] Santolik O. and J. Chum (2009), The origin of plasmaspheric hiss, *Science* 324, 5928, 729-730.
- [3] Santolik, O. et al. (2009), Propagation of unducted whistlers from their source lightning: a case study, *J. Geophys. Res.*, 114, A03212, doi:10.1029/2008JA 013776.
- [4] Melnik O., and M. Parrot (1999), Propagation of electromagnetic waves through the Martian ionosphere, *J. Geophys. Res.* 104, 12705-12714
- [5] Antel, C., et al. (2014), Investigating Dunedin whistlers using volcanic lightning, *Geophys. Res. Lett.*, 41, 4420–4426, doi:10.1002/2014GL060332.
- [6] Melnik O., and M. Parrot (1998), Electrostatic discharge in Martian dust storms, *J. Geophys. Res.* 103, 29107-29117.
- [7] Krauss et al. (2003), Experimental evidence for electrostatic discharging of dust near the surface of Mars, *New Journal of Physics* 5 70.1–70.9.
- [8] Renno et al. (2003), Electrical discharges and broadband radio emission by Martian dust devils and dust storms, *Geophys. Res. Lett.*, 30(22), 2140.
- [9] Aplin et al. (2011), Measuring Martian lightning, *Journal of Physics: Conference Series* 301 012007 doi:10.1088/1742-6596/301/1/012007
- [10] Ruf et al. (2009), Emission of non-thermal microwave radiation by a Martian dust storm, *Geophys. Res. Lett.*, 36, L13202, doi:10.1029/2009GL038715.
- [11] Farrell et al. (2004), Electric and magnetic signatures of dust devils from the 2000–2001 MATADOR desert tests, *J. Geophys. Res.*, 109, E03004, doi:10.1029/2003JE002088.
- [12] Yair et al. (2009), A study of the possibility of sprites in the atmospheres of other planets, *J. Geophys. Res.*, 114, E09002, doi:10.1029/2008JE003311.
- [13] Gurnett et al. (2010), Non - detection of impulsive radio signals from lightning in Martian dust storms using the radar receiver on the Mars Express spacecraft, *Geophys. Res. Lett.*, 37, L17802, doi:10.1029/2010GL044368.

## Preliminary results on carbon dioxide and temperature profiles from NOMAD SO

**Loïc Trompet** (1), Ann Carine Vandaele (1), Ian R. Thomas (1), Séverine Robert (1), Shohei Aoki (1,2,3), Justin T. Erwin (1), Arnaud Mahieux (1,2,4), Arianna Piccialli (1), Valérie Wilquet (1), Frank Daerden (1), Lori Neary (1), Sébastien Viscardy (1), Bojan Ristic (1), Bernd Funke (5), Brittany Hill (5), Miguel Ángel López-Valverde (5), Manuel López-Puertas (5), José Juan López-Moreno (5), Maya García-Comas (5), Marco Giuranna (6), Giuseppe Sindoni (6), Fabrizio Oliva (6), Giancarlo Bellucci (6), Manish R. Patel (7) and the NOMAD team  
(1) Royal Belgian Institute for Space Aeronomy, Belgium, (2) Fond National de la Recherche Scientifique, Belgium, (3) Tohoku University, Japan, (4) The University of Texas at Austin, USA, (5) Instituto de Astrofísica de Andalucía, CSIC, Spain, (6) Institute for Space Astrophysics and Planetology, Italy, (7) Open University, UK. ([loic.trompet@aeronomie.be](mailto:loic.trompet@aeronomie.be))

### Introduction

NOMAD (Nadir and Occultation for MARS Discovery) [1, 2] is one of the four instruments on-board the ExoMars 2016 Trace Gas Orbiter (TGO). It consists of three high-resolution spectrometers, SO, LNO and UVIS. It can operate in different geometries: solar occultation, limb and nadir. The SO channel started to make solar occultation measurements on April 21, 2018. It is performing optimally and is now regularly making solar occultation measurements of the atmosphere of Mars.

### 1. The NOMAD SO channel

The SO channel is dedicated to solar occultation measurements, and is a copy of the SOIR instrument [3] that operated successfully during the entire Venus Express mission. It is an infrared spectrometer working in the 2.2 to 4.3  $\mu\text{m}$  spectral range (2325-4545  $\text{cm}^{-1}$ ) with a spectral resolution that varies from 0.15 to 0.2  $\text{cm}^{-1}$ . The instrument is composed of an echelle grating in a near Littrow configuration, and an Acousto-Optical Tunable Filter (AOTF) for the diffraction order selection [4].

The orbit of TGO is circular at an altitude of 400 km. During a solar occultation, six diffraction orders are scanned every second. The spectra are recorded for each order at a one second interval and are summed in 4 bins. In this configuration, the vertical sampling of the SO channel is always smaller than 1 km.

### 2. Profiles retrievals

One of the radiative transfer code used to retrieve NOMAD vertical profiles is ASIMUT-ALVL [5]. This code, developed at BIRA-IASB, is based on the Optimal Estimation Method [6] and includes the

analytical calculation of the Jacobians [6]. It can be used for different geometries including solar occultations. From  $\text{CO}_2$  vertical profiles, temperature profiles are obtained using the hydrostatic equation and the ideal gas law, similar to the work that was accomplished using the SOIR instrument spectra [7].

The preliminary results of retrieved  $\text{CO}_2$  and temperature vertical profiles from the SO channel will be presented, discussed, and compared to results obtained by other instruments as well as models.

### Acknowledgements

The NOMAD experiment is led by the Royal Belgian Institute for Space Aeronomy (BIRA-IASB), assisted by Co-PI teams from Spain (IAA-CSIC), Italy (INAF-IAPS), and the United Kingdom (Open University). This project acknowledges funding by the Belgian Science Policy Office (BELSPO), with the financial and contractual coordination by the ESA Prodex Office (PEA 4000103401, 4000121493), by MICIIN through Plan Nacional (AYA2009-08190 and AYA2012-39691), as well as by UK Space Agency through grant ST/P000886/1 and Italian Space Agency through grant 2018-2-HH.0. The research was performed as part of the “Excellence of Science” project “Evolution and Tracers of Habitability on Mars and the Earth” (FNRS 30442502). This research was supported by the FNRS CRAMIC project under grant number T.0171.16 and by the BrainBe SCOOP project.

### References

[1] Vandaele, A.C., et al.: Science objectives and performances of NOMAD, a spectrometer suite for the ExoMars TGO mission, *Planet. Space Sci.*, Vol. 119, pp 233-249, 2015.

- [2] Neefs, E., et al.: NOMAD spectrometer on the ExoMars trace gas orbiter mission: part I – design, manufacturing and testing of the infrared channels, *Appl. Opt.*, Vol. 54(28), pp 8494-8520, 2015.
- [3] Nevejans, D., et al.: Compact, high resolution space borne echelle grating spectrometer with AOTF based on order sorting for the infrared domain from 2.2 to 4.3 micrometer, *Appl. Opt.*, Vol. 45, pp 5191-5206, 2006.
- [4] Thomas, I.R., et al.: Optical and radiometric models of the NOMAD instrument part II: the infrared channels – SO and LNO, *Opt. Express*, Vol. 24(4), pp 3790-3805, 2016.
- [5] Vandaele, A.C., Kruglanski, M., De Mazière, M., Modeling and retrieval of atmospheric spectra using ASIMUT. Proceedings of the First Atmospheric Science Conference, ESRIN, Frascati, Italy, 2006.
- [6] Rodgers, C.D., Inverse method for atmospheric sounding: theory and practice. Hackensack, N.J. (Ed.), World Scientific University of Oxford, Oxford, 2000.
- [7] Mahieux, A. et al.: Densities and temperatures in the Venus mesosphere and lower thermosphere retrieved from SOIR on board Venus Express: Carbon dioxide measurements at the Venus terminator, *J. Geophys. Res.*, Vol 117, E07001, 2012.

## Preliminary results on water vapor retrievals from the first data of TGO/NOMAD

**Shohei Aoki** (1,2,3), Ann Carine Vandaele (1), Séverine Robert (1), Ian R. Thomas (1), Loïc Trompet (1), Justin T. Erwin (1), Arianna Piccialli (1), Valérie Wilquet (1), Arnaud Mahieux (1), Frank Daerden (1), Lori Neary (1), Sébastien Viscardy (1), Bojan Ristic (1), Geronimo L. Villanueva (4), Giuliano Liuzzi (4), Michael J. Mumma (4), Michael D. Smith (4), James A. Holmes (5), Giuseppe Sindoni (6), Marco Giuranna (6), Sophie Bauduin (7), Manish R. Patel (4), Giancarlo Bellucci (5), Jose Juan Lopez-Moreno (8), and the NOMAD team

(1) Royal Belgian Institute for Space Aeronomy, Belgium, (2) Fonds National de la Recherche Scientifique, Belgium, (3) Tohoku University, Japan, (4) NASA Goddard Space Flight Center, USA, (5) Open University, UK, (6) Istituto di Astrofisica e Planetologia, Italy, (7) Université libre de Bruxelles, Belgium, (8) Instituto de Astrofisica de Andalucía, Spain.  
(e-mail : [shohei.aoki@aeronomie.be](mailto:shohei.aoki@aeronomie.be))

### Abstract

Nadir and Occultation for Mars Discovery (NOMAD) onboard ExoMars Trace Gas Orbiter (TGO) has started the science measurements on 21 April, 2018. We present the preliminary results on the retrievals of water vapor in the Martian atmosphere from the first data measured by TGO/NOMAD.

### 1. The NOMAD instrument

NOMAD is a spectrometer operating in the spectral ranges between 0.2 and 4.3  $\mu\text{m}$  onboard ExoMars TGO [1]. NOMAD has 3 spectral channels: a solar occultation channel (SO – Solar Occultation; 2.3-4.3  $\mu\text{m}$ ), a second infrared channel capable of nadir, solar occultation, and limb sounding (LNO – Limb Nadir and solar Occultation; 2.3-3.8  $\mu\text{m}$ ), and an ultraviolet/visible channel (UVIS – UV visible, 200-650 nm). The infrared channels (SO and LNO) have high spectral resolution ( $\lambda/d\lambda \sim 20,000$ ) provided by echelle grating in combination with an Acousto-Optic Tunable Filter (AOTF) which selects diffraction orders [2]. The concept of the infrared channels are derived from the Solar Occultation in the IR (SOIR) instrument [3] onboard Venus Express. The sampling rate for the solar occultation measurement is 1 km, which provides unprecedented vertical resolution spanning altitudes from the surface to 200 km. Nadir sounding by the LNO channel will acquire spectra with an instantaneous footprint of  $0.5 \times 17 \text{ km}^2$ , which allows us to obtain maps of trace gases and aerosols in the Martian atmosphere.

One of the most remarkable capabilities of NOMAD is its high spectral resolution in the near infrared range. It allows us (1) to investigate vertical profiles of the atmospheric constituents (such as carbon dioxide, carbon monoxide, water vapor, and their isotopic ratio) and (2) to perform sensitive search of organic species (such as  $\text{CH}_4$ ,  $\text{C}_2\text{H}_4$ ,  $\text{C}_2\text{H}_6$ ,  $\text{H}_2\text{CO}$ ) and other trace gases (such as  $\text{HCl}$ ,  $\text{HCN}$ ,  $\text{HO}_2$ ,  $\text{H}_2\text{S}$ ,  $\text{N}_2\text{O}$ ,  $\text{OCS}$ ) by solar occultation measurements with the SO channel, and (3) to obtain maps of the atmospheric constituents (such as carbon dioxide, carbon monoxide, water vapor, and their isotopic ratio) across the planet by nadir viewing with the LNO channel.

### 2. Retrieval of Water Vapor

Measurements of water and its heavier isotopologue (HDO) are a key diagnostic to the escape processes acting on water on Mars. These first vertical profiles provide an unprecedented view on how water is transported into the upper atmosphere, where it is further dissociated and lost into space. Deuterium fractionation also reveals information about the cycle of water on the planet and informs us of its stability on short- and long-term scales.

We plan to analyze the data measured at diffraction order 167, 168, 169, 170, 171 for the  $\text{H}_2\text{O}$  retrieval, and at diffraction order 119, 120, 121, 124 for HDO (see Table 1 for the corresponding wavenumbers). The NOMAD spectra at these diffraction orders will be compared with the one calculated by radiative transfer models in order to retrieve their abundances. In the presentation, the preliminary results of the retrievals will be discussed.

Table1: Wavenumber range of the diffraction orders for the water vapor analysis by the NOMAD SO and LNO channels.

Diffraction order	SO wavenumber limits [cm <sup>-1</sup> ]	LNO wavenumber limits [cm <sup>-1</sup> ]
119	2674.34-2695.65	2674.90-2696.26
120	2696.81-2718.31	2697.37-2718.92
121	2719.28-2740.96	2719.85-2741.58
124	2786.70-2808.92	2787.29-2809.55
167	3753.06-3782.98	3753.84-3783.83
168	3775.53-3805.63	3776.32-3806.49
169	3798.01-3828.28	3798.80-3829.15
170	3820.48-3850.93	3821.28-3851.80
171	3842.96-3873.59	3843.76-3874.46

## Acknowledgements

This research was supported by the FNRS CRAMIC project under grant number T.0171.16. The NOMAD experiment is led by the Royal Belgian Institute for Space Aeronomy (IASB-BIRA), assisted by Co-PI teams from Spain (IAA-CSIC), Italy (INAF-IAPS), and the United Kingdom (Open University). This project acknowledges funding by the Belgian Science Policy Office (BELSPO), with the financial and contractual coordination by the ESA Prodex Office (PEA 4000103401, 4000121493), by MICIIN through Plan Nacional (AYA2009-08190 and AYA2012-39691), as well as by UK Space Agency through grant ST/P000886/1 and Italian Space Agency through grant 2018-2-HH.0. This research was also performed as part of the “Excellence of Science” project “Evolution and Tracers of Habitability on Mars and the Earth” (FNRS 30442502) and supported by the BrainBe SCOOP project. US investigators were supported by the National Aeronautics and Space Administration. The IAA/CSIC team has been supported by Spanish Ministry of Economy, Industry and Competitiveness and by FEDER funds under grant ESP2015-65064-C2-1-P (MINECO/FEDER).

## References

- [1] Vandaele, A.C., Neefs, E., Drummond, R. et al.: Science objectives and performances of NOMAD, a spectrometer suite for the Exo-Mars TGO mission, *Planetary and Space Science*, Vol. 119, pp. 233–249, 2015.
- [2] Neefs, E., Vandaele, A.C., Drummond, R. et al.: NOMAD spectrometer on the ExoMars trace gas orbiter mission: part 1 – design, manufacturing and testing of the infrared channels, *Applied Optics*, Vol. 54 (28), pp. 8494-8520, 2015.
- [3] Nevejans, D., Neefs, E., Ransbeeck, E.V. et al.: Compact high-resolution spaceborne echelle grating spectrometer with acousto-optical tunable filter based order sorting for the infrared domain from 2.2 to 4.3  $\mu\text{m}$ , *Applied Optics*, Vol. 45 (21), pp. 5191-5206, 2006.

## The NOMAD team

*Scientific team:* Vandaele, Ann Carine; Lopez Moreno, Jose Juan; Bellucci, Giancarlo; Patel, Manish; Allen, Mark; Alonso-Rodrigo, Gustavo; Altieri, Francesca; Aoki, Shohei; Bauduin, Sophie; Bolsée, David; F. Giacomo Carrozzo, Clancy, Todd; Cloutis, Edward; Daerden, Frank; D’Aversa, Emiliano; Depiesse, Cédric; Erwin, Justin; Fedorova, Anna; Formisano, Vittorio; Funke, Bernd; Fussen, Didier; Garcia-Comas, Maia; Geminale, Anna; Gérard, Jean-Claude; Gillotay, Didier; Giuranna, Marco; Gonzalez-Galindo, Francisco; Hewson, Will; Homes, James; Ignatiev, Nicolai; Kaminski, Jacek; Karatekin, Ozgur; Kasaba, Yasumasa; Lanciano, Orietta; Lefèvre, Franck; Lewis, Stephen; López-Puertas, Manuel; López-Valverde, Miguel; Mahieux, Arnaud; Mason, Jon; Mc Connell, Jack; Mumma, Mike; Nakagawa, Hiromu, Neary, Lori; Neefs, Eddy; Novak, R.; Oliva, Fabrizio; Piccialli, Arianna; Renotte, Etienne; Robert, Severine; Sindoni, Giuseppe; Smith, Mike; Stiepen, Arnaud; Thomas, Ian; Trokhimovskiy, Alexander; Vander Auwera, Jean; Villanueva, Geronimo; Viscardy, Sébastien; Whiteway, Jim; Willame, Yannick; Wilquet, Valérie; Wolff, Michael; Wolkenberg, Paulina,

*Tech team:* Alonso-Rodrigo, Gustavo; Aparicio del Moral, Beatriz; Barzin, Pascal; Beeckman, Bram; BenMoussa, Ali; Berkenbosch, Sophie; Biondi, David; Bonnewijn, Sabrina; Candini, Gian Paolo; Clairquin, Roland; Cubas, Javier; Giordanengo, Boris; Gissot, Samuel; Gomez, Alejandro; Hathi, Brijen; Jeronimo Zafra, Jose; Leese, Mark; Maes, Jeroen; Mazy, Emmanuel; Mazzoli, Alexandra; Meseguer, Jose; Morales, Rafael; Orban, Anne; Pastor-Morales, M; Perez-grande, Isabel; Queirolo, Claudio; Ristic, Bojan; Rodriguez Gomez, Julio; Saggin, Bortolino; Samain, Valérie; Sanz Andres, Angel; Sanz, Rosario; Simar, Juan-Felipe; Thibert, Tanguy

## Modeling of HDO in the Martian atmosphere

Loïc Rossi (1), F. Montmessin (1), F. Forget (2), E. Millour (2), K. Olsen (1), M. Vals (2), A. Fedorova (3), A. Trokhimovskiy (3), O. Korabev (3) and the ACS team

(1) LATMOS, Guyancourt, France (loic.rossi@latmos.ipsl.fr) (2) Laboratoire de Météorologie Dynamique (LMD), Paris, France (3) Space Research Institute (IKI), Moscow, Russia

### Abstract

HDO and the D/H ratios are important species to study to understand Mars past and present climate, in particular with regards to the evolution through ages of the Martian water cycle. We present here new modeling efforts aimed at rejuvenating the representation of HDO in the LMD Mars GCM motivated by the future comparison with the new observations provided by the Atmospheric Chemistry Suite (ACS) on board the ESA/Roscosmos Trace Gas Orbiter.

### 1. Introduction

Mars is known to have had a significant liquid water reservoir on the surface and the D/H ratio is an important tool to estimate the abundance of the early water reservoir on Mars and its evolution with time. The D/H ratio is a measure of the ratio of the current exchangeable water reservoir to the initial exchangeable water reservoir. Many observations from the ground have shown that the current ratio is five times that of the reference in Earth's oceans [3, 6, 8].

H and D atoms in the upper atmosphere are coming from H<sub>2</sub>O and HDO, their sole precursor in the lower atmosphere. The lower mass of H over D atoms and the fact that H<sub>2</sub>O is preferentially photolysed over HDO [2] explain the differential escape of these two elements. Finally, due to differences in vapor pressure for HDO and H<sub>2</sub>O, the solid phase of water is enriched in deuterium compared to the vapor phase. This effect is known as the Vapor Pressure Isotope Effect (VPIE) and can reduce the D/H ratio above the condensation level to values as low as 10% of the D/H ratio near the surface [1, 4].

### 2. Modeling HDO

These fractionation processes can affect the amount of HDO with latitude, longitude, altitude and with the season. In particular, previous models [7] have

shown that an isotopic gradient should appear between the cold regions where condensation occurs and the warmer regions. This leads to a latitudinal gradient of D/H (with variations greater than a factor of 5) between the warm and moist summer hemisphere and the cold and dry winter hemisphere. Yet some observations [8] also show longitudinal variations of H/D ratios which are not explained so far. It is therefore essential to model the HDO cycle and the associated processes of fractionation in a 3D general climate model (GCM).

Previous work has been done on 3D GCMs of HDO, in particular around the LMD Mars GCM [7]. Since the GCM has considerably evolved since this first HDO introduction in the modeled water cycle, a reappraisal of HDO predictions is needed to account for the detailed microphysics that control cloud formation and thus HDO fractionation. With the TGO mission now entering its mission phase, very strong and precise constraints will be soon available to evaluate the GCM prediction capability.

### 3. Contribution of ACS

The Trace Gas Orbiter, part of the ExoMars mission, has now reached its operational orbit. Onboard is the Atmospheric Chemistry Suite, a set of spectrometers designed to study the atmosphere of Mars with a specific focus on trace gases such as methane.

ACS combines high resolving power (> 10,000), high accuracy (ppb level) and large spectral coverage (0.7 – 17  $\mu\text{m}$ ) to a large variety of observation modes [5].

Thanks to its solar occultation capabilities, ACS will be able to provide vertical profiles of HDO and H<sub>2</sub>O from a few kilometers above the surface up to 60 km, reaching precisions up to 1 ppb. It will thus be possible to detect when the abundance of the two species decreases due to condensation, to observe the cloud formation and to measure the subsequent fractionation.

These measurements will constrain the spatial and

temporal variabilities and help improve our understanding of the HDO and H<sub>2</sub>O cycles.

We will describe here our preliminary work on the update of the HDO model in the LMD Mars GCM and will attempt first comparison with the early TGO/ACS observations.

## Acknowledgements

ExoMars is the space mission of ESA and Roscosmos. The ACS experiment is led by IKI Space Research Institute in Moscow. The project acknowledges funding by Roscosmos and CNES. Science operations of ACS are funded by Roscosmos and ESA. Science support in IKI is funded by Federal agency of science organizations (FANO). L.R. acknowledges support from the Excellence Laboratory "Exploration Spatiale des Environnements Planétaires (ESEP)".

## References

- [1] Bertaux, J. L., & Montmessin, F. (2001). Isotopic fractionation through water vapor condensation: The Deuteropause, a cold trap for deuterium in the atmosphere of Mars. *Journal of Geophysical Research: Planets*, 106(E12), 32879-32884.
- [2] Cheng, B. M., et al. (1999). Photo-induced fractionation of water isotopomers in the Martian atmosphere. *Geophysical Research Letters*, 26(24), 3657-3660.
- [3] Encrenaz, T., et al. (2018). New measurements of D/H on Mars using EXES aboard SOFIA. *Astronomy & Astrophysics*, 612, A112.
- [4] Fouchet, T., & Lellouch, E. (2000). Vapor Pressure Isotope Fractionation Effects in Planetary Atmospheres: Application to Deuterium. *Icarus*, 144, 114-123.
- [5] Korablev, O., Montmessin, F., Trokhimovskiy, A., Fedorova, A. A., Shakun, et al. (2018). The atmospheric chemistry suite (ACS) of three spectrometers for the ExoMars 2016 Trace Gas Orbiter. *Space Science Reviews*, 214(1), 7.
- [6] Krasnopolsky, V. A. (2015). Variations of the HDO/H<sub>2</sub>O ratio in the martian atmosphere and loss of water from Mars. *Icarus*, 257, 377-386.
- [7] Montmessin, F., Fouchet, T., & Forget, F. (2005). Modeling the annual cycle of HDO in the Martian atmosphere. *Journal of Geophysical Research: Planets*, 110(E3).
- [8] Villanueva, G. L., et al. (2015). Strong water isotopic anomalies in the martian atmosphere: Probing current and ancient reservoirs. *Science*, 348(6231), 218-221.

## Performance and the sensitivity of the ACS MIR channel, first months of solar occultations

Alexander Trokhimovskiy (1), Anna Fedorova (1), Andrey Patrakeev (1), Nikita Kokonkov (1), Jean-Loup Bertaux (1,2), Alexey Shakun (1), Franck Montmessin (2), Oleg Korablev (1)  
(1) Space Research Institute (IKI), Moscow, Russia, (2) LATMOS/CNRS, Guyancourt, France (a.trokh@gmail.com)

### Abstract

The Atmospheric Chemistry Suite (ACS) package is a part of Russian contribution to ExoMars 2016 Trace Gas Orbiter (TGO) ESA-Roscosmos mission for studies of the Martian atmosphere and climate [1]. The cross-dispersion ACS MIR spectrometer was designed to meet major scientific goal of the mission – precise observations of known and trace atmospheric components. Having both, high spectral resolution and signal to noise ratio (SNR) of acquired spectra, MIR channel operates in solar occultation only. The spectral range of MIR is 2.3-4.24  $\mu\text{m}$ . Regular observations from Martian orbit have started in April 2018. For the upper layers of the atmosphere the standard deviation of the calibrated transmittance spectra calculated for a single detector line is better than 0.02%. Detector lines coadding can be used to obtain a further increase of the SNR yet at the expense of a decrease in vertical resolution. The tangent altitude range of observations through the Martian atmosphere starts from several kilometers above the surface, increasing up to 200 kilometers where strong  $\text{CO}_2$  lines can still be detected in the thermosphere.

The most tantalizing goal of ACS MIR is to do sensitive measurements of methane with detection threshold at ppt level. Besides methane, ACS MIR will be able to establish new results for a number of minor species:  $\text{C}_2\text{H}_2$ ,  $\text{C}_2\text{H}_4$ ,  $\text{C}_2\text{H}_6$ ,  $\text{HO}_2$ ,  $\text{H}_2\text{O}_2$ ,  $\text{H}_2\text{CO}$ ,  $\text{HCl}$ ,  $\text{SO}_2$ ,  $\text{OCS}$  etc. For the first time in Mars exploration of the vertical profile of the  $\text{HDO}/\text{H}_2\text{O}$  ratio in Martian atmosphere will be performed. The spectral range of spectrometer includes several  $\text{CO}_2$  absorption bands allows to measure density, temperature profiles and isotopic ratios. The short-wavelength side of MIR's spectral range is extended to cover almost the whole carbon monoxide band.

The general performance, sensitivity levels and further observation plans of the ACS MIR will be presented.

### Acknowledgements

ExoMars is the space mission of ESA and Roscosmos. The ACS experiment is led by IKI Space Research Institute in Moscow. The project acknowledges funding by Roscosmos and CNES. Science operations of ACS are funded by Roscosmos and ESA. Science support in IKI is funded by Federal agency of science organizations (FANO).

### References

- [1] Korablev, O., Montmessin, F., and ACS Team: The Atmospheric Chemistry Suite (ACS) of three spectrometers for the ExoMars 2016 Trace Gas Orbiter, *Space Sci. Rev.*, 214:7, 2018.

# CO<sub>2</sub> density and temperature profiles of Mars atmosphere: first retrievals from the ACS MIR solar occultations

Denis Belyaev (1), Franck Montmessin (2), Anna Fedorova (1), Jean-Loup Bertaux (1, 2), Kevin Olsen (2), Alexander Trokhimovskiy (1), Andrey Patrakeev (1), Alexey Shakun (1), and Oleg Korablev (1)  
(1) Space Research Institute (IKI), Moscow, Russia, (2) LATMOS/CNRS, Guyancourt, France (bdenya.iki@gmail.com)

## Abstract

The Atmospheric Chemistry Suite (ACS) began nominal science operations in April 2018 onboard the Trace Gas Orbiter (TGO) of the ExoMars mission. The mid-infrared channel (MIR) of the instrument is a cross-dispersion echelle spectrometer dedicated to solar occultation measurements in the 2.3–4.3  $\mu\text{m}$  range [1]. This experiment achieves the signal-to-noise ratio  $\text{SNR} \sim 3000$  with the instrumental resolving power of  $>50,000$ . It is able to accomplish the most sensitive measurements of the trace gases ever present in the Martian atmosphere. In parallel, the tiniest atmospheric layers – even up to 200 km – may be probed along the occultation line of sight measuring in strong CO<sub>2</sub> absorption bands (2.7 and 4.3  $\mu\text{m}$ ). It gives us possibility to retrieve density, scale height and temperature of the Martian thermosphere.

In this paper we present first results of CO<sub>2</sub> density and temperature retrievals from the ACS MIR solar occultations. The statistics of observations counts a few sunsets and sunrises per day in the both Martian hemispheres. Each session is devoted to a spectral interval correspondent to one of ten positions of the secondary MIR grating [1]. Such coverage allows measuring all significant CO<sub>2</sub> bands in the 2.3–4.3  $\mu\text{m}$  range orbit by orbit. Depending on absorption line intensities and its temperature behavior several transition bands were selected for density and temperature retrievals at different altitude ranges. An example of absorption band around 4.3  $\mu\text{m}$  is presented in Figure 1. Here strongest transitions R18e...R38e are shown at different temperatures on a background of weak ones (1a). This spectral interval is suitable to measure high atmospheric altitudes: 100-200 km (1b). Those strong lines are clearly detected at 200 km. Except the main isotope <sup>16</sup>O<sup>12</sup>C<sup>16</sup>O, a few others (<sup>16</sup>O<sup>12</sup>C<sup>18</sup>O, <sup>16</sup>O<sup>13</sup>C<sup>16</sup>O) are also analyzed by the MIR, providing additional

possibility to study the oxygen and carbon isotopic ratios.

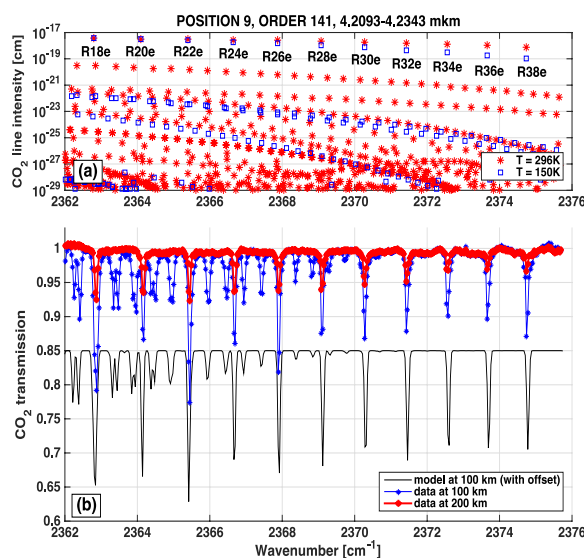


Figure 1: An example of CO<sub>2</sub> absorption measurement at 4.3  $\mu\text{m}$  band at high altitudes of Martian atmosphere. (a): line intensities at temperatures 296 K (red stars) and 150 K (blue squares), calculated from HITRAN 2016. (b): transmission spectra, measured at 100 km (in blue) and at 200 km (in red) in echelle order #141, 25<sup>th</sup> April. To compare, modeled transmission (in black, with offset) was estimated for 100 km on a basis of the MCD (<http://www-mars.lmd.jussieu.fr>).

## Acknowledgements

ExoMars is the space mission of ESA and Roscosmos. The ACS experiment is led by IKI Space Research Institute in Moscow. The project acknowledges funding by Roscosmos and CNES. Science operations of ACS are funded by Roscosmos

and ESA. Science support in IKI is funded by the Russian Government Grant ##14.W03.31.0017.

## **References**

[1] Korablev, O., Montmessin, F., and ACS Team: The Atmospheric Chemistry Suite (ACS) of three spectrometers for the ExoMars 2016 Trace Gas Orbiter, *Space Sci. Rev.*, 214:7, 2018.

## Preliminary results on sensitive search of minor species using the first data of TGO/NOMAD

**Shohei Aoki** (1,2,3), Ann Carine Vandaele (1), Séverine Robert (1), Ian R. Thomas (1), Loïc Trompet (1), Justin T. Erwin (1), Arianna Piccialli (1), Valérie Wilquet (1), Arnaud Mahieux (1), Frank Daerden (1), Lori Neary (1), Sébastien Viscardy (1), Bojan Ristic (1), Geronimo L. Villanueva (4), Giuliano Liuzzi (4), Michael J. Mumma (4), Brittany Hill (5), Bernd Funke (5), Miguel A. Lopez Valverde (5), James A. Holmes (6), Giuseppe Sindoni (7), Marco Giuranna (7), Giuseppe Etiope (8), Nicholas A. Teanby (9), Manish R. Patel (6), Giancarlo Bellucci (7), Jose Juan Lopez-Moreno (5) and the NOMAD team

(1) Royal Belgian Institute for Space Aeronomy, Belgium, (2) Fonds National de la Recherche Scientifique, Belgium, (3) Tohoku University, Japan, (4) NASA Goddard Space Flight Center, USA, (5) Instituto de Astrofísica de Andalucía, Spain, (6) Open University, UK, (7) Istituto di Astrofisica e Planetologia, Italy, (8) Istituto Nazionale di Geofisica e Vulcanologia, Italy, (9) University of Bristol, UK. (e-mail : [shohei.aoki@aeronomie.be](mailto:shohei.aoki@aeronomie.be))

### Abstract

Nadir and Occultation for Mars Discovery (NOMAD) onboard ExoMars Trace Gas Orbiter (TGO) has started the science measurements on 21 April, 2018. We present the preliminary results on the sensitive search of minor species in the Martian atmosphere from the first data measured by TGO/NOMAD.

### 1. The NOMAD instrument

NOMAD is a spectrometer operating in the spectral ranges between 0.2 and 4.3  $\mu\text{m}$  onboard ExoMars TGO [1]. NOMAD has 3 spectral channels: a solar occultation channel (SO – Solar Occultation; 2.3-4.3  $\mu\text{m}$ ), a second infrared channel capable of nadir, solar occultation, and limb sounding (LNO – Limb Nadir and solar Occultation; 2.3-3.8  $\mu\text{m}$ ), and an ultraviolet/visible channel (UVIS – UV visible, 200-650 nm). The infrared channels (SO and LNO) have high spectral resolution ( $\lambda/d\lambda \sim 20,000$ ) provided by echelle grating in combination with an Acousto-Optic Tunable Filter (AOTF) which selects diffraction orders [2]. The concept of the infrared channels are derived from the Solar Occultation in the IR (SOIR) instrument [3] onboard Venus Express. The sampling rate for the solar occultation measurement is 1 km, which provides unprecedented vertical resolution spanning altitudes from the surface to 200 km. Nadir sounding by the LNO channel will acquire spectra with an instantaneous footprint of 0.5 x 17  $\text{km}^2$ , which allows us to obtain maps of trace gases and aerosols in the Martian atmosphere.

One of the most remarkable capabilities of NOMAD is its high spectral resolution in the near infrared range. It allows us (1) to investigate vertical profiles of the atmospheric constituents (such as carbon dioxide, carbon monoxide, water vapor, and their isotopic ratio) and (2) to perform sensitive search of organic species (such as  $\text{CH}_4$ ,  $\text{C}_2\text{H}_4$ ,  $\text{C}_2\text{H}_6$ ,  $\text{H}_2\text{CO}$ ) and other trace gases (such as  $\text{HCl}$ ,  $\text{HCN}$ ,  $\text{HO}_2$ ,  $\text{H}_2\text{S}$ ,  $\text{N}_2\text{O}$ ,  $\text{OCS}$ ) by solar occultation measurements by the SO channel, and (3) to obtain maps of the atmospheric constituents (such as carbon dioxide, carbon monoxide, water vapor, and their isotopic ratio), across the planet by nadir viewing by the LNO channel.

### 2. Search of the minor species

In this study, we focus on the sensitive search of minor species such as  $\text{C}_2\text{H}_2$ ,  $\text{C}_2\text{H}_4$ ,  $\text{C}_2\text{H}_6$ ,  $\text{HCl}$ ,  $\text{HCN}$ ,  $\text{H}_2\text{CO}$ , and  $\text{HO}_2$  using the data measured by the SO channel.

Based on the expected performance, we calculated theoretical detections limit of the minor species by NOMAD [4]. These results for the minor species listed above are summarized in Table 1. We note that these estimations were performed based on the radiative transfer calculation for clear sky conditions. Thus, we expect that the actual detection limits will be slightly higher than the values shown in Table 1. In the presentation, the preliminary results of the analysis using the first data will be discussed.

Table 1: The minor species investigated in this study, their upper limits (3-sigma) by the previous studies, and their theoretical detection limits by NOMAD solar occultation measurements at 20 km by the SO channel [4].

Species	Upper limits by the previous studies (column-integrated)	Theoretical detection limits by NOMAD SO channel (at 20 km alt.)
C <sub>2</sub> H <sub>2</sub>	3 ppb [5]	0.03 ppb
C <sub>2</sub> H <sub>4</sub>	4 ppb [6]	0.2 ppb
C <sub>2</sub> H <sub>6</sub>	0.2 ppb [6]	0.03 ppb
HCl	0.3 ppb [7]	0.03 ppb
HCN	2 ppb [6]	0.03 ppb
H <sub>2</sub> CO	4 ppb [6]	0.04 ppb
HO <sub>2</sub>	200 ppb [6]	1 ppb
H <sub>2</sub> S	2 ppb [8]	4 ppb
N <sub>2</sub> O	65 ppb [6]	0.2 ppb
OCS	70 ppb [9]	0.3 ppb

## Acknowledgements

This research was supported by the FNRS CRAMIC project under grant number T.0171.16. The NOMAD experiment is led by the Royal Belgian Institute for Space Aeronomy (IASB-BIRA), assisted by Co-PI teams from Spain (IAA-CSIC), Italy (INAF-IAPS), and the United Kingdom (Open University). This project acknowledges funding by the Belgian Science Policy Office (BELSPO), with the financial and contractual coordination by the ESA Prodex Office (PEA 4000103401, 4000121493), by MICIIN through Plan Nacional (AYA2009-08190 and AYA2012-39691), as well as by UK Space Agency through grant ST/P000886/1 and Italian Space Agency through grant 2018-2-HH.0. This research was also performed as part of the ‘‘Excellence of Science’’ project ‘‘Evolution and Tracers of Habitability on Mars and the Earth’’ (FNRS 30442502) and supported by the BrainBe SCOOP project. US investigators were supported by the National Aeronautics and Space Administration. The IAA/CSIC team has been supported by Spanish Ministry of Economy, Industry and Competitiveness and by FEDER funds under grant ESP2015-65064-C2-1-P (MINECO/FEDER).

## References

- [1] Vandaele, A.C. et al, Planetary and Space Science, 119, 233–249, 2015.
- [2] Neefs, E. et al, Applied Optics, 54(28), 8494-8520, 2015.
- [3] Nevejans, D. et al., Applied Optics, 45(21), 5191-5206, 2006.
- [4] Robert, S. et al., Planetary and Space Science, 124, 94-104, 2016.
- [5] Maguire, W.C., Icarus, 32, 85-97, 1977.
- [6] Villanueva, G.L. et al., Icarus, 223, 11-27, 2013.
- [7] Hartogh, P. et al., Astron. Astrophys. 521 (L49), 1–5, 2010.
- [9] Khayat, A.S. et al, Icarus, 253, 130-141, 2015.
- [10] Encrenaz, T. et al., Planetary and Space Science, 49, 731–741, 1991.

## The NOMAD team

*Scientific team:* Vandaele, Ann Carine; Lopez Moreno, Jose Juan; Bellucci, Giancarlo; Patel, Manish; Allen, Mark; Alonso-Rodrigo, Gustavo; Altieri, Francesca; Aoki, Shohei; Bauduin, Sophie; Bolsée, David; F. Giacomo Carrozzo, Clancy, Todd; Cloutis, Edward; Daerden, Frank; D’Aversa, Emiliano; Depiesse, Cédric; Erwin, Justin; Fedorova, Anna; Formisano, Vittorio; Funke, Bernd; Fussen, Didier; Garcia-Comas, Maia; Geminale, Anna; Gérard, Jean-Claude; Gillotay, Didier; Giuranna, Marco; Gonzalez-Galindo, Francisco; Hewson, Will; Homes, James; Ignatiev, Nicolai; Kaminski, Jacek; Karatekin, Ozgur; Kasaba, Yasumasa; Lanciano, Orietta; Lefèvre, Franck; Lewis, Stephen; López-Puertas, Manuel; López-Valverde, Miguel; Mahieux, Arnaud; Mason, Jon; Mc Connell, Jack; Mumma, Mike; Nakagawa, Hiromu, Neary, Lori; Neefs, Eddy; Novak, R.; Oliva, Fabrizio; Piccialli, Arianna; Renotte, Etienne; Robert, Severine; Sindoni, Giuseppe; Smith, Mike; Stiepen, Arnaud; Thomas, Ian; Trokhimovskiy, Alexander; Vander Auwera, Jean; Villanueva, Geronimo; Viscardy, Sébastien; Whiteway, Jim; Willame, Yannick; Wilquet, Valérie; Wolff, Michael; Wolkenberg, Paulina.

*Tech team:* Alonso-Rodrigo, Gustavo; Aparicio del Moral, Beatriz; Barzin, Pascal; Beeckman, Bram; BenMoussa, Ali; Berkenbosch, Sophie; Biondi, David; Bonnewijn, Sabrina; Candini, Gian Paolo; Clairquin, Roland; Cubas, Javier; Giordanengo, Boris; Gissot, Samuel; Gomez, Alejandro; Hathi, Brijen; Jeronimo Zafra, Jose; Leese, Mark; Maes, Jeroen; Mazy, Emmanuel; Mazzoli, Alexandra; Meseguer, Jose; Morales, Rafael; Orban, Anne; Pastor-Morales, M; Perez-grande, Isabel; Queirolo, Claudio; Ristic, Bojan; Rodriguez Gomez, Julio; Saggin, Bortolino; Samain, Valérie; Sanz Andres, Angel; Sanz, Rosario; Simar, Juan-Felipe; Thibert, Tanguy

# The Exomars 2020 mission and the search for chemotrophic biosignatures

F. Westall<sup>1</sup>, J. Vago<sup>2</sup>, J. Bridges<sup>3</sup> and the ExoMars Landing Site Selection Committee, K. Hickman-Lewis<sup>1</sup>, F. Foucher<sup>1</sup>, B. Cavalazzi<sup>4</sup>, P. Gautret<sup>5</sup>, K.A. Campbell<sup>6</sup>, C.S. Cockell<sup>7</sup>. <sup>1</sup> CNRS-CBM, Orléans, France (frances.westall@cnrs-orleans.fr), <sup>2</sup>ESA-ESTEC, Noordwijk, The Netherlands, <sup>3</sup>Univ. Leicester, UK, <sup>4</sup>Univ. Bologna, Italy, <sup>5</sup>CNRS-ISTO, Orléans, France, <sup>6</sup>Univ. Auckland, New Zealand, <sup>7</sup>Univ. Edinburgh, UK.

## Abstract

This is the abstract section of your paper. Please replace these instructions with the text of your abstract. The text will appear in two columns. In the final abstract file (after uploading into Copernicus Office) each of those two columns are 75 mm wide. If you are including figures, tables and equations, they MUST be imported into this file. The text will automatically wrap to a second page if necessary.

## 1. Introduction

The ExoMars 2020 mission aims at searching primarily for traces of past life within a specific geological context. The potential landing sites, Oxia Planum and Mawrth Vallis represent a variety of sediment types, including volcanoclastic sediments and their alteration products, such as clays, as well as possibly chemical sediments (salts, amorphous silica) of Early Noachian to Hesperian ages. In both areas, finely layered Noachian deposits have been altered by aqueous processes to produce Fe/Mg clays (~300 m in Mawrth and ~20m in Oxia) that are overlain by fluvial (Mawrth) and fluvio-deltaic sediments (Oxia) of Early Hesperian age [1-3]. In addition, the Mawrth deposits were later traversed by fluids that infilled cross-cutting fractures, possibly related to the nearby Oyama impact, indicating fluid circulation. The top of the Mawrth succession was then altered to Al phyllosilicates and hydrated silica. Both locations were subsequently covered by other deposits that are slowly being eroded away.

In terms of habitability, Mawrth and Oxia have seen varying environmental conditions ranging from possibly subaqueous, through fluvial/deltaic to pedogenic, with the possibility of hydrothermal or groundwater percolations. In an overall anoxic

context and the fact that the lack of long-term habitability of the isolated and temporally distant habitats, means that it is unlikely that, if life did emerge on the planet, that it evolved beyond a chemotrophic metabolism [4], any preserved life forms from these two locations would be chemotrophic in origin [4]. On Earth, the only habitat that shares some of these environmental constraints was that of the early anoxic Earth [Westall 2015] and certain “extreme” environments on more recent times. Understanding the preservation of chemotrophic life forms and their fossilized signatures in lithified (cemented) sediments is, thus, greatly aided by study of relevant terrestrial analogues.

## 2. Fossilised chemotrophs in Early Archaean rocks

Early Archaean volcanic sediments altered to phyllosilicates (smectite) in aqueous environments and influenced by hydrothermal fluids are excellent analogues for early Mars [4]. Deposited in similar anoxic conditions, they host fossilized traces of chemotrophic life forms [4, 5]. Chemotrophs (lithotrophs) colonized the surfaces of volcanic grains, becoming colonised in turn by organotrophs, and they also formed spiky colonies that grew *in situ* in hydrothermally-precipitated, siliceous chemical sediments. However, while the lithotrophs appear to have been fairly widespread in their distribution, even in relatively oligotrophic waters (i.e. poor in nutrients), the distribution of the organotrophs was distinctly controlled by their vicinity to nutrient-rich hydrothermal fluids.

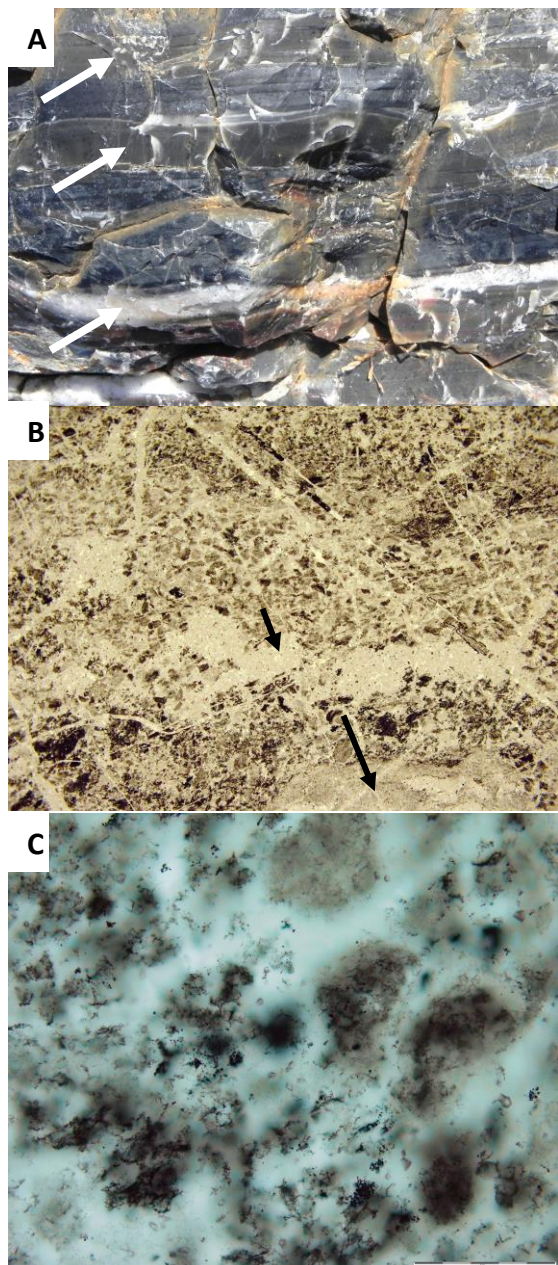


**Figure 1.** A Field photograph of layered hydrothermal sediments (arrows show macroscopic hydrothermal infiltrations) containing (B, C) chemotrophic colonies (dark clots) infiltrated by hydrothermal fluids (black arrows). Early Archaean, Barberton, South Africa.

These primitive organisms were preserved by rapid encapsulation in a mineral cement (silica in this case) resulting in a variety of biosignatures: (1) the physical remains of cells, colonies of cells, biofilms,

(2) degraded organic carbon either associated with the fossils of disseminated in the fine-grained argillaceous or chemical sediments, (3) as corrosion tunnels in the surfaces of volcanic grains.

For the ExoMars payload, while individual fossil cells are too small to be identified ( $<1\mu$ ), colonies in the form of clots or biofilms could be observed microscopically as dark patches or layers within martian sediments. The presence of carbon associated with potential biosignatures would be revealed by Raman and IR spectroscopy and the structure of the carbon molecules, including their chirality would be revealed by the MS techniques. Geological context on large to microscopic scales is essential for correct biosignature identification and would be also provided by the rover instrument suite.

### 3. Conclusions

While the Early Archaean fossils are highly relevant for understanding how chemotrophic life forms can be preserved, the fossilised remains have undergone a greater degree of metamorphism than that expected on Mars. Younger chemotrophic colonies, e.g. those forming carbonate mud mounds (sulphate reducing bacteria), inhabited an inherently oxygenic environment and were preserved in oxygen-controlled conditions. Their relevance is therefore limited. The remains of microbes in evaporite environments also suffer from the same problem. The solution is to use experimental studies to provide preserve chemotrophs from these diverse environments and to age them in martian conditions.

### Acknowledgements

ESA, CNES, the MASE project (FP7 Grant 607297).

### References

- [1] Qantin, C., et al., LPSC, #2863, 2016. [2] Carter, J. et al., LPSC, # 2064, 2016. [3]Loizeau, D. et al., JGR Planets, 120, 1820. [4] Westall, F. et al., Astrobiology, 15, 99, 2015. [5] Westall, F. et al., (2015) Geology, 43, 615–618.

## The Atmospheric Chemistry Suite (ACS) on board the ExoMars Trace Gas Orbiter

Oleg Korablev (1), Franck Montmessin (2), Alexander Trokhimovskiy (1), Anna Fedorova (1), Nikolay Ignatiev (1), Alexey Shakun (1), Alexey Grigoriev (1), and the ACS Team.  
(1) Space Research Institute (IKI), Moscow, Russia, (2) LATMOS-CNRS, Guyancourt, France (korab@iki.rssi.ru)

### Abstract

The Atmospheric Chemistry Suite (ACS) package is an element of the Russian contribution to the ESA-Roscosmos ExoMars 2016 Trace Gas Orbiter (TGO) mission. ACS consists of three separate infrared spectrometers [1]. This ensemble has been designed and developed in response to the Trace Gas Orbiter mission objectives that specifically address the requirement of high sensitivity instruments to enable the unambiguous detection of trace gases of potential geophysical or biological interest. ACS embarks a set of instruments achieving simultaneously very high accuracy (ppt level), very high resolving power ( $>10,000$ ) and broad spectral coverage ( $0.7$  to  $17 \mu\text{m}$  – the visible to thermal infrared range).

The near-infrared (NIR) channel is a versatile spectrometer covering the  $0.7$ - $1.6 \mu\text{m}$  spectral range with a resolving power of  $\geq 20,000$ . This channel is operated in solar occultation and nadir. In nadir NIR is mostly measuring water vapor and dayside oxygen emission. In solar occultation NIR provides profiling of  $\text{CO}_2$ ,  $\text{H}_2\text{O}$ , and the molecular oxygen  $\text{O}_2$  [Fedorova et al. EPSC 2018]. NIR can observe occultations together with the two other ACS channels MIR and TIRVIM, or together with another spectrometer aboard TGO, NOMAD, and TIRVIM.

The mid-infrared (MIR) channel is a high spectral resolution (resolving power of  $\geq 50,000$ ) instrument dedicated to solar occultation measurements in the  $2.2$ - $4.4 \mu\text{m}$  range. MIR targets to accomplish the most sensitive measurements of the trace gases in the Martian atmosphere. Also the abundant components, such as  $\text{CO}_2$ ,  $\text{CO}$ ,  $\text{H}_2\text{O}$  are profiled in a broad altitude range [Trokhimovskiy et al. EPSC 2018].

The thermal-infrared channel (TIRVIM) is a Fourier-transform spectrometer encompassing the spectral range of  $1.7$ - $17 \mu\text{m}$ . TIRVIM is being continuously operated in nadir to profile the temperature from the

surface up to  $50$ - $60 \text{ km}$  and to monitor dust and water ice clouds in nadir. Also the surface temperature is measured [Ignatiev et al. EPSC 2018]. In solar occultation TIRVIM is mostly operated in “climatology” mode, with spectral resolution of  $0.8 \text{ cm}^{-1}$ , delivering profiles of  $\text{CO}_2$ ,  $\text{CO}$ ,  $\text{H}_2\text{O}$  and aerosols. In a more “sensitive” mode, which requires dedicated spacecraft pointing TIRVIM observes through the full nadir aperture with the spectral resolution of  $0.13 \text{ cm}^{-1}$  giving access to trace gases [Grigoriev et al. EPSC 2018].

The overall status of the ACS experiment and key findings available by the time of the conference will be reported.

### Acknowledgements

ExoMars is the space mission of ESA and Roscosmos. The ACS experiment is led by IKI Space Research Institute in Moscow. The project acknowledges funding by Roscosmos and CNES. Science operations of ACS are funded by Roscosmos and ESA. OK, AT, AF, NI acknowledge support from the Ministry of Education and Science of the Russian Federation, Grant 14.W03.31.0017.

### References

- [1] Korablev, O. et al. The Atmospheric Chemistry Suite (ACS) of Three Spectrometers for the ExoMars 2016 Trace Gas Orbiter. *Space Science Reviews*, 214(1), 7, 2018. <http://doi.org/10.1007/s11214-017-0437-6>

## Spectrometer ISEM for ExoMars-2020 space mission: from qualification prototype to flight model

**Yury Dobrolenskiy** (1), Oleg Korablev (1), Anna Fedorova (1), Sergey Mantsevich (1,2), Yury Kalinnikov (3), Nikita Vyazovetskiy (1), Yuriy Ivanov (4), Ivan Syniavskiy (4), Andrey Titov (1), Alexander Stepanov (1,2), Alexander Sapgir (1), Nadezhda Evdokimova (1) and Ruslan Kuzmin (1,5)

(1) Space Research Institute of Russian Academy of Sciences, Profsoyuznaya 84/32, 117997 Moscow, Russia

(2) Faculty of Physics, M. V. Lomonosov Moscow State University, Vorob'evy Gory, 119991, Moscow, Russia

(3) G. Ya. Guskov Scientific Research Institute of Microdevices, Konstruktora Guskova 1, 124460, Zelenograd, Moscow, Russia

(4) Main Astronomical Observatory of National Academy of Sciences of Ukraine, Akademika Zabolotnogo str. 27, 03143, Kyiv, Ukraine

(5) V. I. Vernadsky Institute of Geochemistry and Analytical Chemistry of Russian Academy of Sciences, Kosygina 19, 119334, Moscow, Russia

### Abstract

Robust design, small dimensions and mass, the absence of moving parts in acousto-optic tunable filters (AOTFs) make them popular for space applications [1-3]. Here we introduce a pencil-beam near-infrared AOTF-based spectrometer ISEM for context assessment of the surface mineralogy in the vicinity of a planetary probe or a rover analyzing the reflected solar radiation in the near infrared range [4,5]. The ISEM (Infrared Spectrometer for ExoMars) instrument is to be deployed on the mast of ExoMars Rover planned for launch in 2020.

### ISEM spectrometer

The instrument covers the spectral range of 1.15–3.3  $\mu\text{m}$  with the spectral resolution of  $\sim 25 \text{ cm}^{-1}$  and is intended to study mineralogical and petrographic composition of the uppermost layer of the regolith and to estimate H<sub>2</sub>O/OH content and behavior in this layer. The instrument is able to detect the most important water-bearing minerals (i.e. phyllosilicates, sulfates, opal) and other minerals formed in the aqueous environments. Besides, it will help in real-time assessment of surface composition in selected areas, in support of identifying and selection of the most promising drilling sites. A study of variations of the atmospheric dust properties and of the atmospheric gaseous composition is also of interest.

The instrument (Fig. 1) consists of two parts: Optical Box and Electronic Box. The optical scheme includes entry optics, the AOTF, focusing optics, and a

Peltier-cooled InAs detector. A wide-angle acousto-optic tunable filter manufactured on the base of TeO<sub>2</sub> crystal is used. Incident optical radiation has ordinary polarization and the diffracted optical beam has the extraordinary polarization. The angle between the passed and diffracted optical beams is 6° at the output of the AO crystal. A pair of polarizers with crossed polarizing planes is used to filter out the non-desired zero diffraction order.



Figure 1: ISEM spectrometer: Optical Box (on the right) and Electronic Box.

Two qualification models of the instrument were manufactured. One of them has passed qualification tests including thermal-vacuum tests down to  $-130^{\circ}\text{C}$ . The second one is delivered to ESA for integration into ground-test model of the rover. At present, test

campaign and planetary protection activities with the flight model of the instrument has started.

Example of the gypsum reflectance spectrum obtained by qualification model of ISEM is shown in Fig. 2. Sample was crashed to powder.

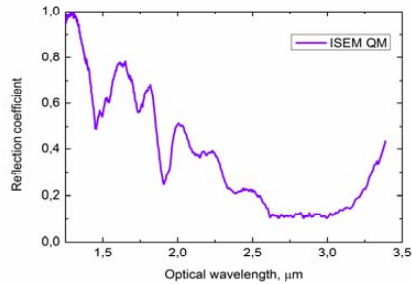


Figure 2: Gypsum spectra measured by ISEM.

## Acknowledgements.

We acknowledge FSF #16-12-10453 for the support in this work.

## References

- [1] O. Korablev, J. Bertaux, A. Fedorova et al., "SPICAM IR acousto-optic spectrometer experiment on MarsExpress," *Journal of Geophysical Research-Planets*, Vol. 111(E9), p. E09S03, 2006.
- [2] J. Bertaux, D. Nevejans, O. Korablev et al., "SPICAV on Venus Express: Three spectrometers to study the global structure and composition of the Venus atmosphere," *Planetary and Space Science*, Vol. 55(12), p. 1673, 2007.
- [3] O. Korablev, A. Trokhimovsky, A. V. Grigoriev et al., "Three infrared spectrometers, an atmospheric chemistry suite for the ExoMars 2016 trace gas orbiter," *Journal of Applied Remote Sensing*, N 8, p. 4983, 2014.
- [4] O. Korablev, A. Ivanov, A. Fedorova et al., "Development of a mast or robotic arm-mounted infrared AOTF spectrometer for surface Moon and Mars probes", *Proc. of SPIE*, Vol. 9608, p. 960807-1, 2015.

[5] O. Korablev, Y. Dobrolensky, N. Evdokimova et al., "Infrared Spectrometer for ExoMars: A Mast-Mounted Instrument for the Rover", *Astrobiology*, Vol. 17, N 6 and 7, p. 542, 2017.

## Preliminary retrievals of CO<sub>2</sub> column densities using the first data of TGO/NOMAD

**Arianna Piccialli** (1), Ann Carine Vandaele (1), Ian R. Thomas (1), Séverine Robert (1), Shohei Aoki (1,2,3), Loïc Trompet (1), Justin T. Erwin (1), Valérie Wilquet (1), Arnaud Mahieux (1), Frank Daerden (1), Lori Neary (1), Sébastien Viscardy (1), Bojan Ristic (1), Ozgur Karatekin (4), Michael D. Smith (5), Giuseppe Sindoni (6), Fabrizio Oliva (6), Sophie Bauduin (7), Paulina Wolkenberg (6), José Juan López-Moreno (8), Giancarlo Bellucci (6), Manish R. Patel (9) and the NOMAD team

(1) Royal Belgian Institute for Space Aeronomy, Belgium, (2) Fonds National de la Recherche Scientifique, Belgium, (3) Tohoku University, Japan, (4) Royal Observatory of Belgium, (5) NASA Goddard Space Flight Center, USA, (6) INAF, Istituto di Astrofisica e Planetologia Spaziali, Italy, (7) Université libre de Bruxelles, Belgium, (8) Instituto de Astrofísica de Andalucía, Spain, (9) Open University, UK. (email: [arianna.piccialli@aeronomie.be](mailto:arianna.piccialli@aeronomie.be), Twitter: [@apic79](https://twitter.com/apic79))

### Abstract

The NOMAD (Nadir and Occultation for MArS Discovery) – operating on board the ExoMars 2016 Trace Gas Orbiter mission – started to acquire the first scientific measurements on 21 April 2018.

Here, we will present first retrievals of CO<sub>2</sub> column density and surface pressure measured by the NOMAD LNO channel in the nadir mode.

### 1. The NOMAD LNO channel

NOMAD is a spectrometer operating in 3 channels: 1) a solar occultation channel (SO) operating in the infrared (2.3-4.3  $\mu\text{m}$ ); 2) a second infrared channel LNO (2.3-3.8  $\mu\text{m}$ ) capable of doing nadir, as well as solar occultation and limb; and 3) an ultraviolet/visible channel UVIS (200-650 nm) that can work in the three observation modes [1,2]. The LNO infrared channel has a high spectral resolution ( $\lambda/d\lambda \sim 10,000$ ) provided by an echelle grating in combination with an Acousto-Optical Tunable Filter which allows the selection of spectral windows (diffraction orders).

In nadir mode, LNO has an instantaneous footprint of  $0.5 \times 17 \text{ km}^2$ , therefore it is very well suited to measure the horizontal and local time distribution of total column density of several species such as CO<sub>2</sub>, CO, H<sub>2</sub>O, and isotopic ratio.

### 2. CO<sub>2</sub> column densities and surface pressure

Since carbon dioxide constitutes 95% of the Martian atmosphere, CO<sub>2</sub> column densities can be reasonably used as a proxy for surface pressure [3].

We plan to analyze the data measured in diffraction orders 149, 167, 168, 169 for the CO<sub>2</sub> retrievals (Table 1). Orders 167-169 are particularly interesting since they contain water vapor as well, which may be retrieved simultaneously with CO<sub>2</sub> (See [4]). We will use the line-by-line radiative transfer code ASIMUT-ALVL developed at IASB-BIRA [5] to retrieve CO<sub>2</sub> column density and surface pressure. These retrieved quantities will then be compared with values predicted by the 3D GEM-Mars v4 Global Circulation Model (GCM) [6].

**Table 1:** Wavenumber ranges of the diffraction orders for the CO<sub>2</sub> analysis by the NOMAD LNO channel.

Diffraction order	LNO wavenumber limits [ $\text{cm}^{-1}$ ]
149	3349.24-3375.99
167	3753.84-3783.83
168	3776.32-3806.49
169	3798.80-3829.15

## Acknowledgements

The NOMAD experiment is led by the Royal Belgian Institute for Space Aeronomy (BIRA-IASB), assisted by Co-PI teams from Spain (IAA-CSIC), Italy (INAF-IAPS), and the United Kingdom (Open University). This project acknowledges funding by the Belgian Science Policy Office (BELSPO), with the financial and contractual coordination by the ESA Prodex Office (PEA 4000103401, 4000121493), by MICIIN through Plan Nacional (AYA2009-08190 and AYA2012-39691), as well as by UK Space Agency through grant ST/P000886/1 and Italian Space Agency through grant 2018-2-HH.0. The research was performed as part of the “Excellence of Science” project “Evolution and Tracers of Habitability on Mars and the Earth” (FNRS 30442502. This research was supported by the FNRS CRAMIC project under grant number T.0171.16 and by the BrainBe SCOOP project.

## References

- [1] Vandaele, A.C., Neefs, E., Drummond, R. et al.: Science objectives and performances of NOMAD, a spectrometer suite for the Exo-Mars TGO mission, *Planetary and Space Science*, Vol. 119, pp. 233–249, 2015.
- [2] Neefs, E., Vandaele, A.C., Drummond, R. et al.: NOMAD spectrometer on the ExoMars trace gas orbiter mission: part 1 – design, manufacturing and testing of the infrared channels, *Applied Optics*, Vol. 54 (28), pp. 8494–8520, 2015.
- [3] Forget, F. Spiga, A.; Dolla, B.; Vinatier, S.; Melchiorri, R.; Drossart, P.; Gendrin, A.; Bibring, J-P; Langevin, Y.; Gondet, B. Remote sensing of surface pressure on Mars with the Mars Express/OMEGA spectrometer: 1. Retrieval method. *JGR*, 2007, 112, doi:10.1029/2006JE002871
- [4] Aoki, S., EPSC 2018.
- [5] Vandaele, A.C., M. De Mazière, R. Drummond, A. Mahieux, E. Neefs, V. Wilquet, O. Korablev, A. Fedorova, D. Belyaev, F. Montmessin, and J.L. Bertaux, Composition of the Venus mesosphere measured by SOIR on board Venus Express. *JGR*, 2008. 113 doi:10.1029/2008JE003140.
- [6] Neary, L., and F. Daerden (2018), The GEM-Mars general circulation model for Mars: Description and evaluation, *Icarus*, 300, 458–476, doi:10.1016/j.icarus.2017.09.028

## The NOMAD Team

*Scientific team:* Vandaele, Ann Carine; Lopez Moreno, Jose Juan; Bellucci, Giancarlo; Patel, Manish; Allen, Mark; Alonso-Rodrigo, Gustavo; Altieri, Francesca; Aoki, Shohei; Bauduin, Sophie; Bolsée, David; F. Giacomo Carrozzo, Clancy, Todd; Cloutis, Edward; Daerden, Frank; D’Aversa, Emiliano; Depiesse, Cédric; Erwin, Justin; Fedorova, Anna; Formisano, Vittorio; Funke, Bernd; Fussen, Didier; Garcia-Comas, Maia; Geminale, Anna; Gérard, Jean-Claude; Gillotay, Didier; Giuranna, Marco; Gonzalez-Galindo, Francisco; Hewson, Will; Homes, James; Ignatiev, Nicolai; Kaminski, Jacek; Karatekin, Ozgur; Kasaba, Yasumasa; Lanciano, Orietta; Lefèvre, Franck; Lewis, Stephen; López-Puertas, Manuel; López-Valverde, Miguel; Mahieux, Arnaud; Mason, Jon; Mc Connell, Jack; Mumma, Mike; Nakagawa, Hiromu, Neary, Lori; Neefs, Eddy; Novak, R.; Oliva, Fabrizio; Piccialli, Arianna; Renotte, Etienne; Robert, Severine; Sindoni, Giuseppe; Smith, Mike; Stiepen, Arnaud; Thomas, Ian; Trokhimovskiy, Alexander; Vander Auwera, Jean; Villanueva, Geronimo; Viscardy, Sébastien; Whiteway, Jim; Willame, Yannick; Wilquet, Valérie; Wolff, Michael; Wolkenberg, Paulina – *Tech team:* Alonso-Rodrigo, Gustavo; Aparicio del Moral, Beatriz; Barzin, Pascal; Beeckman, Bram; BenMoussa, Ali; Berkenbosch, Sophie; Biondi, David; Bonnewijn, Sabrina; Candini, Gian Paolo; Clairquin, Roland; Cubas, Javier; Giordanengo, Boris; Gissot, Samuel; Gomez, Alejandro; Hathi, Brijen; Jeronimo Zafra, Jose; Leese, Mark; Maes, Jeroen; Mazy, Emmanuel; Mazzoli, Alexandra; Meseguer, Jose; Morales, Rafael; Orban, Anne; Pastor-Morales, M; Perez-grande, Isabel; Queirolo, Claudio; Ristic, Bojan; Rodriguez Gomez, Julio; Saggin, Bortolino; Samain, Valérie; Sanz Andres, Angel; Sanz, Rosario; Simar, Juan-Felipe; Thibert, Tanguy

# Spectral characterization of the Ma\_MISS instrument on board the ExoMars 2020 rover

M. Ferrari (1), S. De Angelis (1), M.C. De Sanctis (1), F. Altieri (1), E. Ammannito (2), P. Tinivelli (1), D. Biondi (1), R. Mugnuolo (2), S. Pirrotta (2) and the Ma\_MISS team.

(1) Institute for Space Astrophysics and Planetology, IAPS-INAF, Rome, Italy ([marco.ferrari@iaps.inaf.it](mailto:marco.ferrari@iaps.inaf.it))

(2) Italian Space Agency, ASI, Italy

## Abstract

During the calibration campaign, laboratory measurements were performed on different minerals and rocks that can be considered as Mars analogs with the aim of characterizing the scientific performance of the Ma\_MISS (Mars Multispectral Imager for Subsurface Studies) flight spectrometer.

## 1. Introduction

Ma\_MISS is a visible and near infrared (VNIR, 0.4–2.2  $\mu\text{m}$ ) miniaturized spectrometer hosted by the drill system of the ExoMars 2020 rover [1]. Ma\_MISS will characterize the mineralogy and stratigraphy of the shallow subsurface down to two meters [2]. ExoMars will focus on the search for signs of life from both a morphological and a chemical point of view. Ma\_MISS will be implemented to accomplish the following scientific objectives: (1) determine the composition of the subsurface materials; (2) map the distribution of the subsurface  $\text{H}_2\text{O}$  and volatiles; (3) characterize important optical and physical properties of the materials (e.g., grain size); (4) produce a stratigraphic column that will provide information on the subsurface geology. The detector operating temperature is  $-50^\circ\text{C}$ . The thermal excursions at the equatorial and mid latitudes that the ExoMars mission can target for landing oscillate between a few degrees above 0 and  $-120^\circ\text{C}$ . Ma\_MISS will operate periodically during pauses in drilling activity and will produce hyperspectral images of the drill's borehole.

## 2. The Ma\_MISS instrument

The Ma\_MISS instrument main requirement is its miniaturization because it is embedded within the drill (Fig. 1). The spectrometer is placed in a box on the side wall of the drill box. The spectral range is 0.4–2.2  $\mu\text{m}$ , with a spectral sampling of 20 nm a SNR~100 and a spatial resolution of 120  $\mu\text{m}$ . The light from a 5W lamp is collected and carried,

through an optical fiber bundle, to the miniaturized Optical Head, hosted within the drill tip. A Sapphire Window with high hardness and transparency on the drill tip protects the Ma\_MISS optical head allowing to observe the borehole wall. Different depths can be reached by the use of three extension rods, 50 cm long, each containing optical fibers and a collimator. The first extension rod is connected to the non-rotating part of the Drill, hosted on the rover, through a Fiber Optical Rotating Joint (FORJ), that allows the continuity of the signal link between the rotating part of the drill and the spectrometer.

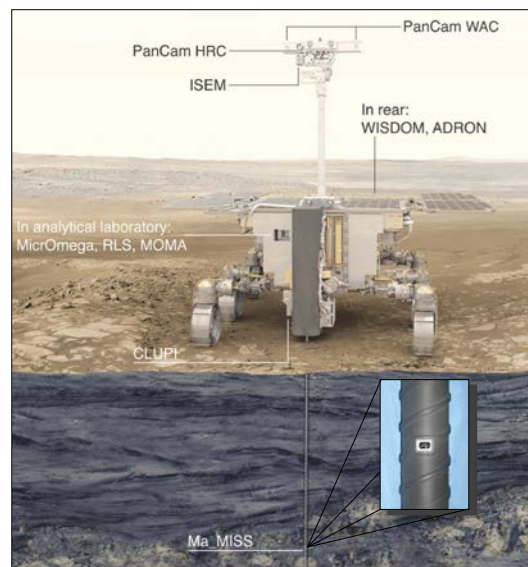


Fig. 1: Artistic view of the ExoMars-Pasteur Rover with instruments allocations. Ma\_MISS is integrated within the drill.

## 3. Experimental setup

The characterization of the scientific performances of the Ma\_MISS instrument was made in April 2018, at the Leonardo calibration facility in Florence (Italy). During this activity, the Ma\_MISS spectrometer was inside a thermo-vacuum chamber (TVC) to maintain the detector unit at the operating temperature. The setup also included the GSE Tip Drill Tool

comprising the optical head with the illuminating system, the optical fibers with the FORJ, and the mini-AVIM connection adapters to pass the signal inside the TVC. During the characterization phase we selected three samples: a slab of Dunite rock, a slab of Montiferru lava and a slab of gypsum, a mineral that shows several spectral features in the range of Ma\_MISS. All the samples were mounted on an ad-hoc sample holder (Fig. 2) screwed on a guide to permit micrometric movement, which was necessary to reach the focus position or to illuminate specific features of interest on the selected sample.

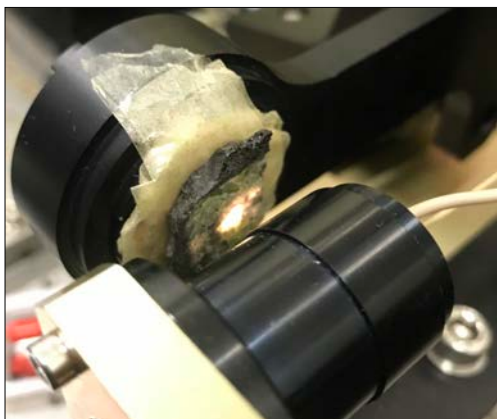


Fig. 2: The GSE Tip Drill Tool illuminating a dunite sample during the measurement session.

## 4. Discussion

Several measurements have been performed on samples of different nature to test the spectral performance of the Ma\_MISS instrument. Data are reported here as function of spectral channels on X-axis. The spectra collected on the three points on the slab of Montiferru lava (purple, blue and black spectra in fig. 3) are quite similar to each other. The weak absorption features indicated with the gray dashed line (at  $\sim 340$  px) represents the absorption at  $1.9 \mu\text{m}$  due to the presence of hydrated phases in the sample.

The spectra obtained on the gypsum slab (cyan spectra in fig. 3) show all its typical absorption features reported in literature [3].

The green spectrum acquired on the dunite sample shows the wide absorption band (from 125 to 275 px) near  $1 \mu\text{m}$  typical of olivine. All the samples were measured a second time using a FieldSpecPro spectrometer in the INAF-IAPS laboratories to cross-check the obtained results, which are consistent with each other. However, the different spatial resolution between the two instruments (Ma\_MISS  $120 \mu\text{m}$  and

FieldSpecPro  $6 \text{ mm}$ ) can lead to collect quite different spectra when analyzing heterogeneous samples.

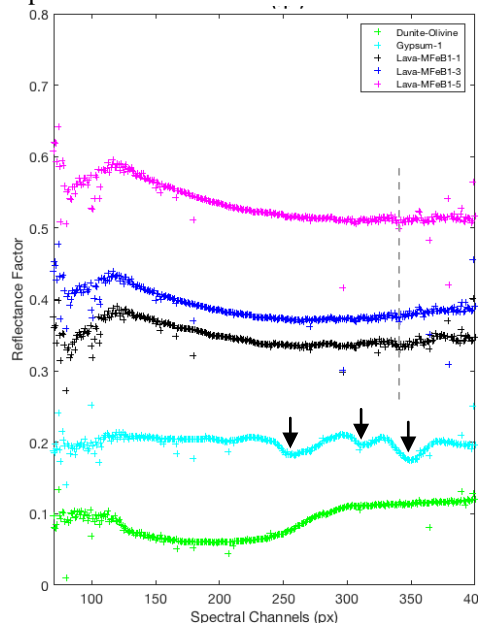


Fig. 3: Spectra obtained on Montiferru Lava, gypsum and dunite. The value on the x axis is referred to the number of pixels on the detector and not to the wavelength.

## 5. Summary and Conclusions

The Ma\_MISS instrument has been developed to provide hyperspectral images of boreholes excavated by the ExoMars rover drill. The obtained results on the mineral/rock samples confirm that the Ma\_MISS spectrometer have a spectral range, resolution and imaging capabilities suitable for the Mars subsurface characterization. An unambiguous understanding of the landing site subsurface composition will be crucial to reconstruct the geological evolution of Mars and determine whether life might have occurred on the planet.

## Acknowledgements

We thank the European Space Agency (ESA) for the ExoMars Project, ROSCOSMOS and Thales Alenia Space for rover development, and Italian Space Agency (ASI) for funding and fully supporting Ma\_MISS experiment (ASI/INAF grant I/060/10/0).

## References

- [1]Vago J.L. et al. (2017): Astrobiology, 17, 6, 7.
- [2]De Sanctis et al. (2017): Astrobiology, 17, 6, 7.
- [3]Clark R.N. et al. (1990) JGR, 95, N.B8, P. 12,653- 12,680.

# Martian aerosol-free reflectance spectra as input to better constrain atmospheric dust content in the NOMAD/TGO nadir observations

**Francesca Altieri** (1), Valérie Wilquet (2), Fabrizio Oliva (1), Emiliano D'Aversa (1), Filippo Giacomo Carrozzo (1), Giancarlo Bellucci (1), Giuseppe Sindoni (1), Anna Geminale (1), Manish R. Patel (3), Ian R. Thomas (2), Yannick Willame (2), Shohei Aoki (2, 4, 5), Cédric Depiesse (2), Edward Cloutis (2), Frank Daerden (2), Will Hewson (3), Ozgur Karatekin (6), Orietta Lanciano (7), Arnaud Mahieux (2, 5, 8), Jon Mason (3), José Juan Lopez-Moreno (9), Manuel López-Puertas (9), Arianna Piccialli (2), Bojan Ristic (2), Séverine Robert (2), Frédéric Schmidt (10), Ann Carine Vandaele (2), and the NOMAD Team

(1) INAF-IAPS, Rome, Italy, (2) Royal Belgian Institute for Space Aeronomy, BIRA-IASB, Belgium, (3) Open University, United Kingdom, (4) Fonds National de la Recherche Scientifique, Belgium, (5) Tohoku University, Japan, (6) Royal Observatory of Belgium, KSB-ORB, Belgium, (7) ASI, Rome, Italy, (8) University of Texas at Austin, Austin, USA, (9) IAA-CSIC, Spain, (10) Université Paris Sud, Orsay, France ([francesca.altieri@iaps.inaf.it](mailto:francesca.altieri@iaps.inaf.it))

## Abstract

The Martian atmosphere is characterized by the presence of dust particles that during dust storms (global or regional) can reach opacities  $> 1$ . The aim of the present work is to identify and validate a strategy to better constrain atmospheric dust content in the NOMAD/TGO nadir observations making use of aerosol-free reflectance spectra derived from the OMEGA/MEX data set.

## 1. Rationale

NOMAD, the "Nadir and Occultation for Mars Discovery" experiment [1], is a suite of spectrometers on board the ExoMars Trace Gas Orbiter (TGO) mission that will operate in nadir, limb and solar occultation viewing modes. Nadir spectra will be collected by the Limb, Nadir and Occultation (LNO) and Ultraviolet and Visible Spectrometer (UVIS) channels, covering respectively the 2.3-3.8  $\mu\text{m}$  and the 0.2-0.65  $\mu\text{m}$  spectral ranges. In the visible and infra-red ranges covered by NOMAD dust does not show well-defined absorption bands, although this indication is being tested by other members of the NOMAD team. Airborne dust particles can increase/decrease the albedo for dark/bright terrains and introduce specific slopes depending on opacity and grain size. Surface reflectance in aerosol-free conditions is thus a crucial parameter in the retrieval codes used to assess the dust content in nadir viewing mode. The OMEGA (Observatoire pour la Minéralogie, l'Eau, les Glaces et l'Activité [2]) instrument on board the Mars

Express mission investigated Martian surface properties on a global scale between 0.4-5.1  $\mu\text{m}$  in nadir-pointing geometry and provide a valuable dataset to derive reflectance spectra of the surface in dust-free conditions [e.g. 3].

## 2. Method

Figure 1 shows two spectra from OMEGA sessions collected in two different seasons but covering the same location (LON= 68.6°E, LAT =15.9°N).

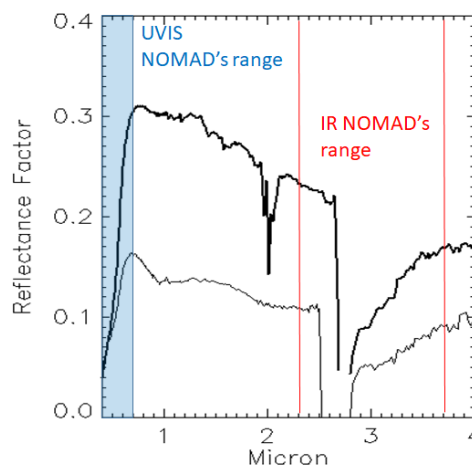


Figure 1: An example of OMEGA spectra, showing the overlap with NOMAD ranges.

The thin spectrum represents the atmosphere corrected reflectance retrieved from the OMEGA session ORB2458\_5 using the SAS (Surface

Atmosphere Separation) method [3]. Here, atmospheric features (dust and CO<sub>2</sub> absorptions at 1.5 μm and 2.2 μm) have been removed. The thick spectrum has been measured at the same location during the OMEGA session ORB4558\_4 but presents a higher dust content. It represents the top of dusty atmosphere, showing the CO<sub>2</sub> atmospheric features as well. For the dusty spectrum, opacity of the order of 3 has been estimated by means of the method described in [4], using the thin spectrum as input for the surface in dust-free conditions.

### 3. Summary

Aerosol-free reflectance spectra derived from the OMEGA data set can be used as input for the surface reflectance into NOMAD retrieval codes. Uncertainties due to the different spectral ranges covered by NOMAD and OMEGA will be evaluated and reported in this work. Water ice cloud effects will be also investigated. Improvements in the aerosol properties gathered thanks to NOMAD limb/occultation measurements will be taken into account.

### Acknowledgements

This work was supported by Italian Space Agency under grant 2018-2-HH.0. The NOMAD experiment is led by the Royal Belgian Institute for Space Aeronomy (IASB-BIRA), assisted by Co-PI teams from Spain (IAA-CSIC), Italy (INAF-IAPS), and the United Kingdom (Open University). This project acknowledges funding by the Belgian Science Policy Office (BELSPO), with the financial and contractual coordination by the ESA Prodex Office (PEA 4000103401), by Spanish Ministry of Economy, Industry and Competitiveness and by FEDER funds under grant ESP2015-65064-C2-1-P (MINECO/FEDER), as well as by UK Space Agency through grant ST/P000886/1. This work was supported by the European Union's Horizon 2020 Programme under grant agreement UPWARDS-633127.

### The NOMAD Team

*Scientific team:* Vandaele, Ann Carine; Lopez Moreno, Jose Juan; Bellucci, Giancarlo; Patel, Manish; Allen, Mark; Alonso-Rodrigo, Gustavo; Altieri, Francesca; Aoki, Shohei; Bauduin, Sophie; Bolsée, David; F. Giacomo Carrozzo, Clancy, Todd; Cloutis, Edward; Daerden, Frank; D'Aversa,

Emiliano; Depiesse, Cédric; Erwin, Justin; Fedorova, Anna; Formisano, Vittorio; Funke, Bernd; Fussen, Didier; Garcia-Comas, Maia; Geminale, Anna; Gérard, Jean-Claude; Gillotay, Didier; Giuranna, Marco; Gonzalez-Galindo, Francisco; Hewson, Will; Homes, James; Ignatiev, Nicolai; Kaminski, Jacek; Karatekin, Ozgur; Kasaba, Yasumasa; Lanciano, Orietta; Lefèvre, Franck; Lewis, Stephen; López-Puertas, Manuel; López-Valverde, Miguel; Mahieux, Arnaud; Mason, Jon; Mc Connell, Jack; Mumma, Michael J.; Nakagawa, Hiromu, Neary, Lori; Neefs, Eddy; Novak, R.; Oliva, Fabrizio; Piccialli, Arianna; Renotte, Etienne; Robert, Severine; Sindoni, Giuseppe; Smith, Mike; Stiepen, Arnaud; Thomas, Ian; Trokhimovskiy, Alexander; Vander Auwera, Jean; Villanueva, Geronimo; Viscardy, Sébastien; Whiteway, Jim; Willame, Yannick; Wilquet, Valérie; Wolff, Michael; Wolkenberg, Paulina – *Tech team:* Alonso-Rodrigo, Gustavo; Aparicio del Moral, Beatriz; Barzin, Pascal; Beeckman, Bram; BenMoussa, Ali; Berkenbosch, Sophie; Biondi, David; Bonnewijn, Sabrina; Candini, Gian Paolo; Clairquin, Roland; Cubas, Javier; Giordanengo, Boris; Gissot, Samuel; Gomez, Alejandro; Hathi, Brijen; Jeronimo Zafra, Jose; Leese, Mark; Maes, Jeroen; Mazy, Emmanuel; Mazzoli, Alexandra; Meseguer, Jose; Morales, Rafael; ; Orban, Anne; Pastor-Morales, M; Perez-grande, Isabel; Queirolo, Claudio; Ristic, Bojan; Rodriguez Gomez, Julio; Saggin, Bortolino; Samain, Valérie; Sanz Andres, Angel; Sanz, Rosario; Simar, Juan-Felipe; Thibert, Tanguy

### References

- [1] Vandaele, A.C., Neefs, E., Drummond, R. et al.: Science objectives and performances of NOMAD, a spectrometer suite for the Exo-Mars TGO mission, *Planetary and Space Science*, 119, 233–249, 2015.
- [2] Bibring, J-P., et al.: Omega: Observatoire pour La minéralogie, l'eau, Les Glaces Et l'activité. ESA SP-1240: Mars Express: The Scientific Payload. ESA Publications Division, ESTEC, Noordwijk, The Netherlands, pp. 37–49, 2004.
- [3] Geminale, A., et al.: Removal of atmospheric features in near infrared spectra by means of principal component analysis and target transformation on Mars: I method. *Icarus* 253, 51–65, 2015.
- [4] Oliva, F., et al.: Properties of a Martian local dust storm in Atlantis Chaos from OMEGA/MEX data, *Icarus*, 300, 1–11, 2018.

# Monitoring of the atmosphere of Mars with ACS TIRVIM nadir observations on ExoMars TGO.

**Nikolay Ignatiev** (1), Alexey Grigoriev (1), Alexey Shakun (1), Boris Moshkin (1), Dmitry Patsaev (1), Alexander Trokhimovskiy (1), Oleg Korablev (1), Davide Grassi (2), Pavel Vlasov (1,3), Ludmila Zasova (1), Sandrine Guerlet (4), François Forget (4), Franck Montmessin (5), Gabriele Arnold (6), Oleg Sazonov(1), Alexander Zharkov(1), Igor Maslov(1), Andrey Kungurov(1), Aleksandr Santos-Skripko(1), Viktor Shashkin(1), Fedor Martynovich(1), Igor Stupin(1), Dmitry Merzlyakov(1), Yuri Nikolskiy(1), Dmitry Gorinov(1).

(1) Space Research Institute of Russian Academy of Sciences, Moscow, Russia, (2) Istituto di Astrofisica e Planetologia Spaziali – Istituto Nazionale di Astrofisica, Rome, Italy, (3) Moscow Institute of Physics and Technology, Dolgoprudny, Russia, (4) Laboratoire de Météorologie Dynamique (LMD), Paris, France, (5) LATMOS, Guyancourt, France, (6) German Aerospace Center (DLR), Berlin, Germany (ignatiev@iki.rssi.ru)

## Abstract

The ExoMars Trace Gas Orbiter (TGO), a mission by ESA and Roscosmos started its operational scientific phase in March 2018. The Atmospheric Chemistry Suite (ACS) is a set of three spectrometers (NIR, MIR, and TIRVIM) designed to observe the Martian atmosphere in solar occultation, nadir and limb geometry [1]. The thermal infrared channel — TIRVIM is a Fourier-transform spectrometer encompassing the spectral range of 1.7–17  $\mu\text{m}$ , with the best spectral resolution 0.13  $\text{cm}^{-1}$ . In nadir operation mode, the primary goal of TIRVIM is the long-term monitoring of atmospheric temperature and aerosol (dust and ice clouds) state from the surface to approximately 60 km. We present the results of the first half year operation in orbit around Mars.

## 1. ACS TIRVIM Fourier transform spectrometer

TIRVIM is a 2-inch double pendulum Fourier-transform spectrometer with cryogenically-cooled HgCdTe detector, allowing both nadir and solar occultation observations. In nadir operation mode TIRVIM effective spectral range is limited to 5–17  $\mu\text{m}$  (590–2000  $\text{cm}^{-1}$ ) with the apodized spectral resolution of 1.2  $\text{cm}^{-1}$ . The capabilities of TIRVIM are similar to those of the previous experiments: IRIS/Mariner 9, TES/MGS and PFS/Mars Express, with advantages provided by the highest spectral resolution and better noise equivalent radiance (from 0.08  $\text{mW}/\text{m}^2/\text{sr}/\text{cm}^{-1}$ ) of the instrument, as well as the

dense spatial coverage of the Martian surface due to TGO 400 km circular orbit. The altitude sensitivity range extends from the surface to 60 km with the vertical resolution from 3 km near the surface to 20 km at high altitudes. The best spatial resolution on the surface of 17 km is defined by the 2.5° field of view. In flight calibrations of TIRVIM are carried out with alternating observations of the deep space and the internal calibration black body.

## 2. Observations

First trial observations of TIRVIM were carried out from the equatorial capture orbit in November, 2016, and repeated from an intermediate orbit in February – March 2017. Routine operations started in March 2018. In nominal operation mode, 600 spectra are recorded from each orbit lasting 2 hours. The whole planet is covered with observations in just a couple of weeks. Examples of Martian spectra recorded by TIRVIM for a variety of locations and local times are shown in Figure 1.

## 3. First results

Inverse problem solution methods for the atmospheric thermal sounding are well known. We used both Bayesian approach, known also as statistical regularization, coupled with line-by-line radiative transfer for final result presentation with associated formal error, and a relaxation method coupled with convolved transmittance technique for fast evaluation of the temperature field. Vertical temperature profiles with the surface temperature in

the bottom of each curve are presented in Fig. 2, while 2-D temperature field along the sub-spacecraft track on the surface is presented in Fig. 3. Half year of TGO operation should provide a unique opportunity to monitor a daily cycle of temperature field in addition to its seasonal variations.

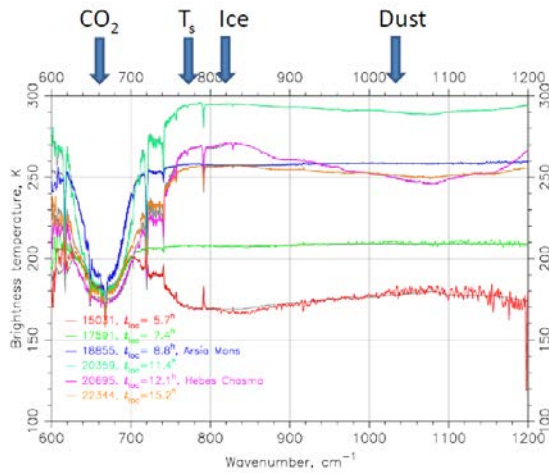


Figure 1: Examples of ACS TIRVIM measured and model spectra recorded at various locations and local times. Absorption bands of CO<sub>2</sub>, dust and water ice, as well as the region with minimum opacity used for monitoring of the surface temperature are marked with arrows.

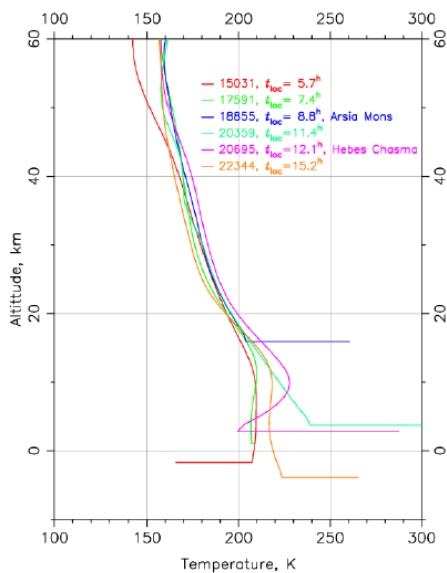


Figure 2: Temperature profiles retrieved for the spectra shown in Figure 1.

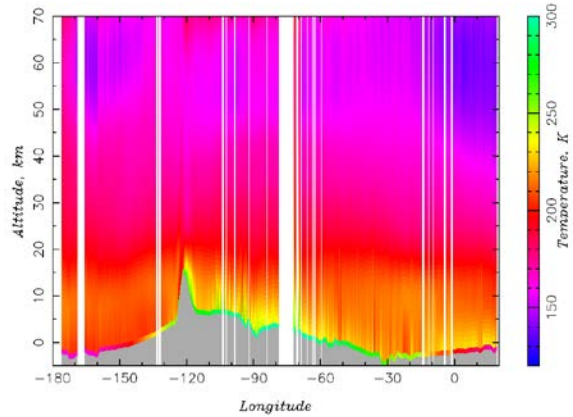


Figure 3: Temperature field along the sub-spacecraft track on the Martian surface measured from the equatorial capture orbit.

## Acknowledgements

ExoMars is the space mission of ESA and Roscosmos. The ACS experiment is led by IKI Space Research Institute in Moscow. The project acknowledges funding by Roscosmos and CNES. Science operations of ACS are funded by Roscosmos and ESA.

## References

- [1] Korabev, O. et al.: The Atmospheric Chemistry Suite (ACS) of Three Spectrometers for the ExoMars 2016 Trace Gas Orbiter, Space Science Reviews, Vol. 214, Issue 1, 2018.

## Preliminary assimilation of observations from ACS/TIRVIM on board ExoMars TGO into the LMD Mars GCM

**R. M. B. Young** (1), F. Forget (1), S. Guerlet (1), E. Millour (1), T. Navarro (1,2), N. Ignatiev (3), A. V. Grigoriev (3), A. V. Shakun (3), A. Trokhimovskiy (3), F. Montmessin (4), and O. Korablev (3)

(1) Laboratoire de Météorologie Dynamique (LMD/IPSL), Sorbonne Université, Centre National de la Recherche Scientifique, École Polytechnique, École Normale Supérieure, Paris, France, (2) Department of Earth, Planetary, and Space Sciences, University of California, Los Angeles, California, USA, (3) Space Research Institute (IKI), 84/32 Profsoyuznaya, 117997 Moscow, Russia, (4) LATMOS/IPSL, UVSQ Université Paris-Saclay, UPMC Univ. Paris 06, CNRS, Guyancourt, France (ryoung@lmd.jussieu.fr)

### Abstract

We present preliminary results from data assimilation of observations from the thermal infrared instrument TIRVIM, part of the Atmospheric Chemistry Suite on board ESA-Roscosmos' ExoMars Trace Gas Orbiter. These assimilations focus on atmospheric temperatures retrieved from the first few months of nadir data. We use the Local Ensemble Transform Kalman Filter technique to assimilate observations into the LMD Mars General Circulation Model.

### 1. Introduction

The ExoMars Trace Gas Orbiter (TGO), a collaborative project between the European Space Agency (ESA) and Roscosmos (Russia), was successfully inserted into Mars orbit on 19 October 2016, and reached its final science orbit on 7 April 2018. TGO began taking observations as part of commissioning operations in March 2018.

At the Laboratoire de Météorologie Dynamique (LMD) we are responsible for data assimilation of observations from the Atmospheric Chemistry Suite (ACS) thermal infrared instrument (TIRVIM) on board TGO [4]. This instrument measures vertical profiles of temperature as well as dust and water ice integrated content, at various local times, latitudes and seasons. Our aims are to generate analyses of the Martian atmosphere in a semi-operational way, provide these to the community in the short term, and use them to better understand Mars' climate.

### 2. Observational data

TIRVIM is a thermal infrared spectrometer with spectral range 1.7–17  $\mu\text{m}$ , whose main purpose is to con-

tinuously monitor the Martian environment in nadir in support of solar occultation measurements by ACS's near-infrared and mid-infrared channels [4]. Its primary observations are vertical profiles of atmospheric temperature, but it also produces surface temperatures and column-integrated dust, water ice, and other aerosol opacities.

We use the first few months of nadir data from TIRVIM. These have been calibrated and then retrieved using a line-by-line radiative transfer model [2]. We focus on assimilation of atmospheric temperatures, with assimilation of the other available data to follow. The observations cover various local times of day with full coverage in longitude every 7–10 days, over  $\pm 75^\circ$  latitude, with vertical coverage between  $\sim 5 - 45$  km altitude.

### 3. Model and assimilation

The LMD Mars General Circulation Model (GCM) [1] is a detailed model of Mars' atmosphere that includes representations of the dust cycle, water cycle, boundary layer, subsurface, aerosols, upper atmosphere, and other parametrizations relevant to the Martian environment.

Assimilation of observations into the LMD Mars GCM is achieved using the Local Ensemble Transform Kalman Filter [3, 6]. The LETKF is an ensemble-based assimilation scheme where we typically use 16 ensemble members and multiplicative inflation to adjust the background ensemble error covariance.

Assimilation of Martian atmospheric data provides a significant challenge for ensemble-based data assimilation. Quantities available to assimilate are strongly inter-dependent, and Mars' atmosphere is less chaotic than the Earth's, so the ensemble can converge over time, with bias dominating the ensemble in a way that

cannot be alleviated by synoptic variability.

## 4. Previous work

Work up to now has assimilated temperature, dust, and water ice observations from the Mars Climate Sounder on NASA's Mars Reconnaissance Orbiter [5, 6]. Figures 1 and 2 show example comparisons between temperature analyses and MCS observations, varying the time between assimilations. The errors are reduced visibly as the time between assimilations is reduced to 2 hours (Fig. 1), and error diagnostics (Fig. 2) show that a 1 hour cycle improves this even further.

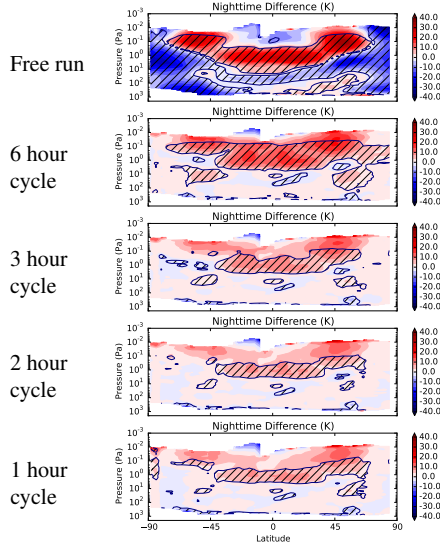


Figure 1: Difference between analysis mean and observed night-time ( $\sim 3$  am) temperatures for MCS observations binned over  $L_s = 175-180^\circ$  during MY29. The top panel has no assimilation, and the others vary the time between assimilations. In hatched regions the difference is larger than observational error.

## 5. Summary and Conclusions

The LMD Mars data assimilation scheme is ready to analyse data from the TIRVIM instrument, part of the ACS suite on board ExoMars TGO. We shall present our preliminary analysis of the first few months of assimilated atmospheric temperature observations.

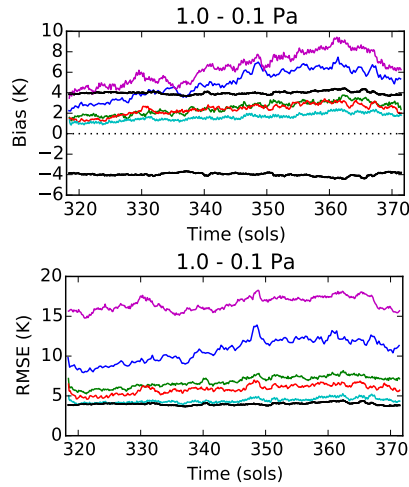


Figure 2: Temperature bias and RMS error in the analysis mean compared with raw observations, globally and diurnally averaged over 10–1.0 Pa between  $L_s = 150-180^\circ$  during MY29 (same period as Fig. 1). We show the pressure range where the assimilation is poorest. Lines show the free run and 6, 3, 2, and 1 hour assimilation cycles. Black lines show observational error.

## Acknowledgements

RMBY acknowledges funding from CNES. ExoMars is the space mission of ESA and Roscosmos. The ACS experiment is led by IKI Space Research Institute in Moscow. The project acknowledges funding by Roscosmos and CNES. Science operations of ACS are funded by Roscosmos and ESA. Science support in IKI is funded by Federal agency of science organizations (FANO).

## References

- [1] Forget, F. et al., JGR, 104, 24155-24175, 1999.
- [2] Guerlet, S. et al., EPSC, Berlin, 16–21 September 2018.
- [3] Hunt, B. R., Kostelich, E. J., and Szunyogh, I., Physica D, 230, 112-126, 2007.
- [4] Korabev, O. et al., Space Sci. Rev., 214, 7, 2018.
- [5] Navarro, T. et al., GRL, 41, 6620-6626, 2014.
- [6] Navarro, T. et al., Earth Space Sci., 4, 690–722, 2017.

# Spectroscopy and trace gas retrievals for the ExoMars Trace Gas Orbiter (TGO) Atmospheric Chemistry Suite mid-infrared (ACS MIR) solar occultation spectrometer using the JPL Gas Fitting software (GFIT)

**K. S. Olsen** (1), F. Montmessin (1), C. B. Boone (2), G. C. Toon (3), A. Fedorova (4), A. Trokhimovskiy (4), A. Grigoriev (4), A. Patrakeev (4), O. Korablev (4) and the ExoMars TGO Science Working Team

(1) Laboratoire Atmosphères, Milieux, Observations Spatiales (LATMOS/CNRS), Paris, France, (2) University of Waterloo, Waterloo, Canada, (3) Jet Propulsion Laboratory (JPL), California Institute of Technology, Pasadena, USA, (4) Space Research Institute (IKI), Moscow, Russia (kevin.olsen@latmos.ipsl.fr)

## Abstract

The ExoMars Trace Gas Orbiter (TGO) intends to study the composition of the Martian atmosphere. It was jointly developed by ESA and Roscosmos and successfully entered orbit around Mars in October 2016. After a lengthy, but crucial, aerobreaking campaign, its orbit was nominally reduced to a near-circular 400 km altitude, with a 2 hour period, in January 2018. There are four scientific instruments on TGO: the Atmospheric Chemistry Suite (ACS), the Nadir and Occultation for Mars Discovery (NOMAD), the Colour and Stereo Surface Imaging System (CaSSIS), and the Fine-Resolution Epithermal Neutron Detector (FREND). This presentation will focus on trace gas retrievals for the mid-infrared (MIR) channel of the ACS instrument operating in solar occultation mode. The first solar occultation observations were made on April 21, 2018, with nominal science operations to follow. We will present the retrieval scheme, our evaluation of spectroscopic parameters, sensitivity to *a priori* data, results from retrievals for simulations of the Mars atmosphere, and spectral fitting results for the first set of solar occultation observations made by ACS MIR.

ACS is a set of three spectrometers that are designed to better characterize the atmosphere of Mars with unprecedented accuracy (Korablev et al., 2018). It aims to detect and quantify unknown trace gases diagnostic of active geological or biological processes, to map their distribution and attempt to identify sources, and to refine our knowledge of the vertical distribution of major and minor atmospheric gases. It has three channels: near-infrared (NIR), thermal-infrared (TIRVIM) and MIR. The ACS MIR channel uses a novel concept for atmospheric studies: a cross-dispersion spectrom-

eter combining an echelle grating with a wide blaze angle and secondary, steerable diffraction grating (Korablev et al., 2018). It covers the wavenumber range of 2375–4340  $\text{cm}^{-1}$ .

ACS MIR data is being processed by several groups. This presentation will focus on the data product generated at LATMOS using the Gas Fitting software (GFIT) maintained by NASA's Jet Propulsion Laboratory. GFIT is a part of the GGG software suite and is designed to be a multipurpose and robust spectral fitting suite (e.g., Sen et al., 1996; Irion et al., 2002). It was derived from early versions of the Occultation Display Spectra (ODS) software developed for the ATMOS spectrometer flown on the space shuttles (Norton and Rinsland, 1991). It is currently used for the MkIV balloon missions (Toon, 1991) and the Total Carbon Column Observing Network (TCCON) of ground-based FTSs (Wunch et al., 2011).

GFIT computes volume absorption coefficients for each gas in a chosen spectral range, computes a spectrum line-by-line, and fits the computed spectrum to the measured spectrum using a non-linear Levenberg-Marquardt minimization. The state vector contains the continuum level and tilt, and volume mixing ratio (VMR) scaling factors (VSFs) for each target gas. GFIT is capable of fitting multiple gases at the same time. The VSF is a multiplicative scaling factor applied to the *a priori* VMR vertical profile. In principle, GFIT only modifies the magnitude, and not the shape of, the *a priori* VMR vertical profile. However, in solar occultation mode, the *a priori* can be scaled for each observed spectrum at each tangent altitude. To retrieve a VMR vertical profiles for a target gas from a set of solar occultation spectra, the set of retrieved slant columns abundances from each observation are inverted with calculated slant column paths

traced through the atmosphere using a linear equation solver.

Two major spectroscopic line lists, HITRAN and GEISA, have been recently updated. Both the 2015 edition of the GEISA spectroscopic database (Jacquinet-Husson et al., 2016) and the 2016 edition of the HITRAN spectroscopic database (Gordon et al., 2017) feature significant changes to the spectroscopic parameters for CO<sub>2</sub>. These changes were developed to support greenhouse gas measurements at Earth by TCCON, the Greenhouse Gases Observing Satellite (GOSAT) and the Orbiting Carbon Observatory (OCO-2). On Mars, while the average surface pressure is roughly 200 times less than Earth's, the VMR of CO<sub>2</sub> is over 2000 times that of Earth. Therefore, CO<sub>2</sub> absorption lines in solar occultation spectra can be larger for Mars than for Earth, and minor changes to the spectroscopic parameters can lead to large differences in the calculated spectra. To determine whether these changes lead to improved spectral fits, we have applied both databases, as well as HITRAN 2012 (Rothman et al., 2013) to spectral fitting of Earth-observing solar occultation spectra recorded by the Atmospheric Chemistry Experiment FTS (ACE-FTS) Bernath et al. (2005). We have also investigated the effects of spectroscopic parameters recently made available for air-broadening parameters in a CO<sub>2</sub>-rich atmosphere. Parameters for some gases have been compiled by HITRAN (CO, SO<sub>2</sub>, NH<sub>3</sub>, HF, HCl, OCS, and C<sub>2</sub>H<sub>2</sub>) (Li et al., 2015; Wilzewski et al., 2016), while parameters for water vapour have been made available by Gamache et al. (2016) and Devi et al. (2017). We will present the results of our validation of HITRAN 2016 and GEISA 2015, and also show the effects that CO<sub>2</sub> broadening parameters have on synthetic Mars spectra.

A first attempt at spectral fitting will be done using climatological models from the Mars Climate Database (Forget et al., 1999; Millour et al., 2015). New observations of temperature and pressure made by the Mars Reconnaissance Orbiter's Mars Climate Sounder and the TIRVIM channel will be assimilated into the LMD General Circulation Model. When a more accurate assimilation is ready, the retrievals will be reprocessed using the updated *a priori* vertical profiles of temperature, pressure, CO<sub>2</sub> VMR, and H<sub>2</sub>O VMR. Vertical profiles of temperature and pressure will also be retrieved by simultaneous observation made with ACS NIR and TIRVIM. These will be used to produce a third version of our MIR data product. As the mission progresses, we will quantify the differ-

ences among sources of *a priori* data, and study their effects on retrievals.

Much work has been done to investigate the limits of the retrieval algorithm by generating synthetic spectra for different atmospheric conditions (temperature, pressure, dust loading, and trace gas abundances). Noise is added to the spectra, they are resampled to a uniform fitting grid, and spectral fitting is performed using generic *a priori* to see how well the trace gas VMR vertical profiles used to create the synthetic spectra are reproduced. We found that given accurate temperature and pressure *a priori*, and a CH<sub>4</sub> abundance between 2–6 ppbv, we can accurately reconstruct the vertical profiles of CH<sub>4</sub> in the presence of noise. However, at low altitudes, due to signal attenuation from dust and interference from strong CO<sub>2</sub> absorption features, our retrieval becomes less accurate when the dust is high. Similarly, at high altitudes, where absorption line depths approach the magnitude of the noise, our retrieved profiles diverge from the true state of the atmosphere.

Since the end of April 2018, ACS MIR has been recording sets of solar occultation spectra. We will present our initial investigations into processing and fitting the data, focusing on the spectra and the goodness of fit for target gases in selected micro-windows. We will also present the latest state of our data processing and current best estimates of the composition and vertical structure of the atmosphere as estimated using GGG and ACS MIR.

## References

- Bernath, P. F., McElroy, C. T., Abrams, M. C., Boone, C. D., Butler, M., Camy-Peyret, C., Carleer, M., Clerbaux, C., Coheur, P.-F., Colin, R., DeCola, P., DeMazière, M., Drummond, J. R., Dufour, D., Evans, W. F. J., Fast, H., Fussen, D., Gilbert, K., Jennings, D. E., Llewellyn, E. J., Lowe, R. P., Mahieu, E., McConnell, J. C., McHugh, M., McLeod, S. D., Michaud, R., Midwinter, C., Nassar, R., Nichitiu, F., Nowlan, C., Rinsland, C. P., Rochon, Y. J., Rowlands, N., Semeniuk, K., Simon, P., Skelton, R., Sloan, J. J., Soucy, M.-A., Strong, K., Tremblay, P., Turnbull, D., Walker, K. A., Walkty, I., Wardle, D. A., Wehrle, V., Zander, R., and Zou, J.: Atmospheric Chemistry Experiment (ACE): Mission overview, *Geophys. Res. Lett.*, 32, L15S01, doi:10.1029/2005GL022386, 2005.
- Devi, V. M., Benner, D. C., Sung, K., Crawford, T. J., Gamache, R. R., Renaud, C. L., Smith, M. A. H., Mantz, A. W., and Villanueva, G. L.: Line parameters for CO<sub>2</sub>- and self-broadening in the  $\nu_3$  band of HD<sup>16</sup>O,

- J. Quant. Spectrosc. Radiat. Transfer, 203, 158–174, doi:10.1016/j.jqsrt.2017.02.020, 2017.
- Forget, F., Hourdin, F., Fournier, R., Hourdin, C., Talagrand, O., Collins, M., Lewis, S. R., Read, P. L., and Huot, J.-P.: Improved general circulation models of the Martian atmosphere from the surface to above 80 km. *J. Geophys. Res.*, 104, 24 155–24 176, doi:10.1029/1999JE001025, 1999.
- Gamache, R. R., Faese, M., and Renaud, C. L.: A spectral line list for water isotopologues in the 1100–4100  $\text{cm}^{-1}$  region for application to  $\text{CO}_2$ -rich planetary atmospheres. *J. Mol. Spectrosc.*, 326, 144–150, doi:10.1016/j.jms.2015.09.001, 2016.
- Gordon, I. E., Rothman, L. S., Hill, C., Kochanov, R. V., Tan, Y., Bernath, P. F., Birk, M., Boudon, V., Campargue, A., Chance, K. V., Drouin, B. J., Flaud, J.-M., Gamache, R. R., Hodges, J. T., Jacquemart, D., Perevalov, V. I., Perrin, A., Shine, K. P., Smith, M.-A. H., Tennyson, J., Toon, G. C., Tran, H., Tyuterev, V. G., Barbe, A., Császár, A. G., Devi, V. M., Furtenbacher, T., Harrison, J. J., Hartmann, J.-M., Jolly, A., Johnson, T. J., Karman, T., Kleiner, I., Kyuberis, A. A., Loos, J., Lyulin, O. M., Massie, S. T., Mikhailenko, S. N., Moazzen-Ahmadi, N., Müller, H. S. P., Naumenko, O. V., Nikitin, A. V., Polyansky, O. L., Rey, M., Rotger, M., Sharpe, S. W., Sung, K., Starikova, E., Tashkun, S. A., Auwera, J. V., Wagner, G., Wilzewski, J., Wcisło, P., Yu, S., and Zak, E. J.: The HITRAN2016 molecular spectroscopic database. *J. Quant. Spectrosc. Radiat. Transfer*, 203, 3–69, doi:10.1016/j.jqsrt.2017.06.038, 2017.
- Irion, F. W., Gunson, M. R., Toon, G. C., Chang, A. Y., Eldering, A., Mahieu, E., Manney, G. L., Michelsen, H. A., Moyer, E. J., Newchurch, M. J., Osterman, G. B., Rinsland, C. P., Salawitch, R. J., Sen, B., Yung, Y. L., and Zander, R.: Atmospheric Trace Molecule Spectroscopy (ATMOS) Experiment Version 3 data retrievals. *Appl. Opt.*, 41, 6968–6979, doi:10.1364/AO.41.006968, 2002.
- Jacquinet-Husson, N., Armante, R., Scott, N. A., Chédin, A., Crépeau, L., Boutammine, C., Bouhdaoui, A., Crevoisier, C., Capelle, V., Boonne, C., Poulet-Crovisier, N., Barbe, A., Chris Benner, D., Boudon, V., Brown, L. R., Buldyreva, J., Campargue, A., Coudert, L. H., Devi, V. M., Down, M. J., Drouin, B. J., Fayt, A., Fittschen, C., Flaud, J.-M., Gamache, R. R., Harrison, J. J., Hill, C., Hodnebrog, Ø., Hu, S.-M., Jacquemart, D., Jolly, A., Jiménez, E., Lavrentieva, N. N., Liu, A.-W., Lodi, L., Lyulin, O. M., Massie, S. T., Mikhailenko, S., Müller, H. S. P., Naumenko, O. V., Nikitin, A., Nielsen, C. J., Orphal, J., Perevalov, V. I., Perrin, A., Polovtseva, E., Predoi-Cross, A., Rotger, M., Ruth, A. A., Yu, S. S., Sung, K., Tashkun, S. A., Tennyson, J., Tyuterev, V. G., Vander Auwera, J., Voronin, B. A., and Makie, A.: The 2015 edition of the GEISA spectroscopic database. *J. Mol. Spectrosc.*, 327, 31–72, doi:10.1016/j.jms.2016.06.007, 2016.
- Korablev, O., Montmessin, F., Trokhimovskiy, A., Fedorova, A. A., Shakun, A. V., Grigoriev, A. V., Moshkin, B. E., Ignatiev, N. I., Forget, F., Lefèvre, F., Anufreychik, K., Dzuban, I., Ivanov, Y. S., Kalinnikov, Y. K., Kozlova, T. O., Kungurov, A., Makarov, V., Martynovich, F., Maslov, I., Merzlyakov, D., Moiseev, P. P., Nikolskiy, Y., Patrakeev, A., Patsaev, D., Santos-Skripko, A., Sazonov, O., Semena, N., Semenov, A., Shashkin, V., Sidorov, A., Stepanov, A. V., Stupin, I., Timonin, D., Titov, A. Y., Viktorov, A., Zharkov, A., Altieri, F., Arnold, G., Belyaev, D. A., Bertaux, J. L., Betsis, D. S., Duxbury, N., Encrenaz, T., Fouchet, T., Gérard, J.-C., Grassi, D., Guerlet, S., Hartogh, P., Kasaba, Y., Khatuntsev, I., Krasnopolsky, V. A., Kuzmin, R. O., Lellouch, E., Lopez-Valverde, M. A., Luginin, M., Määttänen, A., Marcq, E., Martin Torres, J., Medvedev, A. S., Millour, E., Olsen, K. S., Patel, M. R., Quantin-Nataf, C., Rodin, A. V., Shematovich, V. I., Thomas, I., Thomas, N., Vazquez, L., Vincendon, M., Wilquet, V., Wilson, C. F., Zasova, L. V., Zelenyi, L. M., and Zorzano, M. P.: The Atmospheric Chemistry Suite (ACS) of Three Spectrometers for the ExoMars 2016 Trace Gas Orbiter. *Space Sci. Rev.*, 214, 7, doi:10.1007/s11214-017-0437-6, 2018.
- Li, G., Gordon, I. E., Rothman, L. S., Tan, Y., Hu, S.-M., Kassi, S., Campargue, A., and Medvedev, E. S.: Rovibrational Line Lists for Nine Isotopologues of the CO Molecule in the  $X^1\Sigma^+$  Ground Electronic State. *Astrophys. J. Suppl. Ser.*, 216, 15, doi:10.1088/0067-0049/216/1/15, 2015.
- Millour, E., Forget, F., Spiga, A., Navarro, T., Madeleine, J.-B., Montabone, L., Pottier, A., Lefevre, F., Montmessin, F., Chaufray, J.-Y., Lopez-Valverde, M. A., Gonzalez-Galindo, F., Lewis, S. R., Read, P. L., Huot, J.-P., Desjean, M.-C., and MCD/GCM development Team: The Mars Climate Database (MCD version 5.2). *European Planetary Science Congress*, 10, EPSC2015-438, 2015.
- Norton, R. H. and Rinsland, C. P.: ATMOS data processing and science analysis methods. *Appl. Opt.*, 30, 389–400, doi:10.1364/AO.30.000389, 1991.
- Rothman, L. S., Gordon, I. E., Babikov, Y., Barbe, A., Chris Benner, D., Bernath, P. F., Birk, M., Bizzocchi, L., Boudon, V., Brown, L. R., Campargue, A., Chance, K., Cohen, E. A., Coudert, L. H., Devi, V. M., Drouin, B. J., Fayt, A., Flaud, J.-M., Gamache, R. R., Harrison, J. J., Hartmann, J.-M., Hill, C., Hodges, J. T., Jacquemart, D., Jolly, A., Lamouroux, J., Le Roy, R. J., Li, G., Long, D. A., Lyulin, O. M., Mackie, C. J., Massie, S. T., Mikhailenko, S., Müller, H. S. P., Naumenko, O. V., Nikitin, A. V., Orphal, J., Perevalov, V., Perrin, A., Polovtseva, E. R., Richard, C., Smith,

- M. A. H., Starikova, E., Sung, K., Tashkun, S., Tennyson, J., Toon, G. C., Tyuterev, V. G., and Wagner, G.: The HITRAN2012 molecular spectroscopic database, *J. Quant. Spectrosc. Radiat. Transfer*, 130, 4–50, doi:10.1016/j.jqsrt.2013.07.002, 2013.
- Sen, B., Toon, G. C., Blavier, J.-F., Fleming, E. L., and Jackman, C. H.: Balloon-borne observations of midlatitude fluorine abundance, *J. Geophys. Res.*, 101, 9045–9054, doi:10.1029/96JD00227, 1996.
- Toon, G. C.: The JPL MkIV interferometer, *Opt. Photonics News*, 2, 19–21, doi:10.1364/OPN.2.10.000019, 1991.
- Wilzewski, J. S., Gordon, I. E., Kochanov, R. V., Hill, C., and Rothman, L. S.: H<sub>2</sub>, He, and CO<sub>2</sub> line-broadening coefficients, pressure shifts and temperature-dependence exponents for the HITRAN database. Part 1: SO<sub>2</sub>, NH<sub>3</sub>, HF, HCl, OCS and C<sub>2</sub>H<sub>2</sub>, *J. Quant. Spectrosc. Radiat. Transfer*, 168, 193–206, doi:10.1016/j.jqsrt.2015.09.003, 2016.
- Wunch, D., Toon, G. C., Blavier, J. L., Washenfelder, R. A., Notholt, J., Connor, B. J., Griffith, D. W. T., Sherlock, V., and Wennberg, P. O.: The Total Carbon Column Observing Network, *Phil. Trans. R. Soc. A*, 369, 2087–2112, doi:10.1098/rsta.2010.0240, 2011.

# The Raman Laser Spectrometer (RLS) for 2020 Exomars (ESA) Mission: Instrument development and operation on Mars

F. Rull (1), S. Maurice (3), I. Hutchinson (4), A. G. Moral (2), C.P. Canora (2), T. Belenguer (2), G. Ramos (2), M. Colombo (2), G. Lopez-Reyes (1), V. García (6), O. Forni (3), J. Popp (5), J. Medina (1) on behalf of the RLS team.

(1) University of Valladolid (UVa)\_CAB Parque Tecnológico de Boecillo, E-47151, Valladolid, Spain (rull@fmc.uva.es) (2) Instituto Nacional de Técnica Aeroespacial (INTA), Ctra. Ajalvir, Km 4, 28850 Torrejón de Ardoz, Spain. (3) Institut de Recherche en Astrophysique et Planetologie (IRAP), Toulouse, France, (4) University of Leicester, University Road, Leicester, LE1 7RH Leicester, UK, (5) Institute of Physical Chemistry, Friedrich-Schiller University, Jena, Germany. (6) Universidad Complutense de Madrid, Dpto. Química Física, Madrid

## Abstract

Raman Laser Spectrometer (RLS) is part of the Exomars 2020 key instruments devoted to the analysis of samples collected below the Martian surface. This paper aims to describe the instrument technical characteristics, the scientific performances and the operation it will perform on Mars in the context of Exomars 2020 rover mission.

## 1. Introduction

The main ExoMars 2020 mission scientific objective is "Searching for evidence of past and present life on Mars". For that purpose the ExoMars rover will carry a drill able to obtain samples up to 2 meters depth under the Martian surface. These samples will be analyzed by a suite of instruments (Pasteur Payload) located inside the Rover's Analytical Laboratory Drawer (ALD) and dedicated to exobiology and geochemistry research at the mineral grain scale after these samples have been crushed and powdered. The Raman Laser Spectrometer (RLS) is one of these key instruments. The RLS will contribute to this scientific goal through the precise identification of the mineral phases and the capability to detect organics on the powdered samples (1). RLS is being developed by a European Consortium composed by Spanish, UK, French and German partners.

## 2. Instrument description

The RLS Instrument is made by the following units: SPU (Spectrometer Unit), iOH (Internal Optical Head), ICEU (Instrument Control and Excitation

Unit) and CT (the calibration target) (see Fig.1). The instrument main scientific characteristics are:

- Laser excitation wavelength: 532 nm
- Irradiance on sample: 0.4 - 8 kW/cm<sup>2</sup>
- Spectral range: 150-3800cm<sup>-1</sup>
- Spectral resolution: between 6 and 8 cm<sup>-1</sup>
- Spectral accuracy: < 1 cm<sup>-1</sup>
- Spot size: 50 microns

And the instrument main technical and physical characteristics are:

- Mass ~ 2.4 kg
- Power consumption between 20W and 30 W (depending on the temperature and operational mode).
- It is designed to provide full performances in a thermal environment between -40°C and 0°C and survive in a non-operational environment between -60°C and +50°C
- Active focusing of laser onto the crushed sample of ±1mm range and sub-µm resolution
- Redundant laser excitation chain
- Processing activities are shared between RLS and rover processors
- Storage needs on Rover memory is around 200Mbits (20 measurements + auxiliary data)

The RLS instrument operation on Mars consists on a micro analysis of the powdered samples along a line defined by the motion of the rover's carousel. This analysis is performed in automatic mode with the optimal spectral acquisition parameters defined by specific algorithms.

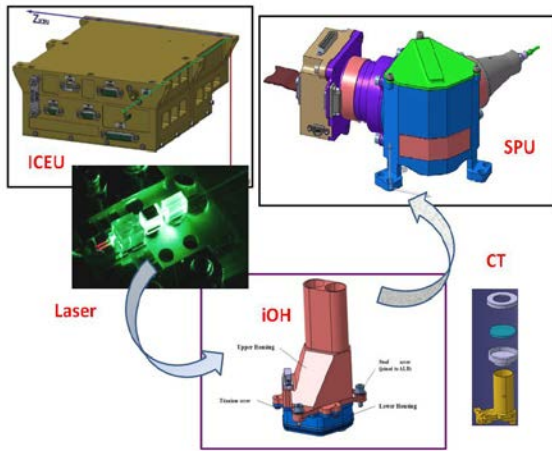


Figure 1: Overview of the RLS instrument showing the main component units.

### 3. Summary and Conclusions

This paper aims to describe the RLS instrument and the operation it will perform on Mars in order to contribute to the Exomars 2020 scientific objectives. The model philosophy and the technical and scientific steps leading to the current flight model (FM) RLS instrument will also be presented and discussed. In particular the results obtained with the EQM model at room conditions and relevant Martian conditions. These results will be compared with those obtained in a specific simulator of the Exomars powder analysis operation. Finally the discussion will include the conclusions obtained from these results and the potential scientific capabilities of the Raman technique in the context of the rover operation on Mars.

### Acknowledgements

Acknowledgments: The authors thank MINECO, project codes ESP2013-48427-C1-3, ESP2014-56138-C1-3-R.

### References

[1] Rull, Maurice, Hutchinson, Moral et al., *Astrobiology*, 2017, 17, 627-654.

## Observations of carbon monoxide (CO) by the Atmospheric Chemistry Suite (ACS) on board the Trace Gas Orbiter

**Franck Lefèvre** (1), Anna Fedorova (2), Alexander Trokhimovskiy (2), Denis Belyaev (2), Nicolay Ignatiev (2), Alexey Grigoriev (2), Natalia Savelyeva (2), Alexey Shakun (2), Kevin Olsen (1), Franck Montmessin (1), and Oleg Korablev (2).  
(1) LATMOS, CNRS/Sorbonne Université, Paris, France, (2) Space Research Institute (IKI), Moscow, Russia  
(franck.lefevre@latmos.ipsl.fr)

### Abstract

The Atmospheric Chemistry Suite (ACS) of three spectrometers started its scientific operations in April 2018 on board the Exomars 2016 Trace Gas Orbiter (TGO). This paper will present the first observations by ACS of the vertical distribution of carbon monoxide (CO) in the atmosphere of Mars.

### 1. CO in the atmosphere of Mars

Carbon monoxide (CO) is formed in the atmosphere of Mars through the photolysis of CO<sub>2</sub> at wavelengths shorter than 200 nm:



Since the 1970s and the classic papers of [1, 2] it has been known that OH and the trace amounts of odd-hydrogen species (HO<sub>x</sub>) produced by H<sub>2</sub>O degradation represent the main loss of CO and can efficiently recycle CO<sub>2</sub> from its photodissociation product:



CO is therefore an important tracer of the catalytic chemistry that explains the remarkable stability of the Mars quasi-pure atmosphere of CO<sub>2</sub>.

The photochemical lifetime of CO is estimated from reaction (2) to 5 terrestrial years [3]. This long lifetime does not authorize chemical variations of CO with local time or even at the seasonal timescale. Yet, observations show a pronounced seasonal cycle of the CO mixing ratio at high latitudes [4,5]. This phenomenon is not of chemical origin but a response to the condensation–sublimation cycle of CO<sub>2</sub> and

from the seasonal ice caps, which leads to enrichment–depletion of all non-condensable gases in polar regions. Thus, CO is also a good tracer of such processes and of atmospheric dynamics in general.

In terms of absolute amounts, previous measurements of Martian CO carried out from space or from the Earth indicate values of 700–1100 ppmv averaged over the atmospheric column [4,5]. Those abundances have historically been a challenge and remain unsolved for chemical models, which typically underestimate CO by a factor 2 to 8 [3]. The fact that such a basic problem persists after decades of research may be indicative that an important process is missing or largely inaccurate in our understanding of the Mars photochemical system.

To date, only column-averaged amounts of CO have been measured on Mars and no measurements of the vertical distribution of CO have been published. Vertical profiles of CO will be provided for the first time by the instruments on board the Trace Gas Orbiter.

### 2. The Atmospheric Chemistry Suite (ACS)

The Atmospheric Chemistry Suite (ACS) package is an element of the Russian contribution to the ESA-Roscosmos ExoMars 2016 Trace Gas Orbiter (TGO) mission [6]. ACS consists of three separate infrared spectrometers, sharing common mechanical, electrical, and thermal interfaces.

Among the three spectrometers of ACS, the mid-infrared channel (MIR) is a cross-dispersion echelle instrument dedicated to solar occultation measurements in the 2.2–4.4 μm range and achieves a resolving power of > 50000. With its unprecedented

sensitivity and its spectral range that covers the 2.3  $\mu\text{m}$  band of CO, MIR is well suited to retrieve accurate vertical profiles of CO from 10 km to about 140 km. In low dust conditions, we anticipate a sensitivity to CO of about 5 ppmv, i.e. less than 1% of the mean mixing ratio of CO on Mars. Measurements of the CO vertical distribution will also be possible with the thermal infrared (TIRVIM) channel of ACS, a Fourier-transform spectrometer encompassing the spectral range 1.7-17  $\mu\text{m}$ . TIRVIM covers the strong CO band at 4.7  $\mu\text{m}$ , which should allow the retrieval of accurate CO profiles in solar occultation mode, despite a lesser spectral resolution than MIR.

### 3. First observations of CO

The first vertical profiles of CO obtained by solar occultation from the MIR and TIRVIM channels of ACS, not retrieved yet at the time of writing, will be presented in this talk. They will be analysed in the context of Mars atmospheric dynamics and photochemistry. We will also present comparisons with three-dimensional simulations of Mars CO carried out with the LMD global climate model with photochemistry.

### Acknowledgements

ExoMars is the space mission of ESA and Roscosmos. The ACS experiment is led by IKI Space Research Institute in Moscow. The project acknowledges funding by Roscosmos and CNES. Science operations of ACS are funded by Roscosmos and ESA.

### References

- [1] McElroy, M. B. and Donahue, T. M., *Science*, 177, 986-988, 1972.
- [2] Parkinson, T. D. and Hunten, D. M., *J. Atmos. Sci.*, 29, 1380-1390, 1972.
- [3] Lefèvre, F. and Krasnopolsky, V., in *The Atmosphere and Climate of Mars*, Cambridge University Press, 2017.
- [4] Krasnopolsky, V., *Icarus*, 190, 93-102, 2007.
- [5] Smith, M. D. et al, *J. Geophys. Res.*, 114, 10.1029/2008JE003288, 2009.
- [6] Korablev, A. et al., *Space Sci. Rev.*, 214:7, 2018.

# The Ancient Fluvial Catchment of the Candidate ExoMars 2020 Rover Landing Site in the Oxia Planum Basin

Peter Fawdon (1), Matthew Balme (1) John Bridges (2) Joel Davies (3) Sanjeev Gupta (4) Cathy Quantan-Nataf

(1) The Open University, United Kingdom, (2) University of Leicester, United Kingdom (3) The Natural History Museum, United Kingdom, (4) Université de Lyon, France. (Peter.fawdon@open.ac.uk)

## 1. Introduction

As part of an ongoing regional study, we present preliminary observations of catchments associated with the Oxia Planum ExoMars 2020 rover landing site in northwest Arabia Terra. With the primary goal of searching for signs of past and present life on Mars, the ExoMars rover will investigate the geochemical environment in the shallow subsurface over a nominal mission of 218 martian days (sols) [1]. To meet this ambitious mission goal, and for the results of the geochemical experiments to be meaningful, it is crucial to understand the context of the landing site as a whole, and to consider the geological processes that might affect the potential for the formation, concentration and preservation of biomarkers within strata exposed in the landing ellipse.

Here, we present the first stage of a study to characterise the Noachian to early Hesperian geological context of the Oxia Planum landing site.

Ancient fluvial systems fed into the Oxia landing site region from the southeast; we compare a hydrological model of the modern topography with geomorphological indicators of ancient fluvial activity such as channels, visible in remote sensing data. We use differences between the two to understand (1) the size of the Oxia Basin catchment which might have sourced potential biomarkers feeding the sediment fan identified within the landing ellipse, and (2) how the catchment may have changed through Martian history.

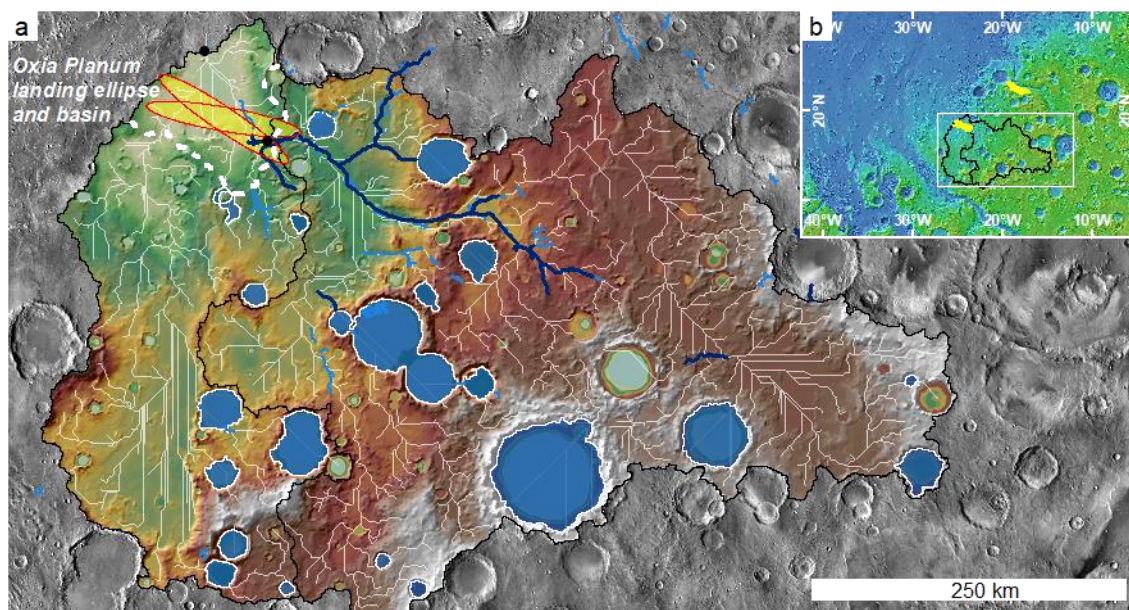


**Figure 1:** Model catchments (black) flow accumulation paths (white) and impact craters with smooth sedimentary floors that fall below the elevation in the catchment that water should pond (blue areas) of the Oxia Planum basin. Overlain with the observed fluvial network from this study (light blue) and Hynek et al (2010): dark blue).

## 2. Method

The model palaeo-watershed area and a drainage network map were calculated using the ArcMap 10.5 Spatial Analyst 'ArcHydro' toolset [2] and MOLA topography data. Ongoing geomorphological observations of fluvial features are being made using THEMIS, HRSC and CTX data, digitized on to a HRSC basemap at a scale of 1:50,000. The data were then visually compared to identify where the model flow accumulation agrees with, or deviates from, the geomorphological observations.

## 3. Observations

The model watershed and flow accumulation (Figure 1) shows that the Oxia Planum landing ellipse lies within an area with two contributing catchments. The larger, covering  $\sim 1.5 \times 10^5 \text{ km}^2$  enters the Oxia Basin at the eastern end of the landing ellipse area and the smaller, of  $\sim 0.6 \times 10^5 \text{ km}^2$ , contributes flow to Oxia Basin from the south.

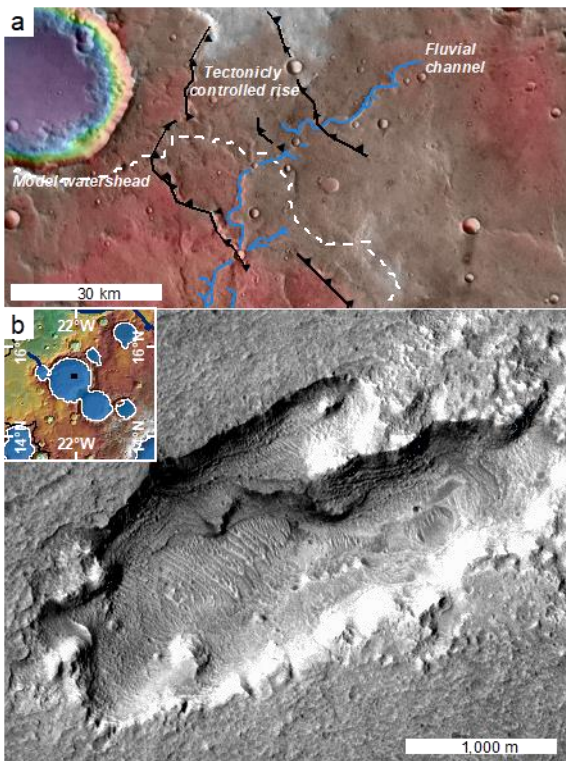


**Figure 2:** (a) Fluvial channel uplifted by a wrinkle ridge crossing the model watershed and (b) a pit in

the smooth floor of a possible crater lake showing layered sediments in CTX image B19\_016961\_1970\_XN\_17N022W.

The model watershed is broadly representative of the observed channel network and includes the large valley *Coogoon Valles* [3]. However, there is an important deviation to the north of Coogoon, where a channel crosses the model watershed (figure 2a). Here the topography has been affected by the formation of a wrinkle ridge, showing that regional tectonic activity postdates the observed fluvial network, and that the true catchment area for the Oxia basin is more extensive than the model suggests.

The model catchments include several basin forming craters (Figure 1), which are found below the elevations at which water should pond. None have previously been identified as candidate paleolakes because they do not have feeder channels. However, they may have channel-like incisions in the interior walls overlapped by smooth, layered crater floor deposits (Figure 2b). The lack of feeder channels may be ascribed to the crater's location on a topographic rise at the edge of the Oxia basin catchment but the possibility of ground water fed paleo lakes remains to be investigated.

## 4. Conclusions

Thus far our ongoing work shows that: (1) The Oxia basin has been fed by an extensive fluvial system with a minimum catchment area of  $\sim 2.1 \times 10^5 \text{ km}^2$ . (2) Tectonic activity postdates the formation of the fluvial network, consequently the catchment may be significantly larger than the model value. (3) Several craters suggest there may be evidence for interior palaeolakes, although, being located on a topographic rise, they do not have feeder channels. It is likely they were sustained by ground water.

## References

- [1] Vago et al., Habitability on Early Mars and the Search for Biosignatures with the ExoMars Rover. *Astrobiology*, 17, 6-7, 471-510, 2017.
- [2] Esri, How Watershed Works, <http://desktop.arcgis.com/en/arcmap/10.5/tools/spatial-analyst-toolbox/how-watershed-works.htm>, 2016.
- [3] Molina et al., Coogoon Valles, western Arabia Terra: Hydrological evolution of a complex Martian channel system, *Icarus*, 293, 27-44, 2017.

# First retrievals of ozone vertical profiles from NOMAD-UVIS

**Arianna Piccialli** (1), Ann Carine Vandaele (1), Y. Willame (1), C. Depiesse (1), L. Trompet (1), L. Neary (1), S. Viscardy (1), F. Daerden (1), Ian R. Thomas (1), Bojan Ristic (1), W. Hewson (2), J.P. Mason (2), M.R. Patel (2), G. Sellers (2), T. Clancy (3), G. Villanueva (4), B. Hubert (5), L. Gkouvelis (5), F. Altieri (6), E. D'Aversa (6), Giancarlo Bellucci (6), Jose-Juan Lopez-Moreno (7), and the NOMAD Team

(1) Belgian Institute for Space Aeronomy, Belgium, (2) Open University, UK, (3) Space Science Institute, USA, (4) Goddard Space Flight Center, USA, (5) University of Liège, Belgium, (6) INAF, Istituto di Astrofisica e Planetologia Spaziali, Italy, (7) IAA/CSIC, Granada, Spain (email: [arianna.piccialli@aeronomie.be](mailto:arianna.piccialli@aeronomie.be), Twitter: [@apic79](https://twitter.com/apic79))

## Abstract

The NOMAD (Nadir and Occultation for MArS Discovery) – operating on board the ExoMars 2016 Trace Gas Orbiter mission – started to acquire the first scientific measurements on 21 April 2018.

Here, we will present first retrievals of ozone vertical profiles obtained with NOMAD UVIS solar occultations.

## 1. The NOMAD UVIS channel

NOMAD is a spectrometer operating in 3 channels: 1) a solar occultation channel (SO) operating in the infrared (2.3-4.3  $\mu\text{m}$ ); 2) a second infrared channel LNO (2.3-3.8  $\mu\text{m}$ ) capable of doing nadir, as well as solar occultation and limb; and 3) an ultraviolet/visible channel UVIS (200-650 nm) that can work in the three observation modes [1,2].

The UVIS channel has a spectral resolution  $<1.5\text{nm}$ . In the solar occultation mode it will be mainly devoted to study the climatology of ozone and aerosols content [3].

## 2. Ozone retrievals

Ozone is a highly reactive species on Mars. In particular, it displays steep gradients across the terminator due to photolysis [4]. Odd hydrogen radicals play an important role in the destruction of ozone. This results in a strong anti-correlation between  $\text{O}_3$  and  $\text{H}_2\text{O}$  [4]. NOMAD will help us improve our knowledge of the climatology of ozone and of its complex photochemistry.

We will present first retrievals of ozone vertical profiles. NOMAD-UVIS spectra will be simulated using the line-by-line radiative transfer code ASIMUT-ALVL developed at IASB-BIRA [5], and the NEMESIS code [10] developed for use on NOMAD-UVIS data at the Open University. In a preliminary study based on SPICAM-UV solar occultations (See [6]), ASIMUT was modified in order to take into account the atmospheric composition and structure at the day-night terminator. We will follow the same method described in [7] to check that the spectra are correctly calibrated and accurately normalized to the solar spectrum. As input for ASIMUT, we will use gradients predicted by the 3D GEM-Mars v4 Global Circulation Model (GCM) [8,9] and the UK version of the LMD GCM. UVIS ozone profiles will also be compared to SPICAM-UV retrievals.

## Acknowledgements

The NOMAD experiment is led by the Royal Belgian Institute for Space Aeronomy (BIRA-IASB), assisted by Co-PI teams from Spain (IAA-CSIC), Italy (INAF-IAPS), and the United Kingdom (Open University). This project acknowledges funding by the Belgian Science Policy Office (BELSPO), with the financial and contractual coordination by the ESA Prodex Office (PEA 4000103401, 4000121493), by MICIIN through Plan Nacional (AYA2009-08190 and AYA2012-39691), as well as by UK Space Agency through grant ST/P000886/1 and Italian Space Agency through grant 2018-2-HH.0. The research was performed as part of the “Excellence of Science” project “Evolution and Tracers of Habitability on Mars and the Earth” (FNRS 30442502). This research was supported by the

## References

- [1] Vandaele, A.C., Neefs, E., Drummond, R. et al.: Science objectives and performances of NOMAD, a spectrometer suite for the Exo-Mars TGO mission, *Planetary and Space Science*, Vol. 119, pp. 233–249, 2015.
- [2] Neefs, E., Vandaele, A.C., Drummond, R. et al.: NOMAD spectrometer on the ExoMars trace gas orbiter mission: part 1 – design, manufacturing and testing of the infrared channels, *Applied Optics*, Vol. 54 (28), pp. 8494-8520, 2015.
- [3] M.R. Patel et al. “NOMAD spectrometer on the ExoMars trace gas orbiter mission: part 2-design, manufacturing, and testing of the ultraviolet and visible channel”. In: *Appl. Opt.* 56.10 (2017), pp. 2771–2782. DOI: 10.1364/AO.56.002771.
- [4] Lefèvre, F., Bertaux, J.L., Clancy, R. T., Encrenaz, T., Fast, K., Forget, F., Lebonnois, S., Montmessin, F., Perrier, S., Aug. 2008. Heterogeneous chemistry in the atmosphere of Mars. *Nature* 454, 971–975.
- [5] Vandaele, A.C., M. De Mazière, R. Drummond, A. Mahieux, E. Neefs, V. Wilquet, O. Korablev, A. Fedorova, D. Belyaev, F. Montmessin, and J.L. Bertaux, Composition of the Venus mesosphere measured by SOIR on board Venus Express. *JGR*, 2008. 113 doi:10.1029/2008JE003140.
- [6] Piccialli, A., EPSC 2018.
- [7] Trompet, L., Mahieux, A., Ristic, B., Robert, S., Wilquet, V., Thomas, I.R., Vandaele, A.C., Bertaux, J.L., 2016. Improved algorithm for the transmittance estimation of spectra obtained with SOIR/Venus Express. *Applied Optics* 55, 9275-9281.
- [8] Neary, L., and F. Daerden (2018), The GEM-Mars general circulation model for Mars: Description and evaluation, *Icarus*, 300, 458–476, doi:10.1016/j.icarus.2017.09.028.
- [9] Daerden, F.; Whiteway, J. A.; Neary, L.; Komguem, L.; Lemmon, M. T.; Heavens, N. G.; Cantor, B. A.; Hébrard, E.; Smith, M. D. A solar escalator on Mars: Self-lifting of dust layers by radiative heating. *GRL*, 2015, 42, 18, 7319-7326.
- [10] P.G.J. Irwin et al. “The NEMESIS planetary atmosphere radiative transfer and retrieval tool”.

## The NOMAD Team

*Scientific team:* Vandaele, Ann Carine; Lopez Moreno, Jose Juan; Bellucci, Giancarlo; Patel, Manish; Allen, Mark; Alonso-Rodrigo, Gustavo; Altieri, Francesca; Aoki, Shohei; Bauduin, Sophie; Bolsée, David; F. Giacomo Carrozzo, Clancy, Todd; Cloutis, Edward; Daerden, Frank; D'Aversa, Emiliano; Depiesse, Cédric; Erwin, Justin; Fedorova, Anna; Formisano, Vittorio; Funke, Bernd; Fussen, Didier; Garcia-Comas, Maia; Geminale, Anna; Gérard, Jean-Claude; Gillotay, Didier; Giuranna, Marco; Gonzalez-Galindo, Francisco; Hewson, Will; Homes, James; Ignatiev, Nicolai; Kaminski, Jacek; Karatekin, Ozgur; Kasaba, Yasumasa; Lanciano, Orietta; Lefèvre, Franck; Lewis, Stephen; López-Puertas, Manuel; López-Valverde, Miguel; Mahieux, Arnaud; Mason, Jon; Mc Connell, Jack; Mumma, Mike; Nakagawa, Hiromu, Neary, Lori; Neefs, Eddy; Novak, R.; Oliva, Fabrizio; Piccialli, Arianna; Renotte, Etienne; Robert, Severine; Sindoni, Giuseppe; Smith, Mike; Stiepen, Arnaud; Thomas, Ian; Trokhimovskiy, Alexander; Vander Auwera, Jean; Villanueva, Geronimo; Viscardy, Sébastien; Whiteway, Jim; Willame, Yannick; Wilquet, Valérie; Wolff, Michael; Wolkenberg, Paulina – *Tech team:* Alonso-Rodrigo, Gustavo; Aparicio del Moral, Beatriz; Barzin, Pascal; Beeckman, Bram; BenMoussa, Ali; Berkenbosch, Sophie; Biondi, David; Bonnewijn, Sabrina; Candini, Gian Paolo; Clairquin, Roland; Cubas, Javier; Giordanengo, Boris; Gissot, Samuel; Gomez, Alejandro; Hathi, Brijen; Jeronimo Zafra, Jose; Leese, Mark; Maes, Jeroen; Mazy, Emmanuel; Mazzoli, Alexandra; Meseguer, Jose; Morales, Rafael; Orban, Anne; Pastor-Morales, M; Perez-grande, Isabel; Queirolo, Claudio; Ristic, Bojan; Rodriguez Gomez, Julio; Saggin, Bortolino; Samain, Valérie; Sanz Andres, Angel; Sanz, Rosario; Simar, Juan-Felipe; Thibert, Tanguy.

# Evaluating the performance of CaSSIS elevation data for geomorphological and geological analyses

Susan J. Conway (1), Riccardo Pozzobon (2, 3), Alice Lucchetti (3), Matteo Massironi (2,3), Emanuele Simioni (3), Cristina Re (3), Teo Mudric (3), Maurizio Pajola (3), Gabriele Cremonese (3) and Nick Thomas (4)  
(1) CNRS, LPG, University of Nantes, France (2) Dept. of Geoscience, University of Padova, Italy, (3) INAF – OAPD Astronomical Observatory of Padova, Italy (4) Physikalisches Inst., University of Bern, Sidlerstrasse 5, CH-3012 Bern, Switzerland. (susan.conway@univ-nantes.fr)

## Abstract

The Colour and Stereo Surface Imaging System (CaSSIS[1-4]) aboard ESA's Trace Gas Orbiter is enabling the acquisition of elevation data at ~20 m/pixel of the surface of Mars. Here we evaluate the performance of CaSSIS for geomorphological and geological studies by comparing with other elevation data used for such a purpose. These datasets are from the ConTeXT (CTX) and the High Resolution Imaging Science Experiment (HiRISE) cameras on NASA's Mars Reconnaissance Orbiter, whose elevation datasets are produced at 20-25 and 1-2 m/pixel, respectively. We find that CaSSIS elevation data have similar potential to those from CTX, yet CaSSIS will have better coverage and the addition of colour across the whole swath.

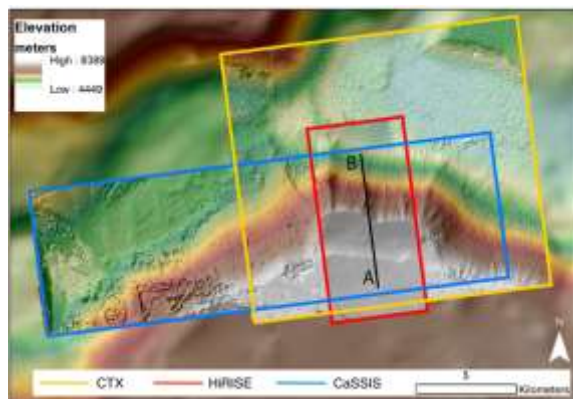
## 1. Technical details and methods

CaSSIS operates a pushframe image-capture system and performs in-track stereo by rotation of the telescope assembly in flight. Via this mechanism a stereo convergence angle of ~20° is obtained and the delay between subsequent images is on the order of 15-20s [1]. The CaSSIS elevation data shown here were produced by the team at the Astronomical Observatory of Padova (OAPD-INAF) from data acquired during the aerobraking phase of TGO in 20 November 2016. Two sets of framelets have been acquired from a mean distance of 520 km with a mean pixel scale of 6 m/px. At this time the orbit was highly elliptical and the spacecraft was rapidly changing altitude and speed across the scene causing unique challenges for the stereo reconstruction. Hence, the analysis of these elevation data should be considered as a minimum estimate of CaSSIS' performance. The production of the elevation data performed by 3DPD [5] includes: initial identification of tie-points using a SURF-type algorithm [6], production of an initial disparity map based on Delaunay triangulation, refined by a fast normalized cross correlation (NCC)

[7], and an iterative sub-pixel refinement with a least square matching algorithm [8]. CTX and HiRISE elevation data of the same region were produced from bundle adjusted images using the Ames Stereo Pipeline [9]. They were vertically controlled to the HRSC elevation data H3210\_0000da4 with 125 m horizontal resolution.

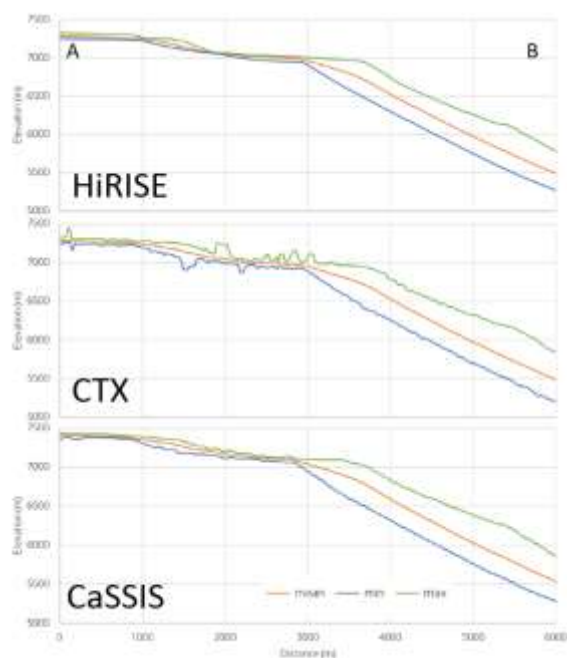
## 2. Initial Results

Fig. 1 shows the location of the three elevation datasets produced for this study. The horizontal resolution is 18, 25 and 2 meters for CTX, CaSSIS and HiRISE, respectively. The data are located over Noctis Labyrinthus to the west of Valles Marineris (6°1'10"S, 10°45'10"W). This area is characterised by steep escarpments with bedrock at the top and a talus slope below – a configuration characteristic of many zones with active slope processes on Mars (e.g. RSL [10], slope streaks [11], gullies [12]) – hence particularly suited to test the performance of CaSSIS.



**Figure 1:** Map showing the footprints of the CaSSIS, HiRISE and CTX elevation data with shaded relief. Background elevation is from HRSC H3210\_000. The black line marks the trace of the centre of the swath profile, spanning up to the edge of the HiRISE DTM footprint.

Fig. 2 shows the comparison between the three topographic swath profiles for CTX, CaSSIS and HiRISE. The sampling step along the profile has been chosen according to the horizontal resolution of the DTMs and the swath profiles have been collected across width of 3 km. Both values have been chosen in order to gather the maximum information in the overlapping area of the three datasets. The topographic information captured by the three datasets is consistent and comparable, despite the widely differing resolutions and noise.



**Figure 2:** Topographic swath profiles derived from the HiRISE, CTX and CaSSIS elevation datasets along A-B in Fig.1. No vertical exaggeration.

### 3. Summary and outlook

Our initial analyses have revealed that CaSSIS elevation data have a similar potential to data derived from CTX stereo pairs. The main advantages of CaSSIS over stereo acquisitions of CTX/HiRISE are: (1) the ability to take near-instantaneous stereo images meaning elevation data can be taken over areas that often change between CTX/HiRISE images making stereo reconstruction difficult or impossible (dunes, seasonally frosted areas, polar caps), (2) more data-volume is specifically allocated to stereo acquisitions than is possible for CTX/HiRISE which obtain stereo data by using different orbits and (3) co-registered colour data can be made available across the whole

swath width, which is particularly important when measuring active slope processes [13].

### Acknowledgements

SJC recognises the support of the French Space Agency CNES in funding her CaSSIS and HiRISE related work. The authors wish to thank the spacecraft and instrument engineering teams for the successful completion and operation of the instrument. CaSSIS is a project of the University of Bern and funded through the Swiss Space Office via ESA's PRODEX programme. The instrument hardware development was also supported by the Italian Space Agency (ASI) (ASI-INAF agreement no. I/018/12/0), INAF/Astronomical Observatory of Padova, and the Space Research Center (CBK) in Warsaw. Support from SGF (Budapest), the University of Arizona (Lunar and Planetary Lab.) and NASA are also gratefully acknowledged.

### References

- [1] Thomas, N., et al. (2017). The Colour and Stereo Surface Imaging System (CaSSIS) for the ExoMars Trace Gas Orbiter. *Space Science Reviews*, 212(3-4), 1897-1944.
- [2] Roloff, V., et al. (2017). On-ground performance and calibration of the ExoMars trace gas orbiter CaSSIS imager. *Space Science Reviews*, 212(3-4), 1871-1896.
- [3] Tulyakov, et al. (2018). Geometric calibration of colour and stereo surface imaging system of ESA's Trace Gas Orbiter. *Advances in Space Research*, 61(1), 487-496.
- [4] Gambicorti, L., et al. (2017). First light of CaSSIS: the stereo surface imaging system onboard the ExoMars TGO. In *International Conference on Space Optics—ICSO 2016* (Vol. 10562, p. 105620A).
- [5] Simioni et Al. "3DPD application to the first CaSSIS DTMs" EPSC(2018)
- [6] Bay et al., *Comput. Vision Image Und.*, 110, 2008.
- [7] Lewis, J.P. *Vision Interface*. 1995.
- [8] Grün, A. *South African J. Photogramm. Remote Sensing and Cartography*, 14, 3, 1985.
- [9] Shean, D. E., et al. (2016) An automated, open-source pipeline for mass production of digital elevation models (DEMs) from very high-resolution commercial stereo satellite imagery. *ISPRS Journal of Photogrammetry and Remote Sensing*. 116.
- [10] McEwen, A. S., et al. (2011). Seasonal flows on warm Martian slopes. *Science*, 333(6043), 740-743.
- [11] Sullivan, et al. (2001). Mass movement slope streaks imaged by the Mars Orbiter Camera. *Journal of Geophysical Research: Planets*, 106(E10), 23607-23633.
- [12] Malin, M. C., & Edgett, K. S. (2000). Evidence for recent groundwater seepage and surface runoff on Mars. *Science*, 288(5475), 2330-2335.
- [13] Tornabene, L. L., et al. (2018). Image simulation and assessment of the colour and spatial capabilities of the Colour and Stereo Surface Imaging System (CaSSIS) on the ExoMars Trace Gas Orbiter. *Space Science Reviews*, 214(1), 18.

# Terrestrial validation of geological analyses in PRo3D using an emulator for the ExoMars 2020 PanCam

R. Barnes<sup>1</sup>, M. Gunn<sup>2</sup>, S. Gupta<sup>1</sup>, G. Paar<sup>3</sup>, C. Traxler<sup>4</sup>, A. Bauer<sup>3</sup>, B. Nauschnegg<sup>3</sup>, T. Ortner<sup>4</sup>, M. P. Perucha-Caballo<sup>3</sup>.

(1)Department of Earth Science and Engineering, Imperial College London, UK. (2)Aberystwyth University, UK.

(3)Joanneum Research, Austria. (4)VRVis, Austria. (robert.barnes@imperial.ac.uk)

## 1. Abstract

The ExoMars 2020 Rover will use a panoramic stereo-camera system to image outcrops along its traverse, in order to characterise their geology and focus the search for ancient life. Photogrammetric reconstructions of these images are created using the Planetary Robotics Vision Processing tool (PRoViP)[1]. 3D Ordered Point Clouds (OPCs) of the reconstructed stereo images are visualized and interpreted in PRo3D [2], which has been tested using stereo-image data obtained by NASA's MER and MSL rover missions [3][4][5]. The Aberystwyth University PanCam Emulator (AUPE), an emulator for the ExoMars 2020 Rover, has been developed to collect stereo-image data of outcrops in the UK which are analogous to those expected in the candidate landing sites [6]. Stereo-image panoramas collected with AUPE are rendered in PRo3D, and full geological analyses of these outcrops are carried out. The results are compared with detailed field investigation of the same outcrops, allowing us to understand the reliability of this data when the ExoMars 2020 Rover carries out its mission.

## 2. Planetary Robotics 3D Viewer (PRo3D)

The interactive 3D viewing tool *PRo3D* [1][2][3] allows virtual exploration of reconstructed Martian terrain and geologic analysis of 3D datasets. It provides measurement and annotation tools to delineate geological boundaries, obtain dimensions of geologic features as well as the linear and projected distances between surface points and to calculate dip and strike of stratigraphic layers.

## 3. Aberystwyth University PanCam Emulator (AUPE)

AUPE was developed to allow the capture, processing and analysis of PanCam field data during the design, development, testing and qualification of the flight model. AUPE was constructed to match as closely as possible the specifications and capabilities

of the PanCam instrument [7] using Commercial Off The Shelf components. Like PanCam, the AUPE WACs have both RGB colour and multispectral imaging capabilities although only the RGB imaging filters were used in these studies. The transmission properties of the PanCam and AUPE RGB filters are closely matched and have the same center wavelengths and bandwidths. AUPE includes a motorized Pan-Tilt Unit (PTU) to allow panoramas to be captured and ensure the precise and repeatable pointing of the cameras during image capture.

## 4. Validation methodology

The primary concerns of this validation are the accuracy of measurements carried out in PRo3D and the geometry of the processed OPC surfaces, adherence to true geometry at an optimum imaging distance, and how this geometry varies with distance and distance:baseline ratio. We are particularly interested in how any changes in geometry will affect key measurements, particularly vertical and lateral dimensions and layer dip and strike. Field validation also lets us gain a greater understanding as to what details we are likely to miss when just interpreting geology from panoramas and DOMs.

## 5. Validation at Brimham Rocks, Yorkshire, UK.

The first stages of the validation process took place at Brimham Rocks, Yorkshire, UK, in July and August 2017. Three outcrops of spectacular fluvial cross-bedded sandstones were imaged extensively using AUPE. Reference measurements were collected after imaging, for comparison to those taken from the processed OPCs in PRo3D. These included field outcrop interpretations, imaging distance measurements, general scale, bedset thicknesses, layer thicknesses, grain size and variation, as well as the dip and strike of foresets, set boundaries and cross beds. Geo-referencing of these datasets has been carried out, using a handheld GPS and compass to place the OPCs into their true positions. Initial analysis of range maps derived from the OPCs show

that the surfaces are consistent with field measured imaging distances. Set thickness measurements in PRo3D also show a good agreement with the field measured values. Statistical analyses of the dip and strike measurements are ongoing.

## 6. Resolution of sedimentary structures at Pembrokeshire, Wales, UK.

A major issue in interpreting image data returned by the ExoMars rover mission will be the resolution of the images taken. We have imaged a series of Silurian-Ordovician outcrops of fluvial flood-plain mudstones and channel sandstones, which typically consists of thick sequences of mudstones, and fine-medium grained cross-laminated sandstones. Imaging took place at incremental distances of 2, 4, 8, 16 and in some cases 32 m from the outcrop. Automated processing using PRoViP is underway with this data, to create panoramic images and 3D OPCs. Interpretation of mosaics and OPCs taken at the different distances will be carried out to determine the level of image and OPC detail required to robustly identify and analyse key sedimentary structures which can be used for palaeoenvironmental reconstruction. Collection of this data will also help us to understand the reliability of stereo-reconstruction with an increasing distance:baseline ratio. This will provide a valuable basis for interpretation and reconstruction of the ancient environments along the ExoMars traverse, therefore providing context for the instrument science which will take place.

## 7. Summary and Conclusions

We show the first validation for photogrammetrically produced 3D digital outcrop models which are representative of those which will be collected by the 2020 ExoMars Rover PanCam. 3D visualization and analysis of photogrammetrically reconstructed stereo-image data enables geoscientists to extract large amounts of quantitative information from the images, so an understanding of the validity of those 3D digital outcrop models and the measurement tools used to analyse them is essential.

## Acknowledgements

RB and SG were funded by UKSA grant ST/P002064/1. Thanks also to National Trust

Brimham Rocks for allowing us to work on their premises. This work receives ESA-PRODEX funding, supported by the Austrian Research Promotion Agency under ESA PEA Grants 4000105568 & 4000117520.

## References

- [1] Paar, G., et al. Vision and Image Processing. In Gao, Yang, ed. Contemporary Planetary Robotics: An Approach Toward Autonomous Systems (2016). John Wiley & Sons, 2016.
- [2] Traxler, C., Ortner, T., Hesina, G., Barnes, R., Gupta, S., Paar, G., Muller, J.-P. and Tao, Y. (2018) The PRoViDE Framework: Accurate 3D geological models for virtual exploration of the Martian surface from rover and orbital imagery. In: 3D Digital Geological Models: From Terrestrial Outcrops to Planetary Surfaces (Ed. A. Bistacchi), John Wiley & Sons, Hoboken, NJ.
- [3] Barnes, R., Gupta, S., Traxler, C., Ortner, T., Hesina, G., Paar, G., Huber, B., Juhart, K., Fritz, L., Nauschnegg, B., Muller, J. P., Tao, Y. (2018). Geological analysis of Martian rover-derived Digital Outcrop Models using the 3D visualization tool, Planetary Robotics 3D viewer – PRo3D. Earth and Space Science.
- [4] Banham, S. G., Gupta, S., Rubin, D. M., Watkins, J. A., Sumner, D. Y., Edgett, K. S., ... & Barnes, R. (2018). Ancient Martian aeolian processes and palaeomorphology reconstructed from the Stimson formation on the lower slope of Aeolis Mons, Gale crater, Mars. Sedimentology.
- [5] Balme, M., Robson, E., Barnes, R., Butcher, F., Fawdon, P., Huber, B., Ortner, T., Paar, G., Traxler, C., Bridges, J., Gupta, S., Vago, J. L. (2018). Surface-based 3D measurements of small aeolian bedforms on Mars and implications for estimating ExoMars rover traversability hazards. Planetary and Space science. v15, 39-53.
- [6] Vago, J. L., *et al.*, (2017). Habitability on Early Mars and the Search for Biosignatures with the ExoMars Rover. Astrobiology. v17, no 6-7.
- [7] Coates, A.J., *et al.*, (2017). The PanCam instrument for the ExoMars Rover. Astrobiology, v17, no 6-7

# Formation of titanium oxide (TiO<sub>2</sub>) polymorphs in an emerged submarine volcano environment: Implications for Mars.

Patricia Ruiz-Galende, Imanol Torre-Fdez, Julene Aramendia, Leticia Gomez-Nubla, Kepa Castro, Gorka Arana, Juan Manuel Madariaga.  
Department of Analytical Chemistry, University of the Basque Country UPV/EHU, P.O. Box 644, E-48080 Bilbao, Spain.  
([patricia.ruiz@ehu.es](mailto:patricia.ruiz@ehu.es))

## Abstract

The study of terrestrial Martian analogues is crucial for the knowledge of the mineralogy and the formation mechanisms that occur in Mars. This work is focused on the study of titanium oxide polymorphs found in the same volcanic emplacement (a 100 million years old submarine volcano), as their formation need different environmental conditions. The three most common phases (rutile, brookite and anatase) were identified in the same samples by means of Raman spectroscopy, a technique that will be implemented in the next ESA Exomars2020 mission.

## 1. Introduction

The landing site of the Exomars2020 mission could be a sedimentary terrain fractured with volcanic events, formed in a submarine environment. The analysis of such a terrestrial environment is a fundamental step to understand the geological processes that could have happened in Mars. For that purpose, the Meñakoz outcrop (Biscay, northern Spain) is being currently studied and proposed as a terrestrial Martian analogue. It represents a 100 million submarine volcano scenario that erupted at 800-1000 m in depth through sea sediments; the pillow lavas together with the sedimentary units emerged 60 million years ago [1]. Among others, titanium dioxides are commonly found in this kind of emplacements.

On Earth, titanium occurs mainly in oxide or mixed oxide forms. Main polymorphs of TiO<sub>2</sub> are rutile (the most thermodynamically stable phase) brookite and anatase (both metastable and can be transformed into rutile irreversibly at high temperatures) [2] Rutile is the high-pressure and high-temperature polymorph that can be formed, among other reasons, because of hydrothermal alterations [3]. On the other hand, brookite and anatase are the low-temperature

polymorphs, being the latter the one with the lowest formation temperature. Brookite is the rarest of the natural TiO<sub>2</sub> polymorphs due to its lowest stability, although both brookite and anatase are stable even at 700°C. Above this temperature, brookite is converted into rutile while, in some cases, anatase could begin its transition to rutile at ~600°C [4].

## 2. Sample description

The analysed samples were extracted from the cliff on the Meñakoz outcrop with the help of a hammer. Samples were sliced and polished until the surface was free of deformations using progressively finer abrasive grit.

## 3. Materials and methods

For the proper characterization of the titanium oxide polymorphs, Raman spectroscopy was employed. The instrument used was an InVia confocal micro-Raman spectrometer (Renishaw, UK), provided with a 532 nm excitation laser, working in both point by point and Raman image mode using laser power filters to avoid thermal transformations.

## 4. Results and discussion

Rutile (Figure 1) with its main Raman bands at 447 (weak, w) and 610 (medium, m) cm<sup>-1</sup> was detected in the inner part of the samples. In order to clearly see the band at 447 cm<sup>-1</sup>, a band decomposition procedure was performed.

As the high-pressure and temperature polymorph, it can be stated that rutile was formed during the eruption of the volcano, when the pressure and the temperature reached high enough values. Due to its stability, it is still present nowadays inside the rocks.

Brookite (Figure 2, black) was identified also in the inner part of the sample with Raman bands at 154

(strong, s), 214 (w), 248 (w), 284 (w), 322 (m), 366 (w), 410 (very weak, vw), 501 (vw), 543 (vw) and 640 (vw)  $\text{cm}^{-1}$ . Regarding anatase (Figure 2, blue), it was detected both in the inner part and on the surface of the samples. Its Raman bands are 143 (very strong, vs), 198 (vw), 397 (m), 514 (w) and 637 (m)  $\text{cm}^{-1}$ .

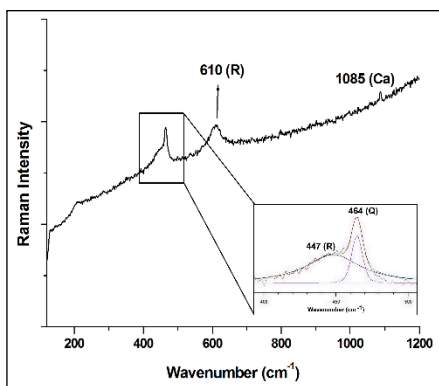


**Figure 1.** Raman spectrum of rutile (R) together with quartz (Q) and calcite (Ca). The decomposition of the band at 447  $\text{cm}^{-1}$  is presented.

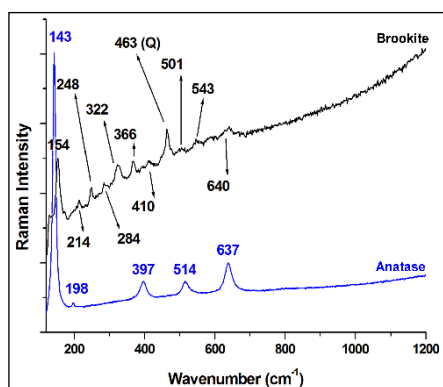


**Figure 2.** Raman spectra of brookite (together with quartz, Q) and anatase.

Formation mechanism of brookite is still unclear. It is an accessory mineral in igneous rocks and it may be formed under hydrothermal conditions [5], but also during the cooling process of the lava. Anatase arises as an alteration product of Ti-rich minerals such as ilmetite ( $\text{FeTiO}_3$ ), which is common in volcanic rocks; the formation of this  $\text{TiO}_2$  polymorph suggest a hydrothermal like origin [6], which could happen in Meñakoz, due to its submarine volcanic nature.

## 5. Conclusions

The identification of titanium oxides is very helpful in the comprehension of the formation mechanisms in Mars. The differences related to the temperature or pressure for their formation could provide clues to establish different formation environments and thus, to understand the environmental and geological history of Martian rocks. The presence of rutile indicates that there was an episode where the temperature and pressure were high, probably during the eruption of the volcano. The other polymorphs (brookite and anatase) arise from alteration processes indicating their later formation.

## Acknowledgements

This work has been financially supported through the Exomars-Raman project (ref. ESP2017-87690-C3-1-R), funded by the Spanish Agency for Research AEI (MINEICO-FEDER/UE).

## References

- [1] Ruiz-Galende, P., Torre-Fdez, I., Arana, G., Aramendia, J., Gomez-Nubla, L. Fdez-Ortiz de Vallejuelo, S., Castro, K., Madariaga, J.M., Geochemical characterisation of a terrestrial Martian analogue: the submarine volcano of Meñakoz (Biscay, Spain), 49<sup>th</sup> Lunar Plan. Sci. Conf. 2018, Abst. 2842, 2018.
- [2] Byrne, C., Fagan, R., Hinder, S., McCormack, D. E., Pillai, S. C.: New approach of modifying the anatase to rutile transition temperature in  $\text{TiO}_2$  photocatalysts., RSC Adv., Vol. 6, pp. 95232-95238, 2016.
- [3] Meinhold G.: Rutile and its applications in earth sciences., Earth-Science Reviews, Vol. 102, pp. 1-28, 2010.
- [4] Hanaor, D. A. H., Sorrel, C. C.: Review of the anatase to rutile phase transformation., J. Mater. Sci., Vol. 46, pp. 855-874, 2011.
- [5] Bakardjieva, S., Stengl, V., Szatmary, L., Subrt, J., Murafa, N., Niznansky D., Cizek, K., Jirkovsky, J., Petrova, N.: Transformation of brookite-type  $\text{TiO}_2$  nanocrystals to rutile: correlation between microstructure and photoactivity., J. Mater. Chem., Vol. 16, pp. 1709-1716, 2006.
- [6] Papoulis, D., Tsolis-Katagas, P., Kalamounias A. G., Tsikouras, B.: Progressive formation of halloysite from the hydrothermal alteration of biotite and the formation mechanisms of anatase in altered volcanic rocks from Limnos island, Northeast Aegean sea, Greece., Clays Clay Miner., Vol. 57, pp. 566-577, 2009.

# The radar WISDOM for the ExoMars rover mission Interpretation of the polarimetric data and contribution to the operations

Valerie Ciarletti (1), Dirk Plettmeier (2), Yann Hervé (1), Alice Le Gall (1), Wolf-Stefan Benedix (2), Yun Lu (2) and the WISDOM team

(1) LATMOS/IPSL, UVSQ (Université Paris-Saclay), UPMC (Sorbonne Univ.), Guyancourt, France (2) Technische Universität Dresden, Dresden, Germany

## Abstract

WISDOM (Water Ice Subsurface Deposits Observation on Mars) is a ground penetrating radar designed to characterize the shallow subsurface of Mars, it will be accommodated on the rover of the ExoMars mission and will provide global information about the landing site geological history as well as accurate descriptions of the buried structures that will be essential to collect the samples at depth. In this paper, we focus on the tools that have been developed to process the signal and the polarimetric data in order to achieve the technical and scientific objectives of WISDOM and contribute to the success of the rover mission. Experimental data acquired in natural environments will be shown and analyzed.

## 1. The WISDOM radar for ExoMars

WISDOM is a polarimetric radar, it can be operated in co/cross-polar mode, which is essential to characterize the shape of buried reflectors, estimate the roughness of the surface.

WISDOM will be accommodated on the rover of the ExoMars 2020 mission [1][2].

The main objectives of WISDOM are to:

- Give clues into the geological context of the investigated site by providing information about the structure of the subsurface (layers, blocks,...), constraining the composition of the detected units (porosity, composition) and mapping the distribution and state of the subsurface water
- Provide input for the identification of the most promising locations for sampling
- Provide guidance for the drilling operations

## 2. The experimental data set

We are leading a series of field tests in natural environments order to acquire experimental data in a variety of environments. These data are currently used to design the data processing pipeline and validate the algorithms. To assess the performances and limits of the tools, it is essential to operate on a number of interesting geological structures (outcrops, layered subsurface, sedimentary rocks ...).

We use a prototype of the instrument representative of the flight model to perform the measurements. The WISDOM prototype is mounted on a cart inside a case and the antenna system is 40 cm above the surface as shown on Fig.1



Fig.1 : WISDOM prototype during a field test in South of France

## 3. Data Processing

For the purpose of the operations on Mars, as automatic as possible codes are developed. They allow to detect in limit time layers and buried blocks.

High resolution algorithms are used to accurately retrieve the surface topography. On smooth surfaces, the amplitude of surface echo provides a first estimate of the permittivity value which is used to convert the measured delays in distances. Entropy computation allows a local characterization of the heterogeneities. Image processing codes are developed to map the interfaces below the surface.

On-going work is done to optimize the processing of the data and a collaboration with the Ma-MISS team has recently be initiated to work on and optimize the necessary synergy with the other instruments.

## **Acknowledgements**

The WISDOM development has be supported by the CNES French agency and DLR German agency.

## **References**

[1] V. Ciarletti, C. Corbel, D. Plettemeier, P. Caïs, S. M. Clifford, and S. E. Hamran, "WISDOM GPR Designed for Shallow and High-Resolution Sounding of the Martian Subsurface " Proceedings of the IEEE, vol. 99, no. 99, pp. 1-13, 2011.

[2] Ciarletti,V. ; Clifford, S. ; Plettemeier,D. ; Le Gall,A.; Hervé,Y. ; et al, "The WISDOM radar: Unveiling the subsurface beneath the ExoMars Rover and identifying for the best location for drilling "2017 Astrobiology.

# Development of a modified Tau-REx retrieval framework for processing the ExoMars TGO NOMAD data

George Cann (1), Jan-Peter Muller (1), Dave Walton (1) and Ingo Waldmann (2).

(1) Imaging Group, Mullard Space Science Laboratory, Department of Space and Climate Physics, University College London, Holmbury St. Mary, Dorking, Surrey, RH5 6NT, UK, ([george.cann.15@ucl.ac.uk](mailto:george.cann.15@ucl.ac.uk))

(2) Astrophysics Group, Department of Physics and Astronomy, University College London, Gower Street, WC1E 6BT, UK.

## Abstract

We present our research on the development of a Mars modified version of Tau-REx (Tau Retrieval for Exoplanets)<sup>[1]</sup>, an exoplanetary atmospheric retrieval framework, designed to retrieve areo-located  $^{13}\text{CH}_4$ ,  $^{12}\text{CH}_4$  and  $\text{C}_2\text{H}_6$  volume mixing ratios (VMRs), using the ESA ExoMars Trace Gas Orbiter (TGO) Nadir and Occultation for Mars Discovery (NOMAD) radiance spectra. The VMRs, of  $\text{C}_2\text{H}_6$  and the isotopologues of  $\text{CH}_4$ , are of great interest in exploring whether  $\text{CH}_4$  in the Martian atmosphere is biotic or abiotic.<sup>[2]</sup> Whilst  $^{13}\text{CH}_4$ ,  $^{12}\text{CH}_4$  and  $\text{C}_2\text{H}_6$  VMRs areo-located retrievals are yet to be obtained, we present transmission and emission spectra, simulated using a Mars modified version of Tau-REx with the Mars Climate Database Version 5.2 (MCDv5.2)<sup>[3]</sup>. Finally, we present a series of movies of the global variation of the atmosphere and climate of Mars, created using the MCDv5.2 and comment on their use in the development of DeepMars, a deep neural network (DNN) retrieval framework.

## 1. Introduction

In 2003, methane,  $\text{CH}_4$ , was detected in the Martian atmosphere (10 ppbv)<sup>[4]</sup>, which has, at most, a photochemical lifetime of a few hundred years.<sup>[5]</sup> This short lifetime of  $\text{CH}_4$  in the Martian atmosphere implies that  $\text{CH}_4$  should be uniformly distributed over Mars. However non-uniform distributions of  $\text{CH}_4$  are observed.<sup>[6]</sup> This raises questions with regard to the source(s) and sink(s) of  $\text{CH}_4$ . Abiotic and biotic sources have been suggested to explain the detection, ranging from serpentinisation of olivine to methanogenesis<sup>[6]</sup> by methanogenic archaea.<sup>[7]</sup> ESA's ExoMars TGO NOMAD instrument is expected to be able to measure the isotopic ratios of carbon-based molecules in the Martian atmosphere.<sup>[8]</sup> On Earth, the ratios of  $^{13}\text{CH}_4/(\text{C}_2\text{H}_6 + \text{C}_3\text{H}_8)$  and  $\delta^{13}\text{C}_{\text{CH}_4}$  and  $\delta^2\text{H}_{\text{CH}_4}$ , can be used to infer whether sources of  $\text{CH}_4$

are biogenic or abiogenic.<sup>[2]</sup> Assuming similar conditions hold on Mars, NOMAD measurements have the potential to address this question.

## 2. Methods

### 2.1 A Mars modified Tau-REx

Tau-REx is a fully Bayesian retrieval framework that uses Multinest/MCMC/Nested Sampling to sample the entire likelihood space, unlike other planetary atmosphere retrieval frameworks that often only find the MAP solution, which may be biased.<sup>[1]</sup> Tau-REx can also be used to produce posterior distributions of model parameters. The posterior distributions of the VMRs of  $^{13}\text{CH}_4$ ,  $^{12}\text{CH}_4$  and  $\text{C}_2\text{H}_6$ , with one another (and other model parameters) are particularly relevant for associating a likelihood to the nature of  $\text{CH}_4$  on Mars; abiotic or biotic, by showing whether the retrievals of different state vector parameters are correlated. Our research has involved modifying the Tau-REx radiative transfer model (RTM) module, which acts within the Tau-REx retrieval framework, for Mars. The RTM has been used with vertical temperature, pressure and VMRs profiles derived from the MCDv5.2 (Figure 1), to produce simulated

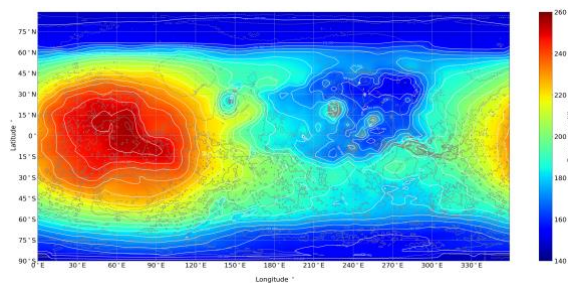


Figure 1: A single frame of a movie of the global atmospheric temperature (K) of Mars at 1m above the local surface, created using the MCDv5.2.

Mars emission (Figure 2) and transmission (Figure 3) spectra over NASA's MSL location (4.5°S, 137.4°E). The developed framework will eventually use calibrated ESA PSA files, generated from NOMAD measurements. These are expected to be publicly released by ESA in September 2018. Through inverting measured radiance spectra, with simulated spectra with  $^{13}\text{CH}_4$ ,  $^{12}\text{CH}_4$  and  $\text{C}_2\text{H}_6$  present, Tau-REx can obtain volume mixing ratios (VMRs). After the Mars modified Tau-REx has obtained areo-located profiles of trace gas VMRs, we intend to attempt to validate these results against the NASA Mars Science Laboratory (MSL) Curiosity rover SAM-TLS measurements in Gale Crater.<sup>[6]</sup>

## 2.2 The Mars Climate Database

We also present a set of movies of the global variation of the atmosphere and climate of Mars created with the MCDv5.2, (Figure 1), e.g. the average solar scenario climatology, with increasing solar longitude and local times, at the local surface and 1m above, can be viewed by the reader online at: <https://www.youtube.com/watch?v=shQGEKYFW8U&t>.

## 2.3 DeepMars

In parallel to a Mars modified Tau-REx retrieval framework, a machine learning Mars retrieval framework is being developed; DeepMars, which uses a DNN to empirically derive a statistical relationship between an ensemble of NOMAD radiance spectra (using an extremely large training database of Mars modified Tau-Rex RTM simulated spectra) and different state vector parameters.<sup>[9]</sup>

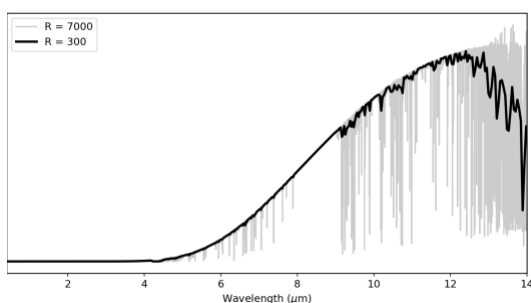


Figure 2: A simulated emission spectrum created, using a Mars modified Tau-REx retrieval framework, exploiting a vertical atmospheric profile at NASA's MSL location (4.5°S, 137.4°E), using the MCDv5.2.

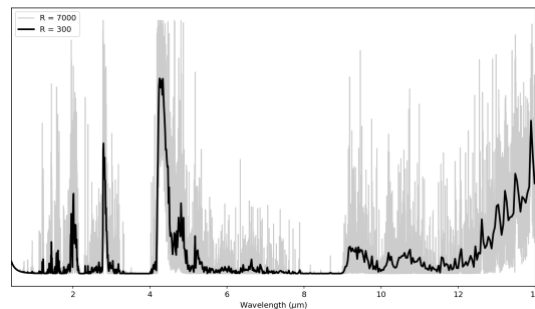


Figure 3: A simulated transmission spectrum, created using a Mars modified Tau-REx retrieval framework.

## 3. Conclusions

Our research has described the development of two retrieval frameworks; a Mars modified Tau-REx together with DeepMars, which will be used for the interpretation of future NOMAD observations, in particular to assess whether  $\text{CH}_4$  detected in the Martian atmosphere is biogenic or abiogenic.

## Acknowledgements

We would like to thank UK Space Agency for their support of this studentship through the Aurora science programme. STFC no: 535385. We would like to thank the LMD for providing a copy of the MCD and Ehouarn Millour for his help in the installation of the MCDv5.2, as well as James Holmes for a set of column averaged methane mixing ratios from Holmes et al. (2015).

## References

- [1] Waldmann et al. (2015), *The Astrophysics Journal*, Volume 802, Number 2. [doi:10.1016/j.icarus.2004.07.004]
- [2] Allen et al. (2006), *EOS*, Vol 87, Issue 41, pp. 433–439, 2006. [doi: 10.1029/2006EO410001].
- [3] Forget, F., Millour, E., and Lewis, S., [http://www.mars.lmd.jussieu.fr/mars/info\\_web/MCD5.2\\_dd.pdf](http://www.mars.lmd.jussieu.fr/mars/info_web/MCD5.2_dd.pdf), 2015.
- [4] Krasnopolsky et al. (2004), *Icarus* 172, pp. 537–547. [doi:10.1016/j.icarus.2004.07.004]
- [5] Formisano et al. (2004), Vol. 306, pp. 1758–1761. [doi: 10.1126/science.1101732].
- [6] Webster et al. (2015), *Science*, Vol. 347 (6220), pp. 415–417. [doi: 10.1126/science.1261713].
- [7] Morozova et al. (2007), Vol. 37, Issue 2, pp. 189–200. [doi: 10.1007/s11084-006-9024-7].
- [8] Robert, S et al. (2016), *Planetary and Space Science* 124, pp. 94–104, 2016. [doi: 10.1016/j.pss.2016.03.003].
- [9] Goodfellow I., Bengio Y., and Courville A., *Deep Learning*, pp., The MIT Press, 2017.

# Processing and Calibration for the WISDOM Radar Applied to Field Measurements

**Dirk Plettemeier** (1), Christoph Statz (1), Yun Lu (1), Wolf-Stefan Benedix (1), Valérie Ciarletti (2), Alice Le Gall (2), Charlotte Corbel (2) and Yann Hervé (2)  
 (1) Technische Universität Dresden, 01062 Dresden, Germany. (dirk.plettemeier@tu-dresden.de)  
 (2) UVSQ/LATMOS, 78280 Guyancourt, France

## Abstract

The capabilities of the WISDOM GPR, which is part of the 2020 ExoMars rover payload, are demonstrated on field test data from two different sites. The objectives of this paper are calibration, data processing and polarimetric classification of buried scatterers.

## 1 Introduction

The WISDOM GPR is part of the 2020 ESA-Roscosmos ExoMars rover payload. It operates at frequencies between 500 MHz and 3 GHz yielding a centimetric resolution and a penetration depth of about 3 m in Martian soil. Its primary scientific objective is the detailed characterization of the material distribution within the first meters of the Martian subsurface as a contribution to the search for evidence of past life [1]. In addition to the primary scientific objectives, the WISDOM data is supposed to be embedded in terrain visualizations [2] in order to support the drilling operations [5].

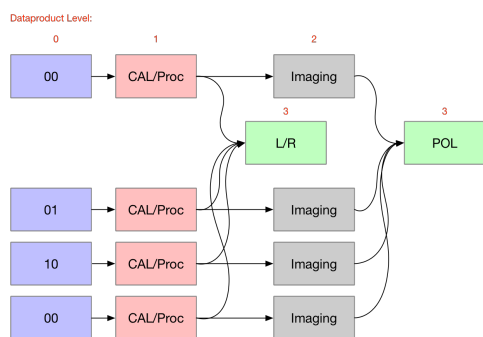


Figure 1: WISDOM calibration and data processing scheme.

## 2 Calibration and Processing

The WISDOM data measured along the rover path is subjected to calibration and pre-processing (removal of ringing artifact). From the fully polarimetric measurements a left-right discrimination [4] and classification of the buried scatterers is possible. The processing scheme is depicted in Fig. 1. The processing consists of a calibration using freespace laboratory measurements of the WISDOM antenna pattern, time-domain transform of the measured data, removal of ringing artifacts, spatial high-pass filtering, imaging (Stolt) and subspace projection. The processed results are decomposed using Entropy- $\alpha$  analysis for classification.

## 3 Field Data

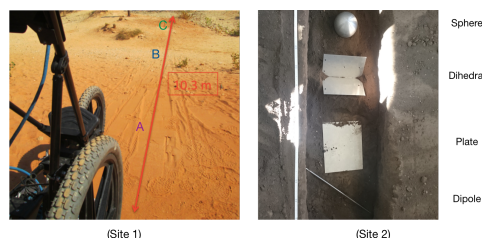


Figure 2: Depiction of the test sites. Left: Site 1, right: Site 2.

The WISDOM data processing, calibration and analysis has been tested on different occasions, e.g. during the SAFER experiments [3].

Here we present further data from field measurements. The two test sites are depicted in Fig. 2. At site 1, the measured track is approx. 10m across plain and flat terrain with limited vegetation and surrounding scatterers. The regions relevant for the radargram processing are marked A,B and C. Feature B seems to

be a channel with distinctive material properties and structure. At site 2 the measured track is approx. 2m across plain soil inside a concrete channel. Inside this channel different scatterers have been buried.

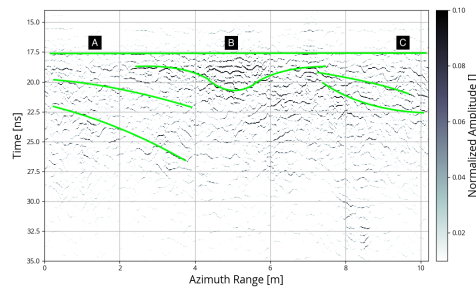


Figure 3: CS (subspace projection) processed radargram of site 1 with marked features.

The processed radargram result of site 1 is depicted in Fig. 3. After processing, the channel B is clearly visible in the data. In region A the signature of a descending subsurface horizon is visible. Region C exhibits different surface structure and density. The classification results of site 2 are depicted in the Fig. 4 and Fig. 5. The buried scatterers are clearly visible in the C-scan and correctly classified in the Entropy- $\alpha$ -plane.

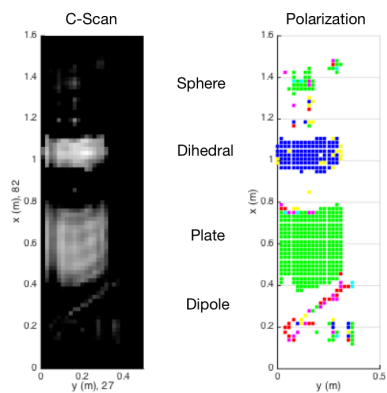


Figure 4: C-Scan and polarization of measurement site 2.

## 4 Conclusions

The derived WISDOM calibration and processing scheme yields stable results at the expected resolution.

The processed data can be embedded in a terrain visualization, aiding in the selection of viable drill sites.

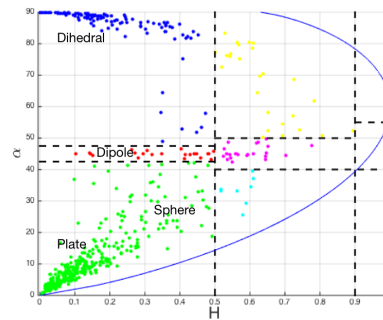


Figure 5: Polarization behavior of site 2. The buried objects are classified correctly in the expected regions.

## Acknowledgements

The research on WISDOM is supported by funding from the Centre National d'Etudes Spatiales (CNES) and the Deutsches Zentrum für Luft- und Raumfahrt (DLR).

## References

- [1] V. Ciarletti, C. Corbel, D. Plettemeier, P. Cais, S. M. Clifford, S.-E. Hamran, "WISDOM GPR Designed for Shallow and High-Resolution Sounding of the Martian Subsurface", Proceedings of the IEEE, Vol. 99, Issue 5, pp. 824-836, May 2011.
- [2] G. Paar, G. Hesina, C. Traxler, V. Ciarletti, D. Plettemeier, C. Statz, K. Sander and B. Nauschnegg, "Embedding Sensor Visualization in Martian Terrain Reconstructions", ASTRA2015, May 2015
- [3] S. Dorizon, V. Ciarletti, A.-J. Vieau, D. Plettemeier, W.-S. Benedix, M. Mütze, R. Hassen-Kodja and O. Humeau, "WISDOM GPR subsurface investigations in the Atacama desert during the SAFER rover operation simulation", EGU2014, Vienna, May 2014
- [4] D. Plettemeier, V. Ciarletti, W.-S. Benedix, S. M. Clifford, S. Dorizon and C. Statz, "ExoMars WISDOM Left-Right-Evaluation of Subsurface Features", EGU2013, Vienna, April 2013
- [5] V. Ciarletti, S. Clifford, D. Plettemeier and the WISDOM Team, "The WISDOM Radar: Unveiling the Subsurface Beneath the ExoMars Rover and Identifying the Best Locations for Drilling", Astrobiology, Vol. 17, No. 6-7, July 2017

## **Martian winds could drive seasonal methane variations observed by MSL-SAM: implications for TGO observations**

Jorge Pla-García<sup>1,2</sup>, Scot C. R. Rafkin<sup>3</sup>, Christopher R. Webster<sup>4</sup>, Paul R. Mahaffy<sup>5</sup>, Özgür Karatekin<sup>6</sup>, Elodie Gloesener<sup>6</sup> and John E. Moores<sup>7</sup>

<sup>1</sup>Centro de Astrobiología (CSIC-INTA), <sup>2</sup>Space Science Institute, <sup>3</sup>Southwest Research Institute (SwRI), <sup>4</sup>NASA Jet Propulsion Laboratory, <sup>5</sup>NASA Goddard Space Flight Center, <sup>6</sup>Royal Observatory of Belgium, <sup>7</sup>Centre for Research in Earth and Space Science (CRESS)

### **Abstract**

The MSL-SAM team recently presented in situ measurements of the background methane levels in Gale Crater that exhibits a strong, repeatable seasonal variability with a mean value of 0.4 ppbv [1]. The Mars Regional Atmospheric Modeling System (hereafter MRAMS, [2]) is ideally suited to study the role of local atmospheric transport and mixing in the evolution of methane from potential source locations using instantaneous and steady-state (Figure 1) in time tracers, and to investigate whether methane releases inside or outside of Gale crater are consistent with TLS-SAM observations. Clathrate hydrates could be a possible source of episodic methane releases on Mars, and are used to estimate atmospheric abundances based on reasonable surface flux rates.

### **1. Experiment configuration**

The model was run for twelve sols. Although the circulation patterns are highly repeatable from sol to sol beginning within a few hours of initialization, the first sol may be regarded as “spin-up”. All simulations were started, at or slightly before local sunrise. In order to characterize seasonal mixing changes throughout the Martian year, simulations were conducted at Ls 270° (the wholesale inundation and flushing season of the crater reported in [3, 4]) and Ls 90° (as a representative of the rest of the year) and Ls 155° (the highest methane values in [5, Mumma]). Using the above model configurations, [3] demonstrate that the model was able to reproduce the meteorological observations obtained by the MSL Curiosity rover REMS instrument [6] in Gale crater.

### **2. Results**

In our simulations, mixing of the crater air with external air is found to be high during all the martian year, being slightly more rapid at Ls 225-315 compared to other seasons. This result is in contrast to prior work, and we find that the crater is not isolated at any period of the year. The mixing time scale is ~1 sol or less. The model simulations further suggest that there must be a continuous release of methane to counteract atmospheric mixing, because the timescale of mixing is much shorter than the observed span of elevated methane levels. The model also indicates that the timing of MSL-SAM sample ingestion is very important, because the modeled methane abundance varies by one order of magnitude over a diurnal cycle (Figure 2). The crater atmospheric circulation is strongly 3-D, not just 1-D or 2-D, and any scenario describing the transport of methane must recognize this dimensionality [7].

### **3. Conclusions**

Presumably, ground temperature controls the release of methane trapped in clathrates on seasonal timescales. The methane flux should be higher during warmer seasons, implying a seasonal hemispheric difference in methane background values if we assume ubiquitous release sources over the planet. During Ls 225-315, the strong northwesterly air flowing down the crater rims during nighttime originates from deep within the northern hemisphere, whereas at other seasons the origin of that external air is from locations closer to the crater or from more tropical regions. The consequence of this is that although the local methane emission in the crater may be highest during the warm Ls 225-315 season, those emissions are rapidly transported away and replaced by methane-poor air emanating from the cold northern hemisphere (red circle in Figure 3). In contrast, the methane flux in the crater at other seasons is similar to the flux for the source air location (blue circle in Figure 3). In this scenario,

mixing has little effect on the overall methane concentration and the concentration should be better correlated with the local ground temperature.

Based on the mean meridional circulation, surface winds would be expected to converge and confine in the equatorial zone as the rising branch transits through the equatorial region from one hemisphere into the other as it migrates to its solstitial location (green circles in Figure 3), containing and circulating methane-rich air in the equatorial zone.

Synergy of our modeling results with TGO observations could help to answer next intriguing questions: Where are the methane release locations? How spatially extensive are the releases? For how long is methane released?

#### 4. Figures

**Figure 1.** Steady state methane release scenarios aerial view. Gale crater encircled. The yellow cross represent the MSL Curiosity rover location. Four independent methane release sources were located outside the crater ~100 km NW, NE, SW and SE of the rover landing site, each with an area of ~6,400 km<sup>2</sup> and another one located inside of the crater ~1 grid point west from the rover with an area of ~149 km<sup>2</sup>:

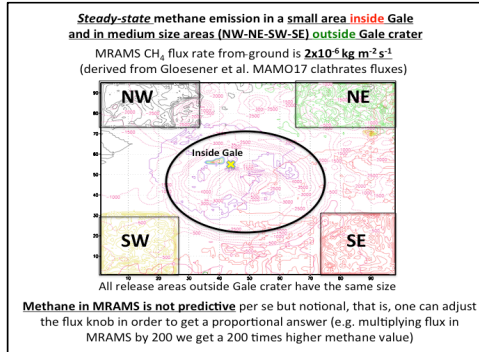


**Figure 2.** Nine-sols timeseries (left) and two-sols timeseries (right) of MRAMS methane abundances sampled ~14.5 m high at release site which is located inside of Gale crater ~1 grid point west from the rover with an area of ~149 km<sup>2</sup>. The release emission is steady state. Only nine of the twelve sols simulated were included into the figure:

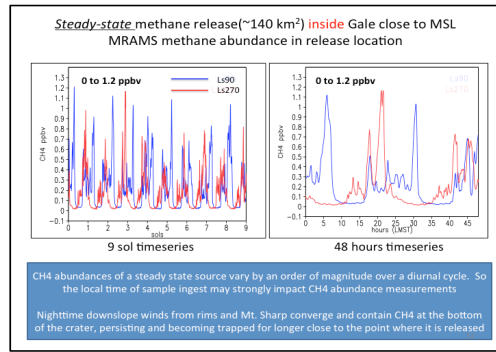
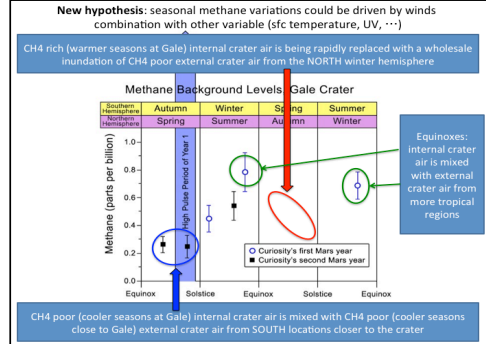


**Figure 3.** SAM methane background levels at Gale crater vs atmospheric mixing periods:



#### Acknowledgements

This work was supported by the Spanish Ministry of Economy and Competitiveness under contract ESP2016-79612-C3-1-R and by the NASA/Jet Propulsion Laboratory under subcontract 1356597.

#### References

- [1] Webster et al, AGU 2017 P33F-07. [2] Rafkin et al, Icarus 2001. [3] Pla-Garcia et al, Icarus 2016. [4] Rafkin et al., Icarus, 2016 [5] Mumma et al, Science 2009. [6] Gómez-Elvira et al, Space Sci. Rev. 2012. [7] Pla-García et al, EGU 2018.

## ExoMars Trace Gas Orbiter – Status and future activities

**Håkan Svedhem** (1), Jorge L. Vago (1), Daniel Rodionov (2) and the ExoMars Team  
(1) ESA/ESTEC, Noordwijk, The Netherlands, (2) IKI, Moscow, Russia (H.Svedhem@esa.int)

### Abstract

The ExoMars programme is a joint activity by the European Space Agency (ESA) and ROSCOSMOS, Russia. It consists of the ExoMars 2016 mission, launched 14 March 2016, with the Trace Gas Orbiter, TGO, and the Entry Descent and Landing Demonstrator, EDM, named Schiaparelli, and the ExoMars 2020 mission, to be launched in July 2020, carrying a Rover and a surface science platform.

TGO arrived at Mars on 19 October 2016 and was inserted into a near equatorial, highly elliptical 4 sol period capture orbit. Two orbits in late November were dedicated to instrument calibration and initial science observations, where an excellent performance of all instruments could be confirmed. In January 2017 the orbital plane was changed to its final inclination of 74 degrees and the period was reduced to one Sol. Early March 2017 an additional two orbits were scheduled for instrument tests and observations, after which a long period of aerobraking commenced. The aerobraking phase was running very smoothly and was suspended for two months during the solar conjunction in the summer of 2017, and then finished with an orbit having an apocentre just above 1000 km on 20 February 2018. After this a series of thruster firings brought the apocentre further down to 400 km. The final near circular 400 km altitude orbit, with a 2 hour period, was reached on 7 April 2018, after which a full check out of the spacecraft and the instrument was performed. The science operations in the Commissioning and Verification Phase, including solar occultation measurements with the two spectrometers, started on 21 April. The commissioning phase will be concluded with a Mars Orbit Commissioning Review on 14 June and the full nominal science operation will start in September 2018.

The TGO scientific payload consists of four instruments. These are: ACS and NOMAD, both being spectrometers for atmospheric measurements

in solar occultation mode and in nadir mode, CASSIS, a multichannel camera with stereo imaging capability, and FRENDA, an epithermal neutron detector for search of subsurface hydrogen. The mass of the TGO is 3700 kg, including fuel and the mass of EDM was 600 kg. The EDM was carried to Mars by the TGO and was separated three days before arrival at Mars but unfortunately failed during the last stage of the descent.

This presentation will cover a brief description of the Trace Gas Orbiter mission, the present status, an overview of the first operations in the science orbit, and the planned future activities.

## TGO limb observations and additional possibilities for upper atmosphere science on Mars

Miguel A. López-Valverde(1) (valverde@iaa.es), Jean-Claude Gérard(2), Francisco González-Galindo(1), Ann Carine Vandaele (3), Oleg Korablev(4) and the NOMAD and ACS teams

(1) Instituto de Astrofísica de Andalucía (IAA/CSIC), Granada, Spain, (2) Laboratoire de Physique Atmosphérique et Planétaire, Université de Liège, Belgium, (3) Royal Belgian Institute for Space Aeronomy, BIRA-IASB, Belgium, (4) Space Research Institute - IKI, Moscow, Russia

### Abstract

The Martian mesosphere and thermosphere (altitudes above 50-60 km), is not the primary target of the Trace Gas Orbiter (TGO) but TGO is exploring the region, both during the aerobraking phase and, after April 21st, 2018, during the science phase using several geometries and instrumentation. Further upper atmospheric science could be obtained during the nominal mission if some “additional” observational modes were implemented ([2]). These would add capabilities to explore the limb off-the-terminator. However some of the new target emissions are weak and variable. In this work we will review the performance of the two key instruments on board TGO for atmospheric science, NOMAD and ACS, and revisit the potential for pursuing those additional observation modes.

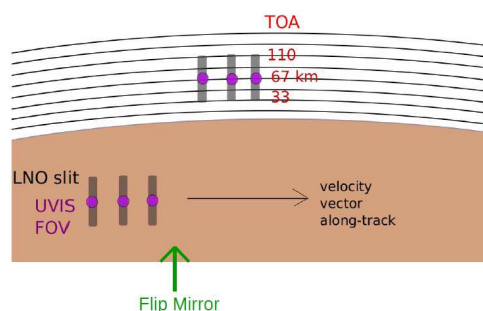


Figure 1: Illustration of the use of NOMAD LNO's flip mirror to observe the limb (at a fixed elevation) during the nadir mapping phase.

### 1. Introduction

During the TGO regular science phase, the Martian upper atmosphere is routinely explored remotely by means of its three nominal observing modes, nadir, solar occultation and limb pointing (using NOMAD's flip mirror, see Figure 1), and by combining the 2 solar occultation spectrometers on board, NOMAD and ACS, which cover from the UV to the IR. This is a superb configuration to detect trace species but also to measure faint absorptions from the solar flux at high altitudes and to investigate atmospheric emissions off-the-terminator ([2]).

Lopez-Valverde et al. (2018) made simulations of possible UV and IR emissions which could be observed with the nominal observing modes, and proposed a few “additional” observational modes for TGO. In particular they mentioned the possibility to perform inertial limb scans, nadir boresight slews, and fixed limb tracking. The obvious goal is to extend the local time of the upper atmosphere observations. None of their additional modes is currently contemplated in the science phase but they would add capabilities to explore the limb off-the-terminator (i.e. the nightside and dayside hemispheres). In particular, they could be useful to improve:

- vertical profiles of minor species and dust
- the daily cycle of minor species
- detection of airglow emissions outside the terminator

Some of their simulations for these modes correspond to solid predictions, some to likely detections, and other ones may be at the limit of detection. Using the better characterization of NOMAD and ACS performances that we will have after the first months of regular operations, we will review those possibilities to study the Mars upper atmosphere with TGO.

Table 1: Characteristics of the NOMAD and ACS channels (before the Science Phase)

Instrument and Channel	Range ( $\mu\text{m}$ )	Resolution ( $\text{cm}^{-1}$ )	LIMB FOV <sup>‡</sup>	NESR <sup>*</sup>
NOMAD SO	2.2 – 4.2	0.15–0.22	1 × 14	$8 \times 10^{-10}$
NOMAD LNO	2.3 – 3.8	0.3–0.5	2 × 67	$2 \times 10^{-8} - 6 \times 10^{-10}$
NOMAD UVIS	0.2 – 0.65	~ 1.5 nm	1 × 1	$10 - 8 \times 10^{-6}$
ACS NIR	0.76 – 1.6	0.4	5 × 50	$5 \times 10^{-7} - 4.5 \times 10^{-10}$
ACS MIR	2.3 – 4.3	0.085	0.5 × 7.5	$5 \times 10^{-10}$
ACS TIRVIM	2 – 17	0.25–1.3	70 × 70	$\sim 2 \times 10^{-8} - 10^{-9}$

<sup>‡</sup> Limb Field-Of-View in km.

<sup>\*</sup> Noise Equivalent Spectral Radiance units:  $W/\text{cm}^2/\text{cm}^{-1}/\text{sr}$ . Estimations based on [4], [3] and [1]

## Acknowledgements

The NOMAD experiment is led by the Royal Belgian Institute for Space Aeronomy (IASB-BIRA), assisted by Co-PI teams from Spain (IAA-CSIC), Italy (INAF-IAPS), and the United Kingdom (Open University). This project acknowledges funding by the Belgian Science Policy Office (BELSPO), with the financial and contractual coordination by the ESA Prodex Office (PEA 4000103401, 4000121493), by Spanish MICINN through its Plan Nacional and European funds under grant ESP2015-65064-C2-1-P (MINECO/FEDER), as well as by UK Space Agency through grant ST/P000886/1 and Italian Space Agency through grant 2018-2-HH.0. OK thanks funding from Roscosmos for the ACS operation support and science funding from The Federal Agency of scientific organization (Planeta No. 0028-2014-0004).

infrared channels - SO and LNO. OPTICS EXPRESS **24**(4), 3790–3805 (2016). DOI 10.1364/OE.24.003790.

## References

- [1] Korabiev, O., et al.: The atmospheric chemistry suite (acs) of three spectrometers for the exomars 2016 trace gas orbiter. Space Sci. Rev **214**(1), 7 (2017). DOI 10.1007/s11214-017-0437-6.
- [2] López-Valverde, et al.: Investigations of the mars upper atmosphere with exomars trace gas orbiter. Space Science Reviews **214**(1), 29 (2018). DOI 10.1007/s11214-017-0463-4.
- [3] Robert, S., et al.: Expected performances of the nomad/exomars instrument. Planetary and Space Science **124**, 94 – 104 (2016). DOI <http://dx.doi.org/10.1016/j.pss.2016.03.003>.
- [4] Thomas, I.R. et al.: Optical and radiometric models of the NOMAD instrument part II: the

# Applications of the ExoMars 2020 PanCam Wide Angle Camera Simulator: Optimising Image Acquisition and Post-Processing

**R. Stabbins** (1,2), A. Griffiths (1,2), M. Gunn (3), A. Coates (1,2) and the PanCam Science Team  
 (1) Mullard Space Science Laboratory, University College London, Holmbury St. Mary, Dorking, Surrey, RH5 6NT, UK, (2) Centre for Planetary Science at UCL/Birkbeck, University College London, Gower Street, Gower Street, London, WC1E 6BT, UK, (3) Department of Physics, Aberystwyth University, UK. (roger.stabbins.10@ucl.ac.uk)

## Abstract

We describe how a simulation of the PanCam Wide Angle Cameras (WACs) can be used as a tool for validating and refining the algorithms and parameters involved in image acquisition and post-processing during the ExoMars 2020 rover mission. We demonstrate how the tool has been used to evaluate and optimise the PanCam WAC auto-exposure algorithm, and discuss on-going work towards validation and optimisation of the noise-removal and calibration pipelines.

## 1. Introduction

The stereo and multispectral image products of the PanCam [1] Wide Angle Cameras (WACs) will be used, in conjunction with the PanCam High-Resolution Camera (HRC), to produce geologic maps of the ExoMars 2020 Rover environment, to assist traverse planning, target selection for in-situ studies, and to support geological and atmospheric studies. The quantitative 3D and surface reflectance reconstructions required to meet these objectives benefit from high signal-to-noise ratio (SNR) images.

Once in operation, SNR for WAC images can be maximised by 3 key tasks: auto-exposure, for optimisation of the dynamic range used in each image; noise-removal; and calibration, against the PanCam Calibration Target and pre-flight characterisation measurements. Developing and validating the algorithms that perform these tasks with the PanCam flight hardware is an expensive process. Large quantities of images must be captured across the range of illumination, surface, and thermal conditions expected at the Mars surface environment, which are difficult, or not possible, to emulate in laboratory conditions.

We present a method for efficiently and autonomously evaluating and optimising trial algorithms, by utilising a full-system simulation of the WACs, as described by Stabbins et al [2], to support further validation with the flight hardware.

## 2. Simulated Algorithm Evaluation

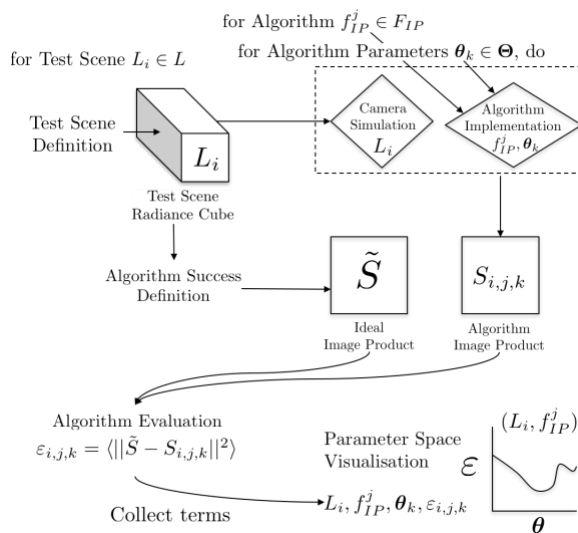


Figure 1 Method for evaluating image acquisition and post-processing algorithms

The general method is illustrated in figure 1. Ideal image products for a given task are defined and synthesized from an input test scene, as a hyperspectral radiance image cube. The parameter spaces of candidate algorithms are sampled, and the input test scenes processed according to the camera system simulation and implementation of the algorithm. Resultant images from the simulation are compared to the ideal examples via a cost-function. Cost-minimisation then guides the selection of optimal algorithms and parameter combinations.

### 3. Example: Auto-Exposure Evaluation and Optimisation

The PanCam WAC Auto-Exposure (AE) algorithm has the objective of finding the optimal exposure time of a given scene, for a selected filter. This is found by acquiring an image at an initial 'seed' exposure time, and then comparing the value of some statistical property of the image to a target value. The distance between the values is used to rescale the exposure time, until this distance is within a tolerance, or a maximum number of iterations are exceeded. The algorithm returns an image acquired at this final exposure time.

We have trialled the algorithm against 4 classes of scene composition (Solar, Horizon, Calibration Target, and Rock Target) and across radiance dynamic ranges scaled according to expectations derived from previous Mars surface measurements (e.g. [3]). The algorithm parameter space has been sampled comprehensively, including 2 statistical parameters over 128 values each (*Target* and *Outliers*) and the *seed* exposure parameter over 64 parameters, generating  $>1 \times 10^6$  images per scene.

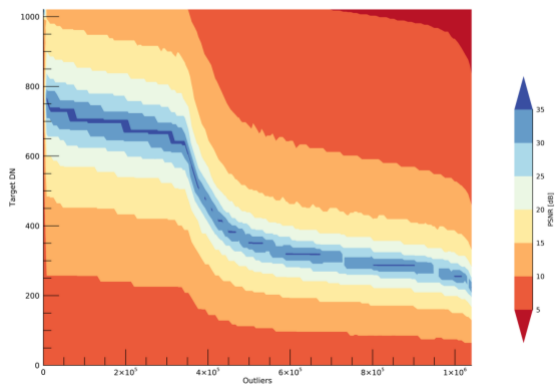


Figure 2 Example of Peak-SNR as a function of the 2 statistical parameters, *Target* and *Outliers*, for the Horizon test scene.

The most challenging part of the analysis is choosing a suitable representation of this high-volume dataset and high-dimensional cost-function, that provides information that can be used to optimise the algorithm. We pair the two statistical parameters, and produce 2D contour plots of the peak-SNR representation of the cost-function (e.g. figure 2). We have found from this representation that optimal values for these parameters lie on a function that can

be derived from the original scene cumulative distribution function.

By comparing cost-function plots for the trialled scenes and radiance dynamic ranges, we found that no optimal solutions exist for all scene compositions, due to the wide diversity between, for example, a simple image of the solar disc and a more complex image of the PanCam Calibration Target.

### 4. Future Work

We have demonstrated how this method can evaluate an algorithm by generating and assessing over 1 million images, a task that would be unfeasible using flight hardware. We currently are leveraging the comprehensive noise simulation of the PanCam WAC Simulator to develop noise-removal algorithms, a less subjective task. This is performed by passing a given scene through the simulator with all noise functions disabled, and using the resultant image as our ideal image product. Similarly, we can tune calibration algorithms by comparing derived radiometric images to the input scene radiance cubes.

Once these key algorithms are refined, we can deploy this complete image chain simulation on simulated scientific observations, allowing for rigorous confidence limits to set on noise-sensitive observations.

### Acknowledgements

This work has been funded by a UK Space Agency Aurora Studentship.

### References

- [1] Coates, A.J. et al.: *Astrobiology*, 17, 6-7, 2017.
- [2] Stabbins, R.B. et al.: 49th LPSC #2099, 19-23 March 2018, The Woodlands, Texas, US, 2018.
- [3] Bell, J.F. III. et al.: *JGR*, 111, E12, 2006.

## ExoMars 2020 is Blossoming: Integration and Test is Underway

Albert Haldemann, **Pietro Baglioni**, Thierry Blancquaert, Giacinto Gianfiglio, Michael Kasper, Francois Spoto, Jorge Vago, and the ExoMars Team  
ESA/ESTEC, Keplerlaan 1, 2200AZ Noordwijk ZH, The Netherlands, (albert.haldemann@esa.int)

### Abstract

The ExoMars programme has a long history, and demonstrated a key milestone with the 2016 mission [1,2]. The next mission for the ESA-Roscosmos cooperative endeavor is the launch in 2020 of the long-awaited Rover with its Pasteur Payload [3] which will be accompanied by a science payload on the Surface Platform of the Descent Module.

### 1. Introduction

This presentation will report on the status of the ExoMars 2020 development at the time of the meeting, given that significant progress is being achieved during 2018.

### 2. ExoMars 2020 Integration and Test

This year, 2018, is planned as a very busy year for ExoMars 2020. The project completed its Critical Design Review in early May, and the year will include:

- Rover Structural and Thermal Model mechanical and thermal testing to qualify the Rover design, in France
- Rover electrical and software verification tests performed on the Avionics Test Benches in U.K. and Italy
- Completion of the Descent Module (DM) and Spacecraft Composite Avionics Test Bench assembly, and software testing, in Italy Entry,
- Descent and Landing comprehensive simulation and verification campaign, supporting DM software development, and responding to the recommendations of the Schiaparelli Investigation Board Report [4]
- Parachute qualification testing with drop tests in Sweden
- Rover Locomotion Verification Model integration, and start of mobility system qualification in Switzerland
- Completion of all Rover subsystems and equipment qualifications and Flight Model unit assemblies
- Delivery of all (and integration of most) flight models of the Pasteur Payload instrument
- Integration and test of the Rover's Analytical Laboratory Drawer Qualification Model and Flight Model in Italy
- Most of the integration of the Rover Flight Model in U.K.
- Most of the integration of the Carrier Module (CM) Proto-Flight Model in Germany
- Most of the integration of the Surface Platform Flight model in Russia and Italy, and start of Descent Module Flight Model integration in Italy
- Spacecraft Composite (DM+CM) mechanical qualification test campaign on structural model in Russia
- Descent Module thermal qualification with a test campaign on thermal model in Russia

### **3. Summary and Conclusions**

With its very full programme of activities during 2018 (and more in 2019), the ExoMars 2020 mission development is on track for the opening of its 3-week launch window on 25 July 2020.

### **Acknowledgements**

The ExoMars developments reported here would of course not be possible without the enormous efforts of the entire ExoMars Team, which in addition to the ESA personnel, and in addition to the science teams of the Pasteur Payload and Surface Platform instruments, includes a wide-ranging industrial consortium in Europe and Russia and beyond. All of those partners are actively contributing to the dedicated, rapid progress towards the launch in 2020, and the authors most heartily thank them all!

### **References**

- [1] Vago et al. ESA Bulletin, 155, Aug.2013.
- [2] Baldwin, ESA Bulletin, 165-168, 2016.
- [3] Vago et al., ASTROBIOLOGY, Vol.17, 6 and 7, 2017  
DOI: 10.1089/ast.2016.1533
- [4] Tolker-Nielsen et al., Schiaparelli Inquiry Board (SIB), 2017, <http://exploration.esa.int/jump.cfm?oid=59176>

# RLS FM performance characterization and calibration campaign with the Instrument Data Analysis Tool (IDAT)

Guillermo Lopez-Reyes (1), Jesús Saiz (1), Álvaro Guzmán (1), Andoni Moral (2), Carlos Pérez (2), Fernando Rull (1), Jose Antonio Manrique (1), Jesús Medina (1) and the RLS team.  
(1) Unidad Asociada UVa-CSIC-CAB (2) Instituto Nacional de Técnica Aeroespacial (guillermo.lopez@cab.inta-csic.es)

## Abstract

The Flight Model (FM) of the RLS instrument for the ExoMars 2020 rover mission has been subject to a thorough campaign before delivery to ESA in order to properly characterize its performances. The Instrument Data Analysis Tool (IDAT) and SpectPro software tools have been key for the acquisition and interpretation of the data from the instrument. The results of the work performed with these tools during the RLS FM performance characterization and calibration campaign is presented here.

## 1. Introduction

The ExoMars 2020 rover mission will carry a drill able to obtain samples up to 2 meters depth under the Martian surface. It also features a suite of instruments (Pasteur Payload) inside the Rover's Analytical Laboratory Drawer (ALD) dedicated to exobiology and geochemistry research at the mineral grain scale after these samples have been crushed and powdered. The Raman Laser Spectrometer (RLS) is one of these key instruments [1]. The main ExoMars 2020 mission scientific objective is "Searching for evidence of past and present life on Mars". The RLS will contribute to this scientific goal through the precise identification of the mineral phases and the capability to detect organics on the powdered samples.

The on-ground characterization of the RLS FM is of utmost importance to guarantee the accuracy of the data received from the operation on Mars. During the RLS FM performance characterization campaign, several representative samples were analyzed, both in ambient and representative operational temperatures, including NIST standards, calibration lamps, the RLS Calibration Target and mineral powdered samples. These samples have allowed the performance

characterization of the instrument, including spectral response characteristics to allow for intensity and wavelength characterization. In addition, the analysis of representative samples has allowed the proper parameterization of the instrument acquisition algorithms [2] for its automated onboard operation.

## 2. IDAT/SpectPro

The Instrument Data Analysis Tool (IDAT) for the RLS instrument is a software tool that is used for the reception, decodification, calibration and verification of the telemetries generated by the RLS instrument, including both science and housekeeping (HK) data, as shown in Figs. 1&2. This allows the verification of the instrument status and the reception and interpretation of science data in a very user-friendly and fast way. The use of this tool is necessary during the system development phase of the instrument to provide a fast means for the decompression and interpretation of data in a fast and friendly way, saving a lot of data treatment time during the always-tight schedule on this development phase.

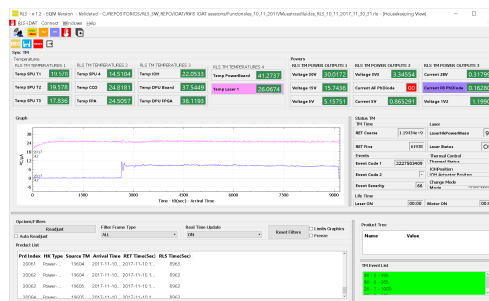


Figure 1: IDAT housekeeping view. This window allows monitoring the HK telemetry from the instrument in real time

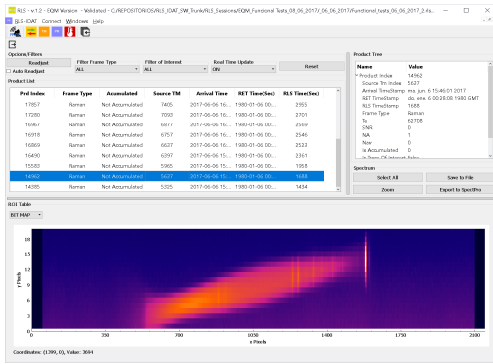


Figure 2: IDAT science product view. This window receives and shows all science products received from the instrument in real time

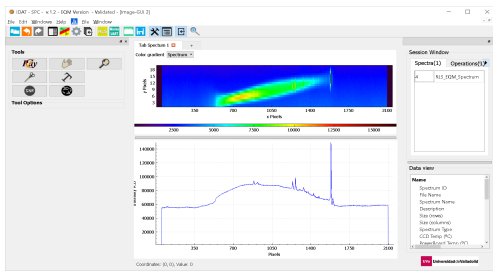


Figure 3: SpectPro image spectra view. This window allows operation on image spectra.

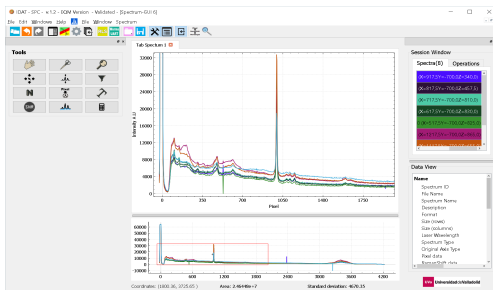


Figure 4: SpectPro linear spectra view. This window allows operation on linear spectra using the available tool palette on the left.

IDAT also incorporates SpectPro, a comprehensive spectra analysis tool for the interpretation and analysis of the science data with tools and operations for both images and binned spectra. This tool includes all types of spectra analysis tools to operate both images (Fig. 3) and linear spectra (Fig. 4), and to perform all kind of operations such as binning, SNR calculation, baseline removal, cosmic ray removal, filtering, cutting, band adjustment, and it even features a spectra calculator to allow operations with spectra in a very simple and reliable way.

### 3. Summary and Conclusions

The development of the appropriate software tools for the analysis of instrument spectra in early stages of development is not only useful but necessary in order to save time during the development phase of the instrument, but also for helping to understand the instrument behavior and performances. In addition, these tools will be further used during the operation of the instrument. For RLS, the development of IDAT and SpectPro has allowed the characterization of the FM of the instrument during the scientific campaign, which will be shown during the conference.

### References

[1] Rull et al., *Astrobiology*, 2017, 17, 627-654.  
 [2] Lopez-Reyes, G. and F. Rull Pérez (2017). "A method for the automated Raman spectra acquisition." *Journal of Raman Spectroscopy* 48(11): 1654-1664.

# Low Temperature Phase Transition in Natural Gypsum: Relevance in Exomars Mission

Ana Isabel Casado (1,2), Óscar Rodríguez Montoro (1), Mercedes Taravillo (1), Valentín G. Baonza (1,2) and Álvaro Lobato (1).

(1) MALTA-Consolider Team and Departamento de Química Física. Facultad de CC. Químicas. Universidad Complutense de Madrid. ([a.lobato@ucm.es](mailto:a.lobato@ucm.es))

(2) Instituto de Geociencias IGEO (CSIC-UCM)

## 1. Introduction

Mineral samples contain information of the Martian geochemistry and water distribution. Differences in their hydration states or crystallographic structure indicate the thermodynamic conditions and paleoclimate changes at which these substances have been submitted, being sensors of the geological history of Mars.

Raman spectroscopy has proved to be a suitable technique to discriminate not only the compositional and structural characteristics of these minerals, but also the pressure and temperature modifications by analysing vibrational bands shifting and broadening. Due to its importance, ExoMars mission incorporate, among others, a Raman Laser spectrometer with the scope of identify and characterize minerals of the Martian subsurface. With that purpose, several terrestrial analogues have been studied in order to create a Raman spectroscopy mineral database. Until now most of the database measurements have been made in mineral terrestrial analogues focusing on the different spectral features given by its composition i.e. sulphates, carbonates and silicates. Moreover, huge amount of these measurements have been made at room temperature conditions. Nonetheless, it is known that the actual Mars surface average temperature is around 218 K with maxima and minima of 308 K, at the equator and 120 K at poles. Such variation in the temperature conditions alter the thermodynamic stability of the minerals which may result in phase transitions which could have implications of the surface processes, and thus on the understanding of the Mars geochemical history.

On the other hand, temperature conditions alter the positions and full width half maximum values of the vibrational Raman bands, and therefore both effects can produce a mismatching assignment of the Raman spectra, making necessary to enlarge the Raman database with the low temperature measurements. In

this sense, few systematic measurements of the low temperature behaviour of Martian minerals making emphasis on the band shifting or phase transitions are found in the literature.

In this work, we show the low temperature history of gypsum mineral ( $\text{CaSO}_4 \cdot 2\text{H}_2\text{O}$ ). Our results show that Mars temperature oscillations could produce phase transitions and Raman spectra modifications evidencing the importance of such kind of measurements in the planetary data interpretation.

## 2. Material and Methods

Gypsum sample is a selenite gypsum collected in the town of Hornillos de Cerrato (Palencia, Spain). Experiments were carried out in a piece cut from the natural large transparent flattened crystal.

Temperature was controlled by a Linkam stage model HFS600E-PB4, with an optical glass window suitable for Raman spectroscopy. Experiments were carried out within the temperature range from 93 to 298 K. Heating rates of 5 °C/min were used with an accuracy of 0.1 °C. Refrigerant was liquid air.

Raman measurements were performed in a confocal Raman spectrometer Jasco NRS-4100, with a 532 nm laser excitation wavelength with an output power of about 6.6 mW. Detector is an air-cooled Peltier Andor CCD with 1650x200 pixels. In order to improve the spectral resolution, measurements were performed using 10 binning rows. A long working distance objective with 50x magnification was used giving a spot size according to the Rayleigh criteria of 2  $\mu\text{m}^2$ . Overall spectra were recorded with a 900 grooves/mm diffraction grating and a rectangular slit of 50x8000  $\mu\text{m}$  which gives a spectral resolution of  $\sim 3 \text{ cm}^{-1}$ . Additionally, high resolution measurements were performed with a 2400 grooves/mm diffraction grating and 10x8000  $\mu\text{m}$  rectangular slit which gives

a spectral resolution of  $\sim 0.5 \text{ cm}^{-1}$ . Spectra were calibrated using an emission Neon lamp.

### 3. Results

#### *Raman spectra of Natural Gypsum at 298 K*

Raman spectrum of gypsum crystal at 298 K between 100 and 4000  $\text{cm}^{-1}$  is shown in Figure 1.

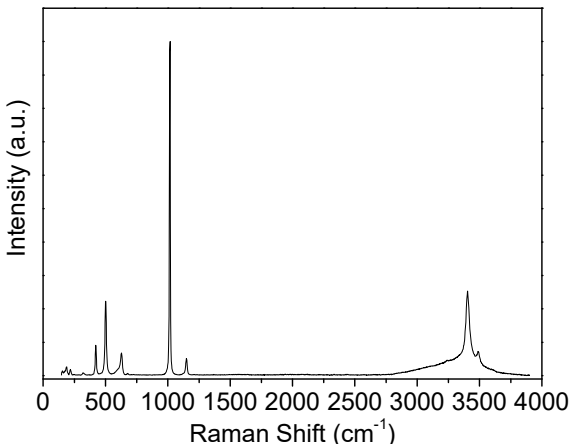


Figure 1: Raman spectra of natural gypsum crystal at 298 K.

Our data agrees well with those previously reported in the literature [1] and are in agreement with a  $C_{2h}^6$  symmetry group of gypsum. However, intensity variations are observed in contrast with previous data. These changes are especially significant in the water stretching region where the band at  $\sim 3400 \text{ cm}^{-1}$  is much stronger than the one located at  $\sim 3480 \text{ cm}^{-1}$ .

These spectral features are due to a partial polarization of the scattered light through the gypsum sample. Indeed, most of the Raman studies of gypsum use powdered or microcrystalline samples, and therefore such measurements are performed with randomly oriented crystals. In this work we have used a natural crystal, which their intensity distributions agree well with those reported by Krishnamur and Soot at an  $xz+zz$  polarization [2].

#### *Low temperature Raman spectra of Natural Gypsum*

Despite of being one of the most probable minerals in the Martian surface, there exist a clearly lack of low temperature data for gypsum mineral. In Figure 2 we show the thermal evolution of the spectral region corresponding to sulphates modes. Cooling to 93 K results in a general decrease of the bandwidth and consequently an increase in the separation of the overlapping bands.

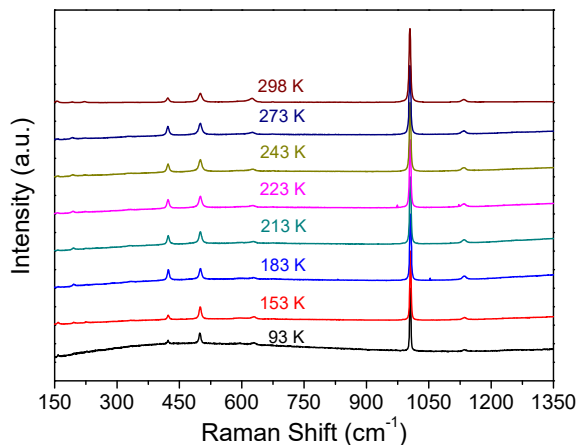


Figure 2: Temperature dependent Raman spectra of natural gypsum crystal within the range between 93 and 298 K.

However, it also produces intensity variations in the  $\nu_2\text{SO}_4$  ( $A_{1g}$ ) bands located at  $\sim 415$  and  $\sim 495 \text{ cm}^{-1}$  specially between 183 and 153 K where the  $415 \text{ cm}^{-1}$  band suffers a drastically intensity reduction. These changes are accompanied with a band splitting of the  $\nu_1\text{SO}_4$  ( $A_{1g}$ ) located at  $\sim 1005 \text{ cm}^{-1}$  as can be seen in Figure 3.

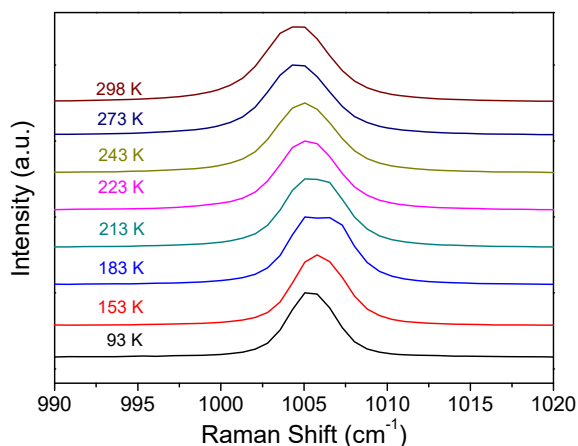


Figure 3: Temperature dependent Raman spectra of the  $\nu_1\text{SO}_4$  ( $A_{1g}$ ) band within the range between 93 and 298 K.

Band splitting can be attributed to a modification of the  $\text{SO}_4$  tetrahedra upon cooling, which results in a decrease of local symmetry and therefore a change in the Raman optical activity. In addition, such features correlate well with the intensity changes observed in the OH stretching region of the Raman spectra, where a sudden increase in the intensity of the band at  $\sim 3480 \text{ cm}^{-1}$  occurs (Figure 4). Such characteristics

could be indicative of phase transition however its confirmation needs a more detailed analysis.

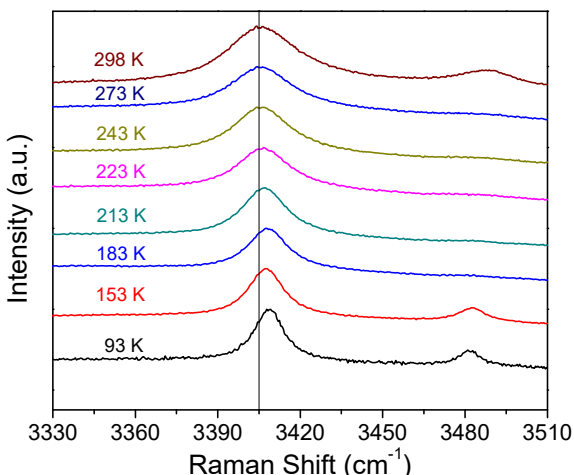


Figure 4: Temperature dependent Raman spectra of the OH stretching bands within the range between 93 and 298 K.

These results are in agreement with those reported for Klopogge and Frost [3]. They studied the Raman spectra of natural gypsum microcrystals at 300 and 77 K, observing intensity changes both in the several  $A_g$ ,  $A_u$  and  $B_g$  sulphate vibrations and in the OH stretching region pointing out also the possibility of a phase transition.

Finally, with regard to anharmonic behavior of the vibrational modes of gypsum, our results show that all sulphates modes suffer approximately a  $3\text{ cm}^{-1}$  upshifting during cooling as consequence of the temperature-induced variations in the vibrational frequency arising from higher-order anharmonic interactions under constant volume (pure temperature effect) and changes in the sample volume under increasing temperatures (pure volume effect). In the case of the OH stretching band located at  $\sim 3480\text{ cm}^{-1}$  undergoes an  $8\text{ cm}^{-1}$  downshifting in its Raman shift from 93 to 298 K, whereas the one at  $\sim 3410\text{ cm}^{-1}$  increases its frequency as the temperature raises, in agreement with data reported by Chio et al [4] for synthetic powder gypsum.

## 4. Summary and Conclusions

Low temperature behavior of natural gypsum crystal within the range from 93 to 298 K was studied. Our results show that upon cooling  $\nu_2\text{SO}_4$  ( $A_{1g}$ ) modes drastically change their intensity at the same time that the  $\nu_1\text{SO}_4$  ( $A_{1g}$ ) splits, pointing out towards a

possible phase transition around 183 and 153 K which can have implications in the mars surface processes. Such behavior correlates with the intensity fluctuations previously reported for the OH stretching bands in the literature but needs further analysis to be confirmed.

Finally, it is shown that low temperature produces substantial changes in the anharmonic behavior of the gypsum vibrational modes, where some vibrational bands increases its frequency as temperature decreases but other specially those related with hydrogen bonding of the hydration water molecules can experience frequency downshifting as temperature decrease. Therefore, an exhaustive database with low temperature measurements in minerals seems to be crucial for the scientific requirements of the next ExoMars mission.

## Acknowledgements

This work has been funded by the Spanish Ministerio de Economía, Industria y Competitividad under grants CSD2007-00045, CTQ2015-67755-C02-1-R and MAT2015-71070-REDC. A. Lobato wish to acknowledge the financial support from FPU grant no. FPU13/05731.

## References

- [1] Berenblut, B.J., Dawson, P. and Wilkinson, G.R., The Raman spectrum of gypsum, *Spectrochimica Acta*, 27, 1849-1863, 1971.
- [2] Krishnamurthy, N. and Soots, V., Raman Spectrum of Gypsum, *Canadian Journal of Physics*, 49, 885-896, 1971.
- [3] Klopogge, J. T. and Frost, R. L., Raman microscopy at 77 K of natural gypsum  $\text{CaSO}_4 \cdot 2\text{H}_2\text{O}$ , *Journal of Material Science Letters*, 19, 229-231, 2000.
- [4] Chio, C. H., Sharma, S. K. and Muenow, D. W., Micro-Raman studies of gypsum in the temperature range between 9 K and 373 K, *American Mineralogist*, 89, 390-395, 2004.

## Ozone and total opacity observation with the NOMAD-UVIS spectrometer

**W. Hewson** (1), M.R. Patel(1), J.P. Mason(1), M. Leese(1), B. Hathi(1), G. Sellers(1), J. Holmes(1), S.R. Lewis(1), P.G.J. Irwin(2), Y. Willame (3), A.-C. Vandaele (3), C. Depiesse (3), I. Thomas (3), B. Ristic (3), A. Piccialli (3), F. Daerden (3), M. Wolff(4), T. Clancy (4), G. Villanueva (5), B. Hubert (6), L. Gkouvelis (6), F. Altieri (7), E. D'Aversa (7) and the NOMAD-UVIS team.

(1) School of Physical Sciences, Faculty of Science, Technology, Engineering and Mathematics, The Open University, Walton Hall, Milton Keynes, U.K., (2) Atmospheric Physics, Clarendon Laboratory, Oxford University, Parks Road, Oxford, U.K., (3) Royal Belgian Institute for Space Aeronomy, Ringlaan-3-Avenue Circulaire, Brussels, Belgium, (4) Space Science Institute, 4750 Walnut St, Suite 205, Boulder, Colorado, U.S.A., (5) Goddard Space Flight Center, 8800 Greenbelt Road, Greenbelt, Maryland, U.S.A., (6) University of Liège, Place du 20 Août 7, 4000 Liège, Belgium, (7) Istituto do Astrofisica e Planetologia Spaziali, Tor Vergata, Via Fosso del Cavaliere 100, Roma, Italy. (will.hewson@open.ac.uk)

### Abstract

The composition of atmospheric trace gases and aerosols is a highly variable and poorly constrained component of the martian atmosphere, and by affecting martian climate and UV surface dose, represents a key parameter in the assessment of suitability for martian habitability. The ExoMars Trace Gas Orbiter (TGO) carries the Open University (OU) designed Ultraviolet and Visible Spectrometer (UVIS) instrument as part of the Belgian led Nadir and Occultation for Mars Discovery (NOMAD) spectrometer suite. NOMAD began transmitting science observations of martian surface and atmosphere back-scattered UltraViolet (UV) and visible radiation in Spring 2018. These are being processed to derive spatially and temporally averaged atmospheric trace gas and aerosol concentrations, intended to provide a better understanding of martian atmospheric photo-chemistry and dynamics, and also improve models of martian atmospheric chemistry, climate and habitability. Work presented here illustrates the development and application of the nadir O<sub>3</sub> and aerosol retrieval algorithms to new data from the NOMAD-UVIS instrument. Comparisons will be drawn with UVIS retrievals made by the OU team, and parallel retrievals by BIRA-IASB colleagues using an updated version of an algorithm used for Mars-Express SPICAM/UV analysis [1].

UVIS is part of the NOMAD instrument suite [2, 3] on board the joint ESA–Roscosmos ExoMars mission orbiting Mars, and is a UV / visible spectrometer operating in nadir and solar occultation modes between 200–650 nm, with 1.5 nm spectral resolution. The main objectives of UVIS are to improve the

O<sub>3</sub> climatology and deliver information on the aerosol content and variability of the martian atmosphere. O<sub>3</sub> is a highly reactive gas in the martian atmosphere, and through assimilation of O<sub>3</sub> measurements made by UVIS into martian climate models, understanding of martian atmospheric chemistry is set to be greatly improved.

The back-scattered signal sensed by UVIS is composed of solar light scattered by surface and atmospheric constituents of Mars, with absorbing signatures of trace gases imprinted on this signal. The simultaneous contribution of these factors in varying quantities make the separation of each scattering and absorbing component (e.g. aerosols and trace gases) a complex procedure.

The NOMAD team uses several different retrievals methods for derivation of ozone abundance. For example, to estimate atmospheric quantities of components contributing to sensed radiation in this manner, the NEMESIS radiative transfer model [4] is employed in an iterative least squares fitting procedure to simulate martian atmospheric radiances and provide a best-fit against UVIS observed values. Modelled radiances take into account the instrument's viewing geometry, martian surface reflectance, and atmospheric composition.

Preliminary results of UVIS observation of martian total column O<sub>3</sub> and aerosol optical depth are presented, as well as plans for future retrievals. This brand new dataset is constructed with the OU optimal estimation O<sub>3</sub> retrieval as applied to recently acquired nadir sounding data from the UVIS instrument, with the dataset expected to grow to provide climatological mapping over the next 4 years of the TGO mission.

## Acknowledgements

The NOMAD experiment is led by the Royal Belgian Institute for Space Aeronomy (IASB-BIRA), assisted by Co-PI teams from Spain (IAA-CSIC), Italy (INAF-IAPS), and the United Kingdom (Open University). This project acknowledges funding by the Belgian Science Policy Office (BELSPO), with the financial and contractual coordination by the ESA Prodex Office (PEA 4000103401, 4000121493), by MICIIN through Plan Nacional (AYA2009-08190 and AYA2012-39691), as well as by UK Space Agency through grant ST/P000886/1 and Italian Space Agency through grant 2018-2-HH.0.

## The NOMAD team

### Science

Vandaele, A.-C.; Lopez Moreno, J. J.; Bellucci, G.; Patel, M. R.; Allen, M.; Alonso-Rodrigo, G.; Altieri, F.; Aoki, S.; Bauduin, S.; Bolsée, D.; Giacomo Carrozzo, F.; Clancy, T.; Cloutis, E.; Daerden, F.; D’Aversa, E.; Depiesse, C.; Erwin, J.; Fedorova, A.; Formisano, V.; Funke, B.; Fussen, D.; Garcia-Comas, M.; Geminale, A.; Gérard, J.-C.; Gillotay, D.; Giuranna, M.; Gonzalez-Galindo, F.; Hewson, W.; Holmes, J.; Ignatiev, N.; Kaminski, J.; Karatekin, O.; Kasaba, Y.; Lanciano, O.; Lefèvre, F.; Lewis, S. R.; López-Puertas, M.; López-Valverde, M.; Mahieux, A.; Mason, J.; Mc Connell, J.; Mumma, M. J.; Nakagawa, H.; Neary, L.; Neefs, E.; Novak, R.; Oliva, F.; Piccialli, A.; Renotte, E.; Robert, S.; Sindoni, G.; Smith, M.; Stiepen, A.; Thomas, I.; Trokhimovskiy, A.; Vander Auwera, J.; Villanueva, G.; Viscardy, S.; Whiteway, J.; Willame, Y.; Wilquet, V.; Wolff, M. J.; Wolkenberg, P.

### Operations

Alonso-Rodrigo, G.; Aparicio del Moral, B.; Barzin, P.; Beeckman, B.; BenMoussa, A.; Berkenbosch, S.; Biondi, D.; Bonnewijn, S.; Candini, G. P.; Clairquin, R.; Cubas, J.; Giordanengo, B.; Gissot, S.; Gomez, A.; Hathi, B.; Jeronimo Zafra, J.; Leese, M.; Maes, J.; Mazy, E.; Mazzoli, A.; Meseguer, J.; Morales, R.; Orban, A.; Pastor-Morales, M.; Perez-Grande, I.; Queirolo, C.; Ristic, B.; Rodriguez Gomez, J.; Saggin, B.; Samain, V.; Sanz Andres, A.; Sanz, R.; Simar, J.-F.; Thibert, T.

## References

- [1] Y. Willame et al. “Retrieving cloud, dust and ozone abundances in the Martian atmosphere using SPICAM/UV nadir spectra”. In: *Planetary and Space Science* (2017). DOI: <https://doi.org/10.1016/j.pss.2017.04.011>.
- [2] M.R. Patel et al. “NOMAD spectrometer on the ExoMars trace gas orbiter mission: part 2—design, manufacturing, and testing of the ultraviolet and visible channel”. In: *Appl. Opt.* 56.10 (2017), pp. 2771–2782. DOI: 10.1364/AO.56.002771.
- [3] A.C. Vandaele et al. “Science objectives and performances of NOMAD, a spectrometer suite for the ExoMars TGO mission”. In: *Planetary and Space Science* 119 (2015), pp. 233–249. DOI: 10.1016/j.pss.2015.10.003.
- [4] P.G.J. Irwin et al. “The NEMESIS planetary atmosphere radiative transfer and retrieval tool”. In: *Journal of Quantitative Spectroscopy and Radiative Transfer* 109.6 (2008), pp. 1136–1150. DOI: 10.1016/j.jqsrt.2007.11.006.

## **CLUPI, a high-performance imaging system on the rover of the ExoMars mission 2020 to discover biofabrics on Mars. Science objectives and development status.**

J.-L. Josset<sup>1\*</sup>, F. Westall<sup>2</sup>, B. A. Hofmann<sup>3</sup>, J. G. Spray<sup>4</sup>, C. Cockell<sup>5</sup>, S. Kempe<sup>6</sup>, A. D. Griffiths<sup>7</sup>, M.C. De Sanctis<sup>8</sup>, L. Colangeli<sup>9</sup>, D. Koschny<sup>9</sup>, K. Föllmi<sup>10</sup>, E. Verrecchia<sup>11</sup>, L. Diamond<sup>12</sup>, M. Josset<sup>1</sup>, E. Javaux<sup>13</sup>, F. Esposito<sup>14</sup>, M. Gunn<sup>15</sup>, S. Gasc<sup>1</sup>, T. Bontognali<sup>1,16</sup>, O. Korablev<sup>17</sup>, S. Erkman<sup>18</sup>, G. Paar<sup>19</sup>, S. Ulamec<sup>20</sup>, F. Foucher<sup>2</sup>, N. Kuhn<sup>21</sup>, M. Tanevski<sup>1</sup>, P. Martin<sup>22</sup>, J. Vago<sup>9</sup>

<sup>1</sup>Space Exploration Institute, Neuchâtel, Switzerland; <sup>2</sup>Centre de Biophysique Moléculaire, Orléans, France; <sup>3</sup>Natural History Museum, Bern, Switzerland; <sup>4</sup>Planetary and Space Science Centre, University of New Brunswick, Canada; <sup>5</sup>UK Center for Astrobiology, University of Edinburgh, Scotland; <sup>6</sup>Geosciences University of Technology Darmstadt, Germany; <sup>7</sup>University College London, United Kingdom; <sup>8</sup>Istituto di Astrofisica e Planetologia Spaziali, Roma, Italy; <sup>9</sup>ESA, RSSD, The Netherlands; <sup>10</sup>Institute of Geology and Paleontology, University of Lausanne, Switzerland; <sup>11</sup>Institute of Earth Surface Dynamics, University of Lausanne, Switzerland; <sup>12</sup>Institute for Geological sciences, University of Bern, Switzerland; <sup>13</sup>Departement de Géologie, Unité PPM, University of Liège, Belgium; <sup>14</sup>Osservatorio Astronomico di Capodimonte, Napoli, Italy; <sup>15</sup>Aberystwyth University, United Kingdom; <sup>16</sup>ETHZ, Geologisches Institut, Zurich, Switzerland; <sup>17</sup>IKI, Space Research Institute, Moscow, Russia; <sup>18</sup>Faculty of Geosciences and Environment, University of Lausanne, Switzerland; <sup>19</sup>Joanneum Research, Graz, Austria; <sup>20</sup>DLR, Space Operations, Cologne, Germany; <sup>21</sup>Physical Geography and Environmental Change, University of Basel, Switzerland; <sup>22</sup>LPCEE, Orléans, France

\*Corresponding author: Dr Jean-Luc Josset, email address: jean-luc.josset@space-x.ch, telephone: + 41 32 889 68 69, fax number: + 41 32 889 69 73

### **Abstract**

The scientific objectives of the 2020 ExoMars rover mission are to search for traces of past or present life and to characterise the near-subsurface. Both objectives require study of the rock/regolith materials in terms of structure, textures, mineralogy, and elemental and organic composition. The 2020 ExoMars rover payload consists of a suite of complementary instruments designed to reach these objectives.

CLUPI, the high-performance colour close up imager, on board the 2020 ExoMars Rover plays an important role in attaining the mission objectives: it is the equivalent of the hand lens that no geologist is without when undertaking field work. CLUPI is a powerful, highly integrated miniaturized (<900g) low-power robust imaging system, able to sustain very low temperatures (-120°C). CLUPI has a working distance from 11.5cm to infinity providing outstanding pictures with a color detector of

2652x1768x3. At 11.5cm, the spatial resolution is 8 micrometer/pixel in color. The optical-mechanical interface is a smart assembly that can sustain a wide temperature range. The concept benefits from well-proven heritage: Proba, Rosetta, MarsExpress and Smart-1 missions...

In a typical field scenario, the geologist will use his/her eyes to make an overview of an area and the outcrops within it to determine sites of particular interest for more detailed study. In the ExoMars scenario, the PanCam wide angle cameras (WACS) will be used for this task. After having made a preliminary general evaluation, the geologist will approach a particular outcrop for closer observation of structures at the decimetre to subdecimeter scale (PanCam HRC) before finally getting very close up to the surface with a hand lens (CLUPI), and/or taking a hand specimen, for detailed observation of textures and minerals. Using structural, textural and

preliminary compositional analysis, the geologist identifies the materials and makes a decision as to whether they are of sufficient interest to be subsampled for laboratory analysis (using the ExoMars drill and laboratory instruments).

Given the time and energy expense necessary for drilling and analysing samples in the rover laboratory, preliminary screening of the materials to choose those most likely to be of interest is essential. ExoMars will be choosing the samples exactly as a field geologist does – by observation (backed up by years and years of field experience in rock interpretation in the field). Because the main science objective of ExoMars concerns the search for life, whose traces on Mars are likely to be cryptic, close up observation of the rocks and granular regolith will be critical to the decision as to whether to drill and sample the nearby underlying materials. Thus, CLUPI is the essential final step in the choice of drill site. But not only are CLUPI's observations of the rock outcrops important, but they also serve other purposes. CLUPI, could observe the placement of the drill head. It will also be able to observe the fines that come out of the drill hole, including any colour stratification linked to lithological changes with depth. Finally, CLUPI will provide detailed observation of the surface of the core drilled materials when they are in the sample drawer at a spatial resolution of about 15 micrometer/pixel in color.

The science objectives and the development status of the close-up imager CLUPI on the 2020 ExoMars Rover will be described together with its capabilities to provide important information significantly contributing to the understanding of the geological environment and could identify outstanding potential biofabrics of past life on Mars.

## Wide-altitude range H<sub>2</sub>O profile from ACS MIR and ACS NIR data

Anna Fedorova (1), Franck Montmessin (2), Alexander Trokhimovskiy (1), Oleg Korablev (1), Kevin Olsen (2), Alexander Lomakin (1, 3), Svyatoslav Korsas (1), Andrey Patrakeev (1), Alexey Shakun (1), Jean-Loup Bertaux (2, 1) and the ACS team (1) Space Research Institute (IKI), Moscow, Russia ([fedorova@iki.rssi.ru](mailto:fedorova@iki.rssi.ru)), (2) LATMOS-UVSQ, Guyancourt, France; (3) MIPT, Dolgoprudnyi, Russia

### Abstract

While the H<sub>2</sub>O column density in the Martian atmosphere has been characterized in depth, with decades of monitoring by different missions, the vertical distribution of water and its behavior in the middle atmosphere, its interannual and seasonal variability is still poorly understood. Direct and long-term observations of the H<sub>2</sub>O vertical distribution in the Martian atmosphere have been delivered by SPICAM on Mars Express for several Martian years [1, 2] but the Mars Express occultations are limited in season/location, and the profiling accuracy of SPICAM is perfectible.

Recent findings proved that water vertical distribution plays major role in the hydrogen escape processes on Mars and the water loss from the atmosphere [2, 3, 4]. Contrarily to our previous understanding, it has been discovered that water molecules reaching altitudes of 80 km in the perihelion season on Mars can be a direct source of escaping hydrogen.

The Atmospheric Chemistry Suite (ACS) began nominal science operations in March 2018 onboard the Trace Gas Orbiter (TGO) of the ExoMars mission [5]. ACS is a set of three spectrometers (NIR, MIR, and TIRVIM) intended to observe Mars atmosphere. The spectrometers can measure the vertical distribution of water vapour in different spectral bands providing a wide coverage of altitudes.

The H<sub>2</sub>O profile is best measured with the strong 2.6 μm band by MIR channel. ACS will be sensitive up to 100 km with the accuracy better than 1 ppm. At the lower altitude bound, MIR can detect water lines down to 3 km provided the aerosol content is low. This can help us better constrain poorly known water distribution within the lowermost scale height. However, measuring the 2.6-μm band with MIR requires a special secondary grating position, and

these sensitive H<sub>2</sub>O measurements can be implemented only during dedicated campaigns. Routine monitoring of water profiles are planned with the NIR channel in the 1.38 μm band with an accuracy better than 10 ppm at 90 km. Such measurements can be performed in parallel with any other ACS channel.

In this talk we will present the first water vertical distributions obtained by NIR and MIR channels with the wide altitude extension from 0 to 100 km, discuss the retrieval algorithms and specifics of observations in different channels.

### Acknowledgements

ExoMars is the space mission of ESA and Roscosmos. The ACS experiment is led by IKI Space Research Institute in Moscow. The project acknowledges funding by Roscosmos and CNES. Science operations of ACS are funded by Roscosmos and ESA. This work has been supported partially by the Ministry of Education and Science of Russian Federation grant 14.W03.31.0017.

### References

- [1] Maltagliati, L., Montmessin, F., Korablev, O., et al. 2013. Annual survey of water vapor vertical distribution and water-aerosol coupling in the martian atmosphere observed by SPICAM/MEx solar occultations. *Icarus* 223, 942-962.
- [2] Fedorova A., Jean-Loup Bertaux, Daria Betsis, Franck Montmessin, Oleg Korablev, Luca Maltagliati, John Clarke, Water vapor in the middle atmosphere of Mars during the 2007 global dust storm, *Icarus* 300, 15 January 2018, Pages 440-457.
- [3] Heavens, N. G., et al. (2018). "Hydrogen escape from Mars enhanced by deep convection in dust storms." *Nature Astronomy* 2(2): 126-132.
- [4] Chaffin, M.S., Deighan, J., Schneider, N.M., Stewart, A.I.F., 2017. Elevated atmospheric escape of atomic

hydrogen from Mars induced by high-altitude water.  
Nature Geoscience 10, 174–178.  
<https://doi.org/10.1038/ngeo2887>

[5] Korablev, O., Montmessin, F., and ACS Team: The Atmospheric Chemistry Suite (ACS) of three spectrometers for the ExoMars 2016 Trace Gas Orbiter, Space Sci. Rev., 214:7, 2018.

# The characterization of airborne dust close to the surface of Mars: the Dust Complex/MicroMED sensor on board the ExoMars 2020 Surface Platform

**F. Esposito** (1), C. Molfese (1), F. Cozzolino (1), F. Cortecchia (2), G. Mongelluzzo (1), B. Saggin (3), D. Scaccabarozzi (3), I. Arruego Rodríguez (4), A. Martín Ortega Rico (4), N. Andrés Santiuste (4), J. Ramón de Mingo (4), P. Schipani (1), S. Silvestro (1), C.I. Popa (1), M. Dall’Ora (1), Brienza (5), J. Robert Brucato (6), A. Zakharov (7), G. Dolnikov (7), A. Lyash (7), I. Kuznetsov (7), R. Mugnuolo (8), S. Pirrotta (8)

(1) INAF - Osservatorio Astronomico di Capodimonte, Napoli, Italy, (2) INAF – Osservatorio Astronomico di Bologna, Bologna, Italy, (3) Politecnico di Milano, Milano, Italy, (4) INTA, Madrid, Spain, (5) INAF-IAPS, Rome, Italy, (6) INAF – Astrophysical Observatory of Arcetri, Florence, Italy (7), IKI, Moscow, Russia, (8) Italian Space Agency, Italy

## Abstract

The ExoMars 2020 mission will deliver a rover and a surface platform on the surface of Mars. The rover has been designed to search for signs of life in the subsurface of Mars, while the surface platform will characterize the surface environment at the landing site.

MicroMED sensor is an Optical Particle Counter aimed to the characterization of the airborne dust at surface level. It is one of the sensors included in the suite named *Dust Complex* to be accommodated on the Surface Platform of the ExoMars 2020 mission. It is a novel experiment, never developed for space applications. It has been designed to measure, for the first time directly and in situ, the size distribution and number density vs size of dust particles suspended into the atmosphere of Mars, close to the surface. This information represents a key input in different areas of interest: 1) to improve knowledge on airborne mineral dust in terms of physical properties and lifting mechanism, 2) to improve climate models and 3) to address potential hazards for future landed Martian exploration missions.

## 1. Introduction

The Dust Complex (DC) is a suite of sensors devoted to the study of Aeolian processes on Mars. It includes three units: an Impact Sensor, the MicroMED sensor, and a Mast. The Impact Sensor contains the main electronics of the DC and two different elements: a piezoelectric based sensor, for the detection of the saltating sand grain flux and momentum, and a Charge-Sensitive Grid for the measurement of the

grains’ electric charges. MicroMED is an optical particle counter for the measurement of airborne dust size distribution and number density. The Mast accommodates the following sensors: 1) a second Impact Sensor, with the same sensors of the first one, 2) two Electric Probes for the measurement of the atmospheric electric field, 3) a Conductive Sensor, for the measurement of the electric conductivity of the Martian atmosphere and 4) an EM Sensor (antenna), which scans the atmosphere at frequencies up to 1 MHz to monitor electric discharges in the atmosphere.

The Dust Complex primary scientific goal is to monitor the dust cycle by direct measurements of dust flux at the surface of Mars. This has never been performed on Mars. Indeed, the dust cycle and the resulting feedback on atmospheric circulation are still poorly known for Mars. The unpredictability of the global dust storms on Mars is one of the most evident consequences of this lack of understanding.

ExoMars 2020 mission will offer a unique opportunity to study these processes by monitoring dust dynamics for one Martian year. This will allow spanning from periods of relatively clear sky to more dusty periods, where an important load of dust is expected to be injected into the atmosphere.

Monitoring of airborne dust is very important in planetary climatology. Indeed, dust absorbs and scatter solar and thermal radiation, severely affecting atmospheric thermal structure, balance and dynamics (in terms of circulations). Main dust parameters influencing the atmosphere heating are size distribution, abundance, albedo, single scattering

phase function, imaginary part of the index of refraction. The first two parameters can be measured by MicroMED. Moreover, wind and windblown dust represent nowadays the most active processes having long term effects on Martian surface morphological and chemical evolution. Aeolian erosion, dust redistribution on surface and weathering are mechanisms coupling surface and atmospheric evolution and are driven by wind intensity and grain properties. It is clear that the knowledge of the atmospheric dust properties and the mechanisms of dust settling and raising into the atmosphere are important to understand planetary climate and surface evolution.

### 1.1 MicroMED

MicroMED (Figure 1) is a miniaturized/optimized version of the MEDUSA instrument, which was selected by ESA for the Humboldt Payload, on board the lander of the previous configuration of the ESA ExoMars, before the mission changes approved in 2009. It has been designed to measure the size of single dust grains entering into the instrument from 0.2 to 10  $\mu\text{m}$  radius, giving as products the dust size distribution and abundance. It analyses light scattered from single dust particles. A pump is used to sample the Martian atmosphere, generating a flux of gas and dust across the instrument trough the inlet. When the dust grains reach the Optical Sensor, they cross a collimated IR laser beam volume (named sampling volume) emitted by a laser diode. The light scattered by the grains is detected by a photodiode, which is amplified and processed by the Electronics. The detected signal is related to the size of sampled dust particle.

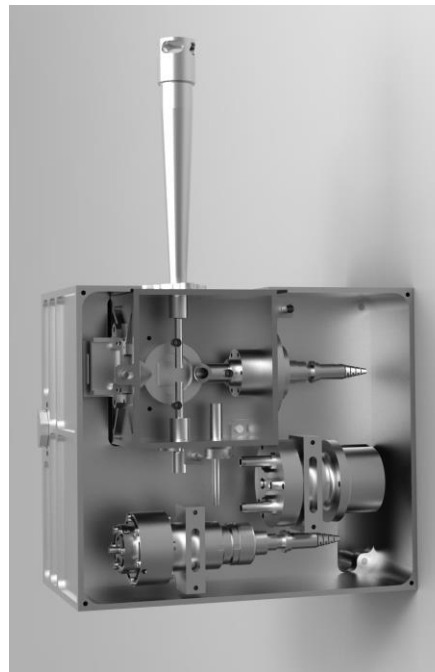


Figure 1. Sketch of the MicroMED sensor.

An optical fiber is used to connect the laser diode with the optical sensor. This allows moving the diode laser source outside the main body of the instrument allowing a flexible accommodation; moreover, it eases the instrument optical alignment. The optical system comprises a focusing system and a parabolic mirror to collect the scattered light onto the instrument detector, a photodiode. Moreover, in order to monitor the laser diode performance, an additional detector acquires a calibrated fraction of laser radiation. A sketch of the instrument optical layout is shown in Figure 2.

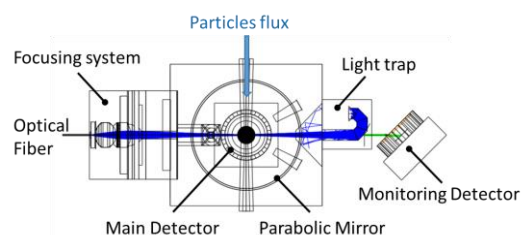


Figure 2. Sketch of the MicroMED optical layout.

In order to correctly detect inhaled particles, dust grains have to cross a 1  $\text{mm}^2$  sampling region where the laser spot is focused. Therefore computational fluid dynamic simulations were performed, aimed at

the optimization of the instrument fluid dynamics, achieving maximum sampling efficiency (95 and 100%) in the interesting size measurement range.

In order to achieve the dust flux through the optical head, a pumping system had been properly designed. Gardner Denver Thomas G 6/04 EB was used as a reference for the design phase. Pump mass budget was limited to 30g. The geometry and the size of the compression chamber, inlet and outlet ports were derived from the geometry of a commercial pump, but only space qualified materials had been considered. Thus, the commercial pump underwent to a process of reverse engineering that allowed identifying the criticalities for space usage. These were mainly related to the outgassing of the materials, resistance against the expected mechanical loading and compliance with the thermal environment. A mockup of the pumping system (as shown in Fig. 3) had been manufactured and underwent preliminary testing in representative environment, highlighting compatibility with expected performance from CFD analyses.



Figure 3. MicroMED pumping system mockup.

Instrument Central Electronics Board is based on micro-controller with high speed co-processor FPGA in order to provide enhanced processing capability, high speed analog acquisition beside advance capability to control motor and laser.

The presentation will detail the challenges in the development of MicroMED sensor and its status.

## ExoMars 2016 Schiaparelli at Mars: AMELIA results from the ‘terrific’ six minutes before crashing

Francesca Ferri (1), Ozgur Karatekin (2), Alessio Aboudan (1), Giacomo Colombatti (1), Bart VanHove (2), Carlo Bettanini (1), Stefano Debei (1), Stephen Lewis (3), François Forget (4)

(1) Università degli Studi di Padova, Centro di Ateneo di Studi e Attività Spaziali “Giuseppe Colombo” (CISAS) (francesca.ferri@unipd.it / Fax +39-049-8276855),

(2) Royal Observatory of Belgium (ROB), Brussels, Belgium,

(3) School of Physical Sciences, The Open University, Walton Hall, Milton Keynes MK7 6AA, UK,

(4) Laboratoire de Météorologie Dynamique, UPMC BP 99, 4 place Jussieu, 75005, Paris, France

### Abstract

On the 19th October 2016, Schiaparelli, the Entry Demonstrator Module (EDM) of the ESA ExoMars Program entered into the martian atmosphere. Although it did not complete a safe landing on Mars, it transmitted data throughout its descent to the surface, until the loss of signal at 1 minute before the expected touch-down on Mars’ surface [1].

The flight data received from Schiaparelli, although more limited than expected, were essential to investigate the anomaly that caused the crash landing and for the achievement of the Atmospheric Mars Entry and Landing Investigations and Analysis (AMELIA) experiment. AMELIA aimed at the assessment of the atmospheric science and landing site by exploiting the Entry Descent and Landing System (EDLS) sensors of Schiaparelli beyond their designed role of monitoring and evaluating the performance of the EDL technology demonstrator [2].

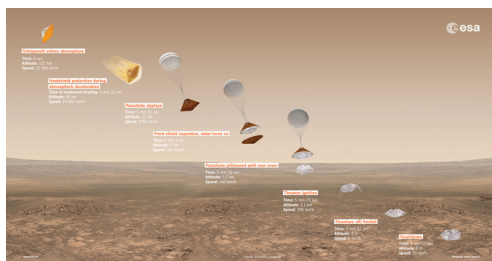


Figure 1: ExoMars 2016 Schiaparelli EDL scenario.

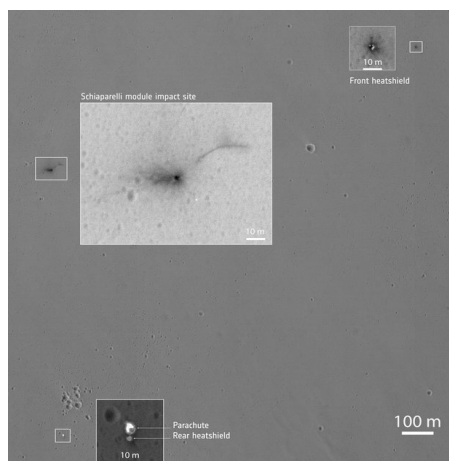


Figure 2: HIRISE image of Schiaparelli crash landing

Despite its ultimate failure to land safely, Schiaparelli allowed for sounding the atmosphere along its trajectory, so as per the seven atmospheric profiles retrieved by previous successful Mars entry probes (Viking 1 & 2 [3], Mars PathFinder [4,5], MER Spirit & Opportunity [6,7], Phoenix, MSL [8]). Sufficient EDL data were returned in order to reconstruct the trajectory and the attitude of Schiaparelli EDM and to retrieve the atmospheric profiles over the altitude range from 121 km to 4 km above the surface.

We will report on AMELIA results of the atmospheric reconstruction and the analysis of the atmospheric structure observed by Schiaparelli also in the context with other observations, atmospheric modelling and data assimilation.

## Acknowledgements

AMELIA is an experiment for scientific investigations of Mars' atmosphere and surface by means of the Schiaparelli measurements during its entry, descent and landing on Mars. The International AMELIA team built under the joint coordination of Principal Investigator: Francesca Ferri (Italy) and 3 Co-Principal Investigators (CoPIs): Özgür Karatekin (Belgium), Stephen R. Lewis (United Kingdom), François Forget (France) (*Interdisciplinary Scientist*). The team included scientists from Italy, France, UK, Belgium, Finland, Germany, Australia and USA. The support of the national funding agencies of Italy (ASI, grant n. 2017-03-17), Belgium (BELSPO and PRODEX), UK (UKSA) and France (CNES) is gratefully acknowledged.

## References

- [1] T. Blancquaert et al., (2017) *14<sup>th</sup> International Planetary Probe Workshop*, The Hague, NL.
- [2] F. Ferri et al. (2017) in press on *Space Science Rev.-ExoMars2016 special issue*
- [3] Seiff, A., D.B. Kirk, (1977) *J. Geophys. Res* **82**, 4364.
- [4] Schofield, T., et al. (1997) *Science* **278**, 1752-1758.
- [5] Magalhães, J.A., J.T. Schofield, A. Seiff, (1999) *J. Geophys. Res.* **104**, 8943-8945.
- [6] Withers, P. and M. D. Smith (2006) *Icarus* **185**.
- [7] Withers, P., Catling, D.C. (2010) *Geophys. Res. Lett.* **37**.
- [8] Holstein-Rathlou, C., A. Maue, and P. Withers (2016) *Planet. Space Scie.* **120**: 15-23.

## Reconstruction of the Mars atmosphere using the flight data from ExoMars Schiaparelli's instrumented heat shield and radio communications

Özgür Karatekin (1), Bart Van Hove (1) F. Ferri (2) Alessio Aboudan (2) G. Colombatti (2)  
(1) Royal Observatory of Belgium, (2) CISAS G. Colombo - University of Padova (o.karatekin@observatory.be)

### Abstract

Schiaparelli, the Entry Demonstrator Module (EDM) of ESA's ExoMars 2016 mission entered Mars atmosphere at 14:42 GMT on 19 October 2016. As part of the ESA-Roscosmos ExoMars mission, Schiaparelli was intended to demonstrate European EDL capability on Mars. While a successful landing was not achieved, fortunately the Schiaparelli lander was equipped with instrumentation that recorded and transmitted valuable flight data. The flight data indicate that hypersonic entry was successful, ending with supersonic parachute deployment starting the descent phase. About ~1.5 minutes into the descent phase, during which the frontal heat shield and back cover were released, contact with Schiaparelli was lost when it was only a few kilometers above the ground. Nevertheless, the transmission of real-time 'essential data' allows for post-flight analysis of the trajectory and the in-situ atmospheric conditions on Mars.

In the current work, we reconstruct the trajectory and atmospheric reconstruction using flight data recorded during atmospheric entry, with emphasis on the heat shield pressure instrumentation and radio link data.

### 1. Flight Data

Schiaparelli was equipped with an onboard guidance, navigation, and control computer (GNC). The GNC processed 3-axis accelerometer and gyroscope rates measured by an Inertial Measurement Unit (IMU). IMU flight data provide information on the trajectory state (i.e. position, velocity, attitude, rotation rates). The initial state before atmospheric entry, used as a starting condition for the GNC numerical integration, was based on a trajectory simulation after separation from the carrier spacecraft 72 hours before entry and

was refined further after the mission. The GNC also used data from a sun sensor on the back cover to estimate initial attitude. During the parachute descent phase, ranging measurements from down-facing radar Doppler altimeters (RDA) were performed after front shield release.

In addition to the IMU flight sensors, which are typical for EDL vehicles and essential to mission success, the frontal heat shield was further equipped with pressure and temperature sensors. In particular, 4 pressure sensors compose a Flush Air Data System (FADS), used to reconstruct attitude and in-situ atmospheric conditions. Methodology to reconstruct the angle of attack, sideslip angle, and atmospheric density, pressure, and temperature are presented. We performed 3-D Navier-Stokes flow simulations (CFD) to construct a surface pressure model on the forebody of Schiaparelli, in collaboration with DLR. The FADS method then combines the pressure data and CFD pressure model, by finding atmospheric density and flow angles that best fit the FADS measurements. Atmospheric pressure and temperature are derived from density as function of altitude from IMU, while assuming hydrostatic equilibrium and the ideal gas law. The 2012 Mars Science Laboratory was the only other mission to have recorded similar flight data, so the FADS onboard Schiaparelli provided a unique and valuable data set for Mars EDL [1,2].

Radio communications during the atmospheric entry were transmitted with the UHF (ultra-high frequency) radio antenna on the backshell. During descent, the spiral-shaped antenna on top of the lander was used, after separating the lander from the parachute. UHF was selected to be used in the Proximity Relay Communications. Nevertheless, the Giant Metrewave Radio Telescope (GMRT), located in Pune, India, was able to track the Schiaparelli in real-time during atmospheric entry and parachute descent, except in

the plasma blackout of about 1 minute between 70 and 30 km altitude. The real-time signal was received with a delay of about 10 minutes due the distance between Mars and Earth. GMRT lost track of EDM shortly before the expected touchdown.

The radio signal was also received and recorded by ESA orbiters in Mars orbit, i.e. Mars Express (MEX) and Trace Gas Orbiter (TGO), and downlinked later to Earth ground stations. On MEX, the Melacom communication system recorded carrier signals from the module in open-loop mode. In addition to the carrier signal, TGO's Electra communication system also recorded data telemetry. Essential flight data, and the Doppler tracking signal, were extracted from radio data relayed by ESOC in the mission control center in Darmstadt.

## 2. Results

In this study we present the analysis ExoMars 2016 Schiaparelli trajectory and atmospheric reconstruction using the engineering sensors. In addition, doppler shifts and power levels received by radio receivers on Earth and the Mars relay orbiters are analyzed to provide information on the trajectory state and the Mars atmosphere. The flow angles, atmospheric density, pressure, temperature, and the Mach number are reconstructed from flight data with associated uncertainties. Results from different flight data sets are presented and compared with observations from Mars orbiters and predictions from atmospheric models.

## References

- [1] Karlgaard, C. D., et al., JSR 51/4, 1029–1047, 2014.
- [2] Van Hove, B., Karatekin, Ö., JSR 54/3, 609–620, 2017.

## Acknowledgements

This work was financially supported by the Belgian Science Policy Office and the European Space Agency (ESA PRODEX Programme). This research was conducted as part of the project UPWARDS-633127 under the European Union's Horizon 2020 Programme (H2020-Compet-08-2014).

# The CaSSIS Digital Terrain Model generation and Archiving at OAPD

Gabriele Cremonese (1), Cristina Re (1), Emanuele Simioni (1), Teo Mudric (1), Amedeo Petrella (1), Matthew Chojnacki (2), Nicolas Thomas (3)

(1) INAF, Osservatorio Astronomico di Padova, Italy (gabriele.cremonese@inaf.it); (2) Lunar and Planetary Laboratory - University of Arizona, Tucson, USA, (3) Physics Institute, Space Research and Planetary Sciences - University of Bern, Switzerland.

## Abstract

The Colour and Stereo Surface Imaging System (CaSSIS) [1] on the ExoMars Trace Gas Orbiter is a multi-spectral stereo push-frame camera. CaSSIS is capable of providing two images of the same target from two different points of view along the same orbit. These acquisitions will be given as inputs for the photogrammetric products generation (digital terrain models and orthophotos). All the stereo data products generated by the different institutes and science teams involved in the CaSSIS project will be archived in a repository set up at INAF (National Institute of Astrophysics) of Padova and by the OAPD (Astronomical Observatory of Padova) team. The repository will be accessed through a website (<http://cassiss.oapd.inaf.it/>), it will provide the ability of on-line visualization and download of the stereo products that will be delivered periodically after their validation. The single archive will offer the benefits of having all the stereo data products from CaSSIS at one place providing easy data accessibility to the entire team. Initially the data will be available only to the CaSSIS team and later on, after the expiration of the proprietary period, also to the public.

The website will be linked to CaST (<http://skoll.unibe.ch/caST/>), the web application for the creation, editing, searching and prioritizing of targets for CaSSIS, and is now accessible for public image suggestions.

## 1. Introduction

The previous and ongoing exploration missions to Mars provide significant amounts of data at different resolution (HRSC [2], HiRISE [3], CTX [4]). CaSSIS is the European stereo acquisition system with the highest resolution operating around the red planet. Eighteen months after its arrival around Mars in October 2016, the TGO is ready for its nominal

science mission and from the end of April 2018, CaSSIS has started to produce its stereo pairs.

The system foresees the acquisition of multiple consecutive framelets that are mosaicked in a single image covering an area of 9.4x47 km.

The camera combines stereo and multispectral capabilities enhancing the ability of the science team to investigate terrain and geology. DTMs and the coloured orthophotos will improve significantly the quantitative analysis of the geomorphology and geology of target areas. In this context, the CaSSIS team is working on the creation of a robust and efficient pipeline that starting from the stereo image pre-processing, through a photogrammetric process, is able to provide accurate three-dimensional data to be collected in the repository for the delivery.

## 2. Stereo Data Product specifications

The stereo data in the OAPD repository will be 8 Bit orthoimages considering the complete mosaics of all the framelets in all the color bands and from both stereo images. These data products will be very useful for the key new science enabled by CaSSIS.

The repository will include also the DTMs that shall be 32-bit signed with elevations relative to the MOLA datum. The DTM spatial resolution is strictly correlated to the image quality and to the accuracy of the orientation data so the grid spacing will depend on the acquisition conditions. For the time being, a nominal stereo pair acquired at 5 m/pix will provide a DTM with 20 m/post sampling as for the case presented in [5] and produced with the 3DPD SW.

The geometric reference for both planimetry and height is a sphere of radius  $r=3396190$  m as defined by the MOLA team.

### 3. Stereo Data Generation

All the institutes affiliated with the CaSSIS team are invited to generate DTMs from the instrument images.

The photogrammetric pipeline proposed by the OAPD will contain automatic procedures for the creation of the complete orthoimages from the framelets, for the definition of an initial disparity map and the disparity refinement at the sub-pixel level and for the triangulation phase arriving to the DTM production [6].

The framelets are mosaicked at the height identified by the triangulation of a set of a tie points extracted with the SURF [7] operator. The DTM generation SW is based on stereo image matching using pyramid-based least-squares correlation process. The 3D point determination by forward intersection is followed by heights interpolation. A bundle adjustment procedure will be considered for the correction of the orientation data applied also for the orthoimage generation.

### 4. Quality Assessment

In order to assess the quality of the DTMs determined by stereo-photogrammetry, from a metrical point of view, the horizontal precision/resolution, the expected vertical precision and the estimated vertical accuracy will be taken in account. Also a qualitative assessment of the abundance and appearance of artifacts in the DTM will be considered. Auxiliary/metadata files describing those aspects will be submitted to the repository for each DTM uploaded in an XML format.

### 5. Data Exploitation

The access to the web repository (Figure 1) linked to the map-based visualisation provided by CaST will be very useful for the exploitation of the CaSSIS data. A shape file, provided to CaST by the stereo data producer, will allow the definition of the target position on the Mars global reference frame connecting different source of data/information at the same time. The science team will benefit in their investigations when taking advantage of all the data sources available.

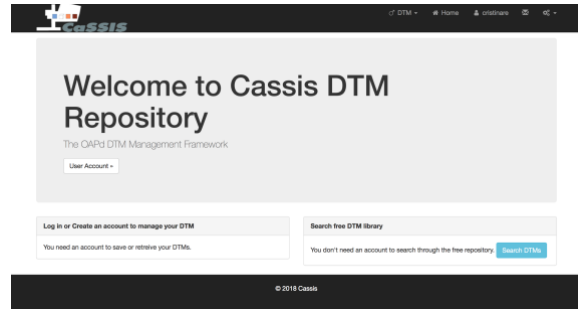


Figure 1: Home page of the Repository set up at the OAPD.

### Acknowledgements

The authors would like to express their gratitude to the CaSSIS team and the Italian Space Agency (ASI) for providing us the opportunity to give our contribution to the project (ASI-INAF agreement no.I/018/12/0).

### References

- [1] Thomas, N., et al. The Colour and Stereo Surface Imaging System (CaSSIS) for ESA's Trace Gas Orbiter. Eighth International Conference on Mars. 2014.
- [2] Jaumann, R., et al. The High Resolution Stereo Camera (HRSC): 10 Years of Imaging Mars. Eighth International Conference on Mars. Vol. 1791. 2014.
- [3] McEwen, Alfred S., et al. Mars reconnaissance orbiter's high resolution imaging science experiment (HiRISE). Journal of Geophysical Research: Planets 112.E5. 2007.
- [4] Malin, Michael C., et al. Context camera investigation on board the Mars Reconnaissance Orbiter. Journal of Geophysical Research: Planets 112.E5. 2007.
- [5] Simioni, E., et al. 3DPD application to the first CaSSIS DTMs. EPSC 2018.
- [6] Simioni, E., et al. A Photogrammetric Pipeline for the 3D Reconstruction of CaSSIS images on board ExoMars TGO. The International Archives of Photogrammetry, Remote Sensing and Spatial Information Sciences 42 : 133-139. 2017.
- [7] Bay, H. et al. Speeded-up robust features (SURF). Computer vision and image understanding 110.3: pp. 346-359. 2008.